PHOTODECOMPOSITIONS OF N-BROMOIMIDES

by

Da-Chuan Zhao

Huaiyin Teacher's College, Huaiyin, China, 1978-1980

THESIS SUBMITTED IN PARTIAL FULFILLMENT OF

THE REQUIREMENTS FOR THE DEGREE OF

DOCTOR OF PHILOSOPHY

in the Department

of

Chemistry

SIMON FRASER UNIVERSITY

January 1989

APPROVAL

Name: Da-Chuan Zhao

Degree: DOCTOR OF PHILOSOPHY

Title of thesis: PHOTODECOMPOSITIONS OF N-BROMOIMIDES

Examining Committee:

Chairman: Dr. P. W. Percival

Dr. Y. L. Chow
Senior Supervisor

Dr. T. N. Bell

Dr. B. M. Pinto

Dr. A. G. Sherwood
Internal Examiner

Dr. J. F. Bunnett
External Examiner
Department of Chemistry
University of California,
Santa Cruz

Date Approved: January 25th, 1989

PARTIAL COPYRIGHT LICENSE

I hereby grant to Simon Fraser University the right to lend my thesis, project or extended essay (the title of which is shown below) to users of the Simon Fraser University Library, and to make partial or single copies only for such users or in response to a request from the library of any other university, or other educational institution, on its own behalf or for one of its users. I further agree that permission for multiple copying of this work for scholarly purposes may be granted by me or the Dean of Graduate Studies. It is understood that copying or publication of this work for financial gain shall not be allowed without my written permission.

Title of Thesis/Project/Extended Essay

PHOTODECOMPOSITIONS OF N-BROMOIMIDES

Author: _____
(signature)

Da-Chuan Zhao
(name)

January 23,1989
(date)

ABSTRACT

The mechanism of photodecomposition of N-bromosuccinimide (NBS) in the presence of 1,1-dichloroethene (DCE) or of Br_2 was investigated in CH_2Cl_2 or in CH_2Cl_2 and cyclohexane. The yields of β-bromopropionyl isocyanate (BPI) from the photolysis of 1) NBS at ≃300 nm in the presence of DCE, 2) NBS at 300 nm in the presence of Br_2, 3) Br_2 at >380 nm in the presence of NBS, and the effects of concentration of benzene on the efficiency of BPI formation indicate 1) the direct photoexcitation of NBS produces a precursor of the succinimidyl radical, 2) both the precursor (†S) and the succinimidyl radical (S·) undergo ring opening to form BPI, and 3) the ring opening of †S is not quenched by benzene but that of S· is. The †S is assumed to be an excited state NBS molecule. An increase in Br_2 concentration caused by the photolysis of a mixture of NBS and Br_2 (<0.03 M) at 300 nm or >380 nm indicates 1) the Br· generated by the photolysis of NBS or Br_2 reacts with NBS to produce Br_2, 2) there is an equilibrium between S· and Br·, and 3) the rate constant previously reported for the bromine atom transfer from NBS to an alkyl radical is too low.

The effects of benzene concentration on the efficiency of hydrogen abstraction or addition of the 3,3-dimethylglutarimidyl radical indicate that only the 3,3-dimethylglutarimidyl radical serves as the chain carrier. The competitive photobrominations of cyclohexane and CH_2Cl_2 with Br_2 in the presence of selected N-bromoimides suggest that the observed product distributions

are mainly due to the bromine atom chain process when the concentration of Br_2 is high, and that the reactivities of the imidyl radicals are suppressed because of the reaction between Br_2 and the imidyl radicals.

The photodecomposition of N-bromo-N-acetylhexanamide and bromine atom-initiated decomposition of the corresponding N-bromoimide indicate 1) the efficient generation of the imidyl radical by the reaction between Br· and the N-bromoimide and 2) the equilibrium between Br· and the imidyl radical.

Selected cyclic N-bromoimides have been synthesized and photolyzed. Some ring-opening products from the corresponding cyclic imidyl radicals have been isolated and characterized. It has been established that thermal reactions of NBS with naphthols produce enones and that the formation of the enone and its subsequent rearrangement are responsible for the bromination products of 1-naphthol.

DEDICATION

To my grandmother

To my parents

To my wife

ACKNOWLEDGMENTS

The author wishes to express his gratitude to:

Dr. Y. L. Chow for his continual encouragement, guidance, and genuine interest during the course of this study,

Dr. T. N. Bell and Dr. B. M. Pinto for their valuable advice,

Dr. A. G. Sherwood, Dr. A. Tracey, Dr. S. K. Lower, and Mrs. S. Black for helping in revising the manuscript,

Dr. P. W. Percival for access to the MINUIT computing program and Mr. D. Yu for operating the program,

members of Dr. Chow's group for their cooporation, discussion and fellowship, and

all the technical staff in Chemistry Department for their assistance.

The generous financial support from Simon Fraser University, the Department of Chemistry, and Dr. Y. L. Chow is gratefully acknowledged.

TABLE OF CONTENTS

LIST OF TABLES

Table

LIST OF FIGURES

Figure

LIST OF SYMBOLS AND ABBREVIATIONS

BPA	β-bromopropionamide
BPI	β-bromopropionyl isocyanate
DCE	1,1-dichloroethene
33G·	3,3-dimethylglutarimidyl radical
33GH	3,3-dimethylglutarimide
33NBG	N-bromo-3,3-dimethylglutarimide
NBP	N-bromophthalimide
NBS	N-bromosuccinimide
1-NpOH	1-naphthol
2-NpOH	2-naphthol
P·	phthalimidyl radical
PH	phthalimide
PhG	N-phenyl-3,3-dimethylglutarimide
PhS	N-phenylsuccinimide
PI·	β-propionylisocyanate radical
S·	succinimidyl radical
SH	succinimide
Φ^0	quantum yield in the absence of benzene
Φ	quantum yield in the presence of benzene

CHAPTER ONE

INTRODUCTION

1.1. Background

The intermediacy of the imidyl radical[1,2] was first proposed in 1944 by Hey and Bloomfield[3], without evidence, in an effort to explain the allylic bromination of alkenes with N-bromosuccinimide (NBS) under Ziegler's conditions. These conditions utilized NBS in a refluxing carbon tetrachloride solution of the olefinic substrate (the solubility of NBS in CCl_4 is 0.005 M[4]). The disappearance of the undissolved NBS from the bottom of the vessel and the formation of the less dense and more insoluble succinimide at the surface indicated the reaction's progress. The "Bloomfield mechanism" suggested that the specificity was due to the unusual selectivity of succinimidyl radical (S·) which was postulated as an allylic hydrogen abstractor.

The Bloomfield Mechanism

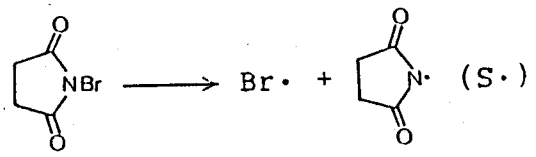

1-1

$$(CH_2CO)_2N\cdot + CH_2{=}CHCH_2R \longrightarrow (CH_2CO)_2NH + CH_2{=}\dot{C}HR \qquad 1\text{-}2$$

(SH)

$$CH_2=CH\dot{C}HR + NBS \longrightarrow S\cdot + CH_2=CHCHBrR \qquad 1\text{-}3$$

This mechanism gained popular acceptance because of its simplicity, and in 1946 Schmid and Karrer showed that the reaction was accelerated by benzoyl peroxide[5]. Dauben and McCoy[6] found that alkenes with tertiary allylic hydrogens could be brominated rapidly if the bromination was initiated by peroxides or light. These were reported as evidence of the radical nature of the reaction.

Goldfinger[7] proposed in 1953 that NBS behaved like N-chlorosuccinimide which had been shown to serve as a source of Cl_2 in low concentration, and that the hydrogen-abstracting species were bromine atoms and not succinimidyl radicals.

The Goldfinger Mechanism

$$Br_2 \longrightarrow 2\ Br\cdot \qquad 1\text{-}4$$

$$Br\cdot + CH_2=CHCH_2R \longrightarrow HBr + CH_2=CH\dot{C}HR \qquad 1\text{-}5$$

$$CH_2=CH\dot{C}HR + Br_2 \longrightarrow CH_2=CHCHBrR + Br\cdot \qquad 1\text{-}6$$

$$NBS + HBr \longrightarrow SH + Br_2 \qquad 1\text{-}7$$

Since then, three decades of widespread effort have indicated that Br· is the chain carrier[8-14]. The curious "Ziegler

requirement" for the use of carbon tetrachloride solvent in allylic bromination of olefins with NBS now has the obvious rationale, that of maintaining a very low concentration of NBS in the liquid phase and thus allowing the Br_2 to be the major radical-trapping agent even though its concentration is very low (presence of olefin). In contrast, if a solvent is used in which NBS has a higher solubility, e.g., acetonitrile or dichloromethane, NBS can compete successfully with the small amounts of Br_2 present in solution in order to react with the alkyl radicals (Eq. 1-3 and 1-6 represent two such competing reactions).

1.2. The Generation of imidyl radicals

The most common and widely used method of generating imidyl radicals is the decomposition of N-haloimides by photolysis[15,16] or thermolysis[17,18]. Since halogen atoms are simultaneously generated with imidyl radicals during the homocleavage of the N-X bond, alkenes without allylic hydrogens are usually used to scavenge the halogen atom to suppress the competing halogen atom chain reactions.

It has however been reported that a phthalimidyl radical (P·) can be generated by the oxidiation of potassium phthalimide with lead tetraacetate in dichloromethane[19] represented in Eq. 1-8

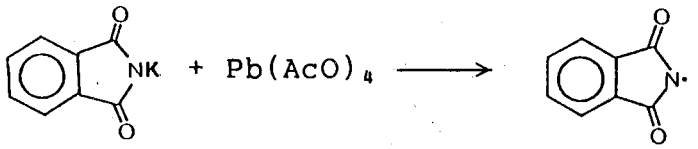

1-8

On the other hand photolysis of *t*-butyl N-succinimidepercarboxylate at 77°K in cumene or toluene (Eq 1-9) was believed to afford succinimidyl radical which could be responsible for the formation of succinimide, the coupling products derived from the solvents (bicumyl or bibenzyl) and t-butyl alcohol[20].

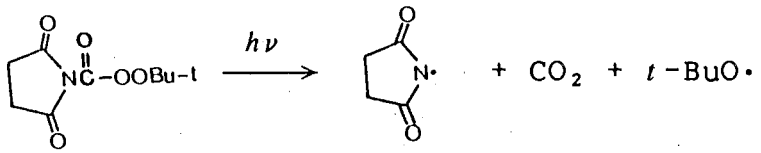

1-9

The authors attributed an observed five line ESR spectrum to the formation of β-propionylisocyanate radical (PI·) from the ring opening of succinimidyl radical (Eq 1-10, see Section 1.4). The attempt to generate succinimidyl radical by photoirradiating N,N'-bisuccinimide failed because of its stability towards the irradiation[20].

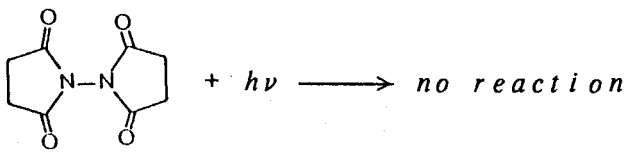

1.3. Detection of Imidyl Radicals with Physical Methods

Even though the existence of imidyl radicals has been suggested by chemists since the 1940's, the effort to characterize them by physical methods was not successful until 1969 when Lagercrantz and Forshult[19] demonstrated that the succinimidyl, tetramethylsuccinimidyl and phthalimidyl radicals generated by photolysis of the corresponding N-bromoimides could be trapped with 2-nitroso-2-methylpropane to exhibit a 3x3 line spectrum. The succinimidyl radical was also identified by esr spectroscopy when succinimide (single crystals) was irradiated with X rays at 26°K[21]. However, the attempt to observe the transient absorption of the succinimidyl radical in solution has not been successful[22].

1.4. Reactions of Imidyl Radicals

1.4.1. Ring Opening Reactions

β-scission, i.e., ring opening reactions of cyclic imidyl radicals, to form β-acylisocyanate radical was proposed by Johnson and Bublitz[23], and Martin and Bartlett[24] in 1957 to explain the isomerization of NBS to β-bromopropionyl isocyanate (BPI).

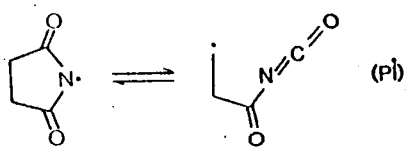

1-10

$$\dot{C}H_2CH_2CONCO + NBS \longrightarrow BrCH_2CH_2CONCO\ (BPI) + S\cdot \qquad 1\text{-}11$$

The reaction was initiated by benzoyl peroxide and this led to the conclusion that the isomerization from NBS to BPI could be described as a radical-chain process with PI· as the radical intermediate. Traces of water in solvent reacts readily with BPI to produce β-bromopropionamide (BPA)[31] (Eq 1-12)

$$BrCH_2CH_2CONCO + H_2O \longrightarrow BrCH_2CH_2CONH_2 + CO_2 \qquad 1\text{-}12$$

Photolysis of *meso*-N-chlorosuccinimide-d_2 afforded *meso*- and *dl*-succinimide-d_2 in about 1:1 ratio[4,25]. This isomerization at the 2,3-position in converting NCS to succinimide suggests that the ring-opening of succinimidyl radical is reversible (Eq 1-10). The reversibility was further confirmed by a recent work reported by Roberts and co-workers[26]: homocleavege of the Br-C bond in BPI initiated by the $(n\text{-Bu})_3P\rightarrow\dot{B}H_2$ radical led to the formation of succinimide and it was isolated by HPLC in about 25% yield. After the rate constant for the bromine transfer from NBS to a primary alkyl (e.g., PI· radical) estimated by Skell was challenged by Chow et al. (see the last paragraph in Section

3.1.4 for the detail), Skell[27] and co-workers, utilizing the cyclopropylcarbinyl-allylcarbinyl free radical "clock", investigated the rate constant for bromine transfer from N-bromo-3,3-dimethylglutarimide (33NBG) and N-bromophthalimide (NBP) to the cyclopropylcarbinyl radical, a primary alkyl radical, to be 1.3×10^{10} and $1.6\times10^{10}M^{-1}s^{-1}$ respectively, about 1×10^{3} times higher than the value reported previously[29] by Skell and Day. Walling and co-workers measured the rate of NBS decomposition, in the presence of 1,1-dichloroethene (DCE) and with dichloromethane as solvent, initiated by benzoyl peroxide at 50°C[18]. Assuming $k_{11}[NBS]>>k_{10}$, and $k_{11}[NBS]>>k_{-10}$, i.e., reversibility of ring opening is minor and the slow steps are those involving k_{10} and hydrogen abstraction by S·, the rate constant of ring opening was calculated to be about 1660 s^{-1}. They reported that addition of cyclohexane produced an unexpected increase in rate corresponding to $k_{10} \simeq 1.5\times10^{4}$ s^{-1}.

The quantum yield of NBS disappearance[4] in degassed bromine-scavenged reaction system (NBS-DCE-CH_2Cl_2) was reported to be 63±3 when NBS was irradiated by a 313-nm light source. Photoinitiation with azobis(isobutyronitrile) (AIBN) at 366 nm in degassed bromine-scavenged system afforded a chain length[4] of 30. The quantum yield of disappearance of a tricyclic N-bromoimide in the presence of 3,3-dimethylbutene was measured by Chow and Naguib[28] to be ≃ 40. The kinetic chain lengths of 10^2 - 10^3 were reported[18] for AIBN-initiated NBS bromination of dichloromethane

in the presence of DCE at 50°C. When DCE was replaced by Br_2 (≃0.1M), the chain lengths decreased to 30 - 70.

Some cyclic N-bromoimides readily undergo opening reaction but others do not[29,30]. The yields of the ring opening products are affected by several factors. For example, the yield of BPI[18,31], the ring opening product of the succinimidyl radical, is low when NBS is photolyzed in the presence of Br_2.

1.4.2. Hydrogen Abstractions

Hydrogen abstractions by imidyl radicals have been studied using substrates unreactive to bromine atoms such as 2,2-dimethylpropane, dichloromethane, *t*-butyl chloride etc. in the presence of an alkene containing no allylic hydrogens in order to scavenge Br_2 and bromine atoms. Yip and Chow[32] reported a value of $>3.5\times10^{3}M^{-1}s^{-1}$ for the rate constant for hydrogen abstraction by 3,3-dimethylglutarimidyl radical (33G·) from cyclohexane from the results of flash photolysis of 33NBG in cyclohexane at 25°C. Studying benzoyl peroxide-initiated bromination of cyclohexane by NBS at 50°C, Walling and coworkers[18] estimated the rate constant for hydrogen abstraction by the succinimidyl radical from cyclohexane to be $>10^{4}M^{-1}s^{-1}$. Walling et al. also reported that the rate constant for hydrogen abstraction by S· from dichloromethane[18] at 55°C was 55±8.

The reactivity of different C-H bonds of alkanes towards imidyl radicals can be determined by means of competitive hydrogen abstractions (Eq 1-13 and 1-14).

$$(RCO)_2N\cdot + A\text{-}H \longrightarrow (RCO)_2NH + A\cdot \qquad 1\text{-}13$$

$$(RCO)_2N\cdot + B\text{-}H \longrightarrow (RCO)_2NH + B\cdot \qquad 1\text{-}14$$

The A· and B· are converted to ABr and BBr by the subsequent bromine transfers from N-bromoimides (if Br_2 is scavenged) or from N-bromoimides and/or Br_2 (if Br_2 is not scavenged). Since the rate constants for hydrogen abstractions from the alkanes are much slower[18,32] than those for the subsequent bromine transfers[27], the product ratio of ABr/BBr from these competitive hydrogen abstractions provides information about the ratio of the rate constants, k_{13}/k_{14}, for the abstraction of various hydrogens in the first chain-propagating step. The latter is reported as the selectivity of the imidyl radical towards hydrogen abstraction from AH and BH[4,18,33-35].

1.4.3. Additions to Alkenes

Imidyl radicals add to the less substituted side of double bonds of alkenes if the alkene is unsymmetric, to form 1:1-addition products in yields up to ≃80%[30,36,38].

$$S\cdot + t\text{-}BuCH{=}CH_2 \longrightarrow t\text{-}Bu\dot{C}H\text{-}CH_2S \qquad 1\text{-}15$$

$$t\text{-}Bu\dot{C}H\text{-}CH_2S + NBS \longrightarrow t\text{-}BuCHBr\text{-}CH_2S + S\cdot \qquad 1\text{-}16$$

It has been reported[38] that the 3,3-dimethylglutarimidyl (33G·) and phthalimidyl (P·) radicals add to electron-rich alkenes such as ethene, vinyl acetate, 2-chloropropene, isobutene, 3,3-dimethyl-1-butene, but these radicals do not add to electron-defficient alkenes such as maleic anhydride and tetrachloroethene[38]. However, recently, a 1:1 addition product of NBS to DCE was isolated by Zhang and co-workers from product mixtures after the photolysis of NBS in the presence of 0.5 M DCE[52].

The rate constant for addition of 33G· to 3,3-dimethyl-1-butene was determined by Yip and Chow, utilizing flash photolysis[32], to be 9×10^6 $M^{-1}s^{-1}$ at 25°C. The chain length for the addition of 33G· to 2-chloropropene was reported to be as high as 2000[38]. A minimum value of the rate constant for the addition step was determined to be 1.3×10^5 - 3.5×10^5 $M^{-1}s^{-1}$ at 35°C[38].

1.4.4. Reactions with Arenes

Imidyl radicals, e.g., succinimidyl and 3,3-dimethylglutarimidyl radicals react with benzene, naphthalene and other aromatic hydrocarbons to form the substitution (imidation) products[36-38].

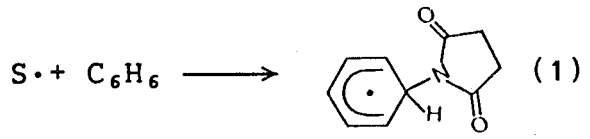

1-17

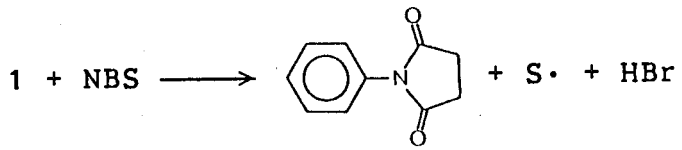

1-18

The imidation was proposed to occur via the cyclohexadienyl radical intermediate (1) followed by bromine transfer from NBS to 1 then dehydrobromination since a tribromo compound 2 in

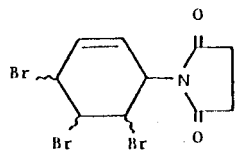

2

addition to N-phenylsuccinimide was isolated by Chow and co-workers from product mixtures after the photolysis of NBS in benzene[37] in the absence of an alkene. A chain length of 10 was reported for substitution of succinimidyl on benzene[30,4]. As to the rate constant for S· adding to benzene there has been no data available so far.

1.5. Theoretical Calculations on Imidyl Radicals

In an imidyl radical the nitrogen accommodates three electrons in two orbitals. The unpaired electron can be either in the σ orbital or in the π orbital. It is a π or σ radical when

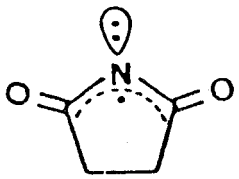

π (or Sπ)

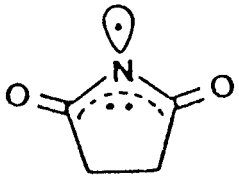

σ (or Sσ)

the unpaired electron is in the π or σ orbital, respectively. For example, the succinimidyl radical may have a π or σ electronic ground state. This has led to many theoretical investigations on the electronic configuration and the ground state of imidyl radicals. Applying simple molecular orbital theory to the relative orbital energy of the succinimidyl radical, Hedaya and co-workers[20] estimated that the ground state would be σ. Using INDO approximation, Koenig and Wielesek[39] have reported that the ground state of succinimidyl radical should be π, and that σ is about 1.6 eV higher in energy than π is. They have pointed out that the ring opening of the Sσ correlates with ground state isocyanate and the same nuclear motions for the Sπ leads to an excited state of the isocyanate (Scheme 1-1). The ring opening of the π radical would thus be slow. It is important to point out that their calculations were based on the assumption that the ring opening proceeds through a transition state which retains the symmetry plane containing the five main atoms. Clark[40] reported (MNDO) that Sπ and Sσ had calculated heats of formation of -30.4 and -16.6 kcal/mol respectively.

Scheme 1-1

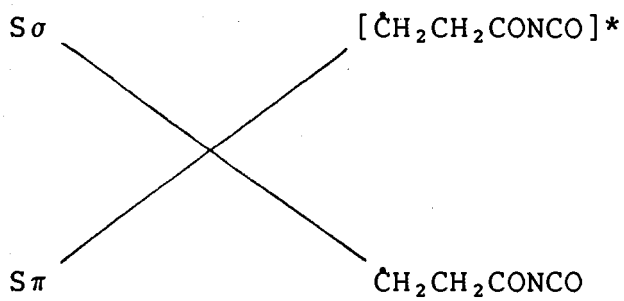

Kikuchi and co-workers[41] (MNDO/3) showed, however, ΔH_f of Sσ was -76 and that of Sπ was -59 kcal/mol respectively, which implies Sσ to be the ground state. Using the spin-unrestricted version of MNDO (UMNDO), Dewar and co-workers[42] show the calculated heats of formation for Sπ and Sσ are -38.3 and -23.7 kcal/mol, and the former is more stable than the latter is by 14.6 kcal/mol. It seems that their calculation of the energy gap is influenced strongly by Skell's previous conclusion that the energy gap between Sπ and Sσ is about 20[43], or <17.7[44] kcal/mol. *Ab initio* studies carried out by Apeloig and co-workers[45] predicts that Sπ is the ground state of the succinimidyl radical with Sσ as its lowest excited state. The energy difference between the two states is 55.0 kcal/mol at STO-3G. The singly occupied molecular orbital (SOMO) of Sπ and Sσ are -280 kcal/mol (-12.10 eV) and -305 kcal/mol (-13.22 eV) respectively. Samskog

and co-workers have investigated the succinimidyl radical by esr spectroscopy[21] in single crystals of succinimide being irradiated with X-rays at 26°K. From the principal values of the hyperfine coupling tensor and the g tensor as well as from *ab initio* MO-LCAO calculation they conclude the succinimidyl radical has a π electron configuration[21]. The ring opening of Sσ has been predicted by Dewar and co-workers to be exothermic by 7.2 kcal/mol with an activation barrier of 12.9 kcal/mol and an activation entropy of 4.8 cal/mol·K at 25°C. This leads to a calculated rate constant of $2.4 \times 10^{4} s^{-1}$ at 25°C[46]. It agrees astonishingly well with the experimental rate constant from Walling's group[18] for the ring-opening of the succinimidyl radical which was generated from the thermal initiated decomposition of NBS in dichloromethane. Walling believed that the succinimidyl radical generated under those conditons should be in its ground state, since that rate constant implied that its lifetime must be about $10^{-4} s^{-1}$, too long for an excited radical[18]. Dewar, however, argued that the lifetime of the succinimidyl radical in its excited state could be that long. In support of this, he and his co-workers calculated the transition moment for the spontaneous decay of Sσ to Sπ. A value of 0.094 a.u. was obtained which leads to a calculated intrinsic emissive lifetime of $4.4 \times 10^{-4} s$[46]. It is necessary to mention that in their calculations Dewar and co-workers made the same assumption as Koenig did[39] that the transition state retained the symmetry plane containing the five main atoms (four carbons and one nitrogen)

and possessed C_S symmetry during the ring-opening.

1.6. The Experimental Investigation on the Electronic Configurations of Imidyl Radicals

From the point of view that the singly occupied orbital of the σ (4σ) or the π radical (4π) is orientated towards a specific direction and that it consequently must show anisotropic behavior in intramolecular hydrogen abstraction reactions, Chow and Naguib[28] studied the electronic configuration of the imidyl radical using the model compound (3).

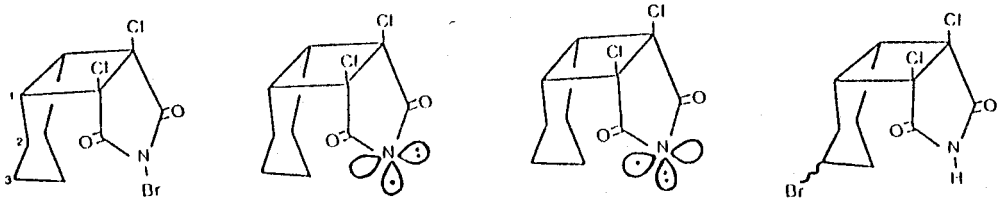

3 4σ 4π 5

If the imidyl radical possesses π electronic configuration (4π), its intramolecular hydrogen abstraction from C-3 position would be expected to be very facile since the distance between the N and the C-3 atoms is only about 2.3 Å. Such a reaction would lead to the formation of 3-bromoimide (5). However, only ring opening products were found from the photolysis of 3 in the presence of an alkene. On this basis they proposed that the imidyl radical generated under the reaction conditions was the σ

Scheme 1-2

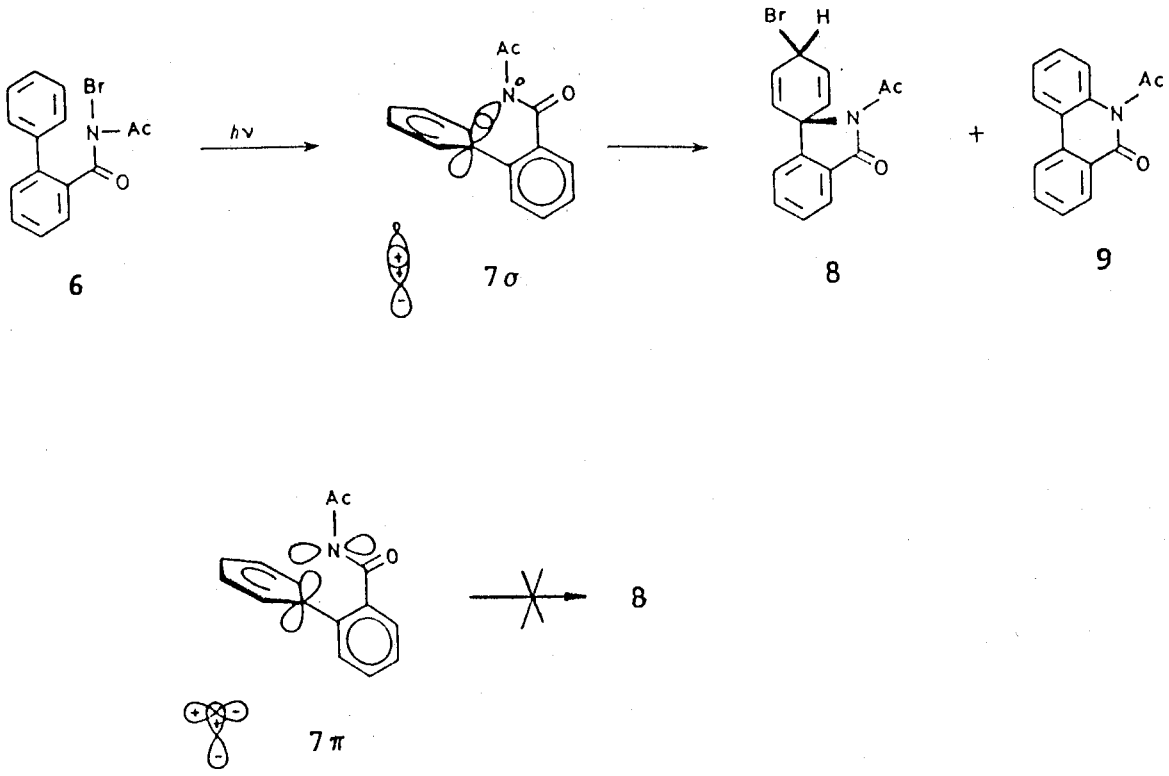

radical (4σ). The conclusion is supported by the results from Glover's group who used an acyclic N-bromoimide (**6**) as a model[47] (see Scheme 1-2). Cyclized products **8** and **9**, in particular **8**, can only be formed when the imidyl radical from photolysis of **6** is a σ radical (7σ)) in which a good overlap of orbitals is allowed between the nitrogen and the C-1'. In contrast, the π radical (7π) presents an orthogonal orbital to the same carbon atom. The poor orbital overlap prevents the formation of **8**. Glover and co-workers attributed the formation of **9** to π-σ mixing[47].

1.7. Recent Controversies

In 1974 Skell and co-workers reported that photolysis of a CH_2Cl_2 solution of NBS in the presence of DCE (the NBS-DCE system) produced a succinimidyl radical which had a selectivity different from bromine atoms[16]. The succinimidyl radical generated under the above conditions adds to alkenes, reacts with arenes[36] and opens its ring to form BPI[43]. To be consistent with Koenig's calculation[39] (see Section 1.5) that only the succinimidyl radical in its excited state, σ, is capable of opening its ring to form BPI, Skell assigned Sσ to the succinimidyl radical generated in the NBS-DCE system. His criterion of involvement of Sσ in a reaction system is the detection of BPI[43,44]. He reported that photolysis of NBS in the presence of Br_2 (the NBS-Br_2 system)[43,44] produced no BPI and the observed selectivity towards hydrogen abstraction from 2,2-dimethylpropane and dichloromethane was different from either the selectivity of Sσ or that of bromine atoms.[1] Theoretical calculations (see Section 1.5) predict the Sπ does not open its ring, Skell assigned the Sπ to the chain carrier operating in the NBS-Br_2 system[43]. The Sσ-Sπ hypothesis was challenged by some workers including Chow[28], Tanner[31], and Walling[18]. The controversy consists of the discrepancies in both experimental results and in the explanation for the results. The major experimental discrepancies are tabulated in Table 1-1 and their explanations in Table 1-2. The

---

[1]For Skell's π radical recipes see references 44 and 48.

cornerstone of Skell's hypothesis is that only Sσ but not Sπ opens its ring. Three different groups[18,28,31,33,35] found ring-opening products under the π conditions (the NBS-Br_2 system). Tanner[33,35,49] proposed that there should only be two chain carriers involved (Br· and S·), and the Sσ which was generated from the NBS-DCE system should be simply a ground state succinimidyl radical (S·). He assigned the chain carrier in the NBS-Br_2 system to the mixture of S· and bromine atoms.

On the basis of the kinetic measurement, Walling[18] proposed that the succinimidyl radical generated under σ conditions was a ground state one, as its rate constant for ring-opening was determined to be 1660 s^{-1}, too slow for an excited radical (see Section 1.5 for Walling's argument). Considering that bromination of CH_2Cl_2 using NBS-Br_2 went some three times as fast as that using NBS-DCE and almost 100 times as fast as that using Br_2 alone, Walling proposed that the chain carrier operating in NBS-Br_2 system was not the mixture of S· and bromine atoms but a reaction product of NBS and a bromine atom, i.e., a radical complex. The two possibilities suggested are as follows:

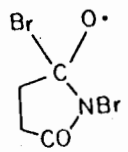

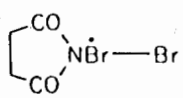

Table 1-1

The Major Experimental Discrepancies among Different Groups

Subject[a]	Skell	Walling	Chow	Tanner
NBS-Br_2 system	No BPI	BPI	Ring Opening	BPI
k_H/k_D (Sσ)	≃1.5	≃10		
k_H/k_D (Sπ)	6	≃10		

a. k_H/k_D, the ratio of rate constants for competitive bromination of CH_2Cl_2 and CD_2Cl_2 with the NBS-Br_2 system.

Independently, Chow and Naguib, on the basis of the extra C_3-Br (5) formation[28] under the π conditions (the 13-Br_2 system), proposed that the intermediate responsible for selectively abstracting hydrogen from the C-3 position to be a bromine radical complex (Eq 1-21).

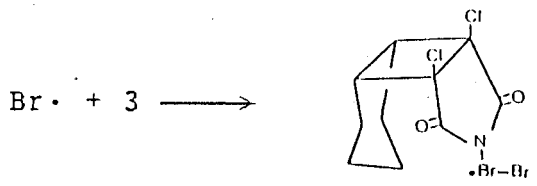

1-21

In a recent joint paper with Tanner, Walling proposed that the chain carrier involved in the NBS-Br_2 system is simply a mixture of S· and Br·[31]. The faster rate of bromination by NBS-Br_2 compared to Br_2 alone was attributed, by Tanner and Walling, to "some deactivation of Br· by complexing with HBr (produced in the bromination) to give unreactive $H\dot{B}r_2$". Considering that the rate constant for bromination of CH_2Cl_2 by bromine atoms is 20 $M^{-1}s^{-1}$ (see reference 31 for the leading references to the older literature), they proposed that the bromination rate constant of 55±8 measured by Walling and co-workers[18] in the NBS-Br_2 system was essentially due to bromine atoms.

In a recent paper Skell withdrew his Sσ-Sπ hypothesis and labeled the succinimidyl radical generated from the NBS-DCE system simply "succinimidyl radical". Its electronic state was left unsettled[25]. Also he realized that the chain carrier(s) in the NBS-Br_2 system was not as simple as previously thought. However, he insisted that the chemistry of the NBS-Br_2 system was not ascribable to a mixture of S· and Br·. Instead he began to accept the proposal that the bromine radical complex acts as the *third* hydrogen-abstracting species and it possesses a unique selectivity. But he did not give its structure explicitly. Nevertheless, he still insisted that the third chain carrier could be a second type of succinimidyl radical[25]. The developments in the controversy are tabulated in Table 1-2.

Table 1-2

Assignments from Different Groups

System	Skell	Walling (before 1985)	Walling (after 1985)	Chow	Tanner
NBS-DCE	S[a]	S·(g)	S·(g)	S·(Σ)	S·(g)
$NBS-Br_2$	S[b] or SBr_2	SBr̈Br	S·+Br·	EQ[c]	S·+Br·

a. The succinimidyl radical, σ or π is not assigned.

b. A second type of succinimidyl radical with its state unsettled.

c. A system in which S·, Br·, and SBr̈Br are in equilibrium.

1.8. Research Proposals

The recent development in the succinimidyl radical chemistry raises some questions:

(1) How many chain carriers are involved in the $NBS-Br_2$ system? What are their identities?

(2) How many reactive intermediates are involved in NBS-DCE system? Skell, Walling, and Tanner believe only one chain carrier, the succinimidyl radical, is involved as the precursor of

BPI.

(3)The following equilibrium has been assumed by various groups[28,31,43] since the begining of the controversy.

$$(CH_2CO)_2N\cdot + Br_2 \rightleftharpoons (CH_2CO)_2N\text{-}Br + Br\cdot \qquad 1\text{-}22$$

Does this equilibrium exist?

(4) What factors affect the ring opening of imidyl radicals and the shifting in the equilibria between the chain carriers?

(5) Bromination of phenols with NBS has been interpreted according to the Goldfinger mechanism that NBS reacts rapidly with HBr to keep a constant, low concentration of Br_2. It has been proposed that the Br_2 attacks phenols[50]. Is that picture correct?

In order to answer those questions, the following studies have been carried out:

(1) the light-initiated and bromine atom-initiated decomposition of the NBS-Br_2 systems at various NBS conversions, with various initial concentrations of Br_2, in the presence of selected hydrocarbons; the selectivity of the NBS-Br_2 system towards hydrogen abstraction from cyclohexane and dichloromethane; the effects of the wavelength of the irradiation, the concentrations of Br_2 and benzene on the yield of BPI and on the quantum yield of BPI formation.

(2) Photolysis of selected N-bromoimides in the presence of

Br_2 or in the presence of an alkene; the effects of the concentrations of Br_2 and alkenes on the product distributions of the photolysis.

(3)kinetics, structure determination, and photochemistry of the products involved in the reaction between NBS and naphthols.

CHAPTER TWO

RESULTS

Section I. Photodecomposition of NBS

2.1.1. Effects of Filters on the Yields of BPI

Since light was used to initiate the decomposition of NBS or Br_2, this work began with the search for suitable light sources to selectively excite NBS or Br_2. For this purpose the absorption spectra of Br_2 and NBS as well as the transmission spectra of a Pyrex filter and a GWV filter were examined, and are shown in Figure 2-1. It should be noted that the absorption of NBS tails to at least 380 nm while Br_2 has an absorption band at about 410 nm. Therefore, when the NBS-Br_2 system is photolyzed with a mercury lamp through a Pyrex filter (cut-off at about 290 nm) both NBS and Br_2 are excited. Unfortunately, all previous experiments reported from Skell's, Tanner's, and Walling's groups were carried out in this way (except a preliminary experiment reported without experimental details by Skell and coworkers[43] in which N-bromoimide-Br_2 systems were irradiated with a >400-nm light source). The effects of Pyrex filter(s) on the yield of BPI were therefore examined first to exclude any misleading artifacts.

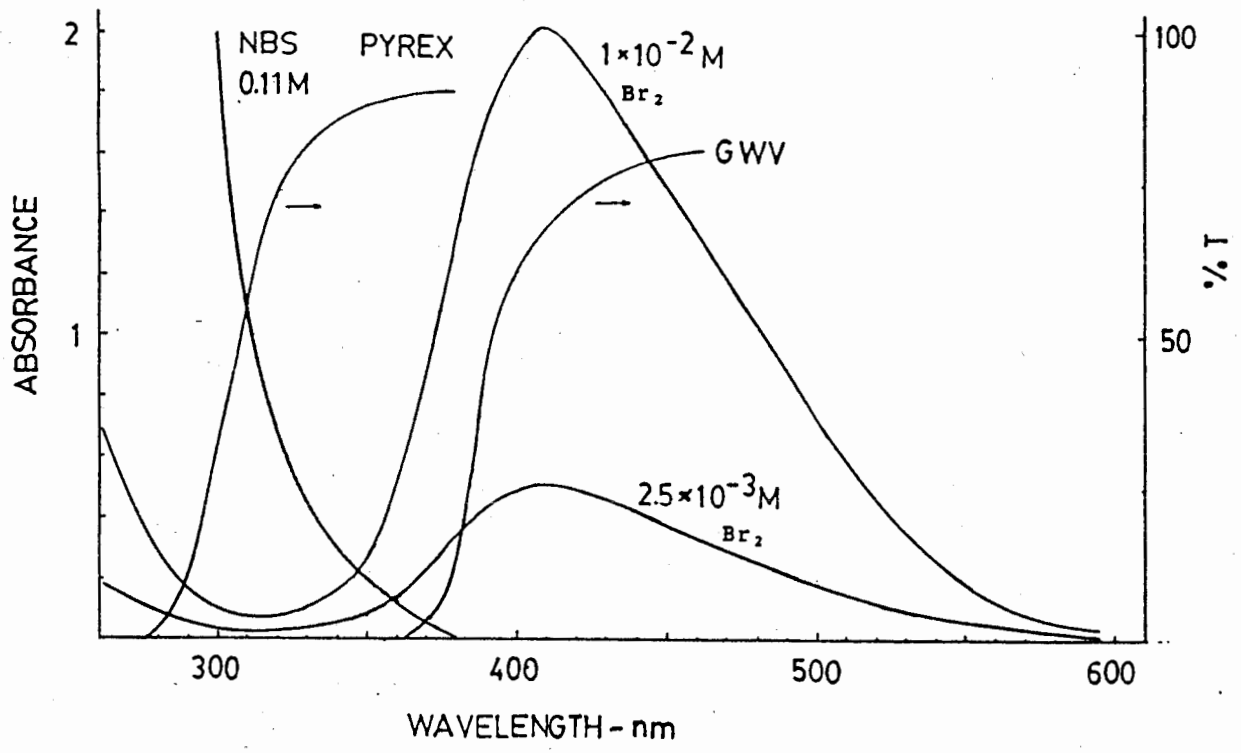

Figure 2-1. UV absorption spectra of NBS and Br_2 and transmission spectra of GWV and Pyrex filters.

When dichloromethane solutions of NBS (0.12 M) containing various amounts of Br_2 were irradiated in NMR tubes with a 200-watt mercury lamp through a GWV filter (cut-off ≥385 nm), only Br_2 was excited under these conditions. 85±5% of the NBS in these solutions was consumed within three hours as shown by ^1H NMR spectroscopy (see Section 4.4.1.2 for details). It was found that the higher the concentration of Br_2 in the solution of NBS the less time needed to consume 85% NBS. Succinimide (SH) was found to be the major product in these photolysates as determined by NMR spectroscopy. In addition, a small amount of BPI was obtained. GC analysis indicated the formation of small amounts of $CHBrCl_2$ (<5 mM), the bromination product of the solvent. The results are listed in Table 2-1 (see experiments 1, 2, and 3). It was found that the yield of BPI was higher in the solution containing lesser amount of Br_2. When the solutions similar to those which were photolyzed through a GWV filter were irradiated with the same lamp through a Pyrex filter (cut-off ≥290 nm, both NBS and Br_2 were excited), 85±5% of the NBS in these solutions disappeared within fifty minutes. More importantly, higher BPI yields were observed as indicated by ^1H NMR spectroscopy (comparing experiments 5, 6, and 7 with 1, 2, and 3 in Table 2-1). The percent yield of BPI (%BPI) in Table 2-1 was calculated based on the amount of NBS consumed in the photolysis. It should be noted that the percent yield of BPI decreased with the increase in the concentration of Br_2 whether a Pyrex or a GWV filter was used. When a dichloromethane solution of NBS in

Table 2-1

Photodecomposition of NBS-Br_2 and the NBS-DCE Systems

Expt.	Solvent	Additive mM	BPI mM	SH mM	*t* min	BPI %
A. Irradiation through a GWV Filter						
1	CH_2Cl_2	Br_2(0.2)	3.1±0.2	100±2	160	3.0±0.2
2	CH_2Cl_2	Br_2(2.0)	2.5±0.2	93.7±2.0	67	2.6±0.2
3	CH_2Cl_2	Br_2(20)	1.1±0.2	90.6±2.0	27	1.2±0.1
4	$CHCl_3$	Br_2(2.0)	<0.5	105±2	80	<1[a]
B. Irradiation through a Pyrex Filter						
5	CH_2Cl_2	Br_2(0.2)	14.1±0.6	90.3±2.2	46	13.5±1.0
6	CH_2Cl_2	Br_2(2.0)	8.0±0.4	95.9±2.0	37	7.7±0.4
7	CH_2Cl_2	Br_2(20)	3.1±0.5	96.9±2.0	20	3.1±0.2
8	CH_2Cl_2	DCE(55)	82.5±4.4	26.4	85	76±4
9	$CHCl_3$	DCE(55)	70.4±3.3	39.6±1.1	90	64±3[a]

a. The heterogeneous solution became homogeneous as the reaction proceeded.

the presence of DCE (a scavenger for Br· and/or Br_2 to suppress the bromine atom chain) was photodecomposed with a mercury lamp through a Pyrex filter, a still higher yield of BPI was obtained (see experiment 8 in Table 2-1). It was found that BPI was obtained by photolysing a $CHCl_3$ solution of NBS in the presence of and absence of Br_2 (see experiments 4 and 9, Table 2-1). These results are contrary to those reported previously[4,44] that photodecomposition of NBS in $CHCl_3$ produces no BPI. In Figure 2-2, the percent yield of BPI from Table 2-1 were plotted against the fraction of incident light absorbed by NBS at various concentrations of Br_2. The plot showed disproportionally higher yields of BPI by direct excitation of NBS (experiments 5-7) compared to those obtained by bromine atom-initiated reactions (experiments 1-3, Table 2-1). These two groups of experiments are identical except for the replacement of the GWV filter by Pyrex. Since the use of a Pyrex filter produces higher yields of BPI than does the use of a GWV filter, all the bromine atom-initiated decompositions of NBS in the NBS-Br_2 system reported in this work were carried out with a >380-nm light source[1] or a ≥400-nm light source.[2] It can be seen that the absorption minimum of Br_2 in 300-330 nm region coincides with the residual absorption of NBS from 300 to 360 nm. Since NBS rather than Br_2 absorbed most of

---

[1]Light from a mercury lamp was filtered through a piece of GWV glass (cut-off at 385 nm).

[2]Light from a mercury lamp was filtered through a aqueous solution of sodium nitrite-sodium hydrogen phthalate (cut-off ≥400 nm)[54].

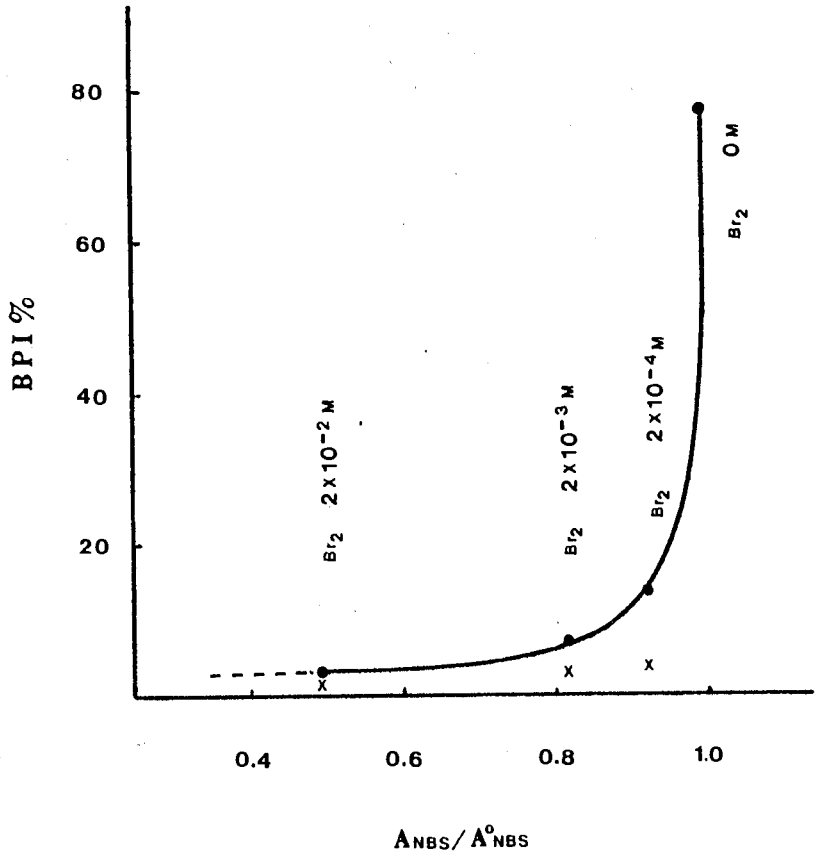

Figure 2-2. Plot of the percent yield of BPI (from photolysis of NBS through a Pyrex filter, see Table 2-1B) vs. the fraction of incident light absorbed by NBS at various concentrations of Br_2 (10^{-4}-10^{-2}M). The corresponding percent yield of BPI (from photolysis of NBS through a GWV filter, see Table 2-1A) are marked by x. A^{o}_{NBS} is the number of light quanta absorbed by NBS in the absence of Br_2, and A_{NBS} is the number of light quanta absorbed by NBS in the presence of Br_2.

the incident light at 300 nm, a 300-nm light source (RPR 3000 Å lamps) was used in this work to irradiate NBS-Br_2 systems when selective excitation of NBS was needed. This technique ensured a predominant but not an exclusive excitation of NBS.

2.1.2. Preparation of BPI

Since the formation and detection of BPI were critical issues in the recent controversy (see Section 1.7, Chapter 1) a suitable method for BPI analysis was needed. For this purpose authentic BPI was synthesized. Photolysis of a dichloromethane solution of NBS (0.2 M) in the presence of 1,1-dichloroethene (DCE) was carried out by irradiating the solution with a 200-watt mercury lamp with a Pyrex filter. BPI was isolated as a yellow oil by vacuum distillation (0.5 mm, 22°C) from product mixtures: IR (CH_2Cl_2) 2245 (s), 1730 (s), 1400 (s), and 1070 cm^{-1}; the solvent (CH_2Cl_2) was distilled over P_2O_5 under nitrogen and the solution of BPI for IR analysis was prepared in a dry box to minimize the introduction of moisture into the solution. The data agree well with those reported elsewhere (see experimental of reference 4). It should be noted that the absorption peak at 2245 cm^{-1} is characteristic of isocyanate group, and has been used as evidence for the formation of BPI in the reaction product mixtures from the photodecomposition of NBS[18].

2.1.3. Investigation of Suitable Methods for BPI analysis

A drop of BPI (5 mg, 0.003 mmol) was added to dichloromethane (1.0 ml) with a pipette in a fumehood and the solution of BPI ($3x10^{-3}M$) was then transferred to a IR cell by pipette. The change in IR absorption of the BPI solution was followed by consecutive scans of the spectrum over the range 2500-2000 cm^{-1}. These scans showed that the absorption of BPI at 2245 cm^{-1} decreased as the absorption of carbon dioxide[51] at 2349 cm^{-1} increased continuously (Figure 2-3), the latter resulting from the hydrolysis of BPI (Eq 1-12). In a sealed cell, the sum of integrals of these two bands increased slightly as CO_2 formed (Table 2-2). The hydrolysis was over in less than ten minutes. BPI is therefore unstable to traces of water present in solvent and introduced during the pipetting of dichloromethane and the preparation of the BPI solution. Since detection of BPI in the reaction system is regarded by Skell[48] as a criterion of $S\sigma$, and since any interpretation of product distributions in terms of competing chains by Tanner and Walling[31] are based critically upon yield determination, an accurate and sensitive method for determining the yield of BPI was necessary. After a dichloromethane solution of NBS was photolyzed the photolysate was transferred by pipette to a flask and the solvent was removed under reduced pressure. The residue was mixed with a precise amount of 3,3-dimethylglutarimide as an internal standard, and the mixture was dissolved in $CDCl_3$. BPI was usually completely destroyed

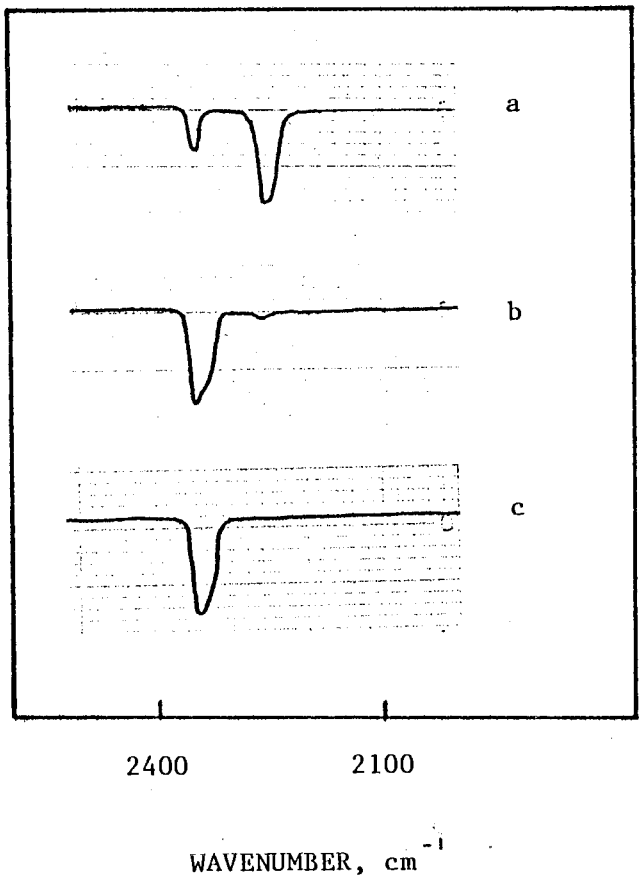

Figure 2-3. IR absorption spectra of dichloromethane solution of BPI (a) 3 min, (b) 5 min, and (c) 8 min after the preparation of the solution (The initial BPI concentration = 3×10^{-3} M).

Table 2-2 Integrals of IR Bands Shown in Figure 2-1

Spect. No.	2349 cm^{-1}	2245 cm^{-1}	Tatal
a	6	24	30
b	30	≃1	≃31
c	33	0	33

during these manipulations, to form β-bromopropionamide (BPA) and CO_2. Nevertheless, a drop of water was added to the photolysate to ensure complete hydrolysis (a control experiment showed that the difference in BPA yields between two samples with and without adding water was only ≃2%, being within experimental error (≃5%)). After the $CDCl_3$ solution was prepared, it was used for ^1H NMR analysis (at 400 MHz) to determine the yield of BPA. An NMR spectrum from a typical experiment is shown in Figure 2-4. The signals of four methylene protons of BPA (triplets at 3.63 and 2.83 ppm) are well separated from those of NBS (singlet at 2.96 ppm) and succinimide (singlet at 2.77 ppm). With 16 to 32 scans, a BPI yield as low as 1%, based on NBS used (0.11-0.12 mmol), can be detected without ambiguity. When the yield is high, GC analysis is also suitable for determining the yield of BPI. In this case, BPI was converted to BPA when the photolysate was washed with aqueous sodium bisulfite solution for the purpose of destroying remained NBS and/or Br_2. The disagreement between NMR and GC analysis is less than 5% when the yield of BPI is higher than 20%. Due to the hydrolysis of BPI and the escape of carbon dioxide from solutions during sample transfer to the IR cells, IR analysis always underestimates the yield and also fails to detect small amounts (<5%) of BPI. Therefore, all the yields of BPA reported in this work were determined by ^1H NMR spectroscopy, and occasionally by GC analysis. The yields of BPA determined in this way are reported as the yields of BPI in the Tables.

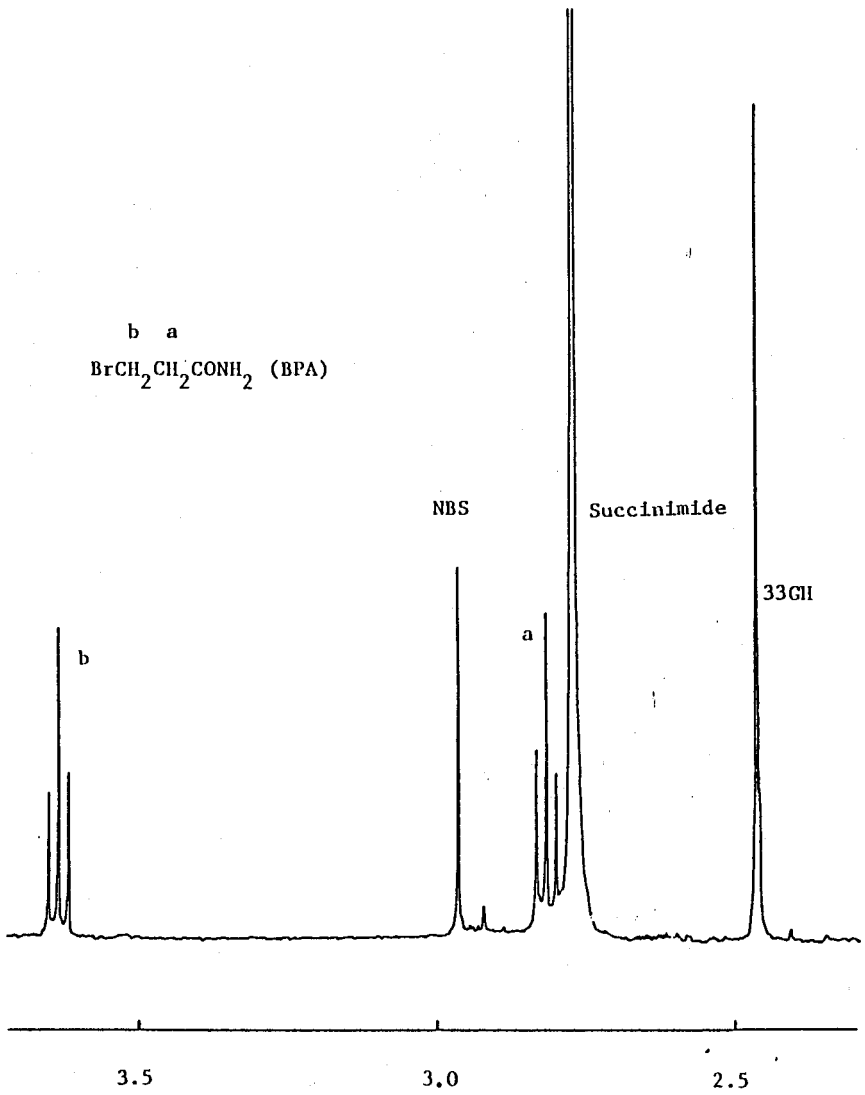

Figure 2-4. 400-MHz ^{1}H NMR spectrum (from $CDCl_3$ solution) of the reaction product mixture (nonvolatile) from the photobromination of cyclohexane (0.046 M) and dichloromethane (15.5 M) with NBS (0.112 M) and Br_2 (0.02 M) as the bromination reagent (a >380-nm light source was used). The singlet at 2.45 ppm is due to the four methylene protons of 3,3-dimethylglutarimide (33GH).

2.1.4. Effects of Hydrocarbons on the Yields of BPI

2,2-Dimethylpropane was added to the NBS-Br_2-CH_2Cl_2(solvent) system by Skell's, Walling's, and Tanner's groups to investigate the selectivities of the chain carriers in the system. The product ratio of BPI/$CHBrCl_2$ was used by Skell's and Walling's groups[4,18] as a reactivity index to identify the chain carriers. Since the index is a function of the yield of BPI, it is necessary to determine whether the yield of BPI is affected by concentrations of the added hydrocarbon. For this purpose, cyclohexane or 2,2,3,3-tetramethylbutane (C_8H_{18}) was added to dichloromethane solutions of NBS and Br_2 (the NBS-Br_2 system) similar to those used in experiments 1, 2 and 3 (Table 2-1). Photolysis of the solutions with a >380-nm light source afforded BPI and succinimide in addition to bromination products such as bromodichloromethane, bromocyclohexane. The yields of BPI are listed in Tables 2-3 and 2-4 to show that the addition of C_8H_{18} or cyclohexane (C_6H_{12}) caused dramatic increases in the yields of BPI (Tables 2-3 and 2-4). Both cyclohexane and C_8H_{18} promoted higher yields of BPI, the former did this with higher efficiency. The higher the concentration of Br_2, however, the lower the percent yield of BPI. This trend was similar in both CH_2Cl_2 and $CHCl_3$ solutions. It is noteworthy that, even in the presence of these hydrocarbons, >200 mM Br_2 could reduce the yield of BPI to

<2%. These relations are shown more clearly in Figure 2-5, where the percent yields of BPI determined under comparable conditions and in the presence of a wide range of $[Br_2]$ and $[C_6H_{12}]$ are summarized. In Figure 2-6, the percent yields of BPI from the NBS-Br_2-cyclohexane(0.092 M) system (Experiments 16-19, Table 2-4A) are plotted against $[Br_2]$ as part of group A. It is important to point out that a >380-nm light source was used to obtain the data represented by group A. For comparison, the same system (NBS-Br_2-cyclohexane) was photolyzed with a 300-nm light source to selectively excite NBS (Experiments 20-23), and the percent yields of BPI obtained are plotted as part of group B (Figure 2-6). Photolysis of similar solutions in the presence of >100 mM Br_2 with the 300-nm light source was not attempted since the absorbance of Br_2 at 300 nm would be as much as that of 112 mM NBS. Figure 2-4 and 2-6 demonstrate that higher BPI yields are always obtained in the NBS-Br_2 system when NBS is photodecomposed than when the Br_2 in the same system is irradiated.

2.1.5. Photobromination of Mixtures of Cyclohexane and Dichloromethane

As mentioned in Chapter 1, if a radical abstracts hydrogen from substrates AH and BH with rate constants k(AH) and k(BH) respectively, the ratio of k(AH)/k(BH) is called (relative) selectivity of the radical towards AH and BH, and its value can be

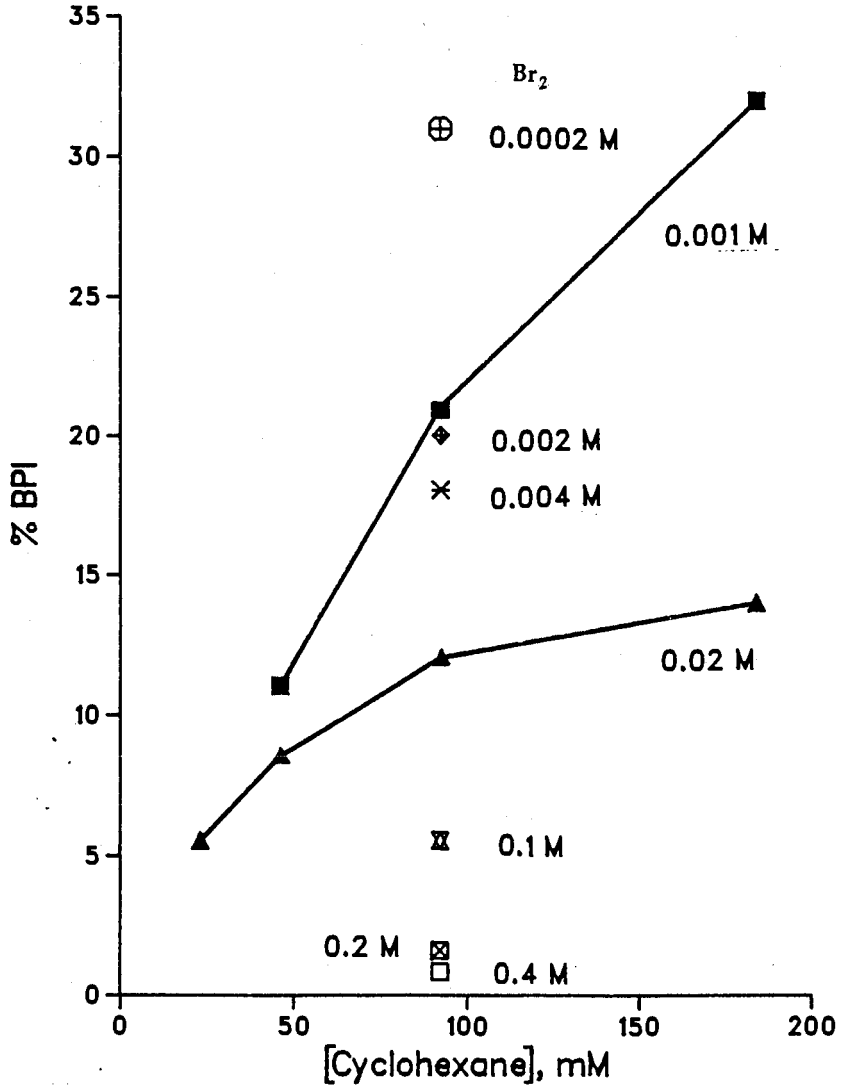

Figure 2-5. Plot of the percent yield of BPI vs. the concentration of cyclohexane. The BPI was obtained from the photobromination of cyclohexane-dichloromethane with the NBS-Br_2 system (A GWV filter was used).

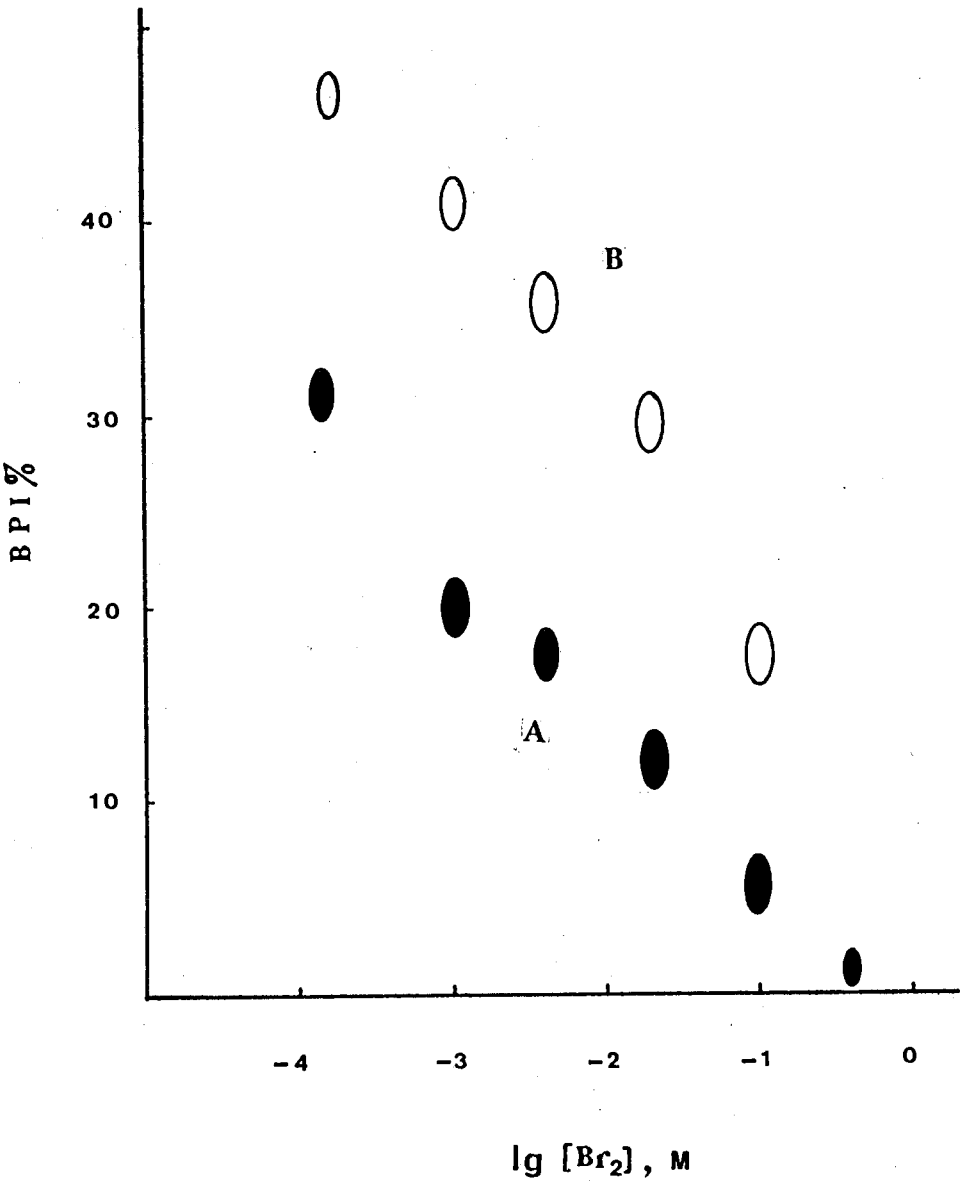

Figure 2-6. Plot of the percent yield of BPI vs. the initial concentration of Br_2 under >380-nm (solid ellipses, group A) and 300-nm irradiations (hollow ellipses, group B). Each ellipse represents two to five experiments and the spreads of the experimental data are shown by the sizes of the ellipses.

Table 2-3

BPI Yields from the NBS(0.112 M)-Br_2-C_8H_{18}(0.065 M) System

Expt.	Br_2, mM	BPI, mM	BPI, %[a]
A. In CH_2Cl_2 Solutions			
10	0.20	11.3±1.2	11±1(3)[b]
11	2.0	8.1±0.9	7.7±0.8(3)[b]
12	20	2.1±0.7	2.0±0.6(3)[b]
B. In $CHCl_3$ Solutions[c]			
13	0.20	11.0±0.3	11±1(3)[b]
14	2.0	8.6±1.8	8.2±1.6(3)[b]
15	20	2.0±1.0	1.9±0.8(2)[b]

a. Samples were irradiated with a 200-watt mercury lamp through a GWV filter and the percent yield of BPI was calculated based on the amount of NBS used.

b. Number of experiments.

c. Heterogeneous solutions before the irradiation became homogeneous as the reaction proceeded.

Table 2-4

BPI Yields from the NBS(0.112 M)-Br_2-C_6H_{12}(0.092 M) System[a]

Expt.	Br_2, mM	BPI, mM	BPI, %
A. In CH_2Cl_2 Solutions			
16	0.20	24.3±2.1	23±2
17	2.0	21.0±2.1	20±2
18	20	10.5±1.1	10±1
19	200	1.7±0.5	1.6±0.4
20	0.25	43.1±2.0	45±2
21	4.0	36.9±1.3	36±1
22	20	30.7±1.4	30±1
23	100	25.9±1.6	25±1
B. In $CHCl_3$ Solutions[b]			
24	0.20	16.5±1.1	16±1
25	20	8.5±1.2	8.0±1.0

a. Samples were irradiated through a GWV filter (experiments 16-19, 24-25) or irradiated with a 300-nm light source (experiments 20-23). The percent yields of BPI were calculated based on the amounts of NBS used.

b. Heterogeneous solutions became homogeneous as the photolysis proceeded.

calculated from the ratio of the products of the competitive hydrogen abstractions.[14] In order to identify the chain carriers involved in the NBS-Br_2 system, mixtures of cyclohexane and dichloromethane were photobrominated with the NBS-DCE, Br_2-K_2CO_3, and NBS-Br_2 systems as brominating reagents. The bromination products, bromocyclohexane ($C_6H_{11}Br$) and $CHBrCl_2$, were analyzed by GC, and the selectivities of these systems for hydrogen abstraction from cyclohexane and dichloromethane were calculated by the use of equation 2-1b (see reference 14 for the derivation of the Eq. 2-1), where $C_6H_{10}Br_2$ is 1,2-dibromocyclohexane. This dibromo compound was obtained from the bromination of dichloromethane-cyclohexane with the Br_2-K_2CO_3 or with NBS-Br_2 system as the brominating reagent. It was not detected when the photobromination was carried out in the NBS-DCE system.

$$r = \frac{k(C_6H_{12})}{k(CH_2Cl_2)}$$

$$= \frac{\ln\{([C_6H_{12}]-[C_6H_{11}Br]-[C_6H_{10}Br_2])/[C_6H_{12}]\}}{6\ln\{([CH_2Cl_2]-[CHBrCl_2])/[CH_2Cl_2]\}} \qquad 2\text{-}1a$$

$$\text{or } r = \frac{\ln\{([C_6H_{12}]-[C_6H_{11}Br]-[C_6H_{10}Br_2])/[C_6H_{12}]\}}{-6[CHBrCl_2]/[CH_2Cl_2]} \qquad 2\text{-}1b$$

The integrated equation 2-1a[14] is approximated to equation 2-1b by the expansion denominator (note: $\ln\{(a-x)/a\} \simeq -x/a$ when x is

small compared to a). The expansion introduces little error (<1%) to the *r* value. It has been accepted by various groups[18,25,31] that the succinimidyl radical is the chain carrier in the hydrogen abstraction step if the NBS-DCE is used as a bromination reagent. The selectivity of NBS-DCE system towards hydrogen abstraction from cyclohexane and dichloromethane was studied first. The dicholoromethane-cyclohexane solutions of NBS and DCE in NMR tubes were photolyzed with a mercury lamp through a Pyrex filter. The conversion of NBS was monitored by NMR spectroscopy at intervals to ensure the photolysis was stopped before all NBS had been consumed. GC analysis showed BPI was obtained in high yield (see Table 2-5). The bromination products were $CHBrCl_2$ and bromocyclohexane. The selectivity was calculated to be ≃190 by the use of Eq. 2-1b. It was found that the *r* values scattered from 170 to 210 in a random fashion (Table 2-5). In the low concentration range of cyclohexane (experiments 25 and 26), the yields of $CHBrCl_2$ and bromocyclohexane were low and much smaller than those of succinimide, even after correction for unreacted NBS. While the error margins of these data must be fairly high, the *r* values are included in Table 2-5 since they do not deviate significantly from those obtained in experiments 27-29. The poor material balance of brominated products was also reported by other groups[18,31].

The selectivity of bromine atoms toward hydrogen abstraction from cyclohexane-dichloromethane was studied next using Br_2 as

Table 2-5

Photobromination of C_6H_{12} and CH_2Cl_2 with the NBS-DCE System[a]

Expt.	C_6H_{12} mM	$CHBrCl_2$ mM	$C_6H_{11}Br$ mM	SH[b] mM	BPI %[c]	t min	r
25	9.20	2.44±0.3	1.61±0.02	36.0±0.2	69±3	90	200
26	27.6	2.12±0.12	3.68±0.09	36.6±0.8	67±3	80	170
27	46.0	2.09±0.06	7.10±0.09	42.4±0.7	66±4	73	210
28	92.0	1.87±0.02	11.0±0.02	45.0±2.0	61±3	60	180
29	276	1.14±0.03	21.8±0.5	53.0±0.7	56±2	47	190
30[c]	4.6(M)	trace	26.1±0.5	49.0±1.1	8.6±0.9[d]	135	

a. Solutions of NBS (0.112 M), DCE (0.060 M) and cyclohexane in dichloromethane (15.5 M) were used except Expt. 30 in which solutions of NBS (0.055 M), DCE (0.028 M), and CH_2Cl_2 in C_6H_{12} (7.75 M) were photolyzed.

b. The yields of succinimide were calculated by the use of [SH]=[NBS]-[BPI] where [NBS] is the initial concentration of NBS (0.112 M).

c. Based on NBS used.

d. This BPI yield was determined by NMR analysis while the rest by GC analysis.

the bromination reagent. Anhydrous K_2CO_3 was added into the cyclohexane-dichloromethane solutions of Br_2 to remove hydrogen bromide[34] which is a by-product of the photobromination. The mixture was stirred vigorously and irradiated with a >380-nm light source. GC analysis of the product mixtures afforded $CHBrCl_2$, bromocyclohexane, and 1,2-dibromocyclohexane. The r values were calculated to be 15-18 (Table 2-6) by the use of Eq. 2-1b, and the results are listed in Table 2-6. It was found that the r values were affected little by changes in concentration of cyclohexane (experiments 36 and 37, Table 2-6). The facile formation of the vicinal dibromocyclohexane at low concentrations of bromocyclohexane with respect to cyclohexane is undoubtedly a result of substantial neighboring group participation from the β-bromo substituent of $C_6H_{11}Br$ in the hydrogen abstraction process by a bromine atom; this has been thoroughly discussed by Skell and Traynham[55].

The selectivity of the NBS-Br_2 system towards hydrogen abstraction from cyclohexane and from dichloromethane was also studied. A cyclohexane-dichloromethane solution of NBS and Br_2 was irradiated with either a >380-nm or ≥400-nm light source. From initial experiments, it was possible to judge the time course of NBS consumption, and subsequently irradiations were stopped at about 85% NBS conversion. The actual extent of the NBS conversion was determined by ^1H NMR spectroscopy, and the concentrations of Br_2 in the photolysates were determined by UV

spectroscopy. The r values were calculated from the yields of $CHBrCl_2$, bromocyclohexane, and 1,2-dibromocyclohexane by the use of Eq. 2-1b, and they are listed in Table 2-7A. It was found that i), the observed $[Br_2]$ increased from its initial value when the latter was <30 mM, ii), the increment in $[Br_2]$ became greater as the NBS conversion increased, and iii), the percent yield of BPI decreased as the conversion of NBS increased. While the percent yield of BPI decreased as the concentration of Br_2 increased (Table 2-7A), the r value did not shift significantly. The r value varied randomly in the range of 17-22, being essentially the selectivity of bromine atoms (see Table 2-6 for the bromine atom selectivity). These experiments were repeated in order to verify these remarkable effects of NBS conversion on the observed $[Br_2]$ and the lack of dependence of the r value on the NBS conversion. One set of experiments is tabulated in Table 2-7. It shows that the increment of $[Br_2]$ relative to the initial $[Br_2]$ was significant when the initial $[Br_2] < 1$ mM. But the observed $[Br_2]$ did not increase from its initial value when the latter was higher than 80 mM (see Table 2-7).

Since the Br_2 in the NBS-Br_2 system absorbs most of the light from the λ>380-nm light source, the results listed in Table 2-7A are from bromine atom-initiated NBS decompositions. When solutions similar to those above (experiments 38-40 and 44-46, see Table 2-7A) were irradiated with a 300-nm light source, much higher BPI yields were obtained. These result are

Table 2-6

Photobromination of C_6H_{12} and CH_2Cl_2 with the Br_2-K_2CO_3 System[a]

Expt.	Br_2 mM	$CHBrCl_2$ mM	$C_6H_{11}Br$ mM	$C_6H_{10}Br_2$ mM	r
31	6.6	3.5±0.2	1.8±0.1	0.13±0.05	16
32	30	5.0±0.4	2.2±0.2	0.64±0.02	16
33	27	16.0±1.4	6.0±0.1	2.08±0.02	15
34	70[b]	17.5±0.1	8.0±0.1	2.35±0.20	18
35	70	30.2±0.8	11.8±0.4	4.68±0.12	17
36	20[c]	6.77±0.09	1.05±0.06	<0.1	18
37	20[d]	2.67±0.11	7.16±0.03	2.1±0.1	20

a. General conditions: Vigorously stirred heterogeneous mixtures consist of CH_2Cl_2 (4.00 ml, 62.0 mmol), cyclohexane (C_6H_{12}, 0.368 mmol, 92.0 mM), Br_2, and K_2CO_3 (molar ratio of the last two compounds = 1:5) in UV cuvettes were irradiated with a mercury lamp through a GWV filter at 15-18°C for 10-30 minutes. Each reaction was duplicated.

b. The light source was a PEK 212 lamp (150 watts) filtered through a Corning filter CS-052 (cut-off ≥300 nm) and a $NaNO_2$-sodium hydrogen phthalate solution (cut-off ≥400 nm).

c. $[C_6H_{12}]$ = 23.0 mM.

d. $[C_6H_{12}]$ = 370 mM.

Table 2-7

Results of Photobromination of Cyclohexane and CH_2Cl_2 with the NBS-Br_2 System[a]

Expt.	Br_2, mM[b]		% NBS	Prdct[c]					BPI	r
	init	obsd	convsn	$CHBrCl_2$	$C_6H_{11}Br$	$C_6H_{10}Br_2$	SH[d]	BPI	%[e]	
				A. Irradiation of Br_2[f]						
38	0.75	2.07	39	14.7±0.9	6.88±0.26	2.35±0.06	32.9	9.60±0.01	22.6	19
39	0.75	2.35	53	17.9±1.0	6.99±0.21	3.56±0.04	46.0	12.0±0.6	20.7	18
40	0.75	3.04	73	24.5±0.5	8.27±0.13	5.77±0.35	67.1	12.7±0.4	15.9	18
41	1.03	1.77	27	10.2±1.8	4.63±0.16	1.44±0.25	23.5	5.76±0.04	19.7	17
42	1.03	2.31	45	17.2±1.1	6.21±0.19	3.46±0.15	39.7	9.85±0.08	19.9	17
43	1.03	3.42	77	27.2±1.2	8.34±0.19	7.32±0.09	70.4	14.2±0.05	16.8	18
44	21.7	22.5	28	14.6±0.1	5.70±0.57	2.68±0.12	26.1	4.25±0.01	14.0	17
45	21.7	23.9	56	23.7±0.2	7.55±0.25	5.63±0.11	54.1	7.03±0.01	11.5	17
46	21.7	24.5	65	27.7±1.0	7.23±0.75	8.24±0.20	64.2	7.29±0.11	10.2	17
47	86.2	85.0	44	18.5±1.4	9.24±0.17	4.19±0.08	44.6	3.21±0.11	6.6	22
48	86.2	84.9	61	26.3±1.8	9.74±0.40	8.65±0.35	63.3	4.31±0.20	6.4	22
49	173	172	26	12.8±1.5	6.28±0.19	2.50±0.08	27.1	1.7±0.2	6.0	20
50	173	173	67	35.0±0.4	10.2±0.3	10.3±0.3	73.0	2.3±0.2	3.1	19
51	200		21	12.4±0.7	5.70±0.24	2.11±0.08	21.9	1.33±0.33	5.7	19
				B. Irradiation of NBS[g]						
52	0.83	1.85	30.6	8.55±0.63	5.10±0.12	1.06±0.03	18.0	15.7±0.5	46.5	20
53	0.83	2.19	47.4	12.2±0.2	6.35±0.13	2.03±0.04	30.0	22.2±0.05	42.5	19
54	0.83	2.58	68.1	17.6±0.3	7.27±0.13	3.37±0.07	42.7	32.2±1.1	43.0	17
55	21.8	25.3	25.5	8.86±0.22	5.04±0.25	1.23±0.06	17.9	10.1±0.5	36.1	20
56	21.8	26.7	55	19.8±0.3	8.83±0.09	4.15±0.05	40.3	20.2±0.8	33.4	18
57	21.8	26.8	74	24.1±2.8	7.53±1.13	5.27±0.29	56.9	24.5±1.0	30.1	15

Footnotes of Table 2-7

a. Solutions of NBS (0.112 M), cyclohexane (0.092 M), and Br_2 in dichloromethane (1.0 ml) were used.

b. The concentration of Br_2 was determined by UV-vis spectroscopy.

c. In mM. The yields (concentrations) of brominated products were analysed with GC, and the yield (concentration) of BPI was determined as BPA by NMR spectroscopy.

d. Calculated by the using of [SH]=[NBS]-[BPI] where [NBS] was the amount of NBS (in mM) converted in the photolysis.

e. Based on the amount of NBS converted in the photolysis.

f. The samples were irradiated with a ≥380-nm light source (a 200-W mercury lamp with a GWV filter) except experiments 38-40 in which a ≥400-nm light source (the mercury lamp with a aqueous filter solution of $NaNO_2$-sodium hydrogen phthalate) was used.

g. The samples were irradiated with a 300-nm light source.

listed in Table 2-7B. Even though the yields of BPI were high when the NBS-Br_2 system was irradiated at ≃300 nm, they were still lower than the BPI yields obtained from photolysis of the NBS-DCE system (see Table 2-5). It is worthwhile to keep in mind that NBS absorbed most of the incident light when a 300-nm light source was used. This was so particularly for the high NBS concentration range, i.e. the conversion of NBS was low. Since the absorbance of Br_2 at ≃300 nm increased with the increase in [Br_2] (see Figure 2-1), solutions containing >20 mM Br_2 were not used to collect data to fill Table 2-7B, as Br_2 would absorb a significant amount of the incident light at such concentration.

2.1.6. Relative Rates of Bromination of Cyclohexane and Dichloromethane with Br_2-K_2CO_3 vs. NBS-Br_2 System

Brominations of cyclohexane-dichloromethane in the Br_2-K_2CO_3 and Br_2-NBS systems were carried out by selectively irradiating Br_2 with >380-nm light souces. Experiments 58 and 59 were identical, and so were 60 and 61, except for the replacement of K_2CO_3 by NBS. That is, each of the samples were irradiated with the same light source for the same period of time. The yields of bromination products were determined by GC. Yields and the r values calculated from them using Eq. 2-1b are listed in Table 2-8. Two uncertainty factors were involved when the Br_2-K_2CO_3 system was irradiated: (1) light quanta might be reflected by the heterogeneous mixtures, and (2) the concentration of Br_2

Table 2-8

Photobromination of C_6H_{12} (0.0920 M) and CH_2Cl_2 (15.5 M) with Br_2-K_2CO_3 and NBS-Br_2 Systems[a]

Expt.	Additive	$CHBrCl_2$ mM	$C_6H_{11}Br$ mM	$C_6H_{10}Br_2$ mM	ΣRBr[d]	r
58	K_2CO_3[b]	11.4±2.2	5.95±1.43	0.86±0.13	19.09	17
59	NBS[b]	18.4±4.4	9.55±1.74	3.06±0.25	34.07	21
60	K_2CO_3[c]	13.8±0.3	6.19±0.28	1.09±0.05	21.45	15
61	NBS[c]	18.4±0.1	9.66±0.70	2.98±0.04	34.02	21

a. See Section 4.4.1.4 for details.

b. These two samples were irradiated for 10 minutes through a GWV filter. The conversion of NBS was 28%, and the BPI yield was 0.0120 mmol (9.7% based on the NBS consumed).

c. These two samples were irradiated for 14 minutes through the filter solution (cut-off ≥400 nm). The conversion of NBS was 26%, and the BPI yield was 0.0116 mmol (10% based on the NBS consumed).

d. The combined yield of $C_6H_{11}Br$ and twice yield of $C_6H_{10}Br_2$.

decreased as the photobromination progressed. These two uncertainties, in particular the second one, were alleviated by using a high concentration of Br_2 which absorbed almost all the incident light with near constancy throughout the irradiation. Taking the rate of bromination in the Br_2-K_2CO_3 system as unity, the rate in the Br_2-NBS system was higher by 60-80% , and this observation was reproducible. The r values from these experiments were in good agreement with those presented in Tables 2-6 and 2-7).

2.1.7. Effects of Concentration of Benzene on the Yield of BPI

Several CH_2Cl_2 solutions of NBS containing various amounts of benzene were placed in a merry-go-round then irradiated with a 300-nm light source (for any given series two samples containing no benzene and one sample for each benzene concentration were used). Small amounts of DCE were present in these solutions to suppress the bromine radical chain. The irradiation was always stopped before $\simeq$ 20% NBS had been consumed. BPI, N-phenylsuccinimide (PhS), 3,4,5-tribromo-6-succinimidylcyclohexene (**2**), and succinimide (SH) were produced. Their yields were determined by 400 MHz ^{1}H NMR spectroscopy with 3,3-dimethylglutarimide (33GH) as an internal standard, and these are listed in Table 2-9. It can be seen that the BPI yield decreases when benzene concentration is increased from zero to about 1 M, but decreases

Table 2-9

Photodecomposition of NBS in the Presence of Benzene[a]

[B] M	10^3Prdct BPI[b]	PhS[c]	2[c]	$\Phi^0/\Phi e$	Φ/Φ_n[f]
Series I (*hν* for 6.0 min., sign by ■)					
0.00	10.6±0.2[d]	0	0	1.00	
0.031	7.29±0.73	0.73±0.07	0.48±0.05	1.45±0.21	6.02
0.061	5.54±0.55	0.64±0.06	0.49±0.05	1.91±0.28	4.90
0.15	3.42±0.34	0.72±0.07	0.62±0.06	3.10±0.45	2.55
Series II (*hν* for 8.0 min., sign by ¤)					
0.00	22.7±0.9[d]	0	0	1.00	
0.10	8.67±0.87	1.38±0.14	0.55±0.06	2.62±0.38	4.49
0.40	4.66±0.47	1.76±0.18	0.69±0.07	4.87±0.71	1.90
0.80	4.07±0.41	2.12±0.21	0.65±0.07	5.58±0.81	1.47
1.0	3.82±0.38	2.94±0.29	0.54±0.05	5.94±0.86	1.10
Series III (*hν* for 7.6 min., sign by Δ)					
0.00	20.0±0.9[d]	0	0	1.00	
0.10	8.05±0.81	1.38±0.14	0.52±0.05	2.48±0.36	4.24
0.20	6.38±0.64	1.83±0.18	0.58±0.06	3.13±0.45	2.65
0.4	4.41±0.41	1.90±0.19	0.57±0.06	4.54±0.66	1.79
0.60	4.04±0.41	2.17±0.22	0.60±0.06	4.95±0.72	1.46
0.80	3.64±0.36	2.17±0.22	0.70±0.07	5.49±0.80	1.31
1.0	3.43±0.34	2.27±0.23	0.71±0.07	5.83±0.85	1.15

Series IV (*hν* for 8.0 min., sign by •)					
0.00	20.5±0.8[d]	0	0	1.00	
1.5	3.22±0.32	2.11±0.21	0.59±0.06	6.37±0.92	1.19
2.0	3.37±0.34	2.45±0.25	0.65±0.07	6.08±0.88	1.09
2.5	2.83±0.28	2.64±0.26	0.72±0.07	7.24±1.05	0.84
3.1	3.25±0.33	2.21±0.22	0.60±0.06	6.31±0.91	1.16
5.1	2.56±0.26	2.80±0.28	0.51±0.05	8.00±1.16	0.77
Series V (*hν* for 7.0 min., sign by o)					
0.00	17.0±0.9[d]	0	0	1.00	
1.5	2.69±0.27	1.97±0.20	0.63±0.06	6.32±0.92	0.996
2.0	3.13±0.31	2.01±0.20	0.64±0.06	5.43±0.79	1.18
2.5	3.21±0.32	2.30±0.23	0.54±0.05	5.30±0.77	1.13
3.1	3.12±0.31	2.18±0.22	0.62±0.06	5.45±0.79	1.11
4.1	2.91±0.29	2.22±0.22	0.63±0.06	5.84±0.85	1.02
5.1	2.17±0.22	2.26±0.23	0.59±0.06	7.83±1.13	0.76

a. Solutions of NBS (20.0 mg, 0.112 mmol, 0.056 M), DCE (0.074 mmol, 0.037 M), and benzene in CH_2Cl_2 (2.00 ml) in Pyrex tubes were used as samples. See Section 4.4.1.3 for details of photolysis and analysis.

b. In mmol. A 10% uncertainty was generously assumed in determining the consequent error accumulation.

c. In mmol. The sum of these two figures is ϕ_n, i.e., $\Phi_n I t$. Each is assumed to possess a 10% uncertainty.

d. The error range is expressed as the average deviation from the mean based on two runs. Its percent uncertainty (≤5%) was not used to calculate the error accumulated in Φ^o/Φ.

e. Errors calculated from square root of the sum of the squares of the percent uncertainty in Y^o(BPI) and Y(BPI).

f. Errors are not listed because of the limited space.

further sluggishly with further increase in benzene concentrations.

since the quantity of BPI generated by the photolysis is equivalent to $\Phi I t$, the product of the quantum yield of BPI formation, the intensity of, and the duration of irradiation (Eq. 2-2), and since samples in each series were photolyzed with the same lamps for the same period of time, equation 2-3 must hold, where the superscript "^{0}" signifies the absence of benzene.

$$Y^0(BPI) = \Phi^0 I t \qquad 2\text{-}2a$$

$$Y(BPI) = \Phi I t \qquad 2\text{-}2b$$

$$Y^0(BPI)/Y(BPI) = \Phi^0 I t / \Phi I t = \Phi^0/\Phi \qquad 2\text{-}3$$

The percent uncertainties in Y^0(BPI) and in Y(BPI) were generously estimated to be 10% even though a much smaller value (5%) was estimated by Tanner and Walling[31] for the uncertainty in Y(BPI) by NMR analysis. The percent uncertainty in Φ^0/Φ was calculated to be 15% according to the rule of accumulation of the uncertainties (a percent uncertainty of 8% would be obtained if 5% uncertainties in Y^0(BPI) and Y(BPI) were assumed).

For convenience, a term, relative quantum yield, is introduced (Eq. 2-4)

$$\phi = \Phi I t \qquad 2\text{-}4$$

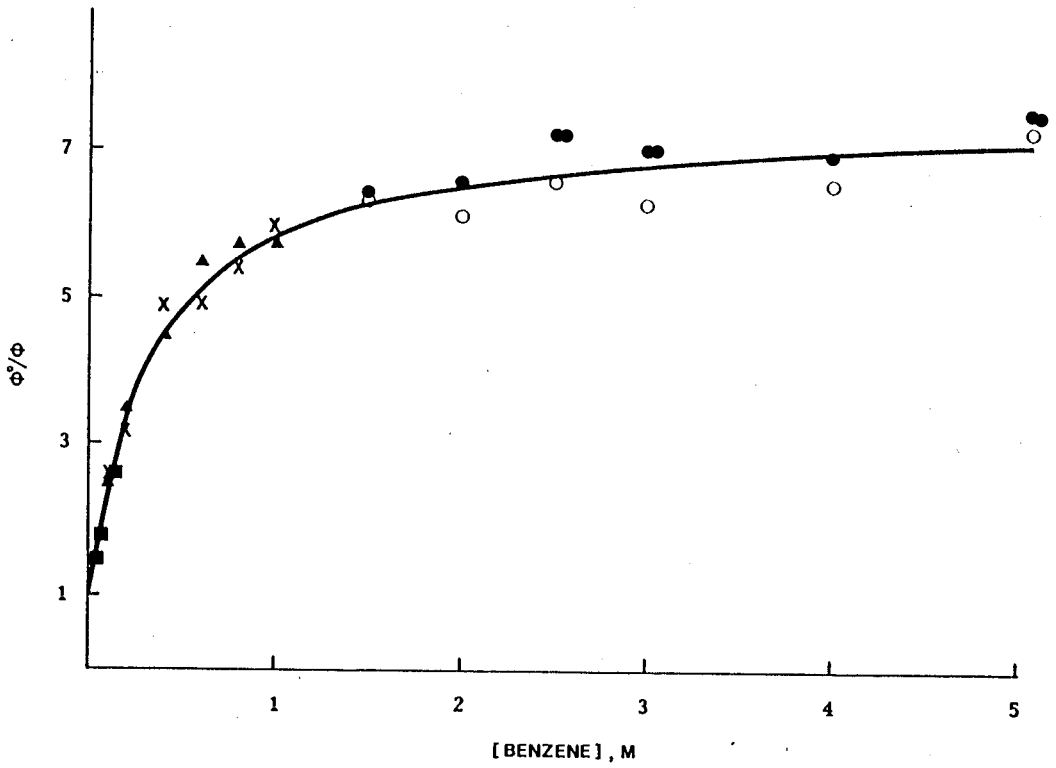

Figure 2-7. Effects of concentration of benzene on the ratio of quantum yields of BPI formation using the data given in Table 2-9.

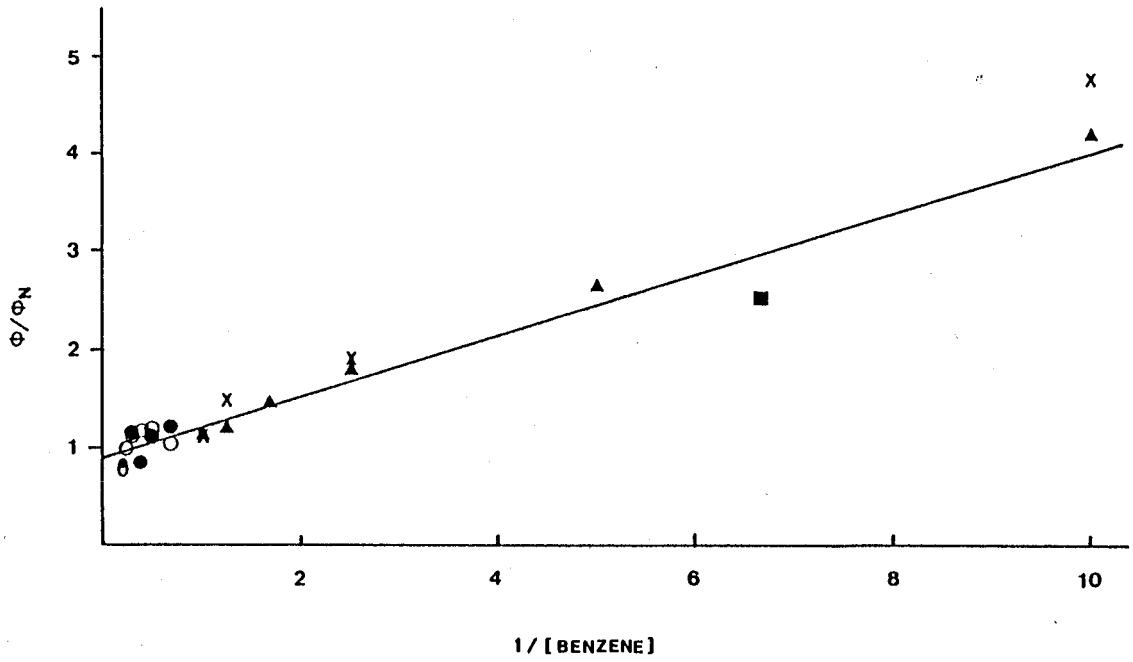

Figure 2-8. Plot of Φ/Φ_n vs. 1/[benzene] using the data given in Table 2-9.

Obviously,

$$\Phi^{o}/\Phi = \phi^{o}/\phi \qquad (2\text{-}5)$$

It is necessary to mention that ϕ^{o} and ϕ are functions of I and t. The ratio of Φ^{o}/Φ calculated from experimental data is plotted against the concentration of benzene in Figure 2-7. It can be seen that Φ^{o}/Φ levels off as benzene concentration increases, approaching an asymptote of about 7.5.

Next, the ratio of the quantum yield of BPI formation to that of N-phenylsuccinimide, Φ/Φ_{n}, i.e. ϕ/ϕ_{n}, is plotted against 1/[benzene] (Figure 2-8). It shows that ϕ/ϕ_{n} decreases linearly when 1/[benzene] decreases. A very important feature of Figure 2-8 is that the intercept of the straight line is not zero. This indicates that the quantum yield of BPI formation (Φ) is not zero when the concentration of benzene becomes very high.

The quantum yield of BPI formation from NBS (0.0562 M) was determined in 5 M benzene in the presence of DCE (0.026 M) at 15-18°C using a 300-nm light source. The light intensity was determined by the benzophenone-benzhydrol actinometer in benzene and the yield of BPI was analysed by ^{1}H NMR spectroscopy. The quantum yield, after correction for the amount of light NBS absorbed, was determined to be 0.78 (see Section 4.4.1.5 for details).

Section II. Photolysis of 33NBG and NBP

2.2.1. Photobromination of Cyclohexane-Dichloromethane with 33NBG-DCE and 33NBG-Br_2 Systems

N-Bromo-3,3-dimethylglutarimide (33NBG) has been used for photobrominations of alkanes and it is believed that 3,3-dimethylglutarimidyl radical is the major chain carrier in the hydrogen abstraction step if an olefin is used to scavenge Br_2.[56] Therefore, the *r* value calculated from photobromination products of cyclohexane-dichloromethane with the 33NBG-DCE system should show the selectivity of 3,3-dimethylglutarimidyl radical. Photolysis of cyclohexane-dichloromethane solutions of 33NBG and DCE with a 200-watt mercury lamp with a Pyrex filter at 15-18°C afforded 3,3-dimethylglutarimide (33GH), $CHBrCl_2$, and bromocyclohexane by GC analysis. No ring opening products were detected by GC-MS analysis. The conversion of 33NBG was monitored by NMR spectroscopy at various intervals, and the photolysis was always stopped before complete consumption of 33NBG. The *r* values are calculated to be ≃95 by the use of Eq. 2-1b, and the results are listed in Table 2-10.

Photolysis of cyclohexane-dichloromethane solutions of 33NBG and Br_2 with a 200-watt mercury lamp through a GWV filter afforded 3,3-dimethylglutarimide (33GH), $CHBrCl_2$, bromocyclohexane, and 1,2-dibromocyclohexane as shown by GC analysis. No ring

Table 2-10

Photobromination of C_6H_{12} (0.0920 M) and CH_2Cl_2 (15.5 M) with 33NBG-DCE System

Expt.	33NBG M	DCE M	$CHBrCl_2$ mM	$C_6H_{11}Br$ mM	33GH mM	*r*
62	0.026	0.019	4.28±0.06	13.7±1.4	13.5±0.8	97
63	0.024	0.014	4.63±0.48	14.5±0.6	17.2±1.6	96

Table 2-11

Photobromination of C_6H_{12} (0.0920 M) and CH_2Cl_2 (15.5 M) with 33NBG-Br_2 System

Expt.	Br_2 M	33NBG M	%33NBG Conv.	$CHBrCl_2$ mM	$C_6H_{11}Br$ mM	$C_6H_{10}Br_2$ mM	*r*
65	0.002	0.093	70.8±1.1	26.8±3.2	15.1±1.9	6.31±0.61	25.6
66	0.002	0.093	84.6±0.6	24.3±1.2	19.4±0.1	7.10±0.08	36.1
67	0.020	0.080	71.5±1.3	28.5±2.5	10.2±1.4	6.48±0.65	18.1
68	0.020	0.074	58.2±1.1	20.6±2.0	9.22±0.71	4.75±0.37	20.7
69	0.13	0.095	44.1±0.1	19.8±1.4	7.66±0.52	3.94±0.27	17.6
70	0.10	0.092	64.5±0.6	26.9±0.1	9.07±0.73	5.90±0.47	17.1

opening products were detected by GC-MS analysis. During the irradiation, samples were withdrawn at various intervals and analysed by NMR. The conversion of 33NBG in the experiments reported in Table 2-11 was <85%. The r values were calculated by the use of Eq. 2-1b and are listed in Table 2-11. When the initial $[Br_2]$ was 0.002 M, the r value calculated was 30±6, lower than that of 3,3-dimethylglutarimidyl radical ($r \simeq 95$, see Table 2-10) but higher than that of bromine atom (r=15-18, see Table 2-6). When the initial $[Br_2]$ was increased to 0.02 M, the r value decreased to ≃20. Further increase in the initial $[Br_2]$ lowered the r values (see expeiments 69 and 70, Table 2-11) close to that of bromine atoms (see Table 2-6).

2.2.2. Photobromination of Cyclohexane-Dichloromethane with NBP-DCE and NBP-Br_2 systems

Photolysis of a cyclohexane-dichloromethane solution of NBP and DCE through a Pyrex filter produced phthalimide (PH), $CHBrCl_2$, and bromocyclohexane. Their yields were determined by GC analysis. No ring opening products were detected by GC-MS analysis. The r value was calculated by the use of Eq. 2-1b to be ≃260 (see Table 2-12), higher than the selectivities of succinimidyl and 3,3-dimethylglutarimidyl radicals (see Tables 2-5

and 2-10).

The selectivity of NBP-Br_2 system towards hydrogen abstraction from cyclohexane and dichloromethane was also studied. Photolysis of a cyclohexane-dichloromethane solution of NBP and Br_2 through a GWV filter afforded phthalimide, $CHBrCl_2$, bromocyclohexane, and 1,2-dibromocyclohexane as detected by GC analysis. The conversions of NBP were monitored by NMR spectroscopy and are listed in Table 2-13. No ring opening products were detected by GC-MS analysis. The *r* values were calculated using Eq. 2-1b and are also listed in the table. When the initial [Br_2] was as low as 0.002 M, a *r* value of 30±1 was obtained (experiments 74 and 75), being between the *r* values of the phthalimidyl radical (≃260) and bromine atoms (≃16). As the initial [Br_2] increased to 0.02 M (experiments 76, 77, and 78), the *r* value decreased to 25-20. As the conversion of NBP increased to 90% from 55%, the *r* value decreased to ≃20 from 25 (compare experiment 76 with 77 and 78). Further increase in the initial [Br_2] from 0.02 M to 0.2 M did not significantly decrease *r* values further (see experiments 79 and 80).

2.2.3. Effects of Concentration of Benzene on the Yields of Bromocyclohexane

Table 2-10 shows that photolysis of cyclohexane-dichloromethane solutions of 33NBG and DCE affords bromocyclohexane in

Table 2-12

Photobromination of C_6H_{12} (0.0920 M)and CH_2Cl_2 (15.5 M) with NBP-DCE System

Expt.	NBP M	DCE M	%NBP Conv.	$CHBrCl_2$ mM	$C_6H_{11}Br$ mM	PH mM	r
71	0.023	0.013	95±5	1.92±0.17	17.1±0.8	-	277
72	0.029	0.018	95±5	2.25±0.20	16.5±1.4	21.4±0.3	226
73	0.029	0.018	95±5	2.08±0.11	18.0±0.5	19.7±0.7	271

Table 2-13

Photobromination of C_6H_{12} (0.0920 M) and CH_2Cl_2 (15.5 M) with NBP-Br_2 System

Expt.	Br_2 M	NBP M	%NBP Conv.	$CHBrCl_2$ mM	$C_6H_{11}Br$ mM	$C_6H_{10}Br_2$ mM[b]	r
74	0.002	0.11	55±5	23.6±1.1	15.1±0.8	6.22±0.33	29
75	0.002	0.11	50±5	21.4±1.5	14.7±0.8	6.13±0.33	31
76	0.020	0.11	55±5	25.1±1.0	13.4±0.4	7.92±0.62	25
77	0.020	0.096	90±5	38.9±1.8	11.7±0.8	12.1±0.8	20
78	0.02	0.075	90±5	34.7±3.1	12.1±0.9	10.3±0.8	21
79	0.20	0.11	60±5	29.6±0.2	11.2±0.5	8.62±0.39	21
80	0.20	0.11	75±5	36.1±1.5	13.0±0.1	10.6±0.2	21

addition to other products. In order to investigate the effects of concentration of benzene on the yield of bromocyclohexane, the following experiments were carried out. Several cyclohexane-dichloromethane solutions of 33NBG containing various amounts of benzene were irradiated in a merry-go-round with a 300-nm light source at 15-18°C. Small amounts of DCE were present in these solutions to scavenge Br_2 and/or bromine atoms to suppress the bromine atom chain. The conversion of 33NBG was determined by NMR spectroscopy to be lower than 20%. The photolysis afforded N-phenyl-3,3-dimethylglutarimide (PhG) and bromocyclohexane in addition to 33GH and $CHBrCl_2$. The yields of PhG and bromocyclohexane were determined quantitatively by GC and are listed in Table 2-14. It was found that the higher the benzene concentration, the higher the yield of PhG, and the lower the yield of bromocyclohexane (Table 2-14).

The ratios of $\Phi^0(C_6H_{11}Br)/\Phi(C_6H_{11}Br)$ were calculated using equation 2-11

$$\Phi^0(C_6H_{11}Br)/\Phi(C_6H_{11}Br) = [C_6H_{11}Br^0]/[C_6H_{11}Br] \qquad (2\text{-}11)$$

where $\Phi(C_6H_{11}Br)$ is the quantum yield of bromocyclohexane formation and $[C_6H_{11}Br]$ is the concentration of bromocyclohexane in the photolysates. The concentration of bromocyclohexane in the solution containing no benzene was taken as $[C_6H_{11}Br^0]$ in calculations. In Figure 2-9, $\Phi^0(C_6H_{11}Br)/\Phi(C_6H_{11}Br)$ is plotted

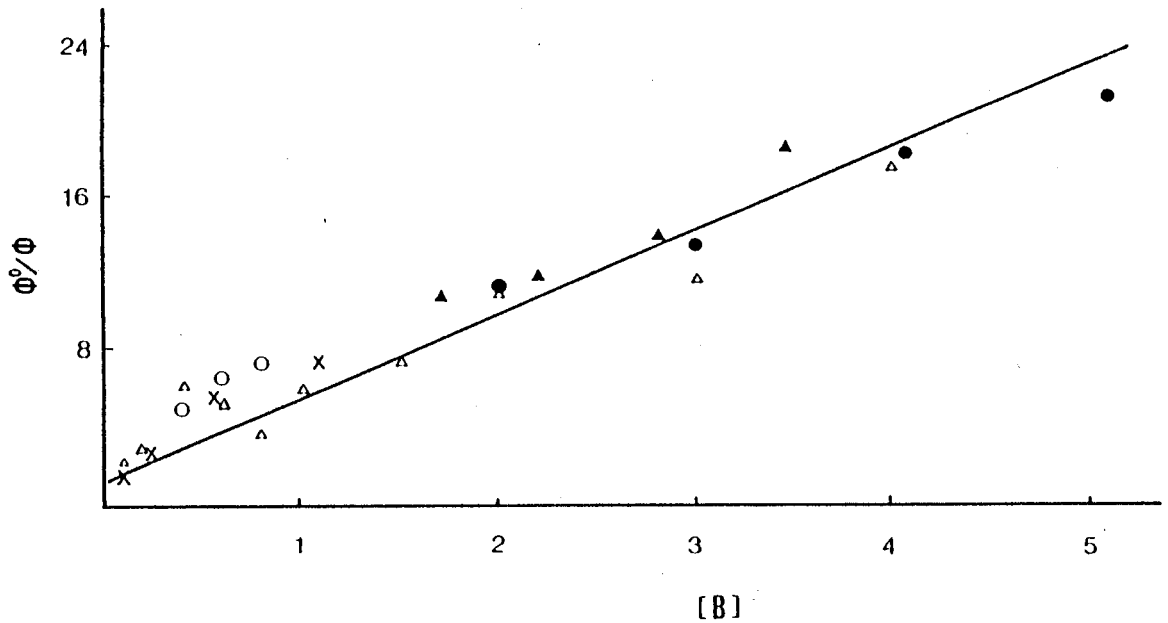

Figure 2-9. Effects of benzene concentration on the ratio of quantum yields of $C_6H_{11}Br$ formation using the data given in Table 2-14.

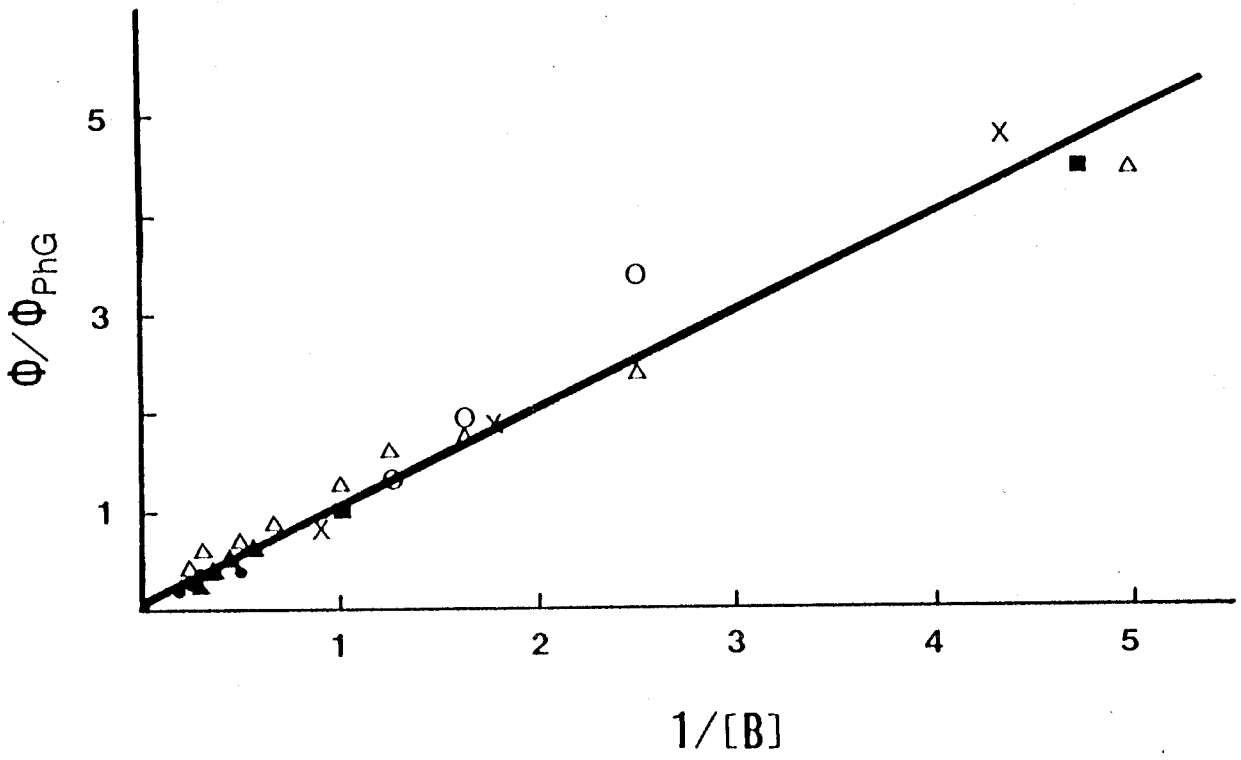

Figure 2-10. Plot of $\phi(C_6H_{11}Br)/\phi(PhG)$ vs. 1/[benzene] using the data given in Table 2-14.

Table 2-14

Photodecomposition of 33NBG in the Presence of Benzene[a]

[B] M	Prdct. mM		Φ^o/Φ^b	$\Phi/\Phi_p{}^c$
	$C_6H_{11}Br$	PhG		
Series A[d] (*hν* for 3.5 min., sign by x)				
0.00	18.1	0	1.00	
0.11	13.0	1.25	1.39	10.4
0.23	6.88	1.43	2.63	4.81
0.56	3.18	1.74	5.69	1.83
1.1	2.43	2.59	7.45	0.938
Series B[e] (*hν* for 2.5 min., sign by Δ)				
0.00	10.7	0	1.00	
0.10	5.30	0.70	2.03	7.57
0.20	3.86	0.872	2.78	4.43
0.40	1.73	0.734	6.20	2.36
0.60	1.90	1.07	5.66	1.78
0.80	3.02	1.84	3.56	1.64
1.0	1.80	1.41	5.97	1.27
1.5	1.43	1.59	7.51	0.902
2.0	0.958	1.38	11.2	0.694
3.0	0.920	1.38	11.7	0.666
4.0	0.622	1.42	17.3	0.437

Series C^f ($h\nu$ for 3.5 min., sign by ▲)				
0.00	18.3	0	1.00	
1.7	1.67	2.80	11.0	0.596
2.2	1.52	2.96	12.0	0.514
2.8	1.3	3.10	14	0.419
3.4	1.00	3.61	18.3	0.277
Series D^g ($h\nu$ for 2.5 min., sign by •)				
0.00	13.9	0	1.00	
2.0	1.23	2.87	11.3	0.429
3.1	1.02	3.28	13.6	0.311
4.1	0.77	3.11	18	0.25
5.1	0.63	3.30	21	0.19
Series E^h ($h\nu$ for 2.5 min., sign by o)				
0.00	10.5	0	1.00	
0.40	2.09	0.63	5.02	3.3
0.60	1.57	0.82	6.69	1.9
0.80	1.41	1.12	7.45	1.26

---

a. See Experimental and footnotes d, e, f, g, and h for details.

b. $\Phi^0(C_6H_{11}Br)/\Phi(C_6H_{11}Br)$

c. $\Phi(C_6H_{11}Br)/\Phi(PhG)$

d. [33NBG] = 0.12 M, $[C_6H_{12}]$ = 0.92 M, and [DCE] = 0.05 M

e. [33NBG] = 0.14 M, $[C_6H_{12}]$ = 0.92 M, and [DCE] = 0.04 M

f. [33NBG] = 0.24 M, $[C_6H_{12}]$ = 0.92 M, and [DCE] = 0.05 M

g. [33NBG] = 0.19 M, $[C_6H_{12}]$ = 0.92 M, and [DCE] = 0.05 M

h. [33NBG] = 0.10 M, $[C_6H_{12}]$ = 0.92 M, and [DCE] = 0.05 M

against benzene concentration to give a straight line. The ratio of the quantum yield of bromocyclohexane to that of PhG is plotted against 1/[benzene] in Figure 2-10. It is a straight line with a slope of 0.99 and an intercept of zero.

It is known that photolysis of 33NBG in the presence of 3,3-dimethylbutene produced a 1:1 adduct[32,38] **10**. The effects of the concentration of benzene on the yield of **10** were also investigated. Several CH_2Cl_2 solutions of 33NBG, cyclohexane (1.0 M), and 3,3-dimethylbutene (0.40 M) containing various amounts of benzene were irradiated with a 300-nm light source to produce **10**, PhG, bromocyclohexane, and 33GH as shown by GC analysis (portions of 33GH was produced by the work-up). The yields of the products are listed in Table 2-15, and the ratio of the quantum yields of formation of **10**, $\Phi^0(10)/\Phi(10)$, is plotted against the concentration of benzene in Figure 2-11.

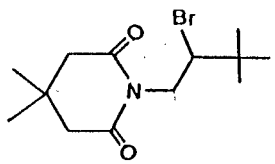

10

Table 2-15

Photodecomposition of 33NBG (0.11 M) in the Presence of Cyclohexane (1.0 M), Benzene, and 3,3-Dimethylbutene (0.40 M)

Tube	$[C_6H_6]$, M	Product[a]			Φ^o/Φ[b]
		$C_6H_{11}Br$	PhG	**10**	
1	0	0.066	0	0.024	1.0
2	0	0.068	0	0.025	1.0
3	0.22	0.038	0.0065	0.019	1.3
4	0.44	0.022	0.0077	0.013	1.9
5	0.88	0.017	0.011	0.0052	4.7
6	2.2	0.0077	0.014	0.0028	8.8
7	3.3	0.0049	0.022	0.002	12

a. In mM. 3,3-dimethylglutarimide was also formed. Its yield was not determined.

b. The ratio of quantum yield of **10** formation. The mean based on two samples containing no benzene was used as Φ^o in calculation of the Φ^o/Φ.

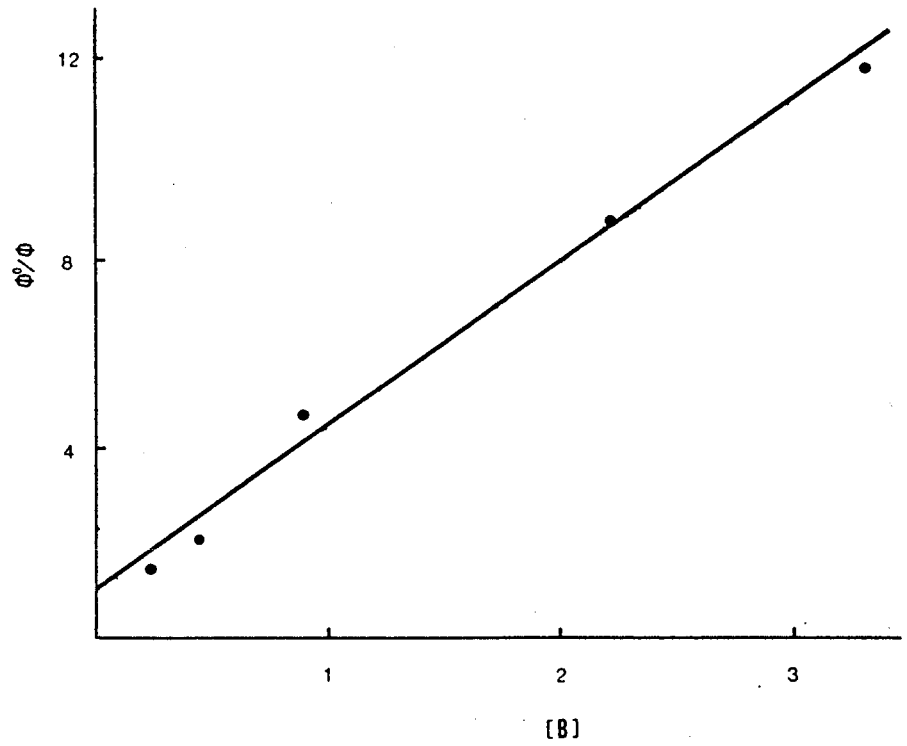

Figure 2-11. Plot of $\Phi^{o}(10)/\Phi(10)$ against [benzene] using the data given in Table 2-15.

Section III. Photodecomposition of N-Bromoimide **11**

2.3.1. Photodecomposition of N-Bromoimide 11

N-bromo-N-acetylhexanamide **11** was synthesized to investigate direct photodecomposition of **11** and bromine atom-initiated decomposition.

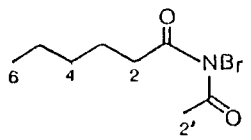

11

Photolysis of a dichloromethane solution of **11** in the presence of 3,3-dimethylbutene through a Pyrex filter at 0°C afforded 4-bromoimide **12** in a high yield (see Table 2-16). In addition there were small amounts of N-acetylhexanamide **13** and an unidentified monobrominated product **A** (Eq. 2-12). The yields of the various products were determined by GC, and the results are reported as experiment 151 in Table 2-16. A high yield of 4-bromoimide **12** was also obtained after a benzene solution of **11** in the presence of DCE was photolysed in a similar way to that described above.

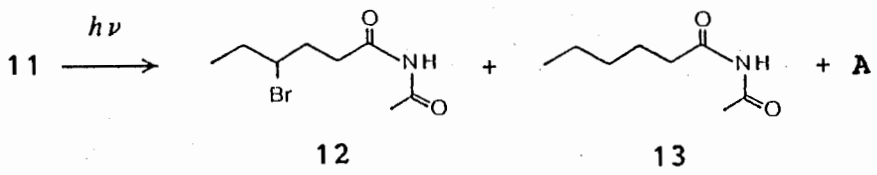

12 13 2-12

Bromobenzene or N-phenyl-N-acetylhexanamide was not detected by GC-MS analysis. The results are reported as experiment 152 in Table 2-16.

The 4-bromoimide 12 was isolated from the product mixture by flash chromatography. The position of the bromine substituent in the compound was assigned on the basis of ^1H coupling obtained from the NMR spectrum as follows: A triplet at 1.07 ppm was easily assigned to the signal due to H_6. Irradiating the signal caused a multiplet at 1.89 ppm to collapse to a broad doublet which was assigned to the signal of H_5. The multiplet at low field (4.03 ppm) was assigned to the proton geminal to the bromine at the C-4 position. Irradiation of this signal caused the signal of H_5 to collapse to a broad quartet. Therefore, the product under examination must be the 4-bromoimide 12.

Bromine atom-initiated decomposition of N-bromoimide 11 was investigated at 0°C by irradiating a carbon tetrachloride solution of 11 in the presence of various amounts of Br_2 with a ≥400-nm light source to ensure that only Br_2 was selectively excited. The time course of the consumption of 11 was judged from

Table 2-16

Photodecomposition of N-Bromoimide 11[a]

Expt.	Additive (mM)	Product. %						14/15	(14+15)/12	Δ15[g]	Δ15/12
		12	13	14	15	16	A				
151	Bute(100)[b]	83	8.5	c	c	0	6.5	-	-	-	
152	DCE(100)[b]	82	8.8	c	c	0	6.4	-	-	-	
153	Br_2(2)[d]	65	17	2.1	6.3	c	2.7	0.33	0.13	5.6	0.086
154A	Br_2(20)[d]	52	20	7.3	9.0	0.7	3.4	0.81	0.31	6.6	0.13
154B	Br_2(20)[d]	55	19	7.0	8.2	0.8	2.1	0.85	0.28	5.9	0.11
155	Br_2(200)[d]	27	34	17	11	1.6	3.9	1.5	1.0	5.3	0.20
156	Br_2(2)[e]	55	27	1	6.2	c	1.6	0.2	0.13	5.9	0.1
157	Br_2(20)[e]	51	28	4.7	7.2	0.6	1.7	0.65	0.23	5.6	0.11
158	Br_2(200)[e]	26	45	12	7.8	1.5	1.8	1.5	0.76	3.8	0.15
159	Br_2(20)[f]	53	26	5.9	7.9	0.7	2.1	0.75	0.26	5.9	0.11

a. General conditions: Solutions of **11** (0.04 M) and additives in CH_2Cl_2 (experiment 151), in benzene (experiment 152), or in CCl_4 were irradiated through a Pyrex filter (experiments 151, 152, and 154 B) or a filter solution (cut-off ≥400 nm) (153-158) at 0°C.

b. Bute = 3,3-dimethylbutene, DCE = 1,1-dichloroethene. The conversion of **11** was ≤95%.

c. Detected by GC but not integrated, owing to their low yields. d. The conversion of **11** was ≤85%.

e. [**11**] = 0.12 M. The conversion of **11** was ≤85%. f. The conversion of **11** was 80%. Temperature = -20±2°C.

g. Calculated by the use of **Δ15** = {**15** - **14**/3}

initial experiments and subsequently irradiations were stopped at about 80% consumption of **11**. The actual extent of the conversion of **11** was subsequently determined by ^{1}H NMR spectroscopy. It was found that **12**, **13**, and 2-bromoimide **14**, 5-bromoimide **15**, and 2'-bromoimide **16** were formed in addition to **A** (Eq. 2-13). Since these compounds had been prepared through different routes or isolated from the product mixtures, their yields could be determined by GC analysis with benzophenone as an internal standard. The results are listed in Table 2-16. GC analysis also detected four small peaks due to unidentified products in small amounts. The photodecomposition of **11** was also carried out by irradiating a CCl_4 solution of **11** and Br_2 through a Pyrex filter (Experiment 154B). The yield of **12** was slightly higher (comparing experiment 154B with 154A).

$$\mathbf{11} + Br_2 \xrightarrow[0^\circ C]{400\ nm} \mathbf{12} + \mathbf{13} + \mathbf{A} + \mathbf{14} + \mathbf{15} + \mathbf{16} \qquad 2\text{-}13$$

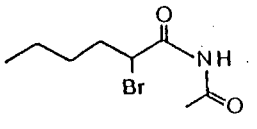

14

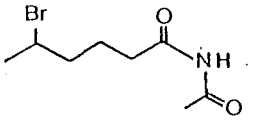

15

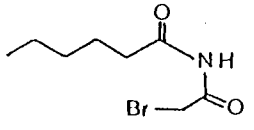

16

The salient feature of the ^{1}H NMR spectrum of **14** is a triplet at 4.43 ppm (1H, J=5.0 Hz). It indicates that the bromine must be at the C-2 position, and that the two magnetically inequivalent protons at the C-3 position happen to couple equally to the proton at the C-2 position. The ^{1}H NMR spectrum of 5-bromoimide **15** shows a doublet at 1.76 ppm (3H, H_6, J=6.7 H_z) and a multiplet at 4.01 ppm (1H, H_5), which was further confirmed by a decoupling experiment. Saturation of the multiplet at 4.01 ppm caused the doublet to collapse to a singlet.

From Table 2-16, it can be seen that the yield of **12** decreased with the increase in the concentration of Br_2. The yield of **12** was nevertheless substantial even at 0.2 M Br_2. It is noteworthy that the ratio of **14/15** increased to ≃1.5 from 0.2 as the concentration of Br_2 increased from 0.002 to 0.2 M. Photolysis of N-bromoimide **11** was also carried out at a lower temperature. A NMR tube containing a carbon tetrachloride solution of **11** (0.04 M) and Br_2 (0.020 M) was placed in a Pyrex beaker full of a mixture of ice and sodium chloride, and the solution, together with the beaker, was irradiated with a ≥400-nm light source. It was found (see experiment 159 in Table 2-16) that the product distribution was not significantly affected by lowering the temperature.

2.3.2. Photobromination of N-Acetylhexanamide 13 with Br_2-K_2CO_3 and NBS-Br_2 Systems

In order to know the selectivity of bromine atoms towards different C-H bonds in the side chain of N-bromoimide **11**, photobromination of **13** with Br_2 was carried out as a blank experiment. It was assumed that the replacement of bromine by hydrogen at the nitrogen would not significantly affect the reactivity of hydrogens in the side chain towards bromine atoms. Since the reverse reaction of 2-14 is significant, complicating the selectivity studies[57],

$$Br\cdot + RH \rightleftharpoons HBr + R\cdot \qquad 2\text{-}14$$

the photobromination was excecuted in the presence of suspended anhydrous K_2CO_3, an HBr scavenger[58]. Alternatively, NBS was used as an HBr scavenger since the latter is trapped rapidly by an ionic reaction with the former to produce Br_2 and succinimide[59]. Solutions of **13**, Br_2, and an HBr scavenger in carbon tetrachloride or in dichloromethane were irradiated with a ≥400-nm light source at 0°C. The conversion of **13** was monitored by GC, and the irradiation was stopped at a low conversion of **13** to minimize polybrominations of the side chain. The 2-bromoimide, **14**, 5-bromoimide, **15**, in addition to small amounts of 4-bromoimide, **12** and 2'-bromoimide, **16**, were obtained. The yields of the products were determined by GC and the results are listed in

Table 2-17

Photobromination of 13 by Br_2[a]

Expt.	Br_2	HBr	Conv.	Product ratio			
	mM	Scvngr.	of **13**	**12**	**14**	**15**	**16**
160	10	K_2CO_3[b]	5%(160)[e]	f	2.9	1.0	f
161	2	NBS[c]	10%(75)[e]	0.5	3.0	1.0	0.3
162	20	NBS[c]	8%(45)[e]	0.4	3.1	1.0	0.2
163	200	NBS[c]	6%(35)[e]	0.4	3.1	1.0	0.2
164	20	NBS[d]	22%(32)[e]	0.5	2.7	1.0	0.3
165	200	NBS[d]	20%(30)[e]	0.5	2.8	1.0	0.2

a. Vigorously stirred solutions of **13** (0.04M, except experiment 160 in which [**13**] = 0.02 M), Br_2, and HBr scavengers in CCl_4 (experiments 160-163) or in CH_2Cl_2 (experiments 164 and 165) were irradiated through a GWV filter and a filter solution (≥400 nm) at 0°C.

b. Heterogeneous during the course of the irradiation, the molar ratio of K_2CO_3 to Br_2 was ≥5.

c. The molar ratio of NBS to **13** was 2:1.

d. The conversion of NBS ([NBS]=0.11 M) was 65% and 45% respectively determined by NMR spectroscopy.

e. The numbers in parenthesis are durations of irradiation, in minutes.

f. The yields were too low to be determined accurately.

Table 2-17, which demonstrates that the 14/15 ratio is *ca.* 3 and that it hardly varies with the change in the solvent and/or the HBr scavenger.

2.3.3. Photobromination of N-Methyl-N-acetylhexanamide 18 with Br_2-K_2CO_3 and NBS-Br_2 Systems

Table 2-17 shows that bromine atoms prefer abstracting hydrogen from the C-2 position as compared to the C-5 position, leading to 14/15 = 3. In order to verify this preference, a similar compound, N-methyl-N-acetylhexanamide (18) was synthesized, and its photobrominations with the Br_2-K_2CO_3 and the NBS-Br_2 systems were carried out in a similar way to that described in the previous section. It was assumed again that the reactivities of hydrogens in the side chains of 18 and 11 were similar towards bromine atoms. To get the product distribution of bromination of 18, mixtures of 18, Br_2, and K_2CO_3 in carbon tetrachloride were irradiated with a ≥400-nm light source at 0°C. The conversion of 18 was monitored by GC analysis at intervals and irradiation was stopped at low conversion of 18 to minimize polybromination of the side chain.

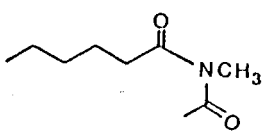

18

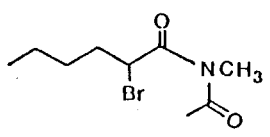

19

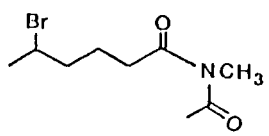

20

Table 2-18

Photobromination of Imide 18 by Br_2-K_2CO_3 and NBS-Br_2 Systems[a]

Expt.	Br_2	HBr	Conv.	Product ratio				
	mM	Scvngr.	of 18	19	20	X	Y	Z
166	20	K_2CO_3	7%	2.4	1.0	0.49	0.17	0.39
167	20	K_2CO_3	15%	3.5	1.0	0.74	0.21	0.38
168	20	NBS[b]	8%	3.1	1.0	1.0	0.18	0.37
169	200	NBS[b]	5%	3.5	1.0	0.92	0.20	0.32
170	200	NBS[b]	6%	3.1	1.0	0.63	0.14	0.25
171A	2	NBS[b]	15%	4.1	1.0	0.49	0.19	0.29
171B	2	NBS[b]	14%	2.0	1.0	0.55	0.23	0.39
172A	2	NBA[c]	6%	3.2	1.0	0.57	0.28	0.29
172B	200	NBA[d]	5%	3.0	1.0	0.56	0.26	0.25

a. Heterogeneous mixtures (except experiment 172) of 18 (0.047 M, except experiment 167 in which [18] = 0.020 M), Br_2, and HBr scavengers in CCl_4 were irradiated with a 200-watt lamp (except experiment 171 in which a 450-watt one was used) through a GWV filter and a filter solution (cut-off ≥400 nm) at 0°C.

b. The molar ratio of NBS to 18 was 1:5.

c. 0.04 M N-bromo-N-acetylacetamide was used.

d. 0.12 M N-bromo-N-acetylacetamide was used.

Again, 2-bromo (**19**) and 5-bromo derivative (**20**) were determined by GC to be the major products. They were isolated by flash chromatography, and the yields of these two products from all subsequent photobrominations of **18** were quantitatively determined by GC with benzophenone as an internal standard. The results are listed in Table 2-18. Three monobrominated products, **X**, **Y**, and **Z** were also formed in smaller amounts. GC-MS analysis indicated that these compounds had the same M^+ values as did 2-bromoimide **19** and 5-bromoimide **20**. They are presumably isomers of **19** and **20**. On the GC trace there was a peak with a shorter retention time in addition to the peak due to **19** itself when a carbon tetrachloride solution of **19** was injected for GC analysis. The former peak was found by GC-MS analysis to arise from a compound possessing a molecular weight 80 and 82 units less than that of **19**, and the compound was bromine-free. It is speculated that this compound is a dehydrobromination product of **19**, and it is formed by a reaction inside the injector of the GC upon **19** being injected. Therefore, the relative yields of **19** listed in Table 2-18 have been corrected by the following method: The sum of areas of the GC signals due to **19** and its decomposition derivative was taken as that due to **19**, and the same molar response factor was assumed for these two compounds.

Photobromination of **18** was also carried out with Br_2 and N-Bromo-N-acetylacetamide (NBA) as the bromination reagent, and the results are listed in Table 2-18 (experiment 172). It can be

seen that the ratio of **19/20** is still ≃3 with preference to bromination at the C-2 position.

Section IV. Photodecomposition of Selected N-Bromoimides

In this section, the photolysis of selected cyclic N-bromoimides in the presence of an olefin is reported. These compounds are derivatives of N-bromosuccinimide and N-bromoglutarimide, and they are prepared from the corresponding imides.

2.4.1. Photodecomposition of N-bromoimide 21

A dichloromethane solution of **21** in the presence of DCE was photolyzed with a 300-nm light source at 15-18°C to give a photolysate showing strong absorptions at 2260 and 2349 cm^{-1} characteristic of isocyanate[60a] and carbon dioxide[51] respectively. It was found that the absorption of the photolysate at 2260 cm^{-1} decreased over the two day period. GC analysis during this time showed that the signal intensity of **24** increased. Chromatography of the product mixtures afforded dicarboximide **22**, **23**, and γ-lactone **24** (Eq. 2-15). Several unidentified compounds in small amounts were also detected by GC.

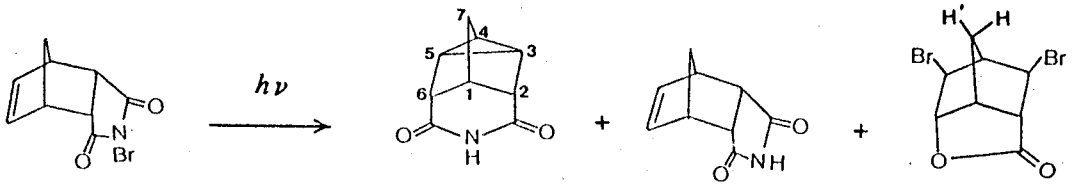

21 22 23 24 2-15

There was a smaller peak next to that due to **24** on the GC trace when the product mixture was analysed. GC-MS analysis showed that this compound possessed the same MS pattern as did γ-lactone **24**. Thus it must be an isomer of **24**. The product distribution of photolysis of N-bromoimide **21** is listed in Table 2-19.

The structure of **22** was determined by ^{1}H and ^{13}C NMR spectral analysis (Tables 4-7 and 4-8), IR (Table 4-9) and mass spectra (Table 4-10). The pertinent arguments in support of the structural assignments are outlined below. A similar pattern in mass spectrum of **22** (*m/e* 163 (M^{+})) to that of imide **23** suggests that **22** is an isomer of **23**. The ^{13}C NMR spectrum of **22** shows a signal due to imidyl carbonyl carbon(s) at 175.14 ppm[62] and indicates a plane of symmetry since only six carbon signals are detected. IR analysis shows N-H absorption (3450 cm^{-1}) and C-H absorption of three-membered ring[60b] at 3080 cm^{-1}. After the broad proton signal[60f] at 7.78 ppm was assigned to NH, the signal at the lowest field (two protons, 2.66 ppm) was assigned to the two chemically equivalent protons H_2 and H_6, since they are α to the carbonyl groups[62]. Assignment of H_3, H_5, and H_7 was based on the homodecoupling (a technique for irradiating a proton with a strong radio frequency signal at its resonance

Table 2-19

Product Distribution of Photodecomposition of N-Bromoimide 21[a]

Expt.	[21], M	[DCE], M	Product %		
			22	**23**	**24**[b]
173	0.067	0.04	20	50	18[c]
174	0.10	0.06	36	38	12(4)
175	0.10	0.06	40	34	7(2)
176	0.10[d]	0.06	33	40	11(4)

a. General conditions: dichloromethane solutions of **21** and DCE were photolyzed at 15-18°C with a 300-nm light source (RPR 3000 Å lamps). The conversion of **21** is >95%, and product yields are based on the amount of **21** used.

b. The number in the parentheses are the yields of the isomer of **24**. The molar response factor of the isomer was assumed to be the same as that of compound **24**.

c. The combined yield of γ-lactone **24** and its isomer.

d. Light source was a 200-watt Hanovia medium pressure mercury lamp with a Pyrex filter.

frequency while scanning other protons to detect which ones are affected by decoupling from the irradiated proton)[63]. Irradiation of H_2 and H_6 caused remarkable simplification of the signal (two protons) at 1.70 ppm but hardly affected the signal (two protons) at 1.73 ppm. Therefore, the former signal was assigned to H_3 and H_5 while the latter to H_7. Irradiation of the H_2 and H_6 signals simplified both signals at 1.67 ppm (one proton) and 2.51 ppm (one proton). The coupling constants, however, could not be estimated since the splitting patterns are complicated by the "w-type" long range coupling[53,64-68] of H_2 (or H_6) to H_4. The signal at 1.67 ppm was assigned to H_4 but not to H_1 on the basis of the consideration that methine protons of three-membered rings resonate at a higher field than do those of six-membered rings.

The structure of γ-lactone **24** was determined by MS, IR, and NMR analysis. The isotopic cluster[69] in the mass spectrum (*m/e* 298, 296, 294 (1:2:1, M^+)) indicates a dibrominated compound. ^{13}C NMR signals at 174.98 and 86.62 ppm suggest the presence of the lactone group[70]. This is supported by a strong IR absorption at 1788 cm^{-1}, characteristic of a five-membered lactone[60d]. The low-field ^1H NMR signal at 4.95 ppm due to the proton in a H-C-O moiety was assigned to H_6 by analogy to a similar compound[71]. The signals at 4.0 and 3.75 ppm were assigned to H_5 and H_3, which are geminal to the bromine atoms. After the signal at the highest field at 2.45 ppm (two protons) was assigned to two

protons at the C-7 position, only the signals of H_1, H_2, and H_4 were left. Irradiation of the signal at 3.3 ppm caused the collapse of the doublet at 2.98 ppm and the doublet due to H_6 at 4.95 ppm to singlets (J=5.0 and 4.8 Hz). The signal at 3.3 ppm was assigned to H_1 and that at 2.98 ppm to H_2 (The coupling between H_4 and H_1 in bicyclo[2,2,1]heptane system is weak[72], i.e. <4.8 Hz, the signal at 2.98 ppm therefore was assigned to H_2 instead of H_4). The stereochemistry of H_3 and H_5 was elucidated by a nuclear Overhauser effect experiment[73,74]. Saturation of H_7 and H_7' resulted in ≃10% enhancement of the H_1 and H_4 signals and approximately 5% enhancement of the H_2 and H_6 signals. The lack of enhancement of H_3 and H_5 signals (Figure 2-12) indicates that H_3 and H_5 occupy the *endo* position, the two bromine atoms geminal to H_3 and H_5 must be in the *exo* positions.

2.4.2. Photodecomposition of N-Bromoimide 25

25 was synthesized by reacting imide **22** with *t*-butyl hypobromite. Photolysis of a dichloromethane solution of **25** in the presence of DCE with a 300-nm light source at 15-18°C produced the parent imide **22** in 78-84% yield determined by GC (Eq. 2-16). A trace amount of the 1:1 adduct of **25** to DCE was detected by GC and GC-MS analysis. The area of the GC signal due to the adduct to that due to **22** was <5/80. The photolysate without work-up showed no absorption at 2260 or 2349 cm^{-1}.

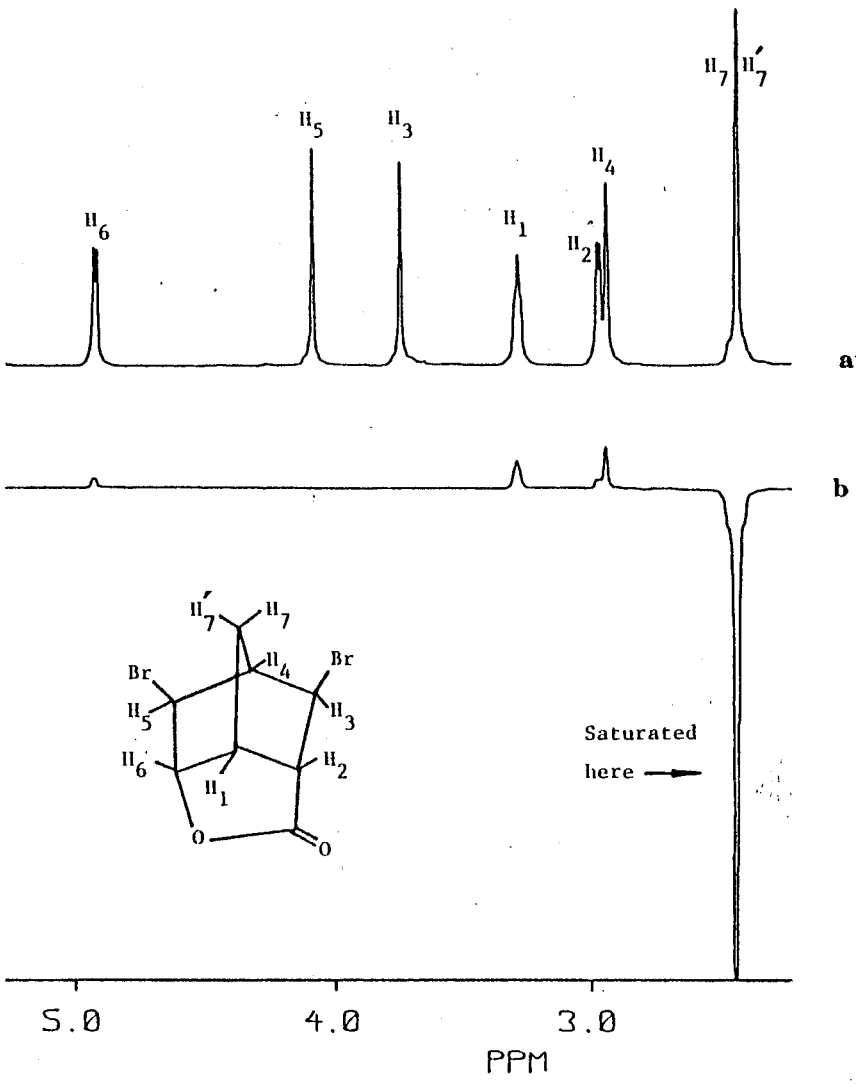

Figure 2-12. 400-MHz ^{1}H NMR spectrum of γ-lactone **24** (a) and difference NOE spectrum obtained by saturation of H_7 and H_7' (b).

Several small peaks due to unidentified compounds were detected by GC analysis, but none of them were the signals of **23** or **24**. This was ascertained by peak matching when the authentic compounds were co-injected with the crude product. The results are tabulated in Table 2-20.

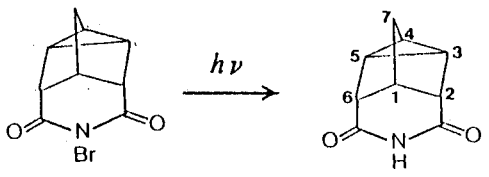

2-16

25 **22**

2.4.3. Photodecomposition of N-Bromoimide 26

When a dichloromethane solution of N-bromoimide **26** (0.26 M) in the presence of DCE (0.16 M) was irradiated with a 300-nm light source at 15-18°C, cloudy precipitation due to polymerization of DCE[38] was observed. GC analysis of the photolysate indicated imide **27** (48%), imide **28** (40%) and phthalimide (≃3%) (Eq. 2-17). The ring opening products, **30** and **31**, were formed only in small amounts (<2%), and IR analysis of the crude photolysate did not show absorption at 2349 or 2250 cm^{-1}. The C-bromoimide **27** was synthesized by a different route (see Section 4.4.7.1).

Table 2-20

Product Distribution of Photodecomposition of N-Bromoimide 25[a]

Expt.	[25], M	[DCE], M	Product %[b]			
			22	23	24	a[c]
177	0.07	0.04	78	nd	nd	2
178	0.07	0.06	84	nd	nd	3
179	0.07	0.05	80	nd	nd	3

a. General conditions: dichloromethane solutions of **25** and DCE were photolyzed with a 300-nm light source at 15-18°C.

b. The product yields are based on the amount of **21** used. The conversion of **21** is >95%.

c. The 1:1 adduct. Its molar response factor was assumed to be the same as that of **22**.

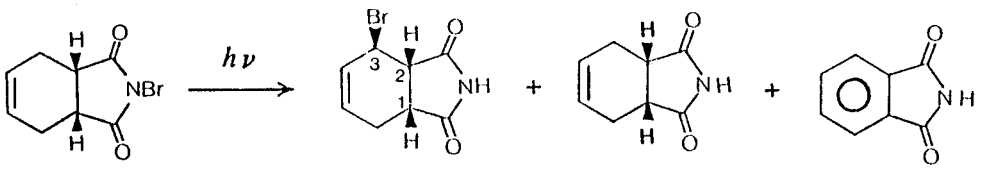

2-17

26 **27** **28** **29**

The coupling constant $J_{2,3}$ of 1.0 Hz was determined for **27** by a decoupling experiment. The small value indicates that H_3 is

trans to H_2 (see Figure 2-13). Therefore, the Br at the C-3 position was assigned to be *cis* to H_2. The small $J_{2,3}$ value is explainable if the dihedral angle ϕ between the H_2-C_2-C_3 and the C_2-C_3-H_3 planes is close to 90°. Assignment of the signal at 2.52 ppm to H_6, the hydrogen *cis* to the H_1, was based on the NOE experiment (Figure 2-13). Irradiating H_1 resulted in ≃5% enhancement of the H_6. The formation of **28** and **29** was confirmed by co-injecting authentic samples with the photolysate in GC analysis.

After photolysis of a dichloromethane solution of **26** (0.1 M) was executed in the presence of 1,3-pentadiene (0.05 M), the photolysate was analyzed by IR spectroscopy without work-up. Surprisingly, strong absorptions at 2349 and 2250 cm^{-1} were observed. The latter absorption is characteristic of isocyanates. A yellow oil was obtained after the solvent was removed under reduced pressure. When it was transferred by a pipette, bubbles evolved from the oil because of the reaction between the isocyanate and the moisture introduced by the pipette. Complete hydrolysis afforded the ring opening products **30** and **31** in 88% yield determined by GC analysis. They and **28** were isolated by flash chromatography (Eq. 2-18).

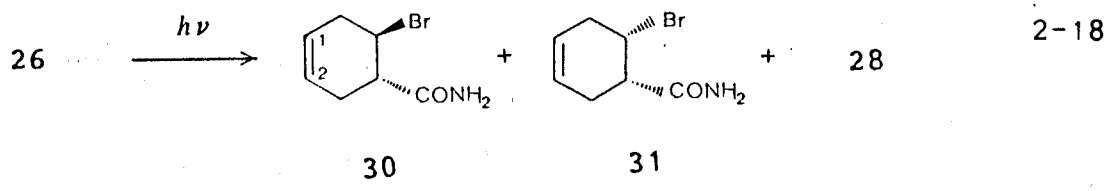

2-18

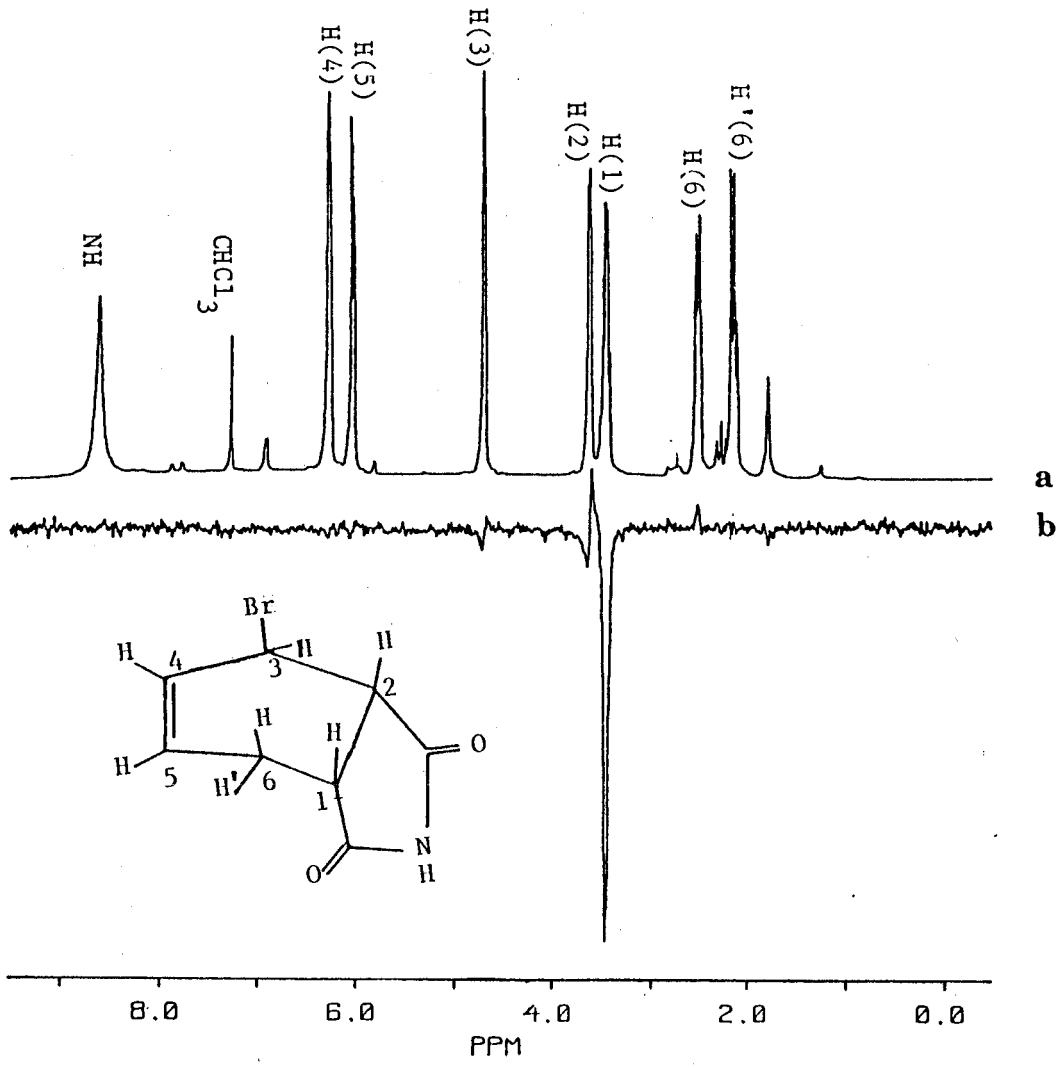

Figure 2-13. 400-MHz ^{1}H NMR spectrum of C-bromoimide **27** (a) and difference NOE spectrum obtained by saturation of H_1 (b).

It is known that 1,3-pentadiene is more reactive than DCE towards bromine atoms[56]. The dramatic change in product distribution may be caused by the use of the more efficient bromine atom scavenger, 1,3-pentadiene. To test this hypothesis, the photolysis of **26** (80 mM) was carried out in different DCE concentrations. It was found that the yields of allylic bromination product **27** decreased and ring opening compounds **30** and **31** became the major products as the concentration of DCE was increased (Table 2-21). Because the precipitation due to polymerization of DCE occurred in all experiments reported in Table 2-21 during the photolysis the actual concentrations of DCE must be lower than those shown in Table 2-21. When photolysis of **26** was carried out in different concentrations of 1,3-pentadiene, however, no remarkable change in product distribution was observed. The ring opening products **30** and **31** were still the major ones even when the photolysis was carried out in the presence of 1.3 M 1,3-pentadiene (see Table 2-22).

The structure and stereochemistry of **30** and **31** were determined by ^{1}H and ^{13}C NMR spectral analysis (Tables 4-7 and 4-8), IR (Table 4-9) and mass spectra (Table 4-10). The pertinent arguments in support of the structural assignment are outlined below. The odd-numbered molecular weight and the isotopic cluster of the mass spectra (*m/e* 205, 203 (1:1, M^{+})) indicates that **30** is a monobromocompound containing one nitrogen atom. The presence of amide carbonyl is suggested by ^{13}C signal at $\simeq$175

Table 2-21

Product Distribution of Photodecomposition of N-Bromoimide 26 in Different DCE Concentrations[a]

Expt.	[DCE], M	Product, mM (%)[b]			
		27	**28**	**30**	**31**
180	0.48	19.6(25)	11.2(14)	18.0(23)	16.6(21)
181	1.2	1.4(2)	15.7(20)	23(29)	29(36)
182	1.8	0.9(1)	14(18)	24(30)	30(38)

a. General conditions: dichloromethane solutions of **26** and DCE were photolyzed with a 300 nm light source at 15-18°C.

b. The figure in the parenthesis is the percent yield based on the amount of **26** (80 mM) used.

ppm. This is further supported by its IR absorptions at ≃3410 cm^{-1} (N-H streching) and ≃1660 cm^{-1} (carbonyl streching of amide). Since amides **30** and **31** show similar mass spectra, it is surmised that they are probably the *cis-trans* isomers. The assignments of *trans* (Br vs. carbamoyl) to **30** and *cis* to **31** were based on the magnitudes of proton-proton splitting of H_5 signals (Figure 2-14). In the *trans* isomer **30**, the axial H_5 is coupled

Table 2-22

Product Distribution of Photodecompositin of N-Bromoimide 26 in Different 1,3-Pentadiene Concentrations[a]

Expt.	[PDE], M	Product, mM[b]			
		27	**28**	**30**	**31**
183	0.05[c]	nd[d]	9.1(9.1)	40(40)	48(48)
184	0.10	nd	7.2(9.0)	31(39)	38(48)
185	0.20	nd	8.2(10)	30(38)	39(49)
186	0.4	nd	9.8(12)	25(31)	29(36)
187	1.3	nd	13(16)	23(29)	30(38)

a. General conditions: solutions of **26** (18.4 mg, 0.080 mmol, 80 mM) and 1,3-pentadiene (PDE) in CH_2Cl_2 (1.0 ml) were photolyzed with a 300-nm light source at 15-18°C.

b. The figure in the parenthesis is the percent yield based on the amount of **26** used.

c. [**26**] = 0.1 M

d. Not detected by GC analysis. [**27**] must be <0.2 mM.

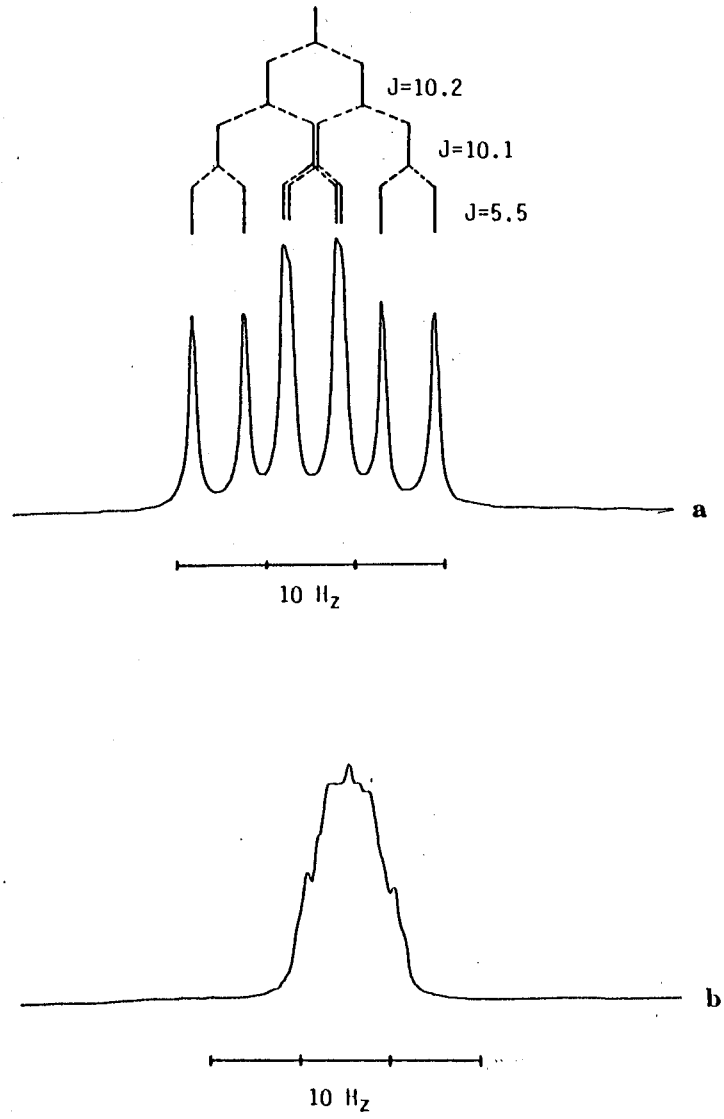

Figure 2-14. 400-MHz ^{1}H NMR signal at 4.38 ppm due to H_5 of **30** (a) and that at 4.85 ppm due to H_5 of **31** (b).

to both H_4 (J=10 Hz) and the axial H_6 (J=10 Hz) in the trans diaxial fashion[75] and to the equatorial H_6 (J=5.5 Hz). In contrast, there is no similar *trans* diaxial coupling observed in the ^1H NMR spectrum of the *cis* isomer (Figure 2-14).

2.4.4. Photodecomposition of N-Bromoimide 32

Photodecomposition of a dichloromethane solution of **32** (0.066 M) in the presence of DCE (0.060 M) with a 300-nm light source afforded amide **33** (75%), amide **34** (7%), and imide **35** (15%) by GC analysis (Eq. 2-19).

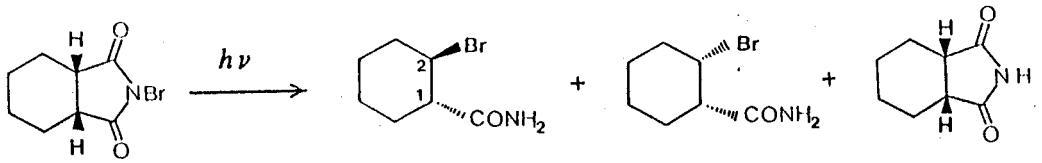

2-19

32 **33** **34** **35**

Compound **33** was isolated by chromatography, and its stereochemistry was elucidated on the basis of its ^1H NMR spectrum. That the bromine at the C-2 position is *trans* to the $CONH_2$ group at C-1 position in **33** is indicated by a coupling constant $J_{1,2}$ of 12.0 Hz. Compound **34** was not isolated because of its low yield. GC-MS analysis showed it had a similar mass spectrum and the same M^+ value as did **33**. These observations suggest **34** is

probably a *cis* isomer of **33**. When the product mixtures were analysed by GC, the same molar response factor was assumed for **33** and **34**, while the molar response factors of **33** and imide **35** relative to benzophenone (the internal standard) were determined by analysing mixtures of these compounds with known ratios.

2.4.5. Photodecomposition of (±)-N-Bromoimide 36

Photolysis of a dichloromethane solution of **36** (0.064 M) in the presence of DCE (0.040 M) was carried out by irradiating the solution with a 300-nm light source. The products were isolated by chromatography as (±)-amide **37** and (±)-imide **38**.

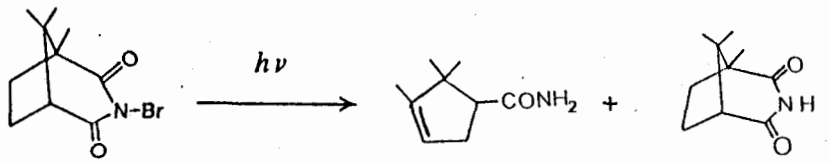

2-20

36 **37** **38**

The yield of **37** was 60%, and that of **38** was 35% according to GC analysis. The structure of **37** was determined from its spectra. The odd numbered value of *m/e* 153 (M^+, 37%) shown by mass spectroscopy and the data obtained from microanalysis (N=8.99%) indicate that **37** contains one nitrogen. The broad proton signal at 5.43 ppm (2H) and the ^{13}C signal at 175.8 ppm suggest the

presence of a carbamoyl group ($CONH_2$). This was confirmed by strong IR absorptions at 3527 and 3410 cm^{-1} due to N-H and those at 1682 and 1589 cm^{-1} due to the carbonyl of the amide moiety. The proton signal at 5.27 ppm and the ^{13}C signals at 121.0 and 146.7 ppm which are characteristic of olefine indicate the presence of a double bond. This information together with the IR absorptions at 2349 and 2250 cm^{-1} (indicating that ring opening has occurred) shown by the crude photolysate led to the assignment of its structure. The formation of the double bond will be discussed in Chapter three.

2.4.6. Photodecomposition of N-Bromoimide 39

Photodecomposition of a dichloromethane solution of **39** (0.034 M) in the presence of DCE (0.03 M) afforded imide **40** in 90% yield as shown by GC analysis (Eq. 2-21). IR analysis did not detect any absorption at 2349 or 2250 cm^{-1} in photolysate. No trace of C-bromoimides were detected by GC-MS (CI) from their calculated *m/e* signals at 236 and 234 (M^++1, one to one intensity ratio for monobrominated compounds).

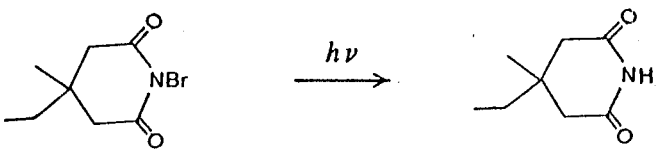

2-21

39 **40**

Formation of a small amount of 1:1 adduct of **39** to DCE was indicated by its M^++1 values shown by GC-MS analysis (see Section 4.4.10); the ratio of area of its GC signal to that of **40** was <3:90.

Section V. Reactions of NBS with Naphthols

2.5.1. Formation of the Products as Monitored by UV, ^{1}H NMR, and IR Spectroscopy

When solutions of 1-naphthol (1-NpOH, 0.01 M) and NBS (0.01 M) in dichloromethane were mixed at room temperature the color of the mixture quickly turned from colorless to light yellow. The solution showed an absorption band at 357 nm where neither 1-NpOH nor NBS have substantial absorptions. In a separate experiment the reaction was followed by consecutive scans of the spectrum over the range 320-390 nm. These scans showed a well defined isosbestic point at 323 nm in addition to the new absorption band at 357 nm. Similarly, scans of the spectrum over the range 250-330 nm showed two isosbestic points at 269 and 323 nm. The absorption band at 357 nm was also studied by a differential UV spectroscopic method; the mixture of 1-NpOH and NBS in dichloromethane placed in a UV cell (the sample cell) was scanned against a double-compartment UV cell (dichloromethane solutions of NBS and 1-NpOH were placed in separate compartments

of the reference cell, the concentrations of which were twice that of the sample cell). The results are shown in Figure 2-15. From a mixture of 2-naphthol and NBS in dichloromethane a new absorption band at 330 nm was detected. When 4-chloro-1-NpOH and 2-bromo-4-chloro-1-NpOH were mixed with NBS in dichloromethane, new absorption bands at 356 and 362 nm, respectively, were observed. Similarly, the reaction of 1-anthrol with NBS produced a product which absorbed at 396 nm. Consecutive scans of the spectrum showed two isosbestic points at 328 and 392 nm. (Figure 2-16). These reactions are expressed with the following equations and their λ_{max} are listed in Table 2-23.

1-NpOH + NBS ⟶ **41** 2-22

2-NpOH + NBS ⟶ **42** 2-23

4-Cl-1-NpOH + NBS ⟶ **43** 2-24

2-Br-4-Cl-1-NpOH + NBS ⟶ **44** 2-25

1-anthrol + NBS ⟶ **45** 2-26

Next, the reaction of 1-NpOH with NBS in $CDCl_3$ was monitored by ^1H NMR spectroscopy. After mixing $CDCl_3$ solutions of NBS and 1-NpOH in an NMR tube for NMR analysis, the methylene signal of NBS at 2.96 ppm kept decreasing in intensity, while a singlet at 2.75 ppm from succinimide appeared and became more intense as

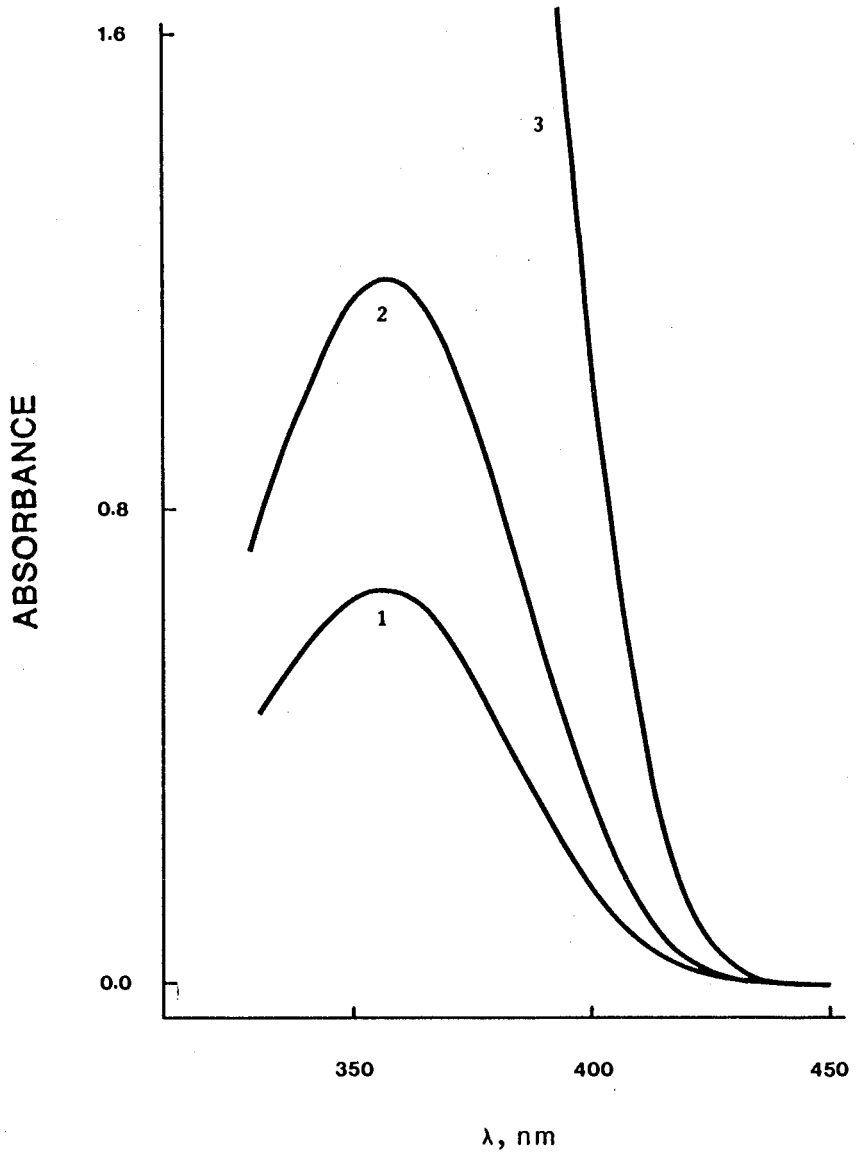

Figure 2-15. Differential absorption spectra.

(1) [NBS]=3.2×10^{-4} M, [1-NpOH]=7.6×10^{-4} M;

(2) [NBS]=1.6×10^{-3} M, [1-NpOH]=7.6×10^{-4} M;

(3) [NBS]=2.0×10^{-3} M, [1-NpOH]=2.5×10^{-3} M;

Table 2-23

UV Absorption Bands and Stability

of 41, 42, 43, 44, and 45 in Dichloromethane

Cmpnd.	λ_{max}, nm	$10^{-3}\epsilon_{max}$	Remarks
41	357	2.0	ϵ(365nm)=1.9x10^3
			$\tau \geq 15$ hr[a]
42	330	5.7	ϵ(355 nm)=4.2x10^3
			$\tau \geq 14$ hr
43	356	2.1	ϵ(375 nm)=1.5x10^3
			$\tau \geq 14$ hr
44	362	2.2	stable
45	396	2.4	$\tau \geq 800$ sec.
	414 (sh)		

a. τ: not the half-life. See the text for the explanation.

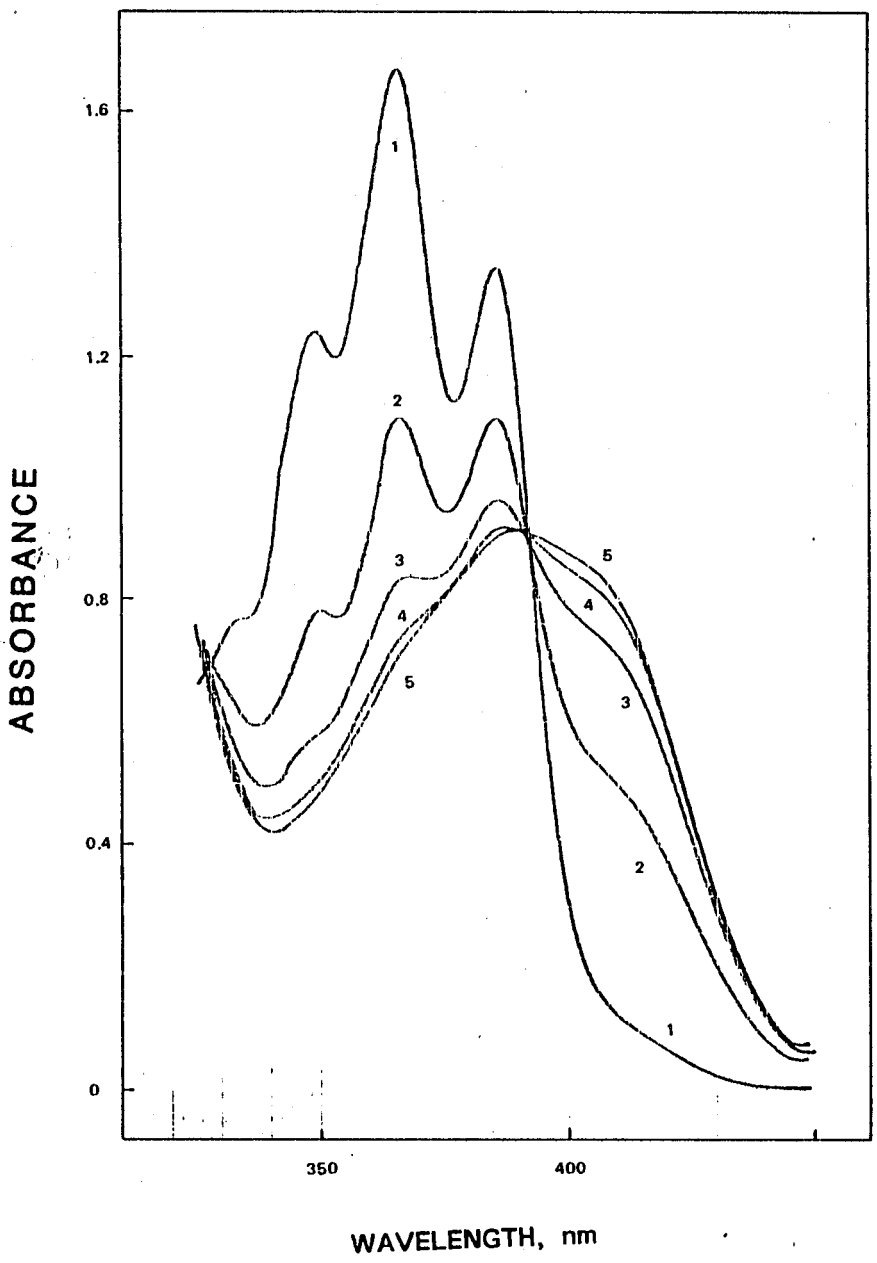

Figure 2-16. Absorption spectra recorded during reaction of 1-anthrol (initially 3.5×10^{-4} M) with NBS (3.6×10^{-4} M) in CH_2Cl_2 at 25°C. Spectra were recorded at the following times (in seconds): 1, 5; 2, 135; 3, 235; 4, 335; 5, 435.

the reaction proceeded. Also, signals of non-aromatic protons (e.g., a doublet at 5.02 ppm) emerged and increased in intensity in contrast to the ever-weakening hydroxy signal of 1-NpOH at 5.3 ppm. This data is listed in Table 2-24. After the intensity of the signals due to the product became constant, the $CDCl_3$ solution was transferred to a 0.1-cm UV cell, and its UV spectrum was recorded. The solution showed an absorption band with λ_{max}=357 nm, and is the same as the band observed from the mixture of 1-NpOH and NBS by UV spectroscopy described previously. This demonstrates that the proton signals recorded in Table 2-24 and the absorption band in Table 2-23 are due to the same species. The reaction of NBS with other naphthols afforded similar results as shown by NMR spectroscopy; the pertinent data are listed in Table 2-24. The chemical shifts of the parent naphthols are also tabulated for comparison.

It should be noted that the NMR data of the products from the reaction of naphthols with NBS were obtained directly from the reaction mixture since most of the products decomposed rapidly when the solutions were concentrated under reduced pressure. Fortunately, most of the signals due to the products are well separated from those of the parent naphthols, NBS, and succinimide.

The reaction of 1-NpOH with NBS in dichloromethane was also followed by IR spectroscopy. The IR spectrum of **41** generated *in*

Table 2-24

^{1}H NMR Parameters of 41, 42, 43, 44 and the Corresponding Naphthols in $CDCl_3$

Cmpnd.	H_1	H_2	H_3	H_4	H_5—H_8
1-NpOH	5.3(s)	6.85(dd)	7.27(dd)	7.40(d)	7.45-8.14
		$J_{2,3}$=6.9	$J_{3,4}$=8.3		
		$J_{2,4}$=1.6			
41		5.02(d)	6.38(dd)	6.70(d)	7.27-8.11
		$J_{2,3}$=4.6	$J_{3,4}$=9.8		
2-NpOH	7.16(s)	5.0(s)	(———	7.32-7.82	———)
42	5.43(s)		6.26(d)	(— 7.16-8.0 —)	
			$J_{3,4}$=10.0		
4-Cl-					
1-NpOH	5.3(s)	6.75(d)	7.40(d)		7.61-8.23
		$J_{2,3}$=8.0			
43		5.11(d)	6.56(d)		7.56-8.42
		$J_{2,3}$=5.5			
2-Br-4-Cl-					
1-NpOH	5.9(s)		7.61(s)		7.56-8.32
44			7.03(s)		7.53-8.29

situ was obtained by subtracting the absorption due to the residual NBS from that due to the reaction mixture (Figure 2-17). The band at 1720 cm^{-1} was easily assigned to the carbonyl stretching of succinimide by running a blank experiment. The new absorption at 1701 cm^{-1} was then attributed to a carbonyl moiety[76] of **41**.

2.5.2. Kinetics of Naphthols Reacting with NBS

The order of the reaction of 1-NpOH with NBS was determined under the experimental conditions where [1-NpOH] and [NBS] were in the range $2.7-5.4\times10^{-4}$ M: doubling of the concentration of either reactant increased the absorbance at 365 nm by a factor of 2.0±0.3 at 20 and 50 seconds after the mixing of reactant solutions. Since second order reaction rate constants calculated from these UV traces agreed well with those (k_2) shown in Table 2-25 (see below), the formation of **41** is first order in each reactant and second order overall.

The rates of formation of **41** were obtained spectrophotometrically by following the absorbance at about 360 nm. Usually, the reactions were carried out under pseudo-first order reaction conditions using excess naphthols. The corresponding graphs of $ln(A_\infty-A_t)$ against time t were linear over at least one half-life (Figure 2-18, A_∞ and A_t being the absorbance at infinite time and at time t). The slopes of the graphs corresponded to the

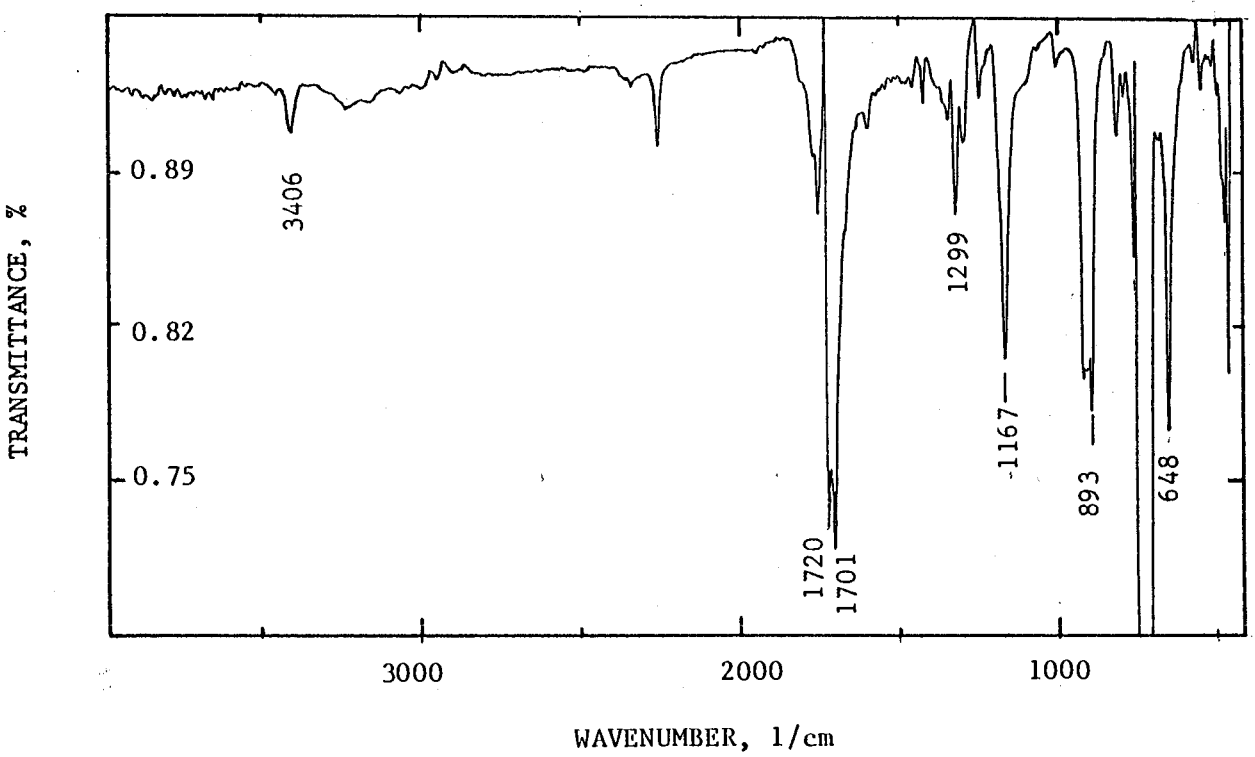

Figure 2-17. The FT-IR spectrum, 35 s after mixing of dichloromethane solutions of 1-NpOH (4.4×10^{-2} M) and NBS (4.1×10^{-2} M); the absorption of NBS has been subtracted.

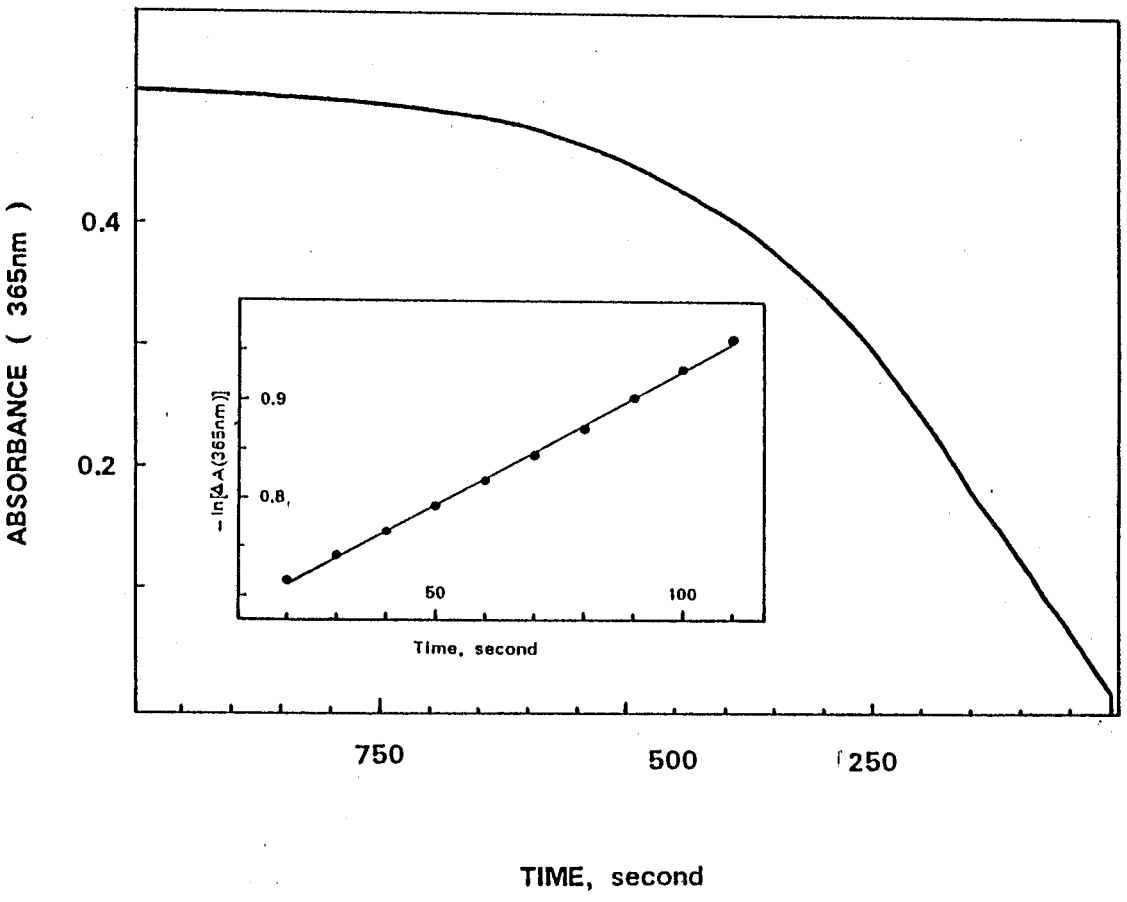

Figure 2-18. A representative single exponential growth of **41** monitored at 365 nm. The insert shows a plot of $\ln(A_\infty - A_t)$ vs. time.

pseudo-first-order rate constants k_{obs} which were then converted to bimolecular rate constants (k_2 in Table 2-25) by simple calculations:

$$k_2 = k_{obs.}/[\text{naphthol}] \qquad 2\text{-}27$$

Since 1-naphthol in dichloromethane had an absorption band at 322 nm, the reaction rate of 1-naphthol with NBS was then studied by monitoring the decrease in absorbance at 322 nm upon mixing 1-naphthol with NBS in CH_2Cl_2 (Figure 2-19). Afterwards the reaction was repeated under the same conditions but the increase in absorbance at 365 nm due to **41** was followed (Figure 2-20). From these two kinetic traces k_{obs} of 0.025 and 0.026 s^{-1}, respectively, were obtained.

In some experiments, a small amount of an olefin, either cyclohexene or DCE (10^{-4}-10^{-5}M) was added to scavenge fortuitous bromine in order to supress radical pathways. It was found, however, that the absence of olefins in the reaction system did not cause any observable difference in the kinetics.

The kinetics of the interaction of NBS with naphthols were sensitive to impurities present in substrates and solvents. For example, the rate increased when NBS was used without purification. In particular, the presence of trace amounts of hydrochloric acid ($<10^{-6}$ M) accelerated rates substantially (see Table 2-25 and its footnotes e and c).

Table 2-25

Rate Constants for the Formation of 41, 42, 43, 44, and 45 in Dichloromethane at 25±1°C

[NpOH] M	[NBS] M	$10^4 k^a_{obs}$ s^{-1}	$10k_2$ $M^{-1}s^{-1}$	λ(monit) nm[b]
1-NpOH				
7.97×10^{-3}	5.26×10^{-4}	30±6	3.8±0.8	360(5)
7.80×10^{-3}	5.09×10^{-4}	27±4	3.5±0.5	360(5)
8.06×10^{-3}	4.91×10^{-4}	98±10	12±1	360(2)[c]
1-AnOH				
6.1×10^{-3}	3.1×10^{-4}	1.5×10^{3}	2.5×10^{2}	430(1)
3.5×10^{-4}	3.6×10^{-4}	-	2.0×10^{2}	430(1)
2-NpOH				
7.7×10^{-3}	4.25×10^{-4}	85±11	11±2	350(3)
9.7×10^{-4}	2.75×10^{-4}	-	1.0×10^{3}	350(1)[d,e]
4-Cl-1-NpOH				
6.93×10^{-3}	4.10×10^{-4}	7.3±2.0	1.0±0.3	365(2)
2-Br-4-Cl-1-NpOH				
6.92×10^{-3}	4.20×10^{-4}	2.5±0.5	0.36±0.07	370(2)

a. The correlation coefficients were ≥0.998.
b. The figure in the parenthesis is the number of runs.
c. 7×10^{-7} M HCl was present in the solution.
d. Measured under second order reaction conditions.
e. NBS was used as supplied in this experiment.

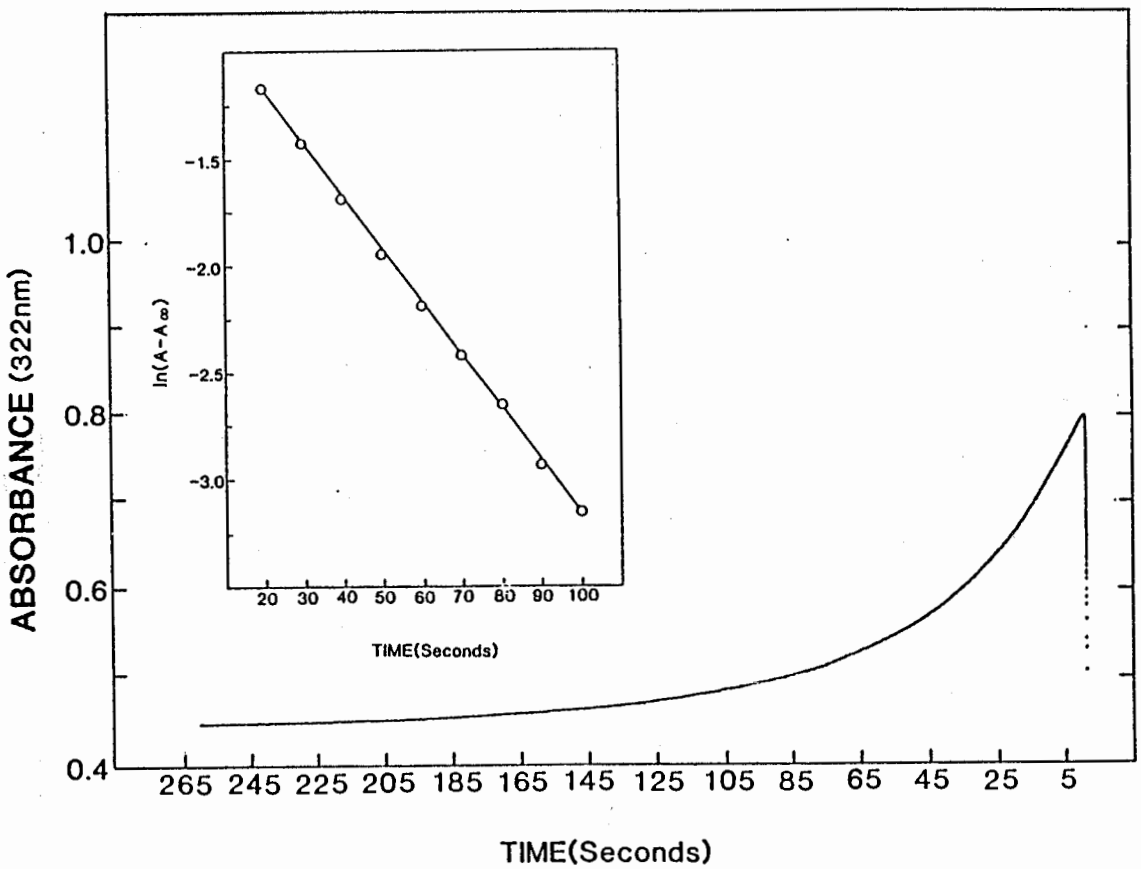

Figure 2-19. A representative.single exponential decay of 1-naphthol monitored at 322 nm. The insert shows a plot of $\ln(A_t - A_\infty)$ vs. time (sec).

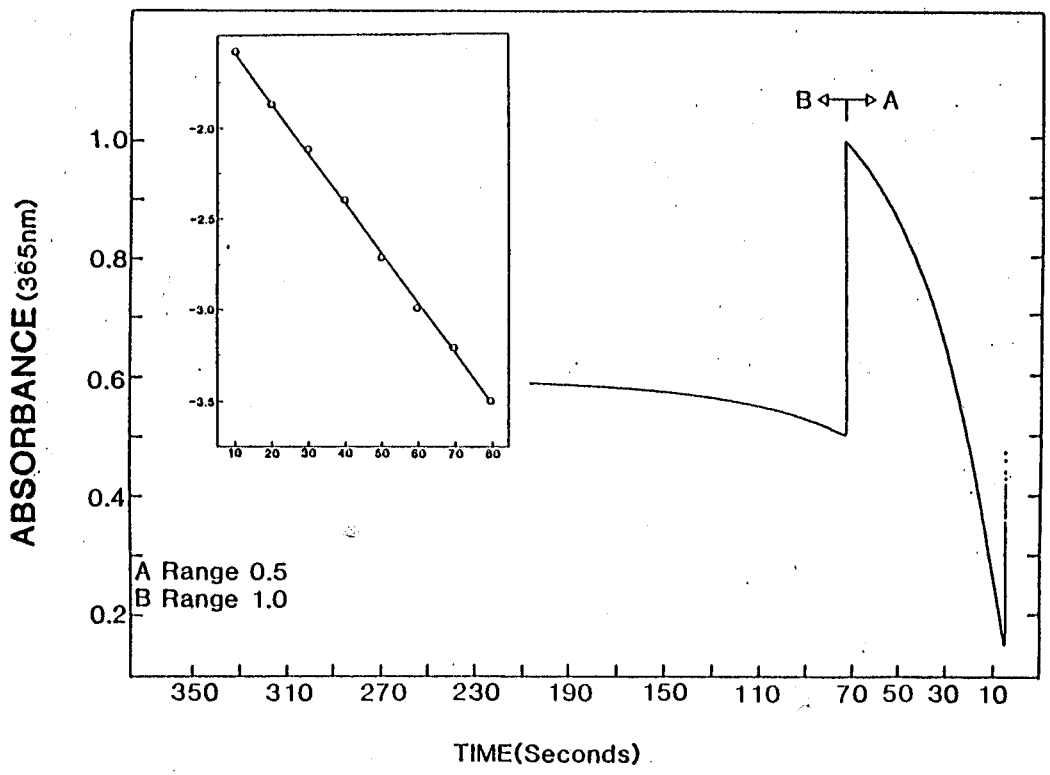

Figure 2-20. A representative single exponential growth of **41** monitored at 365 nm. The insert shows a plot of $\ln(A_{t\,\tau}-A_t)$ vs. time.

2.5.3. Determination of ϵ Values for 41, 42, 43, 44, and 45

In a series of experiments, an excess of 1-NpOH in dichloromethane (3.74×10^{-3}M) was allowed to react with dichloromethane solutions of NBS, the concentration of the latter ranging from 2.5×10^{-5} to 3.9×10^{-4}M. The absorbance at 365 nm after the completion of the reaction was recorded and the values were plotted against the concentration of NBS to give a straight line (Figure 2-21). Its slope represents the molar absorptivity of **41** ($\epsilon = 1.9 \times 10^{3}$, note that 365 nm is not the λ_{max} of **41**). The ϵ values of **42**, **43**, **44**, and **45** were determined in a fixed ratio of [naphthol]/[NBS] with the naphthol in excess, by the use of

$$\epsilon = A_{\infty}/[\text{NBS}] \qquad 2\text{-}28$$

A_{∞} was obtained from a kinetic profile of A_t vs. time t as in Figure 2-18.

2.5.4. Decomposition of 41

After **41**, **42**, **43**, and **44** were formed, they decomposed slowly in the dark at room temperature. For example, the complete decomposition of **41** took more than twenty hours. The decay of the absorbance of **41** which was followed near its λ_{max} did not fit either the equation of the first-order decay or that of the second-order decay. When the data from the decay curve were

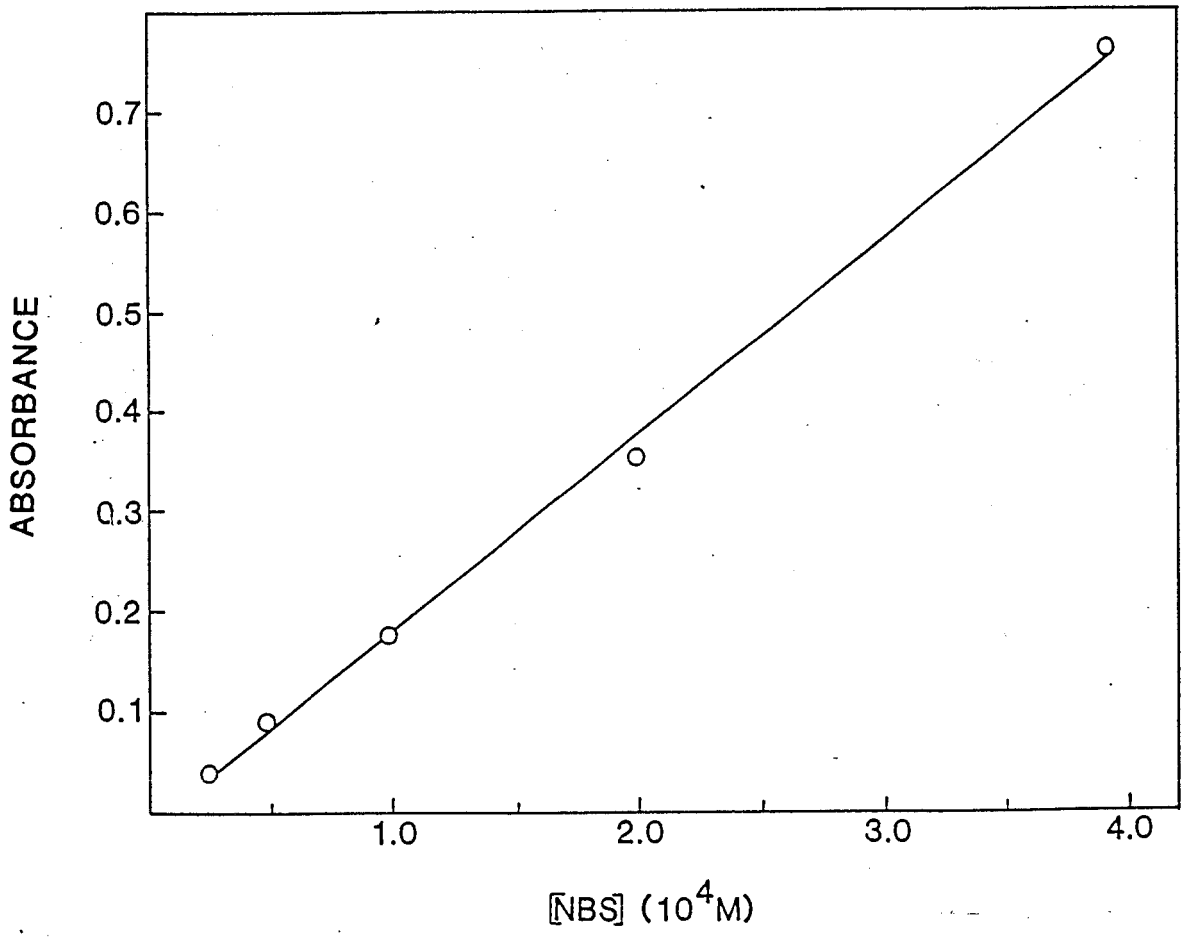

Figure 2-21. Plot of the maximum absorbance at 365 nm due to **41** against the concentration of NBS in CH_2Cl_2 in the presence of 3.74×10^{-3} M 1-naphthol (initial concentration). A small amount of cyclohexene was used to scavenge the fortuitous bromine (the molar ratio of cyclohexene/NBS was 1:5).

treated as a first order decomposition, the plot of $\ln(A_\infty - A_t)$ against time t showed a upward curvature. The same situation occurred when the same data were analysed assuming second order kinetics. These upward curvatures in the plots indicate the decomposition of **41** become faster and faster as the time increased. The time required for the absorbance of **41** at 365 nm to decrease to its half-value, τ, is listed in Table 2-27. The τ values for **42**, **43**, **44**, and **45** are also given in the same Table. These τ's are not true half-lives of these products because of the kinetic complications.

Acid accelerated not only the formation of **41** but also its decompositions. When a small amount of hydrochloric acid (*ca* 7×10^{-7} M) was added, the decomposition of **41** ($\simeq5\times10^{-4}$ M in CH_2Cl_2) showed an excellent first-order decay with a half-life of 40 minutes. The half-life of **41** was further shortened to 10 seconds if 4×10^{-4} M hydrochloric acid was present in the CH_2Cl_2 solution of **41**. Under these conditions, however, the rate constants for the decomposition of **41** did not represent the true value for the unimolecular decomposition of **41**.

41, **42**, and **43** were unstable in aqueous acetic acid solution and decomposed rapidly. For example, when 0.1 ml of CH_2Cl_2 solution of NBS (0.05 M) was added into 3 ml of 90% acetic acid solution of 1-NpOH (0.02 M), the formation of **41** was completed within ten seconds followed by a rapid decomposition. 50% **41** was

decomposed within one minute.

2.5.5. Photodecomposition of 41

A dichloromethane solution of **41** prepared *in situ* in a quartz cuvette was exposed to unfiltered room light or light filtered with a GWV filter and the absorbance at 365 nm was recorded as a function of irradiation time. The plot is linear, indicating a zero order reaction up to 85% conversion (Figure 2-22). The quantum yield of the photodecomposition of **41** was then measured. Dichloromethane solutions of **41** prepared *in situ* were irradiated with monochromatic light (λ=365 nm); the intensity of the incident light had been determined with benzophenone-benzhydrol actinometry as the secondary reference[78]. In a typical experiment, the *observed* quantum yield of 0.66 was obtained for a solution of **41** showing an absorbance change from 0.56 to 0.47: extrapolation to the total absorbance of incident light by **41** gives the *actual* quantum yield of 0.9-1.0. For dichloromethane solutions of **41** with absorbances higher than 1, the observed quantum yield was 1.0±0.1.

2.5.6. Product Distribution of Photodecomposition of 41

41, **42**, and **43** decomposed thermally and photochemically to afford bromonaphthols. For example, the decomposition of **41**

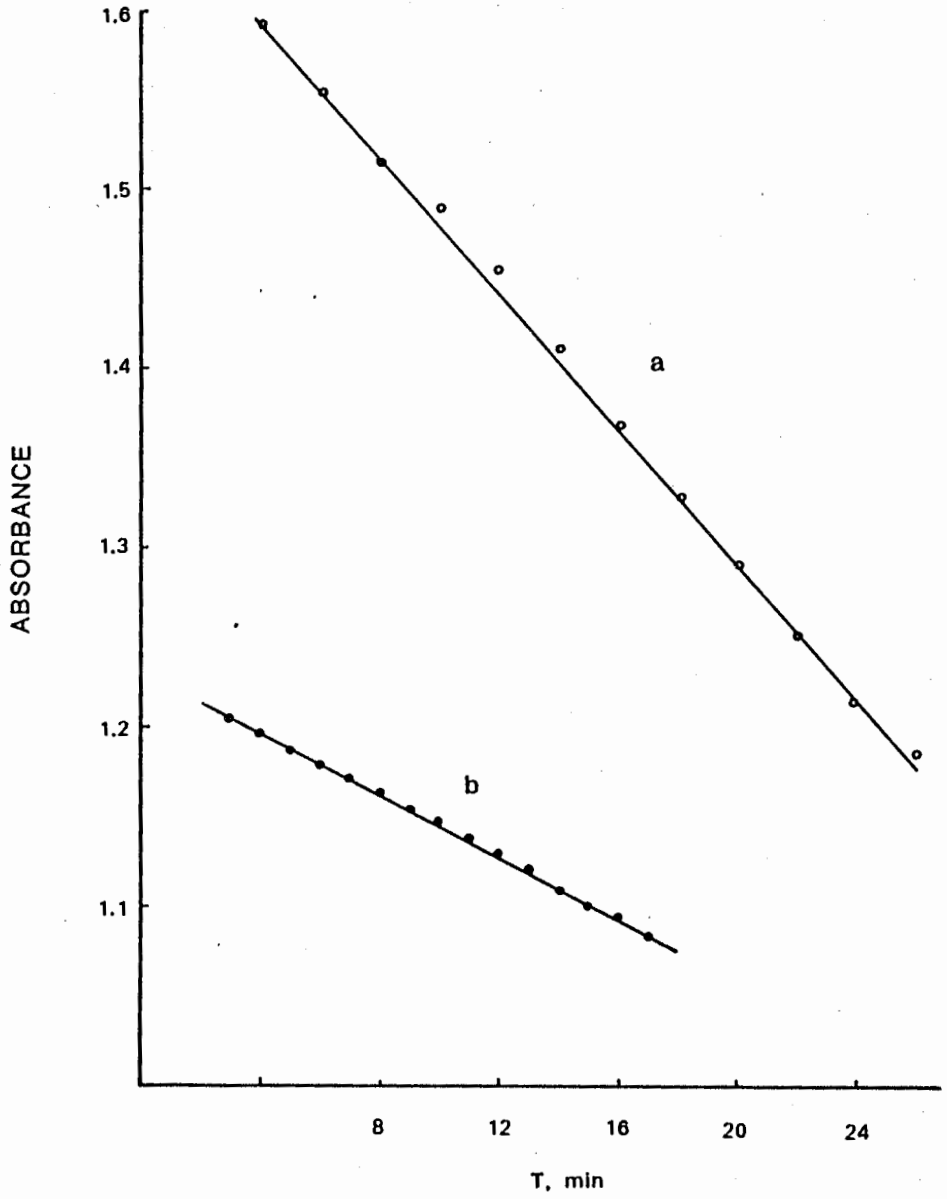

Figure 2-22. Linear decays of 41 monitored at 365 nm.

(a) Caused by room light,

(b) Caused by room light filtered through a GWV filter.

produced 2-bromo-1-NpOH and 4-bromo-1-NpOH, **42** produced 1-bromo-2-NpOH, **43** produced 2-bromo-4-chloro-1-NpOH and **45** produced 2-bromo-1-anthrol.

The product distribution in the photodecomposition of **41** was studied as follows in various solvents. The solutions of **41** were prepared *in situ* with an excess of 1-NpOH and were irradiated with a mercury lamp through a GWV filter to photoexcite **41** alone at >380 nm. The yellow color due to **41** was bleached within fifteen minutes. The yields of 2-bromonaphthol and 4-bromonaphthol produced in the photolysate were analysed by GC with anthracene as an internal standard. The results are tabulated in Table 2-26. It was found that 2-bromo-1-NpOH was the major product whilst the yield of 4-Br-1-NpOH increased significantly as the polarity of solvents increased. These effects of solvent polarity are similar to those observed in the bromination[50,79] of phenols. When unpurified NBS was used to prepare **41**, a higher yield of 4-Br-1-NpOH was obtained after the *in situ* prepared **41** was photolyzed (experiments 197, 200, and 201). When the thermal decomposition of **41** was allowed to preceed for a longer time, the yield of 4-Br-1-NpOH was also slightly increased. In certain photoreactions, 1-methoxynaphthalene (1-$NpOCH_3$) was added as a competing substrate to solutions of **41**. The amount of 4-bromo-1-methoxynaphthalene (4-Br-1-$NpOCH_3$) was negligibly small, indicating that **41** is a poor brominating reagent. The mixture of NBS and 1-methoxy-naphthalene in dichloromethane in the dark for six

Table 2-26

Product Distributions

of Photodecomposition of 41

Expt.	10^2[1-NpOH] M	10^2[NBS] M	Solvent	Product[a] %	
				2-Br	**4-Br**
188	1.4	0.49	Benzene	81	5.3
189	1.7	1.3	Benzene	85	2.6
190	2.6	1.4	Dioxane	75	6.0
191	2.5	1.2	Dioxane	82	5.0
192	5.9	2.75[b]	CCl_4	37	7
193	2.0	1.8	CH_2Cl_2	78	7
194	0.93[c]	0.69	CH_2Cl_2	67	5.8
195	1.8	1.4	CH_2Cl_2	85	9[d]
196	2.0[e]	2.0	CH_2Cl_2	65	12
197	0.5[f]	0.5	CH_2Cl_2	63	24
198	0.43	0.38	CH_3CN	50	17
199	0.62	0.57	CH_3CN	44	28[d]
200	2.4[f,g]	1.9	CH_3CN	29	46
201	2.4[f,h]	1.9	CH_3CN	29	44

a. Based on the amount of NBS used in preparation of **41**. **2-Br:** 2-Br-1-NpOH; **4-Br:** 4-Br-1-NpOH.

b. Heterogeneous throughout because of low solubility of NBS in

CCl_4. The photolysate was separated from the remained NBS, washed, and dried before GC analysis.

c. In the presence of 8.65×10^{-3} M 1-methoxynaphthalene, small amount of 4-bromo-1-methoxynaphthalene (<1%) was detected.

d. Photolysis was executed one hour after **41** was formed.

e. Decomposed in the dark as comparison.

f. Unpurified NBS was used.

g. In the presence of 3.1×10^{-3} M DCE.

h. In the presence of 4.35×10^{-3} M 1-methoxynaphthalene, a small amount of 4-bromo-1-methoxynaphthalene (<1%) was detected.

hours produced no brominated products.

In order to confirm that the bromination of naphthols with NBS is not due to Br_2 in a low concentration but results from the decomposition of **41** itself, some control experiments were carried out. They were competitive brominations of mixtures of 1-NpOH and 1-NpOCH_3, and they were carried out either in the dark or under illumination (Table 2-27). When Br_2 was used as the brominating reagent, 2-bromo-1-NpOH and 4-bromo-1-NpOH in addition to 4-bromo-1-methoxynaphthalene were formed, the ratios being 1:0.6:0.8. A similar reactivity trend has been reported[80]. In contrast, NBS reacted exclusively with 1-NpOH to produce bromonaphthols, showing minimal reactivity towards 1-NpOCH_3 (see the last experiment in Table 2-27).

Table 2-27

Competitive Bromination of 1-Naphthol (OH) and 1-Methoxynaphthalene (OCH_3) in Dichloromethane

10^2[OH] M	10^2[OCH_3] M	10^2[XBr][a] M	Product ratio[b]		
			2-Br-OH	**4-Br-OH**	**4-Br-OMe**
1.2[c]	1.1	0.7	1.0	0.62	0.77
1.2[d]	1.1	0.7	1.0	0.57	0.87
1.3[e]	1.0	0.6	1.0	0.57	0.78
1.3[f]	1.0	0.6	1.0	0.62	0.50
0.9[a]	0.87	0.6	1.0	0.083	<0.04

a. Br_2 was used in all of these experiments except the last one in which NBS was used as brominating reagent.

b. **2-Br-OH:** 2-Br-1-NpOH; **4-Br-OH:** 4-Br-1-NpOH; **4-Br-OMe:** 4-Br-1-NpOMe.

c. A CH_2Cl_2 solution of Br_2 was added while the substrate to be brominated was being irradiated with a 410±6 nm light source (200 watts Xe/He lamp, Kratos intensive monochromator).

d. This experiment was carried out in the dark for 30 minutes and a colorless solution was obtained.

e. A solution in which the molar ratio of $K_2CO_3/Br_2 \geq 5$ was exposed to room light until the the brown color disappeared.

f. A CH_2Cl_2 solution of Br_2 was added while the substrate to be brominated was being irradiated with a 450 watts medium pressure Hanovia mercury lamp through a Pyrex filter.

CHAPTER THREE

DISCUSSION

Section I. Photodecomposition of NBS

3.1.1. Generation of Succinimidyl Radicals

Experiments 8 and 9 in Table 2-1B restate the well-known fact that irradiation of NBS in the presence of an olefin (which contains no readily abstractable hydrogens) to scavenge Br_2 and/or Br· affords a good yield of BPI[18,29]. It is evident that the succinimidyl radical (S·) is generated by photodecomposition of NBS, and the succinimidyl radical undergoes ring opening followed by reaction with NBS to produce BPI (which was isolated as BPA) (see Eq 3-1 — 3-3). The last step also propagates the succinimidyl radical chain.

$$\text{NBS} \xrightarrow{h\nu} \text{S}\cdot + \text{Br}\cdot \qquad 3\text{-}1$$

$$\text{S}\cdot \longrightarrow \text{PI}\cdot \qquad 3\text{-}2$$

$$\text{PI}\cdot + \text{NBS} \longrightarrow \text{BPI} + \text{S}\cdot \qquad 3\text{-}3$$

The fact that BPI is also generated by selectively irradiating

Br_2 in NBS-Br_2 systems (Experiments 1-4, Table 2-1) indicates that Br· initiates the decomposition of NBS to generate S· (Eq. 3-4 and 3-5) and hence BPI.

$$Br_2 \xrightarrow{h\nu} 2Br\cdot \qquad 3\text{-}4$$

$$Br\cdot + NBS \rightleftharpoons Br_2 + S\cdot \qquad 3\text{-}5$$

Comparing the high yields of BPI in experiments 8 and 9 with the low ones in experiments 1-4 (Table 2-1) suggests that the S· chain does not prevail when the decomposition of NBS to form S· is initiated by Br· because S· is easily trapped by Br_2 via the reverse of Eq 3-5 (see Section 3.1.2).

3.1.2. Effects of [Br_2] on the Yield of BPI

Suppression of the percent yield of BPI with the increase in bromine concentration in the NBS-Br_2 system is demonstrated in Tables 2-1, 2-3, 2-4 and 2-7 and Figures 2-2, 2-5, and 2-6; the higher the concentration of Br_2, the lower the percent yield of BPI, regardless of whether NBS or Br_2 in the NBS-Br_2 system is irradiated. Those observations can be satisfactorily explained if a rapid equilibration occurs as shown in Eq. 3-5. Since the dissociation energy of the N-Br bond of NBS[86] is comparable to that of the Br-Br bond of Br_2[87-89] the ΔH of reaction 3-5 is

close to zero. When concentration of Br_2 is high the succinimidyl radical generated through the forward reaction of Eq 3-5 will have better chance to be intercepted by Br_2 to form Br· and NBS. Therefore, the formation of BPI is suppressed. It is particularly noteworthy from Figure 2-2 that the presence of 0.2 mM Br_2 is effective in reducing the yield of BPI from 76% to 3%. If the percent yield of BPI is taken as the extent to which the concentration of the succinimidyl radical is generated in the bromine atom-initiated decomposition of NBS, these data imply that S· is rapidly scavenged by ≃2 mM Br_2 (see Table 2-1A). In bromine atom-initiated reactions (see Figure 2-2, 2-5, and 2-6), the rate of bromine atom generation must remain nearly constant at >10 mM Br_2 because 99-100% of incident light (λ>380 nm) is absorbed by Br_2 (see the absorption spectrum of Br_2, Figure 2-1). In other words, the further increase in $[Br_2]$ does not increase the amount of Br· generated by the irradiation. The steady decrease in the percent yield of BPI with the increase in $[Br_2]$ is a good indication that the succinimidyl radical is scavenged by Br_2 more efficiently, i.e. the equilibrium (Eq. 3-5) is shifted to the left at higher $[Br_2]$. The r values in the presence of Br_2 (Table 2-7) are also drastically reduced from ≃190, the selectivity of the succinimidyl radical (see Table 2-5).

3.1.3. Mixed Chains

The selectivity of the NBS-DCE system shown in Tables 2-5 is substantially different from that of bromine atoms (see Table 2-6). It suggests that as long as the olefin maintains the concentration of Br_2 at levels too low to compete with NBS in trapping of radicals (see Eq 3-8 and 3-7 in Section 3.1.4), the succinimidyl radical is the major chain carrier in the hydrogen abstraction step. Table 2-7 exhibits an unusual feature; as $[Br_2]$ increases, the BPI yield decreases steadily and the r value is close to the selectivity of bromine atoms. (A clearer indication of the trend can be seen in Table 2-11 and 2-13 in which the r value changes from the value for imidyl to the value for bromine atoms as the Br_2 concentration is increased). These data strongly suggest that both the succinimidyl radical and the bromine atom chains are involved in the NBS-Br_2 system, their relative contribution to the product distribution being strongly affected by the concentration of Br_2. The r values of the NBS-Br_2 system shown in part A and B of Table 2-7 are very close to each other, and are almost the same as that of bromine atoms. This indicates that bromine atoms are largely involved as the chain carriers in the intermolecular hydrogen abstractions from cyclohexane and CH_2Cl_2, no matter whether the reaction is initiated by irradiation of Br_2 or by NBS. It follows that the succinimidyl radical, regardless of the mode of irradiation, quickly undergoes two competing reactions, namely, the ring opening to PI· and

trapping by Br_2 (Scheme 3-1). In bromine atom-initiated reactions (Table 2-7A), the *r* values of 17-22 and the decrease in the percent yield of BPI with the increase in $[Br_2]$ suggest that the equilibrium in Scheme 3-1 shifts to the left as $[Br_2]$ increases, causing lower concentrations of succinimidyl radical in the reaction system. The bromine atom generated simultaneously in the process abstracts hydrogen from the hydrocarbons (cyclohexane and dichloromethane), making the predominant contribution to the *r* value observed in Table 2-7 (schemes 3-1 and 3-2).

3.1.4. Effects of Hydrocarbons on the Yield of BPI

As shown in Figure 2-5 the percent yield of BPI in the NBS-Br_2 system increases with the increase in the concentration of cyclohexane. Unlike dichloromethane[84,85], cyclohexane has the secondary CH bonds susceptible to hydrogen abstraction by bromine atoms[33], thereby generating the C_6H_{11} radical. The latter, in turn, generates a succinimidyl radical by bromine atom transfer from NBS as shown in Eq 3-7 where R· stands for the C_6H_{11} radical or any other alkyl radical.

$$R\cdot + NBS \longrightarrow RBr + S\cdot \qquad 3\text{-}7$$

In bromine atom-initiated bromination the addition of cyclohexane to the NBS-Br_2 system, no doubt, causes higher BPI yields through this route as shown in Figure 2-5 and Table 2-4.

Scheme 3-1. Relationship between the succinimidyl radical and the bromine atom

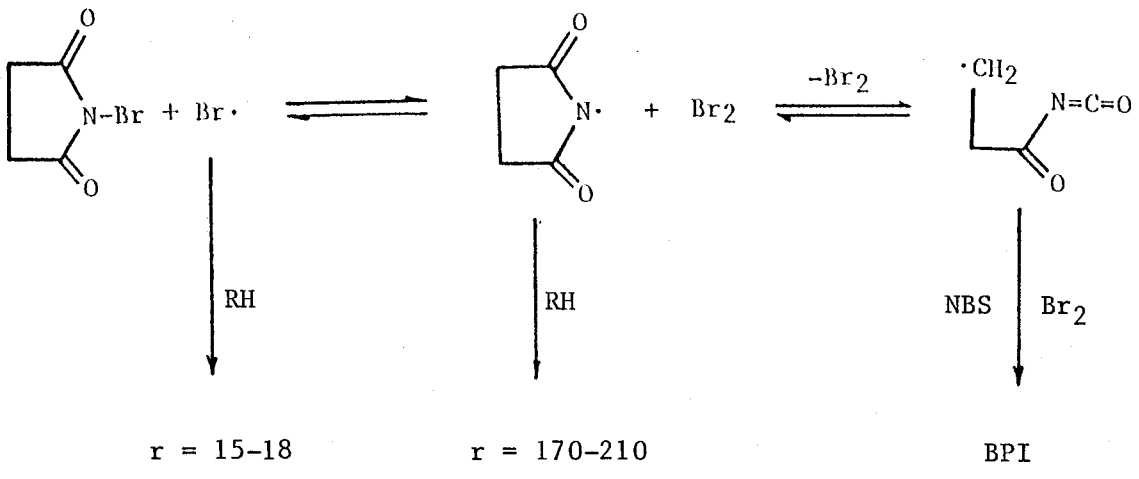

Scheme 3-2. Cyclic diagram for photobromination of RH by Br_2

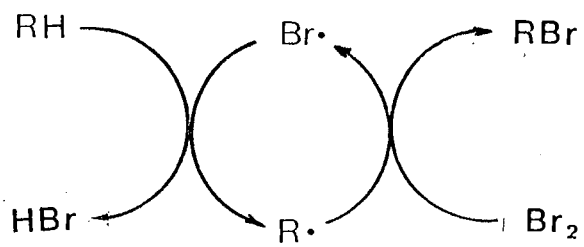

RH stands for mixtures of cyclohexane and CH_2Cl_2

Addition of 2,2,3,3-tetramethylbutane (C_8H_{18}) to the NBS-Br_2 system also increases the percent yield of BPI, but the increment is smaller than that caused by the addition of cyclohexane (comparing Table 2-3 with 2-4). The C_8H_{18} has primary CH bonds which are less reactive than cyclohexane towards hydrogen abstraction by bromine atoms[90] (Eq. 3-9). The C_8H_{17} radical is thus generated from C_8H_{18} less efficiently than the cyclohexyl radical is from cyclohexane. The increment in the yield of BPI by addition of C_8H_{18} to the NBS-Br_2 system is therefore smaller. When the hydrocarbon is added into the NBS-Br_2 system, the increment in the yield of BPI is much larger at 0.001 M Br_2 than that at 0.02 M Br_2 (compare the slopes of the two lines in Figure 2-5). This can be interpreted as follows: when the concentration of Br_2 is high, the cyclohexyl and C_8H_{17} radicals preferentially abstract bromine atoms from Br_2 instead of from NBS (see Eq 3-8 and 3-7).

$$R\cdot + Br_2 \longrightarrow RBr + Br\cdot \qquad 3\text{-}8$$

This causes the decrease in the yield of BPI as the concentration of Br_2 increases. Nevertheless, when $[Br_2] \simeq 20$ mM, the BPI yield remains as high as 8-10% as shown in Tables 2-4 and 2-7. This is surprising since the ratio of the rate of bromine-transfer from Br_2 (Eq 3-8) to that from NBS (Eq 3-7) is >100. This ratio is calculated by taking a conservative value of $k_{3\cdot7}/k_{3\cdot8} = 1/500$, which is one-half the value[29,91] reported by

Skell, $[Br_2]$=20 mM, and the maximum [NBS]=100 mM. This discrepancy indicates that $k_{3\cdot7}/k_{3\cdot8}$ is probably larger than that estimated by Skell; this is also suggested by the following argument.

3.1.5. Formation of Br_2 during Photolysis

In either mode of irradiation, i.e. whether NBS or Br_2 is irradiated, a significant increase in observed $[Br_2]$ in the photodecomposition of the NBS-Br_2 system was observed (Table 2-7); this phenomenon has been known for a long time[4,31,44,48] but no explanation has been proposed. The data in Table 2-7A reveal that the observed $[Br_2]$ is approximately three times the initial $[Br_2]$ when the latter is 0.75 mM. When the NBS-Br_2 system is photolysed with 86 mM Br_2, however, no increase in the concentration of Br_2 was observed during the irradiation. These discoveries suggest the following explanation. When Br· is generated by photolysis of Br_2 in the NBS-Br_2 system, it abstracts hydrogen from RH (e.g., cyclohexane or dichloromethane) to generate HBr (Eq. 3-9) followed by the formation of one Br_2 (Eq. 3-10).

$$Br\cdot + RH \longrightarrow R\cdot + HBr \qquad 3\text{-}9$$

$$HBr + NBS \longrightarrow Br_2 + SH \qquad 3\text{-}10$$

At high [NBS]/[Br_2] ratios, i.e. when [Br_2] is low, the R· (and PI·) react with NBS preferentially instead of with Br_2 in the subsequent process of bromine atom transfer (Eq 3-7). Therefore, whenever a bromine atom abstracts a hydrogen from RH, one R· is generated and one Br_2 is formed by Eq. 3-10. The R· then abstracts a bromine atom from NBS to generate succinimidyl radical, and the latter may open its ring to lead, at last, to BPI. On the other hand, at low [NBS]/[Br_2] ratios, for example, the photolysis of the NBS-Br_2 system is carried out at >50 mM Br_2 (which means [NBS]/[Br_2] $\simeq$1 when 50% NBS is consumed), the bromine atom transfer from Br_2 through reaction 3-8 becomes capable of competing with reaction 3-7. When a molecule of Br_2 is consumed through reactions 3-8 and 3-9, a molecule of Br_2 is concurrently generated through reactions 3-9 and 3-10. The concentration of Br_2 should remain constant. It is surprising that even at an initial concentration of 20 mM Br_2 [Br_2] does increase with the progress of bromination (Table 2-7). Taking [Br_2]=20 mM and [NBS]=100 mM as the concentrations when the rates of bromine atom transfer are about the same for both reagents (NBS and Br_2), the ratio of $k_{3\cdot7}/k_{3\cdot8}$ is calculated to be 1/5, much lower than 1/1000 reported before by Skell[91] and quoted subsequently[29]. After this result was published[108], Skell reinvestigated the rate constant for the bromine atom transfer and a ratio of 1.5/2.2 was reported[27].

3.1.6. Comparison of Bromination Rate of Hydrocarbons by NBS-DCE and Br_2-K_2CO_3

Cyclohexane, 3,3-dimethylpropane, dichloromethane and some other hydrocarbons have been photobrominated with either Br_2 or Br_2-NBS as bromination reagents. The relative rate has been a problem since Skell reopened the controversy. Walling and co-workers[18] reported at first that the rate of bromination with Br_2 alone was at least ten times slower than that with Br_2-NBS. Based on the difference in the rate, they proposed that the chain carrier in the NBS-Br_2 system was not the bromine atom. After recently adopting the mixed chain hypothesis, however, they predicted the rates should not be different in these two systems, and the slower rate observed with Br_2 was attributed to a failure to remove the hydrogen bromide produced in the reactions[31,57].

Bromination rates of cyclohexane-dichloromethane by the Br_2-K_2CO_3 and by the Br_2-NBS systems are certainly different. This is the result of the parallel experiments shown in Table 2-8. The rate increment observed in the latter system is too small to be significant in the radical chain reactions, since its rate measurement can be easily plagued by several factors[14] such as the mode of termination, the presence of trace impurities etc. In the experiments reported in Table 2-8, the concentrations of Br_2 and the rate of generation of Br· by photolysis of Br_2 have been maintained as constant as could be in the

parallel experiments to obtain a meaningful comparison. The small difference in the bromination rates may be attributed to a difference in the way that the Br· is aggregated or weakly complexed in the two systems. Therefore, the reactivity of the bromine atom is somewhat modified in intermolecular hydrogen abstraction, but the selectivity shown remains essentially that of Br· in both systems. It follows that the bromine atom-initiated decomposition of the NBS-Br_2 system is propagated by succinimidyl radicals and bromine atoms as reactive intermediates without the necessity of involving another radical intermediate. It also follows that all the observed chemistry of the NBS-Br_2 system, except the extra BPI formation,[1] is a continuum of two extremes — the chemistry of the bromine atom and that of the succinimidyl radical. The position of the observed chemistry in the continuum is affected by several factors such as the concentrations of NBS and Br_2, the conversion of NBS, etc. (see Section 3.1.7)

3.1.7. Factors Affecting the Yield of BPI in NBS-Br_2 System

As shown in previous sections, there is an equilibrium between bromine atoms and succinimidyl radicals in the NBS-Br_2 system. The dynamics of the equilibrium is governed by several factors which affect the formation of the succinimidyl radical,

---

[1]The extra BPI is the differential yield of BPI obtained by the two modes of irradiation (see Figures 2-2 and 2-6).

therefore, the formation of BPI.

(1) The concentration of Br_2. The increase in $[Br_2]$ shifts the equilibrium (Eq. 3-5) to the left. Therefore, the yield of BPI is reduced because of the lower concentration of succinimidyl radicals, and the *r* value of the system becomes closer to that of the bromine atom.

(2) The $[NBS]/[Br_2]$ ratio. The higher the ratio, the higher the concentration of succinimidyl radicals by reaction 3-7 and thus higher BPI yields. Since the concentration of NBS decreases with the consumption of NBS during the process of photolysis, the $[NBS]/[Br_2]$ ratio keeps changing. Therefore, it is only meaningful to compare the yield of BPI under the same initial concentrations of NBS and Br_2, and the same conversion of NBS. This is a important factor to be kept in mind in comparing the data from different groups. Unfortunately it has been overlooked in the recent controversy.

(3) The presence of hydrocarbons possessing hydrogens susceptible to hydrogen abstraction by bromine atoms. Cyclohexane and 2,2,3,3-tetramethylbutane are such hydrocarbons. The presence of the hydrocarbon in the NBS-Br_2 system opens a new avenue for the reaction of bromine atoms (Eq 3-9), and, in turn, a new pathway for the generation of succinimidyl radicals (Eq 3-7). Therefore, more BPI is produced.

(4) The presence of hydrocarbons possessing benzylic hydrogens. Photolysis of Br_2 in the presence of NBS and toluene afforded only benzyl bromide and no BPI. This is because reaction 3-11 is very facile[92-95], and the succinimidyl chain is totally supressed.

$$Br\cdot + CH_3C_6H_5 \longrightarrow \dot{C}H_2C_6H_5 + HBr \qquad 3\text{-}11$$

This facility may arise from a complex formation between Br· and toluene, since the modification of the reactivity of the halogen atom in aromatic solvents is well established[96-99].

3.1.8. The Extra BPI Formation

Figure 2-2 and 2-6 show that direct irradiation of NBS generates more BPI than does irradiation of the Br_2 in the NBS-Br_2 system. The differential yield of BPI, i.e. the extra BPI, is also observed in Table 2-7. Carefully examination of the table reveals that the direct irradiation of NBS increases the yield of BPI but does not make the *r* value of the system any closer to that of the succinimidyl radical ($\simeq$190, see Table 2-5). It is proposed that the extra BPI does not result from the ring opening of the succinimidyl radical but from a precursor of the succinimidyl radical and that Br_2 in the system does not intercept the precursor as efficiently as it intercepts the succinimidyl radical.

Most photodecompositions reported in recent years from Skell's, Tanner's, and Walling's groups were carried out with Pyrex filters and therefore, the reported yields of BPI must certain fractions which result from direct excitation of NBS in the NBS-Br_2 system (see Figure 2-2 for the differential yields of BPI caused by their techniques). There was a lingering debate between Skell[4,25,34,44,48,57] and Walling[18] and Tanner[31,33,35,49] on whether BPI is formed in the NBS-Br_2 system and whether it is due to the Sσ or the succinimidyl radical (see Chapter 1 for details). However, the BPI formation from photolysis of NBS through Pyrex filters should not be used for diagnoses of the mechanism of the photolysis of the NBS-Br_2 system because of the formation of the extra BPI.

3.1.9. Effects of Benzene Concentration on the Quantum Yield of BPI Formation.

The graph of the quantum yield ratio against the concentration of benzene (Figure 2-7) levels off as the concentration of benzene increases. Figure 2-7 is very similar to the plot of Φ^0/Φ against the concentration of naphthalene reported by Ullman and co-workers[100] where Φ^0 and Φ are the quantum yields of pyrylium oxide formation from 2,3-diphenylindenone oxide in the absence and presence of naphthalene. Since naphthalene only quenches the triplet state reaction but fails to do so with the

singlet reaction, a level-off has been observed in the plot. Such a level-off in the plot of Φ^0/Φ against the concentration of a quencher has been regarded as characteristic of a reaction system in which i) two distinctive intermediates afford the same product and ii) only one of them is quenchable by the quencher. For example, both the singlet and the triplet cyclohexanones undergo a Norrish Type II reaction. But only the triplet reaction can be quenched by 1,3-pentadiene. The plot of Φ^0/Φ against the concentration of the olefin does show a level-off[101], where Φ^0 and Φ are quantum yields of type II product formation in the absence and the presence of 1,3-pentadiene respectively. Intuitively the asymptote in Figure 2-7 suggests that a part of the total BPI formation can not be quenched (or intercepted) even at high concentrations of benzene. Figure 2-8 shows a non-zero intercept. It indicates that ϕ/ϕ_n is not zero as 1/[benzene] approaches zero, i.e., as [benzene] becomes extremely high. Since ϕ_n is by no means zero in the presence of benzene, it follows that ϕ must be nonzero. That is, the quantum yield (or the yield of BPI) will not approach zero as [benzene] becomes very high. The feature strongly supports the proposal that the BPI formation from the precursor can not be suppressed by benzene. This is expressed in Scheme 3-3.

To facilitate the derivation and the subsequent discussion equations relevent to Scheme 3-3 are grouped together and renumbered as Eq 3-12 — 3-20.

Scheme 3-3. Photodecomposition of NBS-DCE in the Presence of Benzene

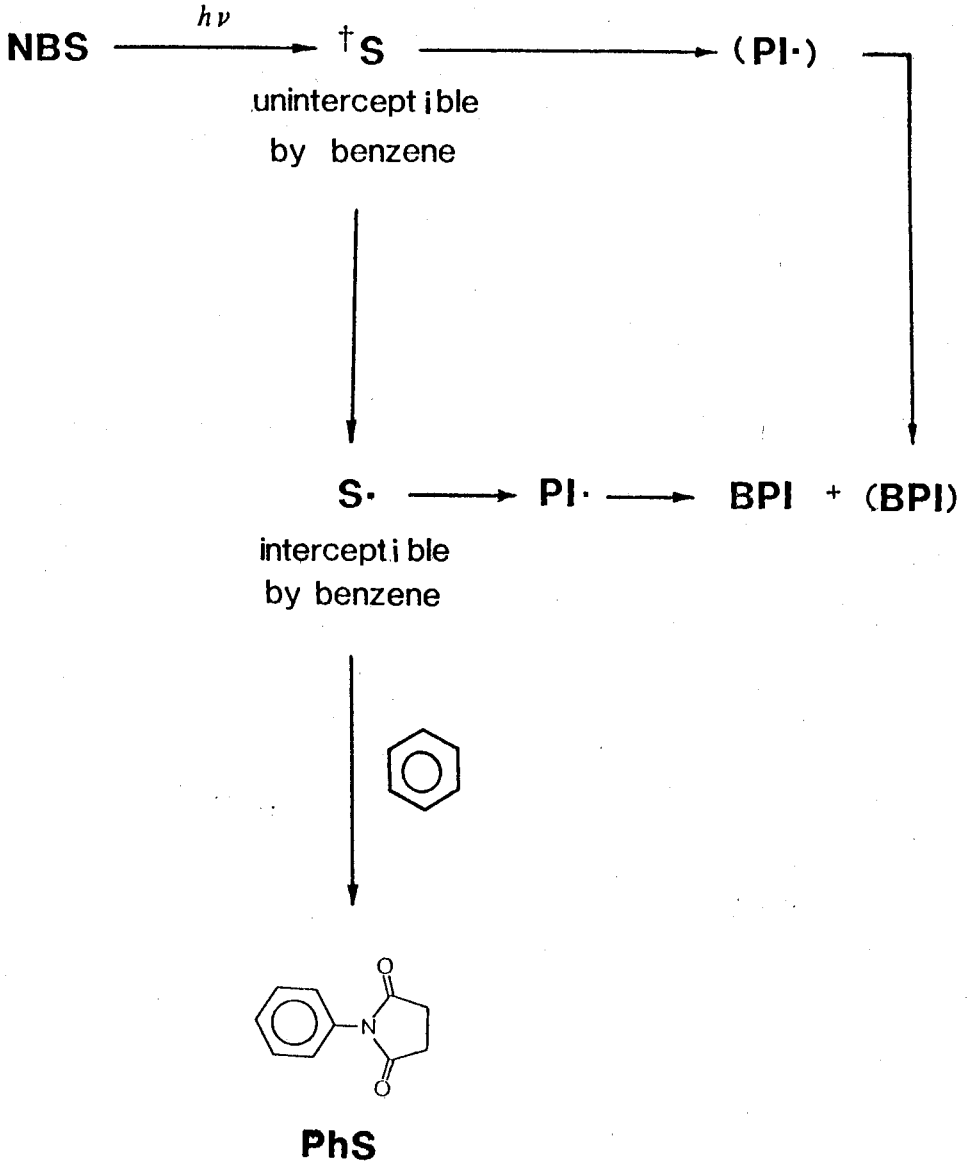

$$NBS + h\nu \longrightarrow \dagger S + Br\cdot \qquad 3\text{-}12$$

$$\dagger S \longrightarrow S\cdot \qquad 3\text{-}13$$

$$\dagger S \longrightarrow (PI\cdot) \qquad 3\text{-}14$$

$$(PI\cdot) + NBS \longrightarrow (BPI) + S\cdot \qquad 3\text{-}15$$

$$S\cdot \longrightarrow PI\cdot \qquad 3\text{-}16$$

$$PI\cdot + NBS \longrightarrow BPI + S\cdot \qquad 3\text{-}17$$

$$S\cdot + CH_2Cl_2 \longrightarrow SH + \cdot CHCl_2 \qquad 3\text{-}18$$

$$S\cdot + C_6H_6 \longrightarrow 1 \qquad 3\text{-}19$$

$$1 + NBS \longrightarrow PhS + S\cdot + HBr \qquad 3\text{-}20$$

It is necessary to point out that the intermediate generated from the direct excitation of NBS (Eq 3-12) is denoted as †S only for convenience. It is tentatively called the precursor, and its identity will be discussed later. The (PI·) and (BPI) generated in Eq 3-14 and 3-15 is indistinguishable chemically from PI· and BPI generated in Eq 3-16 and 3-17. They are designated with parentheses only for convenience of mechanistic discussion and derivation of kinetic equations.

3.1.10. Kinetic Analysis

The mechanistic description of the photodecomposition of NBS in the presence of benzene is complex. It has to be simplified so that kinetic expressions for the quantum yield of BPI formation can be derived. Therefore, some assumptions have to be made and the simplified mechanism is represented by Eq 3-12 to Eq 3-20. The total quantum yield (Φ^0) of BPI formation in the absence of benzene can be treated as the sum of that contributed from the precursor (Φ_e^0) and that from the succinimidyl radical (Φ_g^0) (see Eq 3-21 and 3-22).[2] Similarly the total quantum yield (Φ) of BPI formation in the presence of benzene can be given as the sum of Φ_e^0 and Φ_g, Φ_g being the quantum yield of BPI formation from the succinimidyl radical. Φ_e^0 is not quenchable by benzene while Φ_g is dependent on the concentration of benzene (Eq. 3-23). The quantum yield of imidation (the formation of PhS and its tribromo-derivative **2**) is expressed as Eq. 3-24

$$\Phi_e^0 = k_{14}/(k_{14}+k_{13}) \qquad 3\text{-}21$$

$$\Phi_g^0 = \lambda_b k_{16}/(k_{16}+k_{18}[D]) \qquad 3\text{-}22$$

$$\Phi_g = \lambda_b k_{16}/(k_{16}+k_{18}[D]+k_{19}[B]) \qquad 3\text{-}23$$

---

[2]It should be noted that two assumptions have been made in the derivation of Eq. 3-21: the quantum yield of †S formation is unity or close to unity, and the relaxations and the ring-opening of †S are the most important pathways which govern its lifetime. See appendix 2 for the derivation of Eq. 3-21.

$$\Phi_n = \lambda_n k_{19}[B]/(k_{16}+k_{18}[D]+k_{19}[B]) \qquad 3\text{-}24$$

where k_{13}, k_{14}, k_{16}, k_{18}, and k_{19}, are the rate constants for the reactions 3-13, 3-14, 3-16, 3-18, and 3-19, [D] and [B] are the concentrations of dichloromethane and benzene, and λ_b and λ_n are the chain lengths of succinimidyl radicals generated by the propagation steps (Eq. 3-17 and 3-20). Explicit mathematical expressions for λ_b and λ_n can not be incorporated in the kinetic equations (see Eq 3-22, 3-23, and 3-24) since the mechanism of the termination has not been fully understood. Owing to the nature of a chain reaction, the propagation steps (Eq. 3-15, 3-17, and 3-20) contribute further complication arising from the involvement of NBS concentrations in the regeneration of S·. This complication is alleviated by running the experiments with a fixed initial [NBS] and a low conversion of NBS.

Dividing Φ^o (the sum of Φ_e^o and Φ_g^o) by Φ (the sum of Φ_e^o and Φ_g) gives Eq. 3-25, the relationship between Φ^o/Φ and the concentration of benzene.

$$\Phi^o/\Phi = 1 + \frac{k_{19}\tau_o[B]}{1+ (\Phi_e^o/\Phi_g^o)(1+k_{19}\tau_o[B])} \qquad 3\text{-}25$$

where $\tau_o = 1/(k_{16}+k_{18}[D])$, the lifetime of the succinimidyl radical in the absence of benzene. Eq. 3-25 is further modified to Eq. 3-25' in the region of high concentration of benzene where

the limiting conditions of $k_1\tau_0[B]>>1$ and $k_1\tau_0[B]>>(\Phi_e^0/\Phi_g^0)$ exist.

$$(\Phi^0/\Phi)_{lim} = 1 + \Phi_g^0/\Phi_e^0 = (\phi^0/\phi)_{lim} = \Phi^0/\Phi_e^0 \qquad 3\text{-}25'$$

The data points of Φ^0/Φ ($=\phi^0/\phi$) in the region of >2 M [B] (see Figure 2-7) exhibit the limiting conditions with $(\Phi^0/\Phi)_{lim}$ = Φ^0/Φ_e^0 =7.5 (Figure 2-7). This gives Φ_e^0/Φ_g^0 = 1/6.5 (note: $\Phi^0 = \Phi_e^0 + \Phi_g^0$). Using this value and $k_1\tau_0$ = 21 M^{-1} which was obtained from the slope of Figure 3-1 (see the next paragraph for the detail), the graph of Eq. 3-25 is plotted in Figure 2-7. The agreement between the experimental data points and the graph of Eq. 3-25 drawn by a computer confirms the reasonableness of the proposed scheme and assumptions; that is, both S· and the precursor undergo ring opening to give BPI and the precursor cannot be intercepted by benzene. The Φ_e^0/Φ_g^0 value of 1/6.5 also indicates that about 15% of the total yield of BPI originates from the ring opening of the precursor (Eq. 3-14) which shows no appreciable reactivity with benzene.

The succinimidyl radical is quenchable by benzene through its addition to the benzene ring. If the quantum yields of BPI formation from the succinimidyl radical (Φ_g^0 and Φ_g) are isolated from the total quantum yield of BPI formation (Φ^0 and Φ), and a plot of Φ_g^0/Φ_g against [B] is drawn, a straight line should be obtained. The values of Φ_g^0/Φ_g at various benzene concentrations

can be obtained as described below. The BPI yield in Table 2-9 is the sum of the contribution from †S and S· (see Eq. 2-2 in Section 2.1.7 for the left sides of Eq. 3-26)

$$Y^0(BPI) = \Phi^0 I t = \Phi_e^0 I t + \Phi_g^0 I t \qquad 3\text{-}26a$$

$$Y(BPI) = \Phi I t = \Phi_e^0 I t + \Phi_g I t \qquad 3\text{-}26b$$

The second terms in the right side of Eq 2-26a and 2-26b, i.e. $\Phi_g^0 I t$ and $\Phi_g I t$, are the yields of BPI from the succinimidyl radical in the absence and presence of benzene. They can be calculated from Eq 3-27a and 3-27b. The values of $Y^0(BPI)$ and $Y(BPI)$ were taken from Table 2-9 in Section 2.1.7.

$$\Phi_g^0 I t = \phi_g^0 = Y^0(BPI) - \Phi_e^0 I t = Y^0(BPI) - (1/7.5)Y^0(BPI) \qquad 3\text{-}27a$$

$$\Phi_g I t = \phi_g = Y(BPI) - (1/7.5)Y^0(BPI) \qquad 3\text{-}27b$$

Their values and the corresponding Φ_g^0/Φ_g at various concentrations of benzene are listed in Table 3-1. When Φ_g^0/Φ_g is plotted against the concentration of benzene a straight line with a slope of 21 M^{-1} is obtained (see Figure 3.1; the data corresponding to >1 M benzene are not used because of the higher uncertainty introduced in the measurement of small amounts of BPI). The linearity in Figure 3-1 confirms again that two kinds of intermediates (S· and †S) lead to the formation of BPI (see Scheme 3-3).

Table 3-1

Photodecomposition of NBS in the Presence of Benzene[a]

[B] M	10^3Prdct ϕ_g[b]	ϕ_n[c]	ϕ_g^g[d]	Φ_g^g/Φ_g	Φ_g/Φ_n
Series I (*hν* for 6.0 min., sign by ■) $k_1\tau_0$=23.2±1.0[e](0.998)					
0.00	9.19±1.07	0	1.41±0.14	1.000	
0.031	5.88±0.74	1.21±0.09		1.56	
0.061	4.13±0.57	1.13±0.08		2.23	
0.15	2.01±0.37	1.34±0.09		4.57	1.50
Series II (*hν* for 8.0 min., sign by ¤) $k_1\tau_0$=22.1±1.2[e](0.996)					
0.00	19.7±2.3	0	3.03±0.30	1.00	-
0.10	5.64±0.92	1.93±0.15		3.49	2.92
0.40	1.63±0.56	2.45±0.19		12.1	0.665
0.80	1.04±0.51	2.77±0.22		18.9	0.375
1.0	0.80±0.48	3.47±0.29		24.6	0.231
Series III (*hν* for 7.6 min., sign by Δ) $k_1\tau_0$=20.4±0.7[e](0.997)					
0.00	17.3±0.94	0	2.67±0.27	1.00	
0.10	5.38±0.85	1.90±0.15		3.22	2.83
0.20	3.71±0.70	2.41±0.19		4.66	1.54
0.4	1.74±0.49	2.47±0.20		9.94	0.704
0.60	1.36±0.49	2.77±0.23		12.6	0.495
0.80	0.97±0.45	2.77±0.23		17.8	0.350
1.0	0.76±0.43	2.98±0.24		22.8	0.255

Series IV ($h\nu$ for 8.0 min., sign by •)					
0.00	17.8±2.1[d]	0	2.73±0.27	1.00	
1.5	0.49±0.42	2.70±0.22			0.18
2.0	0.64±0.43	3.10±0.26			0.21
2.5	0.10±0.39	3.36±0.27			0.030
3.1	0.52±0.43	2.81±0.23			0.19
5.1	-0.17±0.37	3.31±0.28			-0.05
Series V ($h\nu$ for 7.0 min., sign by o)					
0.00	14.7±1.7	0	2.27±0.23		
1.5	0.42±0.35	2.70±0.21			0.16
2.0	0.86±0.39	2.65±0.21			0.32
2.5	0.94±0.39	2.84±0.24			0.33
3.1	0.85±0.39	2.80±0.23			0.30
4.1	0.64±0.37	2.85±0.23			0.22
5.1	-0.10±0.32	2.85±0.23			-0.035

a. The data are calculated using the results in Table 2-9.

b. In mmol. Calculated by the use of $\phi_g^0=\phi^0-\phi_e^0$.

c. In mmol. $\phi_n=\phi(\mathrm{PhS})+\phi(\mathbf{2})$, the sum of the relative quantum yields of the formation of PhS and **2**.

d. In mmol. Calculated by the use of $\phi^0/\phi_e^0=7.5$.

e. The uncertainty given for the values $k_1\tau_0$ (M^{-1}) is obtained by assuming that ϕ_g^0, ϕ_g, and [B] have no associated errors. The correlation coeffients are given in parentheses.

Dividing Φ_g^o (Eq. 3-22) by Φ_g (Eq. 3-23) gives Eq 3-28.

$$\Phi_g^o/\Phi_g = 1+k_{19}\tau_o[B] \qquad 3\text{-}28$$

This equation reveals the physical meaning of the slope in Figure 3-1: $k_{19}\tau_o$. The $k_{19}\tau_o$ values listed in Table 3-1 were obtained from a straight-line fit to the data in the table assuming a Stern-Volmer-type kinetic relationship (Eq. 3-28). The kinetics of thermo-initiated NBS decomposition in dichloromethane by Walling's group is the closest to the reactions of the succinimidyl radical proposed in this work. If k_{16} = $2\times10^3 s^{-1}$ and k_{18} = 1 $M^{-1}s^{-1}$ are accepted[18,32], τ_o at [D]=15.5 M is calculated to be 5×10^{-4}s: k_{19} = 4.2×10^4 $M^{-1}s^{-1}$ is obtained. The contribution from k_{18}[D] is negligible.

Multiplying the both sides of Eq. 3-24 by It and taking reciprocals produce Eq 3-29.

$$1/(\Phi_n It) = 1/(\lambda_n It) + \{1/(\lambda_n It k_{19}\tau_o)\}\cdot 1/[B] \qquad 3\text{-}29$$

where $\Phi_n It$ is the combined yield of PhS and **2**, their values at various concentration of benzene being listed in Table 2-9. The linearity of the plot of $1/(\Phi_n It)$ against 1/[B] (Figure 3-2) is not bad, considering the high uncertainty introduced in determining yields of **2** as a part of $1/(\Phi_n It)$ in low concentration range of benzene. From Eq 3-29 it can be seen that dividing its intercept by its slope produces $k_{19}\tau_o$. $k_{19}\tau_o$ values obtained

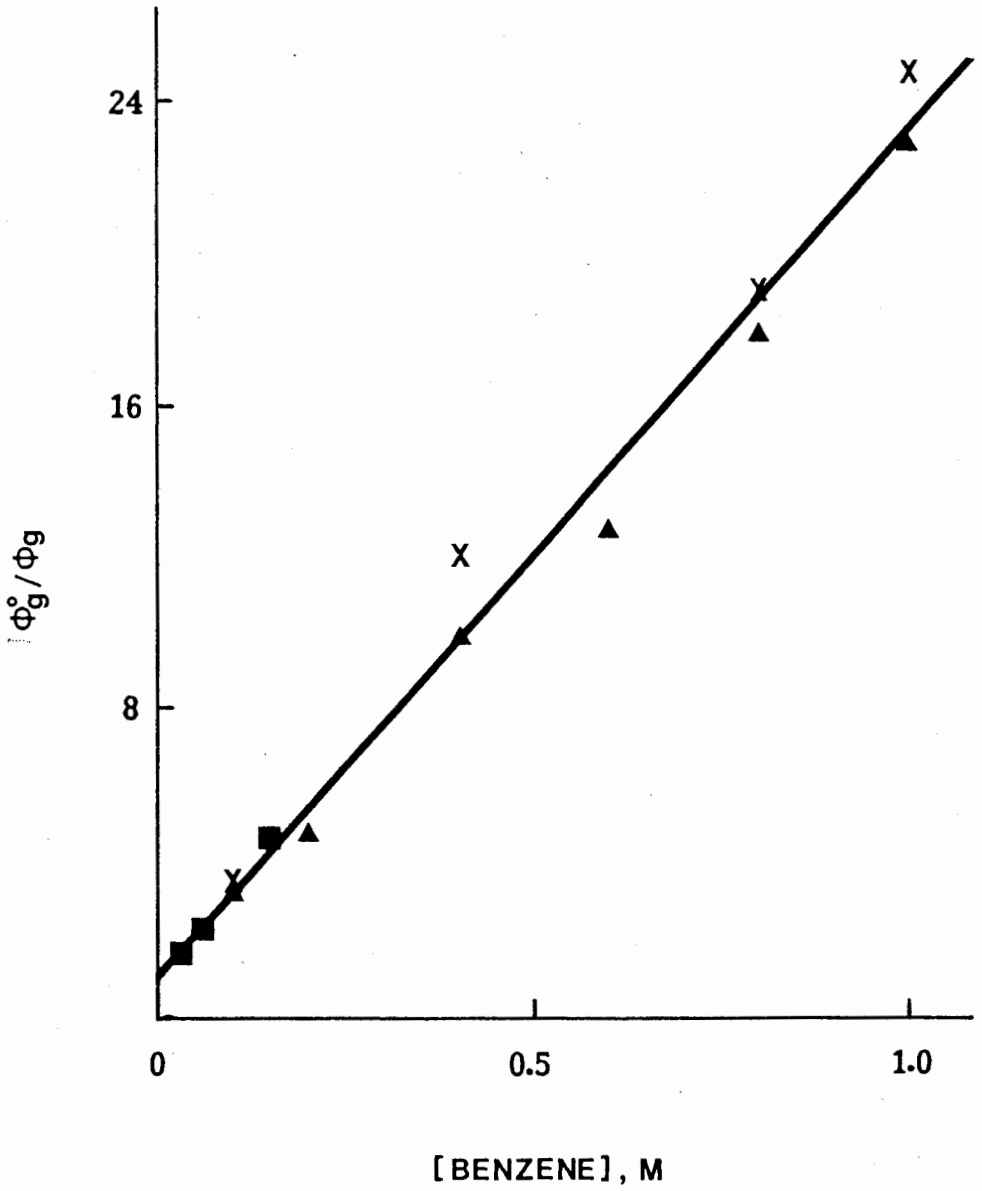

Figure 3-1. Effect of benzene concentration on the ratio of quantum yields of BPI formation from the succinimidyl radical.

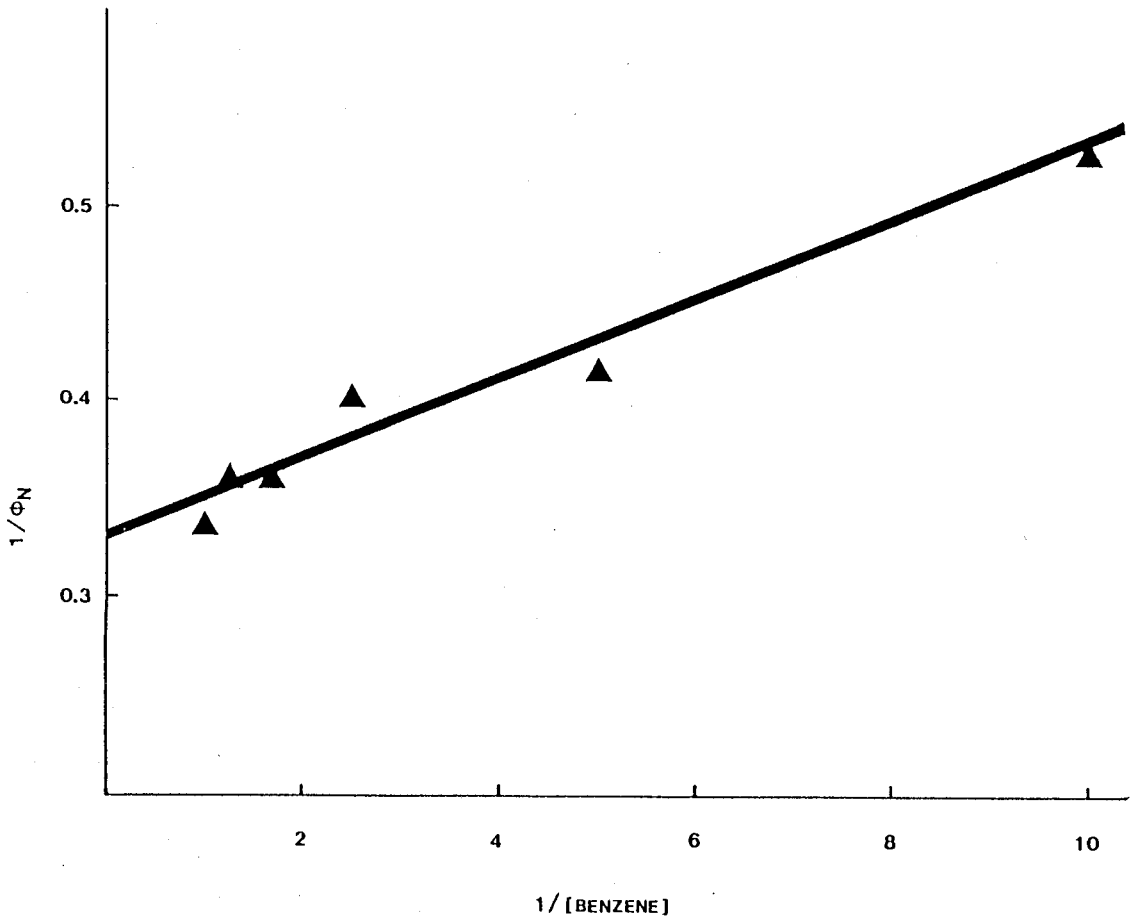

Figure 3-2. Plot of $1/\phi_n$ vs. 1/[B] using the data given in Table 2-7 (Note $1/\phi_n = 1/\Phi_n I t$).

from Series II and III are 15 and 18 M^{-1} respectively, agreeing reasonably well with those obtained from the plot of Φ_g^o/Φ_g against [B] (see Table 3-1 and Figure 3-1).

Dividing Φ_g (Eq. 3-23) by Φ_n (Eq. 3-24) gives

$$\phi_g/\phi_n = \Phi_g/\Phi_n = \{\lambda_b k_{16}/\lambda_n k_{19}\}\cdot 1/[B] \qquad 3\text{-}30a$$

The equation predicts a straight line with an intercept of zero. When Φ_g/Φ_n is plotted against 1/[B] using the data listed in Table 3-1, a straight line passing the point (0,0) is obtained (Figure 3-3). This demonstrates the strategy used in the kinetic analysis is resonable that the total BPI can be treated as the sum of the contribution from the succinimidyl radical and one from another source. Moreover, the intercept of zero indicates that ϕ_g becomes zero when benzene concentration is very high. Hence Φ_g is benzene quenchable. This and the linearity of Figure 3-3 suggest that the ring opening and the addition of the succinimidyl radical to benzene are two competitive reactions.

Dividing the sum of Φ_e^o (Eq. 3-21) and Φ_g (Eq. 3-23) by Φ_n (Eq. 3-24) gives the relationship between ϕ/ϕ_n and 1/[B], Eq 3-30b

$$\phi/\phi_n = \Phi/\Phi_n$$

$$= k_{14}\tau_o'/\lambda_n + \{\lambda_b k_{16}/\lambda_n k_{23} + k_{14}\tau_o'/\lambda_n k_{19}\tau_o\}\cdot 1/[B] \qquad 3\text{-}30b$$

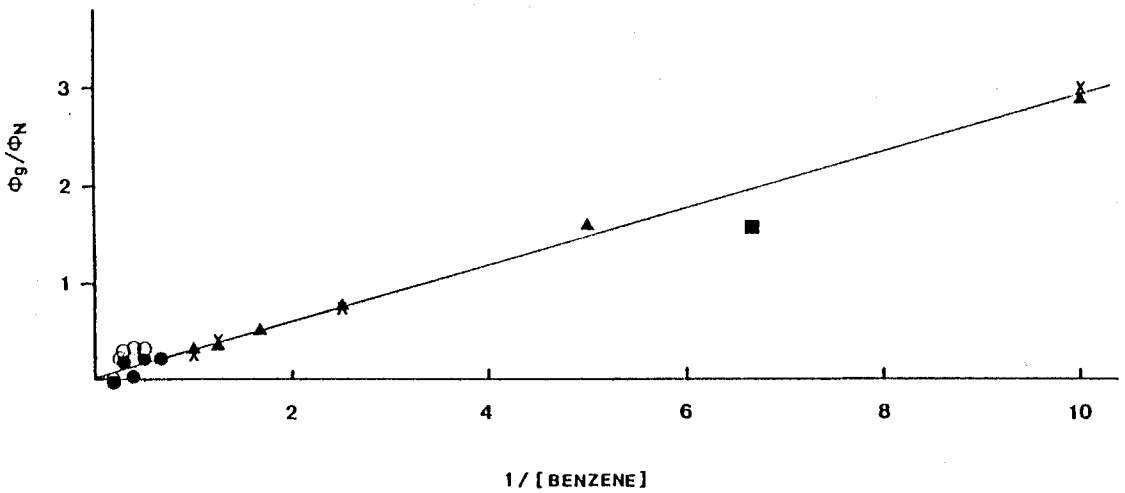

Figure 3-3. Plot of Φ_g/Φ_n vs. 1/[B] using the data given in Table 3-1.

It predicts a straight line with a non-zero intercept. Examining Figure 2-8 reveals that this is the case.

3.1.11. Limiting Quantum Yield of BPI Formation

The quantum yield of BPI formation at 5 M benzene was determined to be 0.78 (Section 2.1.7, Chapter 2). It is reasonable to assume that at such high concentration of benzene the formation of BPI from the succinimidyl radical is entirely suppressed and that only the precursor, †S, produces the observed BPI (the limiting quantum yield of BPI formation). Since the mathematical expression for the quantum yield of BPI formation from the precursor is available (see Eq. 3-21), it follows that

$$k_{14}/(k_{13}+k_{14}) = 0.78$$

Solving this equation gives $k_{14}=3.5k_{13}$. That is, the rate constant for the ring opening of †S (k_{14}) and that of relaxation (or transformation) of †S (i.e. k_{13}) are comparable.

3.1.12. A Hot Succinimidyl as the Precursor

The pseudounimolecular rate constant for collision of solute molecules with benzene at 20°C was estimated by Zimmerman and Wilson[103] to be $1.1\times10^{11}s^{-1}$. If †S is a hot succinimidyl

radical, i.e., a vibrationally excited ground state, the conclusion $k_{14}=3.5k_{13}$ (see the last paragraph of the previous section) requires $k_{14}=3.5\text{x}1.1\text{x}10^{11}=3.9\text{x}10^{11}\text{s}^{-1}$. The k_{14} value was calculated by assuming that deactivation of †S occurs with every collision. Now, the question is — Is ($3.9\text{x}10^{11}\text{s}^{-1}$) too high for k_{14} (the rate constant for the ring opening of †S)?

The Rice-Ramsperger-Kassel (RRK) theory of unimolecular reaction[104,105] provides a method to calculate k, the rate of reaction of a vibrationally excited molecule with vibrational energy E (Eq 3-31)

$$k = A\{(E-E_0)/E\}\exp(n-1) \qquad 3\text{-}31$$

where A is the frequency factor and E_0 the activation energy of the normal thermal reaction, and n is the number of vibrational degrees of freedom that act along the reaction coordinate (n is usually assumed to be (3N-6)/2, N being the number of atoms in the nonlinear molecule). Using 20 kcal/mol as the energy E of a hot succinimidyl radical formed by adiabatic conversion of electronic to vibrational energy[3], and also making the conservative estimate that the ring opening of the ground state succinimidyl radical will not have a lower activation energy than 12.9

---

[3]This is the energy gap between the ground and the excited state succinimidyl radicals calculated by Apeloig and co-workers[45], the vibrational energy of the hot succinimidyl radical can not be higher than this value after the hot species is formed through the intersystem crossing.

kcal/mol[4], and additionally assuming that n is 13, and finally employing a typical frequency factor of $A=10^{13}$, k in Eq 3-31 is given by $6x10^{7}s^{-1}$. It is much lower than that required ($3.9x10^{11}s^{-1}$). Clearly collisional quenching by solvent with a rate of $10^{11}s^{-1}$ is an efficient process which would deactivate such a hot species prior to thermal rearrangement ($6x10^{7}s^{-1}$). It is important to keep in mind that the argument of the unimolecular rate theory for vibrationally excited ground-state reactions begins with the assumption that a vibrationally excited ground-state will have its vibrational energy randomly distributed as if it had been excited through thermal activation. Ullman speculated that, in a vibrationally excited ground state produced by crossing from an electronically excited state, much of the energy required for reaction might already be concentrated at the reaction site[106]. Nevertheless, a hot species is not considered as a probable candidate for †S since Ullman's speculation has not been supported by enough convincing evidence[107].

3.1.13. *S or *NBS as the Precursor

If a succinimidyl radical is considered to be the intermediate for the formation of PI•, the precursor could be another

---

[4]This is the energy barriar calculated for the ring opening of the excited succinimidyl radical by Dewar and Olivella[46]. The energy of activation required for the ring opening of the hot succinimidyl radical should not be lower than this value.

state of S·. since Chow and Naguib have provided reasonable evidence that a related tricyclic succinimidyl radical possesses the σ electronic configuration[28] (see Section 1.6. for details) the precursor could be a succinimidyl radical having the π electronic configuration. However, the theoretical calculations from many groups [40,42,45,46] have been unanimous, with only one exception[41], in claiming that the π electronic state is the ground state and is lower in energy than the σ state which is the lowest excited state of succinimidyl radical. Intuitively, it may be assumed that excited state *NBS decomposes adiabatically, i.e., on the same energy surface to generate an excited state succinimidyl radical.[5] While it is tempting to assign the precursor †S to the lowest excited state as opposed to the assignment of S· to the ground state succinimidyl radical, the obvious disagreement with the theoreticians' conclusions cautions us that such an assignment is not as straightforward as it appears. If reaction 3-13 involves an electronic transition and the energy gap between the ground and excited state succinimidyl radicals is as small as 15-25 kcal/mol as indicated by theoretical studies[40,42], a high value[109] could be assumed for k_{13} (and, therefore, also for k_{14}) unless there is quantum mechanical "forbiddenness" which imposes a high energy barrier for reaction 3-13. From the fact that 5 M benzene fails to quench †S, it is reasonable to assume k_{14} to be at least 100 times greater than

---

[5]The irradiation of NBS with a 300-nm light source provides an energy of about 95 kcal/mol. The dissociation energy of N-Br bond in NBS is belived to be <50 kcal/mol[86,18].

k_{19}[B]; it is estimated that $k_{14}>4x10^7$ s^{-1} by taking [B]=10 M.

At present, there is no strong experimental evidence to suggest that the precursor is a radical. Therefore, it is possible that the precursor is an excited state NBS which does not react with benzene but undergoes a concerted ring opening to give (PI·) and Br· during the course of relaxation (Eq. 3-14a), by-passing the formation of the excited state of succinimidyl radical (Eq 3-32).

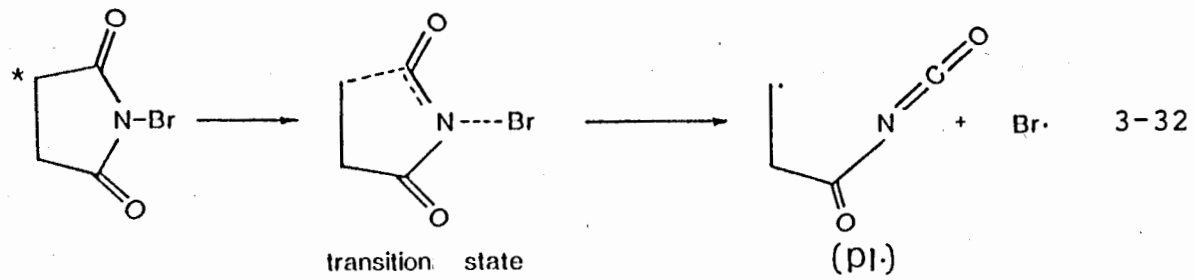

3-32

This hypothesis is consistent with the failure to completely suppress BPI formation with a high concentration of benzene. A similar idea has been mentioned by Walling et al[18], and Chow and Zhao[108]. If Eq. 3-12, 3-13, and 3-14 are replaced by Eq 3-12a, 3-13a, and 3-14a,

$$NBS + h\nu \longrightarrow *NBS \qquad 3\text{-}12a$$

$$*NBS \longrightarrow S\cdot + Br\cdot \qquad 3\text{-}13a$$

$$*NBS \longrightarrow (PI\cdot) + Br\cdot \qquad 3\text{-}14a$$

This new mechanistic scheme predicts the same kinetic

expressions as Eq 3-21—3-24, if Φ_e^0 is defined as the quantum yield of Eq. 3-14a. At present, there is no strong experimental evidence upon which to assign the identity of †S to the excited succinimidyl radical or the excited NBS. The kinetic analysis described above is consistent with either assignment.

3.1.14. Possibility of Sensitization of NBS

The investigation of the photodecomposition of NBS has been treated as a straightforward radical chain problem without consideration of excited-state chemistry. Two aspects of the photodecomposition of NBS in the presence of Br_2 require comment, that is, the possible sensitization processes shown in Eq 3-33 and 3-34.

$$*Br_2 + NBS \longrightarrow Br_2 + *NBS \longrightarrow S\cdot + Br\cdot \qquad 3\text{-}33$$

$$*NBS + Br_2 \longrightarrow NBS + *Br_2 \longrightarrow 2Br\cdot \qquad 3\text{-}34$$

The failure to detect excited NBS by flash-excitation techniques[22] suggests there is good reason to believe that excited NBS possesses a lifetime $<10^{-9}$s. Thus, reaction 3-34 is rather unlikely. The energy transfer from the excited-state Br_2 to NBS (Eq 3-33) is not probable either because of unfavorable energetics. Further, it is known that excitation of Br_2 causes its rapid predissociation[110].

Section II. Photodecomposition of 33NBG and NBP

3.2.1. Selectivities towards Hydrogen Abstraction

Table 2-10 shows the selectivity ($r \simeq 96$) towards hydrogen abstraction from cyclohexane and dichloromethane shown by the 33NBG-DCE system. A selectivity of ≃260 is observed from the NBP-DCE system. These selectivities differ and they are due to the chain carrier 3,3-dimethylglutarimidyl (33G·) and phthalimidyl (P·) radicals since the Br_2 concentrations in these two systems are kept very low by DCE[56]. Unlike the succinimidyl radical, neither 33G· nor phthalimidyl radical (P·) produced in these systems undergoes the ring opening reaction. Examination of the selectivities shown in Table 2-5, 2-10, and 2-12 reveals the following order in the selectivity : 260 (P·), 190 (S·), 96 (33G·). The selectivity of these imidyl radicals are much higher than that of bromine atoms ($r \simeq 17$, see Table 2-6). When the olefin DCE in the 33NBG-DCE system is replaced by Br_2, however, the selectivity dramatically decreases. It can be seen from Table 2-11 that the presence of 0.002 M Br_2 decreases the selectivity to ≃30 and that the further increase in $[Br_2]$ lowers the r value to 17 which is essentially the selectivity of the bromine atom. The same trend is observed from Table 2-13. The r value of the NBP-Br_2 system decreases from 30 to 21 as the $[Br_2]$ increases from 0.002 to 0.2 M. The change in the selectivity shown in Table 2-7, 2-11, and 2-13 indicates the N-bromoimide-Br_2 systems

show similar selectivities to that of bromine atoms at high [Br_2] no matter which N-bromoimide is used whatever the *r* value of the imidyl radical. This strongly suggests that a mixed chain (the imidyl and the bromine atom) operates in the N-bromoimide-Br_2 system and that the bromine atom chain prevails when the Br_2 concentration is high enough.

3.2.2. Effects of Benzene Concentration on the Reactions of 33G·

Figure 2-9 is a straight line up to 5 M benzene. It resembles Figure 3-1. The linearity of Figure 2-9 indicates that only one kind of reactive intermediate, 3,3-dimethylglutarimidyl radical, abstracts hydrogen from cyclohexane to produce bromocyclohexane (Scheme 3-4), and this reaction can be totally suppressed by benzene at high concentration. This is supported by Figure 2-10 where the intercept of zero demonstrates that no bromocyclohexane will be produced when benzene concentration is very high.

Suppressing the addition of 33G· to 3,3-dimethylbutene shows the similar results. The plot of Φ^0/Φ against [B] is a straight line (Figure 2-11). This demonstrates that only one kind of intermediate, 33G·, adds to 3,3-dimethylbutene to form **10**, and the addition can be suppressed by benzene. Therefore, the previous report[32] is not conclusive that both the 33G· and its precursor react with 3,3-dimethylbutene with different rates.

Scheme 3-4. Photodecomposition of 33NBG in the presence of cyclohexane and benzene

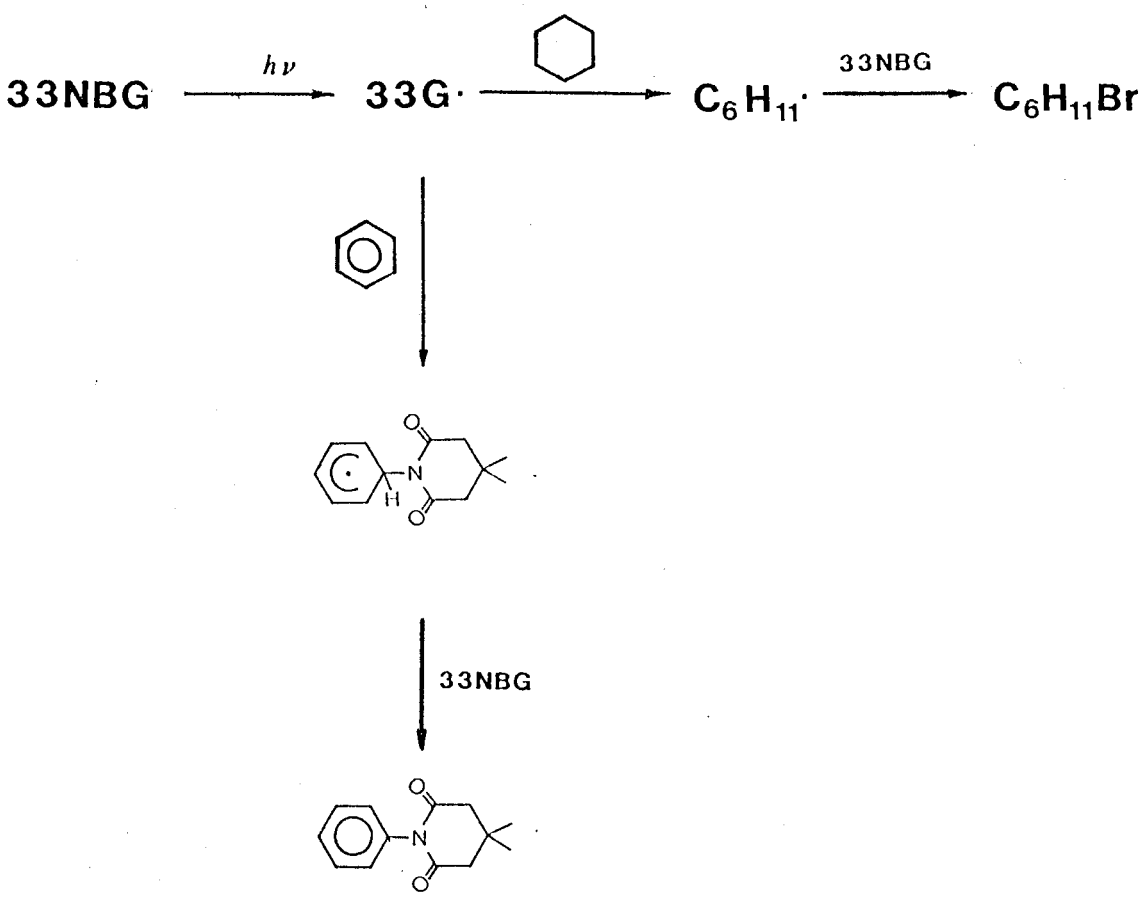

Section III. Photodecomposition of N-Bromoimide **11**

3.3.1. Equilibrium between Br· and Imidyl Radicals

Although NBS is a versitile reagent[111-115], it is not a good model for mechanistic studies of imidyl radical since succinimidyl radical undergoes fast ring opening and the BPI formation is complicated by the contribution from the precursor †S. N-Bromo-N-acetylhexanamide **11** is chosen for probing the mechanism of photolysing N-bromoimide-Br_2 system, since the corresponding imidyl radical **46** (see Eq. 3-35 for its structure) must selectively abstract δ-hydrogen intramolecularly through a six-membered ring transition state, regardless of whether **46** possesses the σ or π configuration, to give 4-bromoimide **12** (Eq 2-12). This hypothesis is based on a related work[116] published in 1964 in conjunction with Chow's work on the intramolecular reactions and model studies of amidyl radical[117-120]. The intramolecular hydrogen abstraction from a δ-hydrogen also serves as a chemical clock[115] to estimate concurrent bimolecular side reactions. Indeed 4-bromoimide **12** has been obtained in an excellent yield from photolysis of N-bromoimide **11** in the presence of an olefin (Experiments 151 and 152, Table 2-16). No products due to β-scission of imidyl radical **46** (caproyl isocyanate and acetyl isocyanate or their hydrolysis products hexanamide or acetamide) have been detected. As neither bromobenzene nor imidylbenzene are produced when **11** is photolysed in

benzene, **46** undergoes intramolecular hydrogen abstraction much faster than it attacks benzene. Since the intramolecular hydrogen abstraction is the predominant pathway for imidyl radical **46**, the formation of 4-bromoimide **12** can be used to estimate the extent to which imidyl radical **46** is produced when **11**-Br_2 is photolysed. On the other hand, the extent to which the bromine atom chain prevails in the reaction system can be evaluated by the ratio of **14**/**15**. Control experiments (see Table 2-17) have shown that bromination of the side chain of imide **13** always produces 2-bromoimide **14** about three times as fast as 5-bromoimide **15**. The tendency does not change substantially when **18**, a N-methyl analogue to **13**, is used as a model compound (Table 2-18). Therefore, it is assumed that the tendency will be the same when the side chains of N-bromoimide **11** are brominated.

When **11**-Br_2 system is irradiated with a >380-nm light source to excite Br_2, there are two pathways available to the bromine atom generated by the photolysis, namely, (1) initiation of the decomposition of N-bromoimide **11** or (2) the bromination of the side chains of **11**. Therefore, bromination of the side chain concurrent to the bromine atom-initiated decomposition of N-bromoimide **11**.

The high yields of 4-bromoimide **12** (>50%) at low concentration of bromine (≤0.02 M) in Table 2-16 demonstrates that the imidyl radical **46** is efficiently generated by the bromine atom (see the forward reaction of Eq. 3-35) and that the

intramolecular hydrogen abstraction by the imidyl radical prevails. The relative low yields of 2-bromoimide **14** and 5-bromoimide **15** indicates that the bromination by bromine atoms can not compete successfully with intramolecular hydrogen abstraction.

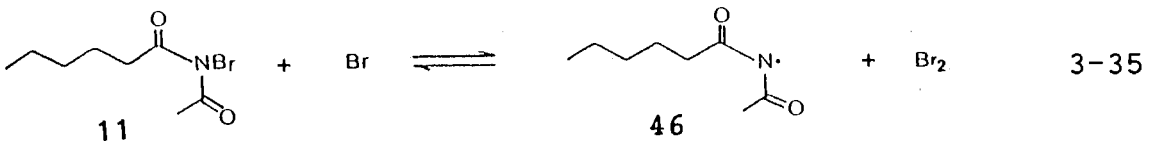

11 **46** 3-35

When the concentration of Br_2 increases to 0.2 M, however, the yields of the side chain-brominated imides **14** and **15** become higher (Table 2-16). Obviously, the contribution to the product distribution from the bromination by bromine atoms increases as the concentration of Br_2 increases. Nevertheless, this change in the product distribution is not caused by the higher concentration of bromine atom generated by photolysis, because the number of photons absorbed by Br_2 is almost the same when concentration of Br_2 increases from 0.02 to 0.2 M (the molar absorptivity of Br_2 at 410 nm is 200). Therefore, it is proposed that the Br_2 intercepts imidyl radical **46** more efficiently as the concentration of Br_2 increases, producing bromine atoms (the reverse reaction of Eq 3-35). The higher product ratios of 2- and 5-bromoimides (**14** and **15**) to 4-bromoimide (**12**) shown in Table 2-16 at higher [Br_2] indicates that the [Br·]/[**46**] ratio increases. When a mixture of **11** and Br_2 is irradiated through a filter solution

(cut off ≥400 nm) to excite Br_2 selectively, the **46**/Br· system (see Eq 3-35) is fed through the Br· side. When both **11** and Br_2 are irradiated through a Pyrex filter, the **46**/Br· system is fed through both the imidyl **46** and the Br· sides. The similar product distributions observed from experiments 154A (through the filter solution) and 154B (through a Pyrex filter, see Table 2-16) suggest that **46** and Br· are in equilibrium. In view of the fact that 0.1 M Br_2 is high enough to suppress 33G· and phthalimidyl radicals in the 33NBG-Br_2 and NBP-Br_2 systems and makes these systems show the selectivity of the bromine atom in hydrogen abstraction from cyclohexane and dichloromethane (Table 2-11 and 2-13), the substantial yield of **12** at 0.2 M Br_2 is surprising. It may be interpreted in term of facile intramolecular hydrogen abstraction by imidyl radical **46**.

3.3.2. Bromination of the Side chain of 11

It seems that the variation in product distribution caused by the increase in the Br_2 concentration (see experiments 153-158, Table 2-16) can be explained in term of an equilibrium between imidyl radical **46** and the bromine atom (Eq. 3-35)—the higher the concentration of Br_2, the lower the concentration of **46** and hence the lower the yield of 4-bromoimide **12** which comes predominantly from the intramolecular hydrogen abstraction by imidyl radical **46**. The following problem, however, cannot be

interpreted in the same way. Photodecomposition of N-bromoimide **11** in the presence of an olefin produces little 2-bromo and 5-bromoimides. Imidyl radical **46** hardly abstracts hydrogen at C-2 or C-5 position (experiments 151 and 152, Table 2-16). It follows that the substantial yields of **14** and **15** produced in experiments 153 - 158 must not come from the hydrogen abstraction from the side chain by **46**. Do they result from the bromination of the side chain of **11** by bromine atoms? The selectivity of the bromine atom towards the side chain can be elucidated from the results in Table 2-17 and 2-18 with the relative yields of 2-bromo and 5-bromoimides as references. Photobrominations of imides **13** and **18** produce 2-bromo and 5-bromoimides in addition to some other C-bromoimides[6] and the ratio of the 2-bromo to the 5-bromo derivative is about three to one. The NBS-Br_2 system is used as a bromination reagent in photobrominations of imide **13** and **18** since it is known from the previous studies that such system shows essentially the selectivity of bromine atoms in hydrogen abstraction (see Section I of the discussion). It follows that one mole of 5-bromoimide **15** should be generated with three moles of 2-bromoimide **14** provided that these two are the bromination products of bromine atoms. Taking experiment 153 as an example. When 2.1% of **14** is formed, one third of that, i,e., 0.7% of **15** should be produced concurrently.

---

[6]For example, X, Y, and Z are also generated when photobromination of **18** is carried out. However, their formation and their yields are not discussed in this section since 2-bromo and 5-bromo derivatives are purposely chosen to obtain the selectivity of bromine atoms towards the side chain.

Scheme 3-5. Relationship between imidyl radicals **46** and bromine atoms

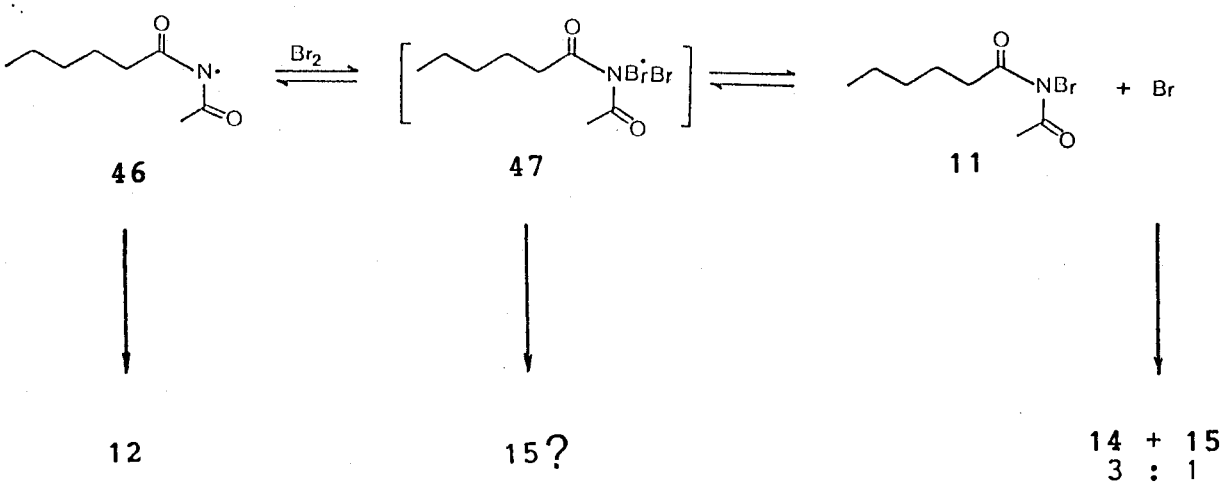

However, 6.3% of **15** is generated. Therefore, the extra **15**, calculated to be 6.5 - (2.1/3) = 5.6, should not be attributed to the bromination by bromine atoms. The formation of the extra **15** (**Δ15**) is much more informative if it is examined against the yield of **12**, the product produced via the intramolecular hydrogen abstraction by imidyl radical **46**. The ratio of (**Δ15**)/**12** is interesting. Table 2-16 shows the higher the concentration of Br_2, the higher the ratio. It follows that the value of **Δ15** becomes greater when the imidyl radical (**46**) chain is suppressed by Br_2. Since the extra **15** is not produced by either the imidyl or bromine atoms it is tempting to propose that the formation of the extra **15** is due to the hydrogen abstraction by the bromine radical complex, and its probable structure is given as **47**

(Scheme 3-5). A similar idea has been proposed by Chow[28] and Walling[18] independently in an analogy to ArĊl radical complex[96,121,122,123]. Recent work by Zhang et al gives support to this proposal[52]. The selectivity of the NBS-Br_2 system towards hydrogen abstraction from different positions of 1-chloropentane was found to become lower than those of the NBS-DCE system (the selectivity of the succinimidyl radical) and the Br_2-K_2CO_3 one (the selectivity of the bromine atom) when the temperature was decreased from 20° to 0°C. The unique selectivity shown by the NBS-Br_2 system is attributed to the intermolecular hydrogen abstraction by a complex between NBS and bromine atom which is stabilized at 0°C and its longer lifetime at the lower temperature allows the radical complex to show its unique selectivity. Nevertheless, it is difficult to rationalize why the radical complex **47** preferentially abstracts hydrogen from the 5-position rather than from the 3-position intramolecularly through a six-membered ring transition state. It seems that such a complex is more crowded than its tricyclic counterpart[28] (see Chapter one for details) because the imidyl moiety of complex **47** is acyclic. The radical complex, if it is formed, tends to squeeze the bulky Br_2 moiety out, producing the more stable imidyl radical **46**. This hypothesis is supported by the observation that high yields of 4-bromoimide were obtained even at 0.2 M Br_2 (see experiments 155 and 158, Table 2-16). Photolysis of Br_2 in the presence of N-bromoimide **11** at a lower temperature shows similar product distributions (see experiment

159, Table 2-16). This indicates that the radical complex **47** is still unstable even at -20°C. If the extra **15** were due to hydrogen abstraction by the complex, the value of **Δ15** should be different when the photolysis of Br_2 in the presence of **11** is carried out at -20°C. But this is not the case (experiment 159, Table 2-16).

The ω-1 effect[124,125] is capable of explaining why 5-bromoimides **15** and **20** are obtained in fairly good yields when the side chains of **13** and **18** are brominated. However, it fails to answer why the **Δ15** is observed when **11** is photobrominated by Br_2. Therefore the question of **Δ15** remains unanswered.

Section IV. Photolysis of Selected N-Bromoimides

3.4.1. Formation of Ring-Opening Products

The production of γ-lactone **24** is rationalized with Scheme 3-6. That amide **51** has not been isolated from the photolysate is not surprising since the conversion of haloamide **51** to lactone **24** is not difficult. Such conversions have been well documented[118,126]. The formation of amides **30** and **31** (from **26**), **33** and **34** (from **32**), and **37** (from **36**) is straightforward, and is explained in Scheme 3-7.

Scheme 3-6. Formation of γ-lactone **24**

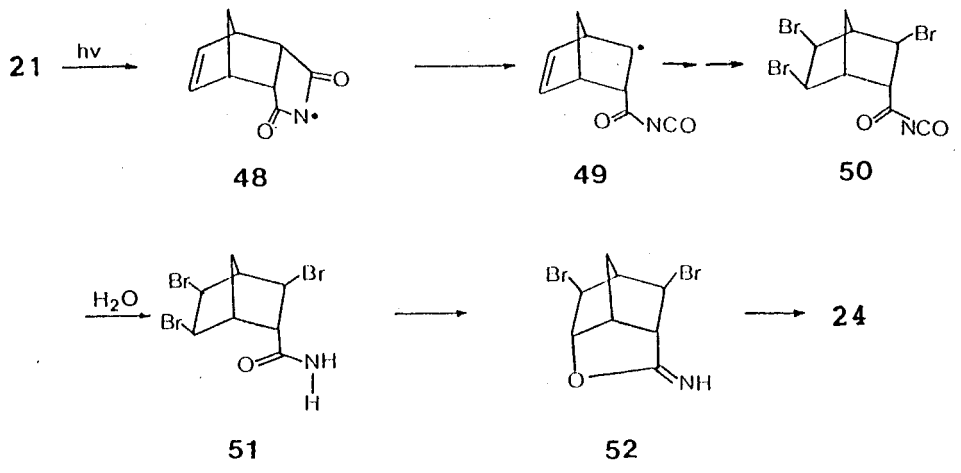

Scheme 3-7. Formation of ring opening products

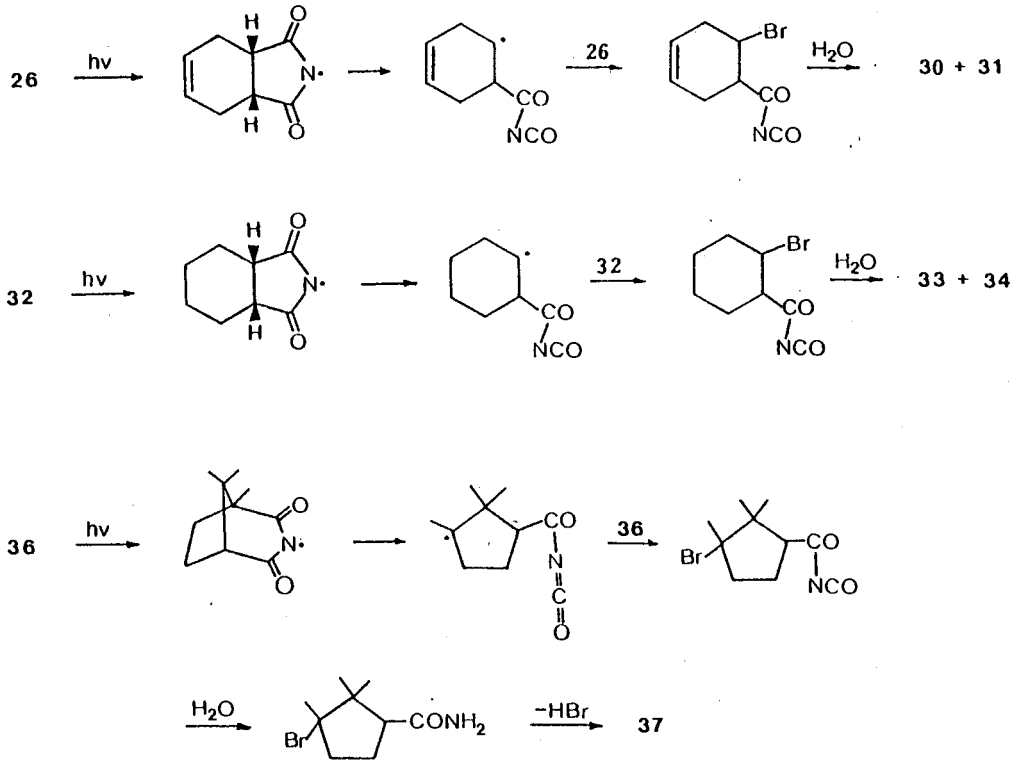

3.4.2. Reversibility of the Ring Opening of Imidyl Radical 48 to Imidyl Radical 53

The formation of imide **22** from N-bromoimide **21** has been reported from this laboratory[127] and needs some comment. Photolysis of N-bromoimide **21** generates imidyl radical **48**. It then opens its ring to afford radical **49** followed by cyclization to produce imidyl radical **53**. The involvement of **53** is indicated by the formation of the corresponding imide **22** through hydrogen abstraction from the solvent (Scheme 3-8). Can imidyl radical **48** be formed from imidyl radical **53** via **49**? It has been demonstrated that **53** can be generated by photocleavage of the N-Br bond of N-bromoimide **25**. If **48** can be generated from **53** via **49** (i.e., the conversion of **48** → **49** → **53** is reversible), photodecomposition of N-bromoimide **25** under the same conditions as photodecomposition of N-bromoimide **21** should lead to the formation of **23** and 24. Tables 2-19 and 2-20 demonstrate unambiguously the different patterns of product distribution when **21** and **25** are photolysed respectively in the presence of DCE. It is noteworthy that **24** has not been detected by GC which can detect at least 0.7 mM **24** (1% yield based on the amount of N-bromoimide **25** used in the photolysis). The result indicates that no **49** is generated during the photolysis. It follows that the step of **49** → **53** must be irreversible[128]. The reversibility of the step of **48** → **49** remains unknown. This is summerized in Scheme 3-8. since **48** is a substituted succinimidyl radical and **49** is a substituted PI

Scheme 3-8.

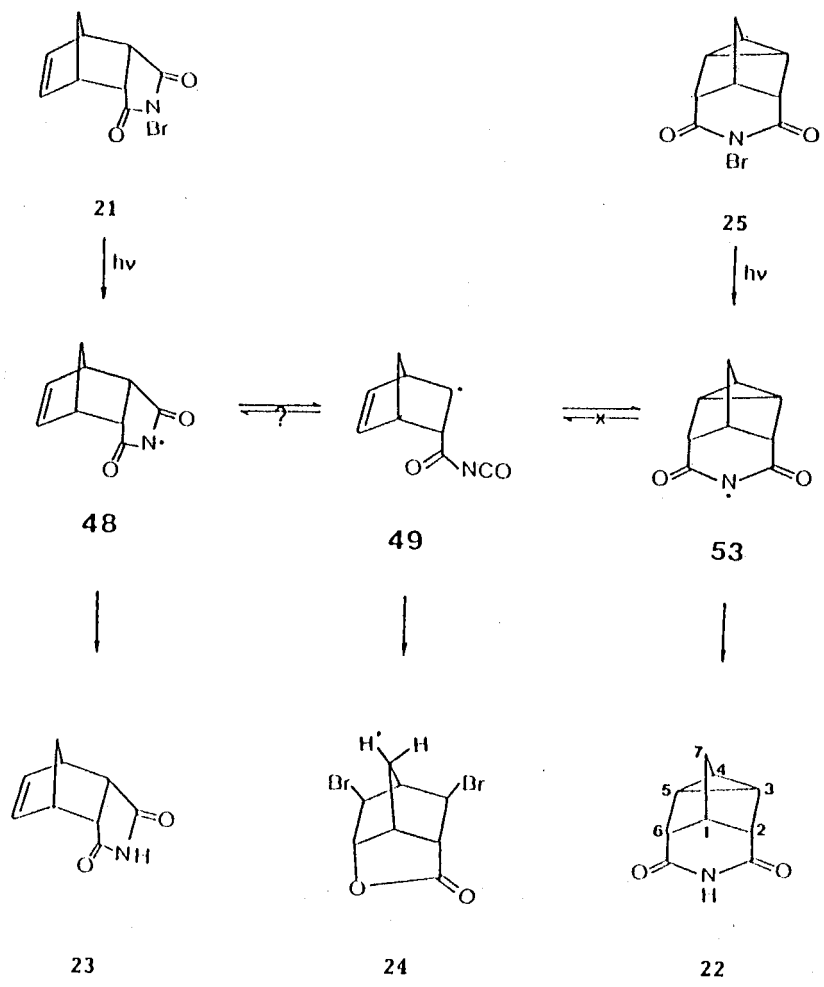

radical, the step of **48** → **49** in Scheme 3-8 is assumed to be reversible by analogy to their unsubstituted counterparts (the succinimidyl and PI· radicals). On the basis of his experimental observation[4], Skell concludes reasonably that the β-scission of succinimidyl radical and the cyclization of PI radical are reversible. He also extrapolates this conclusion to the ring-opening of α-alkyl-glutarimidyl radical[4]. Imidyl radical **53** can be regarded as such an alkyl-substituted glutarimidyl radical. Unfortunately, it fails to ring open (β-scission) as shown in this work. In such a complicated field as imidyl radical chemistry, any extrapolation is unwarranted.

3.4.3. Bromine Atom Chain Domain vs. Imidyl Chain Domain

Photolysis of **32** in 0.06 M DCE produces ring opening products predominantly. Photolysis of **26**, the unsaturated analog of **32**, under similar conditions, however, affords the allylic bromination product **27**, the same one obtained under the Ziegler's conditions using NBS in carbon tetrachloride as the bromination reagent. This demonstrates that even in the presence of a scavenger for Br_2 and/or Br·, the bromine atom chain is still capable of predominating in the bromination of a substrate with allylic and benzylic hydrogen using an N-bromoimide as the bromination reagent. This conclusion has been obtained by the mid 70's and has been frequently reviewed[14,29]. The conclusion that

the allylic brominated compound **27** results from bromination by bromine atoms is further confirmed by the following observations:

(1) An increase in the concentration of DCE makes ring opening products **30** and **31** become major ones through more efficient scavenging of Br_2 and/or Br· (Table 2-21).

(2) Replacement of DCE by a more reactive olefin like 1,3-pentadiene for the scavenging of Br_2 and bromine atoms enables ring opening to be predominant (experiment 183, Table 2-22).

Instead of using more reactive olefin than DCE, removal of reactive C-H bonds towards bromine atoms also suppresses the bromine atom chain. For example, in the case of **21** which carries an additional CH_2 bridge on **26** (see Scheme 3-9), the two allylic hydrogens are not reactive to bromine atoms because of their location at the tertiary bridgehead positions[129]. Now 0.05 M DCE is enough to suppress the allylic bromination by bromine atoms and causes the ring opening of imidyl radical **62** to prevail, producing **22** and **24** (see Table 2-19). It is concluded that for cyclic imidyl radicals which are capable of undergoing ring opening, the failure to observe such a reaction under some conditions is mainly due to the successful competition of the bromine atom chain (see the Goldfinger mechanism described in Section 1.1). In this case, the bromine atom chain is usually facilitated by the presence of reactive substrates towards

Scheme 3-9. Change of chain carriers in photolysis of the N-bromoimide-Br_2 system by changing structure of N-bromoimides

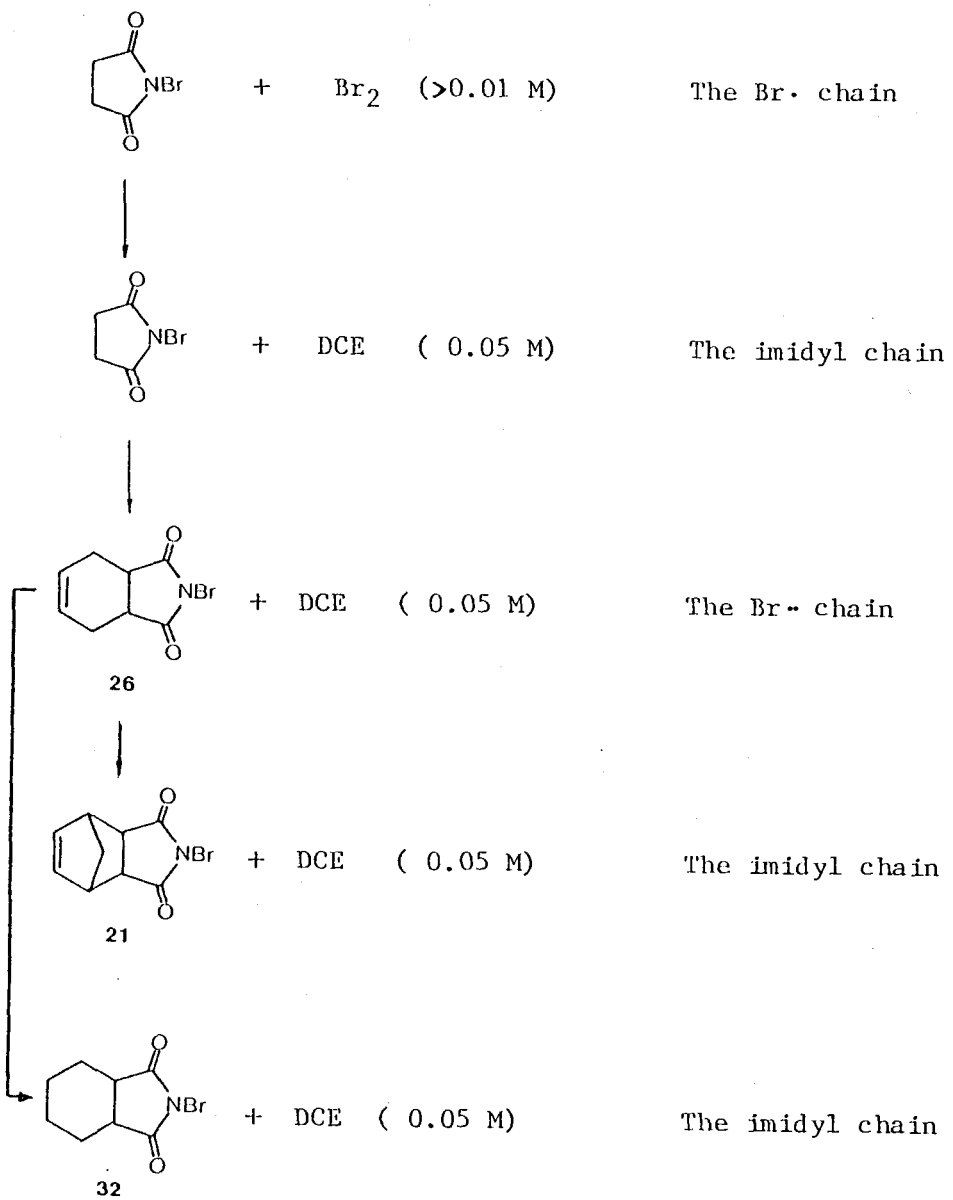

bromine atoms in the reaction systems. Ring opening of such imidyl radicals can be assured by either removing the reactive substrates or using more efficient bromine scavenger.

NBS has no allylic hydrogen, therefore, 0.05 M DCE is enough to ensure its ring opening. But **26** has allylic hydrogens which are very reactive towards the bromine atom. The rate of hydrogen abstraction by Br· from the allylic position is so fast that the Br_2 at the low concentration which survives the DCE's scavenging is enough to perpetuate the bromine atom chain, the imidyl chain being suppressed. In this case, the Goldfinger mechanism operates. The discussion can be expressed with Schemes 3-9.

Section V. Reactions of NBS with Naphthols

3.5.1. Formation of Dienones

Bromination of phenols with bromine has been studied extensively as a prototype electronic reaction[130-135]. NBS has been used as an analytical reagent for phenols such as vanillin and thymol[136,137], but its mechanistic aspects have scarcely received any attention. A semistable product obtained from the reaction of NBS with estradiol has been proposed to be hypobromite **54**[138] although its NMR data are equally compatible with a cyclohexadienone structure **55**.

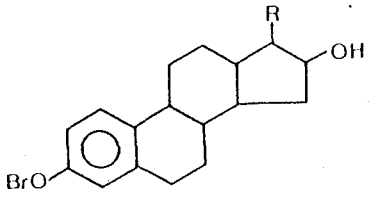

54

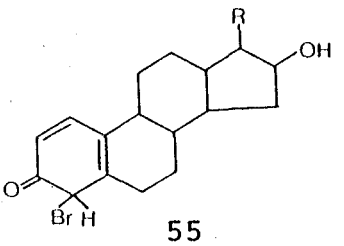

55

In this work the mechanistic studies of the reaction of naphthols with NBS is carried out primarily using 1-NpOH as a model compound. The UV data of the product **41** formed in the reaction of NBS with 1-NpOH are not conclusive as far as its structure determination is concerned, since alkyl hypobromites are reported to absorb near 340 nm[139,140]. The naphthyl hypobromite (**56**) may absorb at a longer wavelength. Nevertheless, the carbonyl absorption at 1701 cm^{-1} due to the product which has λ=357 nm suggests a dienone structure rather than that of the hypobromite. The dienone structures are also assigned to the products from other naphthols in analogy to the 1-NpOH reaction.

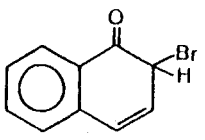

41

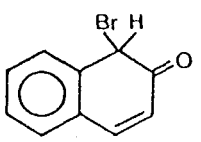

42

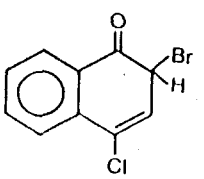

43

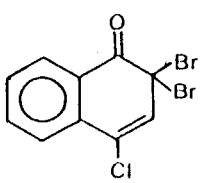

44

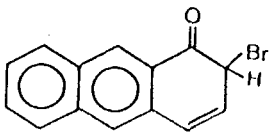

45

3.5.2. Possibility of Hypobromite as precursor of Dienones

The involvement of hypobromites in oxidation of alcohols and bromination of phenols has been conceived for a long time[136,141]. No evidence, however, has been found to substantiate the hyphothesis. If the formation of **41** from 1-NpOH and NBS is not an elementary reaction, the hypobromite **56** might be a mechanistically reasonable precursor of dienone **41** (see Scheme 3-10). The rate of consumption of 1-NpOH has been determined to be the same as that of the formation of **41**. If the formation of **56** from 1-NpOH and NBS is much slower than the intramolecular rearrangement of **56** to **41**, that is, the formation of **56** is rate determining step, route a and route b will show the same kinetics as far as the formation of **41** is concerned. In this case, the formation of **56** is a bottle-neck, and the *observed* rate of formation of dienone **41** can only be, at most, as fast as that of the formation of hypobromite **56**.

Supposing that hypobromite **56** is a short-lived precursor of dienone **41**, an interesting questions arises. How much faster should the rate of rearrangement of **56** to **41** be compared to that of formation of **56** from 1-NpOH and NBS in order for an exponential curve as in Figure 2-18 to be observed? Based on Scheme 3-11 the following equation can be derived[142].

Scheme 3-10.

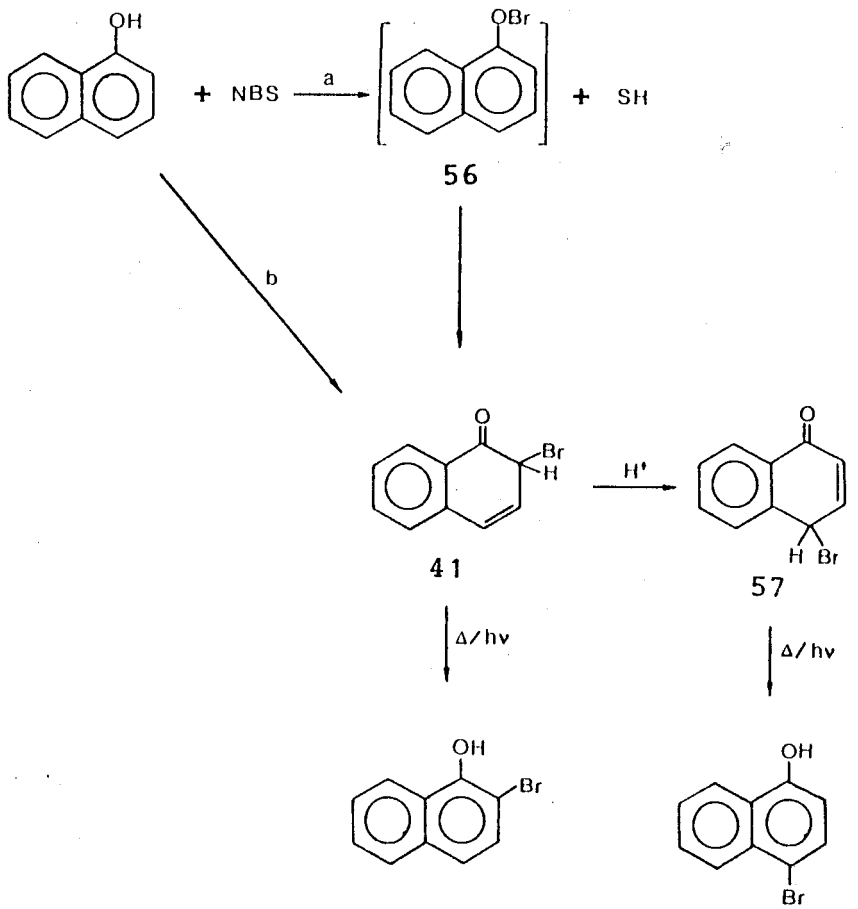

Scheme 3-11.

$$\text{NBS} \xrightarrow{k_1} \mathbf{56} \xrightarrow{k_2} \mathbf{41} \xrightarrow{k_3} \text{Bromophenols}$$

$$\begin{aligned} A(t) = {} & \epsilon_{56}\{k_1[\text{NBS}]^0/(k_2-k_1)\}\exp(-k_1 t) \\ & - \epsilon_{56}\{k_1[\text{NBS}]^0/(k_2-k_1)\}\exp(-k_2 t) \\ & - \epsilon_{41}\{k_1[\text{NBS}]^0/(k_2-k_1)(k_3-k_1)\}\exp(-k_1 t) \\ & + \epsilon_{41}\{k_1[\text{NBS}]^0/(k_2-k_1)(k_3-k_2)\}\exp(-k_2 t) \\ & - \epsilon_{41}\{k_1[\text{NBS}]^0/(k_3-k_1)(k_3-k_2)\}\exp(-k_3 t) \end{aligned}$$

where $A(t)$ is the absorbance observed at a given wavelength (for example, 365 nm), ϵ_{56} and ϵ_{41} are molar absorptivities of **56** and **41** at the given wavelength respectively, $[\text{NBS}]^0$ is the initial concentration of NBS (1-NpOH is in excess therefore k_1 is the pseudo-first order rate constant for the formation of **56**), k_2 is the first order rate constant for the rearrangement of **56** to **41**, and k_3 is the first order rate constant for the thermal decomposition of **41** which makes little contribution to the observed kinetic profile of $A(t)$ vs. time t. It is shown that after the value for k_{obs} in Table 2-25 is fed into a computer as k_1, the best fit is realized when $k_2/k_1=1.7\times10^6$. This means that k_2 is in the order of magnitude of $\simeq10^4$ s^{-1}, which is not too high to be reasonable[143].

An interesting question is the location of the attack of NBS on naphtholic species, i.e., whether it is an attack at the O-center or the C-center. The former leads to the formation of hypobromite **56**, and the latter results in the formation of the dienone directly from the reaction of 1-NpOH with NBS. NBS is formally regarded as a source of positive bromine, and its N-Br bond may be polarized but not dissociated in dichloromethane to provide a bromonium ion. Even though the attempt to detect the O-Br bond stretching absorption by FT-IR spectroscopy failed, there is evidence to suggest that the primary product from NBS and 1-NpOH is hypobromite **56** which rearranges rapidly to dienone **41**. In a mixture of 1-$NpOCH_3$ and 1-NpOH the bromination of 1-NpOH by NBS occurs almost exclusively (Table 2-27). This suggests that the reaction might have occurred at the oxygen but not at the *ortho* position to the hydroxy group of 1-NpOH (the C-2 position). This is a reasonable conclusion in view of the fact that NBS does not add to a carbon-carbon double bond thermally while bromine does so efficiently. It should be mentioned that the direct attack of NBS at the C-2 position does not lead necessarily to the dienone intermediate, even though it produces 2-Br-1-NpOH eventually if the attack occurs at all. In contrast, Br_2 does brominate 1-$NpOCH_3$ as shown in Table 2-27. Molecular bromine has been proposed as the actual reagent in the bromination of phenol with NBS; i.e., NBS acts as a reservoir of molecular bromine in low concentration by reacting with HBr[50,79]. This conclusion is obviously untenable, at least, in

aprotic nonpolar solvents, for the same reason.

The formation of hypobromites from phenols and NBS in aprotic solvent can be regarded as an electrophilic attack of the positively polarized Br of NBS on the phenolic oxygen, or a nucleophilic attack of the phenolic oxygen on the bromine atom of NBS. The mechanism of the latter process is essentially a halophilic reaction[144-145]. The formation of dienones can also be regarded as oxidative electrophilic substitution[146]. Whatever interpretation is used, the failure for *p*-nitro- and *p*-cyanophenols to react with NBS clearly indicates that a low electron density at the O-center retards the reactivities[147].

3.5.3. Decomposition of Dienones

At the onset of the interaction of NBS with 1-NpOH, only dienone **41** is formed as the initial product as indicated by the lack of the IR bands of **57**. Since the prototropy of **57** produces 4-Br-1-NpOH and that of **41** produces 2-Br-1-NpOH, the production of 4-Br-1-NpOH (see Table 2-26) indicates that **57** is formed at a certain point in the reaction. The rearrangement of **41** to **57** is thermodynamically favored, and the latter absorbs in the region 250-310 nm[81-83]. The higher percentage yields of 4-Br-1-NpOH in experiments 197, 200, and 201, where unpurified NBS is used, demonstrates that a trace amount of acid impurities catalyses the rearrangement of **41** $\rightarrow$ **57**.

It is worthwile to mention the following two points. (1) The acid catalysis in the thermal rearrangement of dienone **41** to brominated naphthols is confirmed by kinetic studies in this work, and that an acid could catalyse[50,79] the rearrangement of an extended dienone such as **41** to a cross-conjugated dienone such as **57**, and (2) It is known that brominated phenols are more acidic by about one pK_a unit than the parent phenols[148]. Probably the thermal decomposition of dienone **41** is subject to increasing acid catalysis as more and more 2-Br- and 4-Br-1-NpOH are generated during the thermal decomposition. Therefore, the decay of the absorbance of **41** does not follow either first-order or second-order kinetics. Also, probably the rearrangement of **41** to **57** is catalysed by the bromonaphthols generated during the decomposition of dienone **41**.

Bromination of phenols with Br_2 to produce dienone intermediates has been recognized previously[131-135,50,79], and with some 2- and 4-substituted phenols and naphthols, the corresponding dienones have been isolated and identified[131,50,76]. However, Br_2 as the reagent generally leads to uncontrollable bromination for two reasons: (1) a secondary bromination of dienones, and (2) the generation of HBr which catalyses the rapid rearrangements of dienones. From this point of view, NBS is a good reagent to generate extended dienones such as **41** *in situ* and/or to monobrominate at *ortho*-positions of naphthols, provided that caution is exercized to eliminate trace amounts of

acids.

The solutions of dienones derived from naphthols as shown in Table 2-23 can be used as secondary actinometric solutions in the region 300-400 nm. These solutions are easily prepared and have a sufficiently long lifetime. The concentrations of the dienones are readily determined by UV spectroscopy. The rearrangement of **41** to 2-Br-1-NpOH is accompanied by aromatization, and should be an irreversible process. The efficient and clean photorearrangement of these dienones (e.g., the quantum yield of unity for the case of **41**) makes them excellent compounds as actinometry.

CHAPTER FOUR

EXPERIMENTAL

4.1. General Conditions

Unless otherwise stated, the following experimental conditions prevailed. Melting points (mp) were determined on a Fisher-Johns apparatus, and are uncorrected. Infrared spectra (IR) were recorded with a Perkin-Elmer 559B spectrophotometer using Nujol mull, neat liquid film or solution. Ultraviolet and visible spectra (UV) were taken with a Varian Cary 210 spectrophotometer. Mass spectra (MS) and gas-chromatography-mass spectra (GC-MS) were obtained on a Hewlett-Packard 5985 GC-MS system either by electron ionization (at 70 eV) or by chemical ionization. Proton nuclear magnetic resonance (^{1}H NMR) spectra were recorded with a EM-360, Bruker WM-400, or Bruker SY-100 spectrometer from samples in $CDCl_3$ solution using tetramethylsilane (TMS) or the trace of $CHCl_3$ (7.27 ppm) contained in $CDCl_3$ as an internal standard. Chemical shifts are reported in δ values in ppm and coupling constants (J) in H_Z. The coupling patterns are presented as s (singlet), d (doublet), t (triplet), q (quartet) and m (multiplet). The chemical shifts of ^{13}C NMR spectra are also reported as δ values in ppm relative to TMS. Elemental analyses were carried out by Mr. M. K. Yang using a Carlo Erba Model-1106 Elemental Analyzer. Gas chromatography (GC) analyses

were performed on a Hewlett-Packard 5790A chromatograph (FID), equipped with an OV-1 capillary column (HP, 12 m x 0.20 mm) and a Hewlett-Packard 3390A chart integrator. Retention times are reported in minutes. Separations by column chromatography were carried out on silica gel (Baker, 60-200 mesh)[149]. Fluorescence spectra were taken with a Perkin-Elmer MPF 44B spectrophotometer and were uncorrected.

4.2. Chemicals

In the preparative reactions, solvents of reagent grade were used as supplied. For photochemical reactions and kinetic studies, analytical reagent grade solvents were purified prior to use. Dichloromethane (Fisher) was purified by distillation over phosphorus pentoxide (BDH, reagent). GC analysis showed it to be 99.9% pure. Chloroform (Fisher) was shaken five times with about half its volume of water, then dried over anhydrous magnesium sulphate for one hour followed by distillation over phosphorus pentoxide (BDH, reagent) before use (99.8% pure by GC analysis). Dioxane (Fisher) was distilled from sodium-benzophenone. Carbon tetrachloride (Fisher), cyclohexane (Fisher), 1,1-dichloroethene (Aldrich, 99%), 3,3-dimethylbutene (Aldrich, 95%), benzene (BDH, reagent), and acetonitrile (BDH, reagent) were distilled before use. For spectroscopy, commercial spectrophotometric grade solvents were used as supplied. N-Bromosuccinimide (BDH, reagent) was recrystallized from hot water and dried over anhydrous

calcium chloride under reduced pressure for 48 hours in the dark, after which it was sealed and stored in a refrigerator. The container was warmed to room temperature before opening. N-Bromophthalimide (Aldrich) was used as supplied. Bromine (Anachemia, reagent), hexamethylethane (Aldrich, 99%) were used as supplied. Anhydrous potassium carbonate (BDH, reagent) was ground to a powder and pumped in a vaccum line at 150°C for 24 hours prior to use. 1-Naphthol (Anachemia), 2-naphthol (Anachemia) were recrystallized from toluene twice followed by sublimation twice. 4-Chloro-1-naphthol (Sigma) and 4-methoxyphenol (Sigma) were sublimed, then kept under a nitrogen atmosphere in a refrigerator. Argon (Union Carbide Linde, 99.9995%) and nitrogen (Union Carbide Linde, 99.998%) were used as suppiled.

4.3. Photolysis Apparatus

Method I A 200-watt Hanovia medium pressure mercury lamp, with or without a GWV filter (cut-off at $\lambda \simeq 385$ nm), was placed in a Pyrex cold-finger, the latter was cooled by cold water. Vessels containing samples were placed *ca.* 5 cm away from the lamp. Both the cold-finger and the vessels were placed in a sink full of cold water. The temperature of the water in the sink was 15-18°C throughout irradiation.

When a ≥400-nm light source was needed, the cold-finger was placed in a Pyrex cylinder (8x28 cm) containing $NaNO_2$-sodium

hydrogen phthalate solution (0.0266 M, cut-off at ≥400 nm)[54]. The thickness of the solution was adjusted to about 1 cm.

Method II RPR 3000 Å lamps (6 or 12x21 watts) were placed in a Rayonet Photochemical Reactor. Tubes containing samples were placed in a merry-go-round apparatus inside the reactor, and were cooled by a fan blowing air over dry ice. The temperature inside was 15-18°C throughout irradiation.

4.4. Photodecomposition of N-bromoimides

4.4.1. Photodecomposition of NBS

4.4.1.1. In the Presence of DCE

Two NMR tubes (tube A and tube B, Wilmad, 505 ps) were placed in a dark room, and each was wrapped with a piece of aluminum foil (4x15 cm). To each of the tube was added NBS (22.0 mg, 0.123 mmol), DCE (4.5 μl, 0.055 mmol), and dichloromethane (1.0 ml). Clear solutions were obtained. Each of the tubes was capped with a rubber septum. Using a long metallic needle as a gas inlet and a short one as an outlet, the solution was purged with argon. When argon was bubbled through the solution the tube was cooled with an ice-salt bath to minimize the escape of the solvent and volatile components. After the solution had been purged for five minutes the needles were pulled out quickly and the septum was sealed with a piece of Parafilm wax paper (2x4

cm). The solutions in tube A and B were irradiated with a 200-watt mercury lamp through a Pyrex filter (Method I) for 85 minutes. NMR analysis showed that NBS conversion was 88.9% and 87.7% in tube A and B respectively by the use of Eq. 4-1

$$\text{Conv.} = \{1 - [I_{2.95}/(I_{2.95} + I_{2.75} + 2xI_{3.61})]\}x100\% \qquad 4\text{-}1$$

where $I_{2.95}$ stands for the intensity or area of the signal at 2.95 ppm (s, 4H) due to NBS, $I_{2.75}$ for that of the signal at 2.75 ppm (s, 4H) due to succinimide, and $I_{3.61}$ that of the signal at 3.61 ppm (t, 2H) due to BPI. These signals did not overlap with the signal at 5.3 ppm due to dichloromethane. The photolysate in Tube A was transferred to a 5 ml flask and diluted with dichloromethane (3 ml). The solution was washed with 5% aqueous sodium bisulfite solution (0.6 ml) in a separatory funnel. The aqueous layer was extracted with dichloromethane (1 ml x 3). The organic layer together with the combined organic extracts was dried over anhydrous magnesium sulphate. To the mixture was added a solution of benzophenone (0.0372 mmol) in 100 μl of dichloromethane. The organic phase was collected by filtration and the filtrate was analysed by GC (column temperature, 160°C isothermal; column pressure, 10 psi) to afford succinimide (retention time 1.27 minutes, 0.0332 mmol) and BPA (1.46 minutes, 0.0869 mmol, 79.7% based on the NBS consumed). The retention time of benzophenone under the conditions was 5.78 min. The molar response factors of BPA and succinimide to that

of benzophenone were determined first, with the mixtures of these three compounds.

The photolysate in tube B was transferred to a 5 ml flask. To the flask was added 100 μl of dichloromethane solution containing 3,3-dimethylglutarimide (0.0191 mmol). The solvent was removed under reduced pressure. To make sure that the loss of the internal standard was negligible during the evaporation, a control experiment was carried out as follows. A mixture of succinimide (1.97 mg) and 3,3-dimethylglutarimide (2.79 mg) was dissolved in $CDCl_3$ (0.6 ml), and the solution was analysed with a Bruker SY 100 NMR spectrometer. The ratio of the signal intensity of succinimide at 2.75 ppm (4H) to that of 3,3-dimethylglutarimide at 2.45 ppm (4H) was determined to be 1.00:1.01. The solvent was removed under reduced pressure, and the residue was dissolved in dichloromethane (3 ml). Then the solvent was removed again under reduced pressure. The residue was taken up with $CDCl_3$ (0.6 ml) and the solution was analysed by NMR spectroscopy. A ratio of the signal intensity of 1.00:1.03 was obtained. The difference was within the experimental error (*ca.* 5%). After the solvent in tube B was removed, the residue was left in the dark and exposed to air for ten minutes, after which it was taken up with $CDCl_3$ (1 ml). The yield of BPA, Y(BPA), was determined to be 0.0824 mmol (76.3% based on the NBS consumed) by the use of Eq. 4-2.

$$Y(BPA) = (2xI_{3.65}/I_{2.45})m \qquad 4\text{-}2$$

where $I_{3.65}$ stands for the intergral of the signal of BPA at 3.65 ppm, $I_{2.45}$ for that of 3,3-dimethylglutarimide at 2.45 ppm, and m is the amount of the 3,3-dimethylglutarimide (in mmol) added into the photolysate. The yield of succinimide, Y(SH), was determined to be 0.0264 mmol by the use of Eq. 4-3, where $I_{2.75}$

$$Y(SH) = (I_{2.75}/I_{2.45})m \qquad 4\text{-}3$$

stands for the intergral of the signal of succinimide at 2.75 ppm. The sample was then analysed by GC with benzophenone as an internal standard (see the previous paragraph for details of GC analysis) to afford succinimide (0.0396 mmol) and BPA (0.0781 mmol, 72.3% based on the NBS consumed). The yields of BPA and succinimide determined with GC analysis for tube A and B were averaged and reported in Table 2-1 (see experiment 8).

In a separated experiment, to each of the two NMR tubes (tube C and D) was added NBS (22.0 mg, 0.123 mmol), DCE (4.5 μl, 0.055 mmol) with a 10 μl syringe, and trichloromethane (1.0 ml). Heterogeneous mixtures in the two tubes were obtained. Each of the tubes was capped and purged with argon for five minutes (see the first part of this section for details). After being irradiated with a mercury lamp through a Pyrex filter (Method I) for forty minutes, shaken from time to time, the samples in the NMR

tubes became homogeneous. Then the NBS conversion was monitored with NMR spectroscopy (see the first part of this section for the details). Ninty minutes of irradiation decomposed 90.5% NBS in tube C and 88.3% in tube D. NMR analysis (see the first part of this section for the detail) afforded BPA (0.0737 mmol, 66.4% based on the NBS consumed in tube C; 0.0671 mmol, 61.6% in tube D) and succinimide (0.0385 mmol in tube C and 0.0407 mmol in tube D). The yields of BPA and succinimide determined by NMR analysis were averaged and reported in Table 2-1 (see experiment 9).

4.4.1.2. In the Presence of Br_2

To dichloromethane (5.0 ml) in a test tube (1x10 cm) was added bromine (5.0 μl) with a 1 μl pipette (1 μl x 5). To each of the four NMR tubes was added NBS (20.0 mg, 0.112 mmol), cyclohexane (10.0 μl, 0.0920 mmol), and the prepared CH_2Cl_2 solution (1.00 ml) of bromine. Each tube was capped, and the solution inside was purged with nitrogen for five minutes using a metallic needle connected to a Teflon tube (0.1x15 cm) as a gas inlet and a needle as an outlet. One tube was opened, and the absorbance at 412 nm of the solution was determined to be 0.436 with a UV cell (0.1-cm pathlength). The concentration of bromine was calculated to be 21.8 mM, given the molar absorptivity of bromine at 412 nm = 200 (in dichloromethane). The other three tubes were irradiated with RPR 3000 Å lamps (Method II). The

first tube was withdrawn in ten minutes from the merry-go-round, and 25.5% NBS was consumed according to the NMR analysis (see Section 4.4.1.1 for the detail). The remaining two tubes were taken out at twenty and twenty-nine minutes respectively, and 55% and 74% NBS were consumed. The photolysates were transferred into 0.1-cm UV cells, and their absorbances at 412 nm were determined to be 0.506, 0.534, and 0.536, corresponding to concentrations of bromine of 25.3, 26.7, and 26.8 mM respectively. The photolysates were washed with 10% aqueous solution of sodium bisulfite in separatory funnels, and the organic layers were separated and dried over anhydrous magnesium sulfate. To each mixture, was added tribromomethane (1.80 μl) as an internal standard with a 1 μl syringe (0.90 μl x 2). After the organic phases were separated from the magnesium sulfate by filtration, they were analysed by GC. Typical sets of retention times were 1.84 minutes ($CHBrCl_2$), 4.84 minutes ($CHBr_3$), and 9.40 minutes (bromocyclohexane) under the conditions of 55°C isothermal (column temperature) and 8 psi (column pressure); and 1.25 minutes ($CHBr_3$), 1.55 minutes (bromocyclohexane), and 2.84 minutes (1,2-dibromocyclohexane) under the conditions of 120°-200°C at 10°C/minutes (column temperature) and 8 psi (column pressure). The molar response factor of bromocyclohexane relative to the internal standard ($CHBr_3$) was determined first by analysing the mixtures of these two compounds in various ratios. The molar response factor of 1,2-dibromocyclohexane was assumed to be the same as that of bromocyclohexane. In each analysis, three

injections were executed, and the peak areas were averaged to calculate the absolute yields of these products. The results were listed in Table 2-7 (see experiments 55, 56, and 57). After the GC analysis was over, the three samples were analysed with NMR spectroscopy to determine the yields of BPA (see Section 4.4.1.1 for the details). In each analysis, two measurements were made. The signal areas relative to that of the internal standard (3,3-dimethylglutarimide) were averged to calculate the absolute yields of BPA. The results are listed in Table 2-7.

4.4.1.3. In the Presence of Benzene

Five dichloromethane solutions of NBS (0.056 M), DCE (0.037 M) and various concentrations of benzene (0-0.15 M) were prepared as follows. NBS (625 mg, 3.51 mmol) and DCE (138 μl, 1.72 mmol) were dissolved in CH_2Cl_2 (25.0 ml). Aliquots of the solution (2.00 ml each) were pipetted to each of five 5-ml volumetric flasks, and various amounts of benzene (0, 0, 11.0, 22.0, 54.0 μl) were added into each of these flasks. After diluting with CH_2Cl_2, the solutions (2.0 ml) were transferred into five Pyrex tubes (1x10 cm). The concentration of benzene in these tubes were 0, 0, 0.031, 0.061, and 0.15 M respectively. The tubes were capped, and the solutions inside were purged with nitrogen for five minutes (see Section 4.4.1.1 for the details). The degassed solutions were irradiated on a merry-go-round apparatus in a Rayonet Photochemical Reactor with 300-nm lamps

(21 watts x 6) for six minutes at 15-18°C (Method II). The photolysate (1.0 ml) was taken out and combined with 100 μl of CH_2Cl_2 containing 3,3-dimethylglutarimide (0.00129 mmol) as an internal standard. After the solvent was removed under reduced pressure, the residue was dissolved in 1.5 ml of $CDCl_3$ for 400 MH_Z NMR analysis. The intensities of the signals at 3.65 ppm due to BPA (t, 2H), at 2.75 ppm due to succinimide (s, 4H), at 2.91 ppm due to N-phenylsuccinimide (s, 4H), and at 2.88 ppm due to **2** (s, 4H) relative to the intensity of the signal at 2.45 ppm due to the internal standard (3,3-dimethylglutarimide, s, 4H) were used to calculate their absolute yields (see Section 4.4.1.1 for the formula). The results are listed in Table 2-9 (series I).

4.4.1.4. Relative Rates of Brominations of Cyclohexane and Dichloromethane

Irradiations were carried out on an optical bench. Light from a PEK 212 150-watt high pressure mercury lamp was filtered through a piece of glass, Corning CS-052 (cut-off at ≥300 nm[150]), and an aqueous solution of sodium nitrite-sodium hydrogen phthalate (1 cm thickness, cut-off at ≥400 nm) to provide a ≥400-nm light source. Alternatively, the light beam was filtered through a GWV filter to provide a >380-nm light source.

4.4.1.4.1. Br_2-K_2CO_3 System

To a 1-cm fluorescence cuvette with a long neck, was added CH_2Cl_2 (4.00 ml, 62.0 mmol), Br_2 (13 μl, 0.26 mmol), K_2CO_3 (185 mg, 1.34 mmol), cyclohexane (40.0 μl, 0.368 mmol), and a magnetic bar. The cuvette was sealed, and the heterogeneous mixture inside the cuvette was purged with nitrogen (see Section 4.4.1.2 for the detail). The substrates in the cuvette was stirred vigorously while irradiated with the ≥400-nm light source for 14 minutes. In a separate experiment, a vigorously stirred solution with the same composition as described above was irradiated with the >380-nm light source for 10 minutes. The photolysate was filtered, and the filtrate was washed and dried for GC analysis (see Section 4.4.1.2 for the detail). The yields of $CHBrCl_2$, $C_6H_{11}Br$, and 1,2-dibromocyclohexane ($C_6H_{10}Br$) determined by GC are listed in Table 2-8.

4.4.1.4.2. Br_2-NBS System

To a long neck fluorescence cuvette was added CH_2Cl_2 (4.00 ml, 62.0 mmol), Br_2 (13 μl, 0.26 mmol), NBS (80.0 mg, 0.449 mmol) and cyclohexane (40.0 μl, 0.368 mmol). The cuvette was sealed, and the solution inside the cuvette was first purged with nitrogen (see Section 4.4.1.2 for the detail) and then irradiated with the ≥400-nm light source for 14 minutes with vigorous stirring. In a separate experiment, a vigorously stirred

solution with the same composition as described above was irradiated with the >380-nm light source for 10 minutes. In each case, the photolysate (1.0 ml) was withdrawn from the cuvette with a volumetric pipette for NMR analysis (see Section 4.4.1.1 for the detail) to determine the conversion of NBS and the yield of BPA. The remaining photolysate (3.0 ml) was washed and dried for GC analysis (see Section 4.4.1.2 for the detail). The yields of $CHBrCl_2$, $C_6H_{11}Br$, and 1,2-dibromocyclohexane ($C_6H_{10}Br$) are reported in Table 2-8.

4.4.1.5. Quantum Yield of BPI Formation

The determination of quantum yield of BPI formation in 5 M benzene and in dichloromethane were carried out on a merry-go-round equipped with RPR 3000 Å lamps (Method II). NBS (100 mg, 0.562 mmol), DCE (20 μl, 0.26 mmol), and benzene (5.0 ml) were dissolved in dichloromethane in a 10 ml volumetric flask (solution A, 10.0 ml). To each of three Pyrex tubes (1x10 cm) was added solution A (3.00 ml). Similarly, a solution of NBS (100 mg, 0.562 mmol) and DCE (20 μl, 0.26 mmol) in dichloromethane (solution B) was first prepared in 10 ml volumetric flask, and then added into two Pyrex tubes (3.00 ml each). The rest of solution B was placed in a 1-cm UV cell, and the absorbance at 310 nm due to NBS was determined to be 0.542 (the ϵ value of NBS at 310 nm is 9.6 $M^{-1}cm^{-1}$). An actinometer solution was prepared (see Section 4.5.9 for the detail) and 3.00 ml of

the solution was placed into each of the five Pyrex tubes. The ten tubes which contained solution A, B, and the actinometer solution were placed on the merry-go-round and irradiated for six minutes. The two tubes containing solution B and the two tubes containing the actinometer solution were withdrawn from the merry-go-round. The absorbance of solution B at 310 nm was determined to be 0.410 and 0.438. The quantum yield of NBS decompsition was calculated to be 3.3±0.5 by the use of Eq. 4-4a

$$\Phi = (\Delta A \cdot V(/(\epsilon I t) \qquad 4\text{-}4a$$

where ΔA is the difference in the absorbance at 310 nm due to the NBS consumption (0.542-0.424=0.118, where 0.424 is the mean based on the two readings), V the volumn of the photolysate (3.00×10^{-3} l), ϵ the molar absorptivity of NBS at 310 nm (9.6), t the duration of the irradiation (6.0 minutes), and I the intensity of the incident light, which was determined to be $(1.8 \pm 0.2) \times 10^{-6}$ einstein/min (see 4.5.8 for the method of calculating the intensity of incident light). The three tubes containing solution A and the three tubes containing the actinometer solution were irradiated for eleven minutes (seventeen minutes in total). The photolysate (1.0 ml) was withdrawn from each of the three tubes and each was mixed with 3,3-dimethylglutarimide (3.00×10^{-3} mmol) in dichloromethane (100 μl). After the solvent was removed under reduced pressure, the residue was taken up with $CDCl_3$ (0.6 ml) for 400-MH_Z NMR analysis

(see Section 4.4.1.1 for the detail). The yield of BPA in each of the photolysate (1.0 ml) was determined to be 0.00141, 0.00128, and 0.00121 mmol. The concentration of BPI in the tubes was $(1.3\pm0.1)\times10^{-3}$ M, and the error is expressed as the standard deviation from the mean based on three runs (it was assumed that the BPA yield from each run had no associated error). The quantum yield of BPI formation was calculated to be 0.13±0.02 by the use of Eq. 4-4b

$$\Phi = CV/It \qquad 4\text{-}4b$$

where C is the BPA concentration (1.3×10^{-3} M), V the volumn of the photolysate (3.0×10^{-3} M), t the duration of the irradiation (17.0 minutes), and I the intensity of the incident light, which was determined to be $(1.8\pm0.2)\times10^{-6}$ einstein/min (the error is expressed as the standard deviation from the mean based on five runs).

Concentrations of BPA in solution B and PhS (including 3,4,5-tribromo-6-succinimidylcyclohexene **2**) in solution A were determined by NMR analysis to be $4.76\pm\times10^{-3}$, and 1.4×10^{-3} M respectively (see Section 4.4.1.1 and 4.4.1.3 for the method and the chemical shifts). The corresponding quantum yields were calculated by the use of Eq. 4-4 to be 1.3 and 0.14 respectively. The change in NBS concentration in solution A caused by the irradiation (seventeen minutes) was determined by NMR to be

Table 4-1

Correction Factors for the Quantum Yields of NBS Reactions

λ, nm	α	β	f
290	>>10	0.145	4
300	≥10	0.080	6
310	3.9	0.053	8

6.2×10^{-3} M, and the calculated quantum yield of NBS decomposition in the presence of 5 M benzene was 0.61 according Eq. 4-4a. Since the absorbance of solution A and B is different from that of the actinometer solution in the 300±10 nm region, a correction for the calculated quantum yield was needed. Correction factors (f) at 290, 300, and 310 nm were calculated by the use of Eq 4-5 (see Appendix 1 for the derivation)

$$f = (1-10^{-\alpha})/(1-10^{-\beta}) \qquad 4\text{-}5$$

where α and β are absorbance of the benzophenone solution and the NBS solution respectively at the given wavelengths respectively. These f values were averaged to give a correction factor of 6.

4.4.1.6. Bromination of Aromatic Compounds with NBS

4.4.1.6.1. Bromination of Naphthalene

NBS (105 mg, 0.590 mmol) and DCE (20 μl, 0.25 mmol) were dissolved in dichloromethane in a volumetric flask (5.0 ml). The solution (1.0 ml) was pipetted into each of three NMR tubes (tubes A, B, and C). To these tubes were added naphthalene (13.3 mg, 0.104 mmol; 41.4 mg, 0.323 mmol; and 136 mg, 1.06 mmol) respectively. The solutions were purged with nitrogen then irradiated with RPR 3000 Å lamps (Method II) for 14 minutes. After the solvent was removed under reduced pressure the residues were dissolved in $CDCl_3$ and analyzed by NMR spectroscopy. The conversion of NBS in each of these three tubes was determined to be 39%, 32%, and 31% respectively, and the BPA yield was 0.012 mmol (27% based on the amount of NBS consumed), 0.0072 mmol (19%), and 0.0033 mmol (8.9%) respectively. The washed and dried $CDCl_3$ solutions were analysed by GC with benzophenone as an internal standard (column temperature 140-230°C at 10°/min, column pressure 20 psi, column length 25 m) to afford 1-bromonaphthalene (retention time 3.65 minutes, 0.00014 mmol, 0.06% based on the amount of NBS consumed in tube A; 0.0095 mmol, 5.2% in tube C),[1] 1-succinimidylnaphthalene (retention time 9.59 minutes,

---

[1]Some photolysate in tube B was lost during the sample transfer before benzophenone was added as an internal standard (retention

0.0017 mmol, 7.4% in tube A; 0.00072 mmol, 3.9% in tube C), and 2-succinimidylnaphthalene (retention time 10.34 minutes, 0.00048 mmol, 2.1% in tube A; 0.00028 mmol, 1.5% in tube C). No 2-bromonaphthalene was detected by GC-MS analysis.

4.4.1.6.2. Bromination of Anthracene

A solution of anthracene (18.6 mg, 0.105 mmol) and NBS (17.2 mg, 0.0966 mmol) in CH_2Cl_2 (4.0 ml) in a 1-cm fluorescence cuvette was purged with nitrogen then irradiated with RPR 3000 Å lamps (Method II) for 60 minutes. A cloudy yellow solution was obtained. Removal of the solvent left a yellow powder. To the residue was added $CDCl_3$ (3 ml) to give a yellow solution with some yellowish powder floating on the surface. The mixture was filtered, and the filtrate was analysed to afford BPA (0.0021 mmol, 2% based on 100% NBS conversion) by NMR, and 9-bromoanthracene (0.042 mmol, 38% based on 100% NBS conversion, retention time 5.30 minutes) and 9,10-dibromoanthracene (0.027 mmol, 25%, retention time 6.89 minutes) by GC (column temperature 230°C isothermal, column pressure 10 psi).

In a separate experiment, a solution of anthracene (20 mg, 0.11 mmol) and NBS (19 mg, 0.11 mmol) in CH_2Cl_2 (1.0 ml) in a NMR tube was purged with nitrogen and irradiated with a 200-W mercury lamp through a GWV filter (Method I) for 175 minutes.

---

[1](cont'd) time 4.68 minutes).

The conversion of NBS (90%) and the yield of succinimide (0.096 mmol, 97% based on the the amount of NBS consumed) were determined by NMR spectroscopy. Neither BPI nor BPA was detected by NMR. GC analysis afforded 9-bromoanthracene (0.084 mmol, 85%) and 9,10-dibromoanthracene (0.0026 mmol, 2.6%).

4.4.1.6.3. Bromination of Phenanthrene

A solution of phenanthrene (55 mg, 0.31 mmol) and NBS (20 mg, 0.11 mmol) in CH_2Cl_2 (4.0 ml) in a 1-cm fluorescence cuvette was purged with nitrogen and irradiated with a 200-watt mercury lamp through a GWV filter (Method I) for 160 minutes. The solvent was removed from the photolysate and the residue, dissolved in $CDCl_3$ (0.6 ml), was analysed by NMR spectroscopy to afford succinimide (0.55 mmol, 91% based on 55% NBS conversion). But no BPA or BPI was detected. The $CDCl_3$ solution was washed and dried for GC analysis (column temperature 230°C isothermal, column pressure 20 psi) to afford 9-bromophenanthrene (retention time 3.78 minutes, 0.043 mmol, 71% based on the NBS consumed). A small peak on the GC trace was detected (retention time 6.81 minutes), and the area of the signal was 1/10 of that of 9-bromophenanthrene. GC-MS analysis of this peak provided *m/e* (relative intensity) 338 (M^+, 40), 336 (M^+, 80), 334 (M^+, 45), 257 (M^+-Br, 10), 255 (M^+-Br, 10), 176 (M^+-2Br, 100), 88 (70).

4.4.1.6.4. Bromination of Toluene with NBS-Br_2 System

A solution of NBS (20 mg, 0.11 mmol), toluene (9.5 μl, 0.090 mmol) and Br_2 (1 μl, 0.02 mmol) in CH_2Cl_2 (1.0 ml) in a capped NMR tube was purged with nitrogen, and irradiated with a 200-watt mercury lamp through a GWV filter (Method I) for fifteen minutes. The conversion of NBS was determined to be 89% by NMR spectroscopy (the singlet at 2.31 ppm (3H) due to toluene did not interfere with the NMR analysis). The photolysate was washed and dried for GC analysis to afford benzylbromide (0.095 mmol, 97% based on the amount of NBS consumed). The yield of succinimide was 0.10 mmol. BPA was not detected by either GC or NMR analysis.

4.4.2. Photodecomposition of N-Bromo-3,3-dimethylglutarimide

4.4.2.1. In the Presence of DCE

A solution of N-bromo-3,3-dimethylglutarimide (10.8 mg, 0.0490 mmol), DCE (2.3 μl, 0.028 mmol), and cyclohexane (20.0 μl, 0.184 mmol) in CH_2Cl_2 (2.00 ml, 15.5 mmol) was prepared, and the solution (1.0 ml) was added to each of the two NMR tubes (A and B). Each tube was capped, and the solution in the tube was purged with nitrogen and irradiated through a Pyrex filter (Method I) for 83 minutes. The decomposition of N-bromo-3,3-dimethylglutarimide, D, was determined to be 95% and 90% in these two photolysates by NMR spectroscopy using Eq. 4-6

$$D = \{1-[I_{2.74}/(I_{2.74} + I_{2.45})]\}x100\% \qquad 4\text{-}6$$

where $I_{2.74}$ and $I_{2.45}$ are the intensities of the signals at 2.74 ppm (s, 4H) due to N-bromo-3,3-dimethylglutarimide and 2.45 ppm (s, 4H) due to 3,3-dimethylglutarimide. The photolysates were washed and dried for GC analysis (see Section 4.4.1.1. for the detail) to afford $CHBrCl_2$ (0.00511 mmol in tube A and 0.00415 mmol in tube B) and bromocyclohexane (0.0151 mmol in tube A and 0.0139 mmol in tube B). The yields of $CHBrCl_2$ and those of bromocyclohexane in these two tubes were averaged and reported as experiment 63 in Table 2-10.

4.4.2.2. In the Presence of Br_2

A solution of N-bromo-3,3-dimethylglutarimide (32.4 mg, 0.147 mmol), Br_2 (10 μl, 0.20 mmol), and cyclohexane (20.0 μl, 0.184 mmol) in CH_2Cl_2 (2.00 ml) was prepared, and the solution (1.0 ml) was added to each of the two NMR tubes (A and B). After the tubes were capped, the solutions were purged with nitrogen, and irradiated with a 200-watt mercury lamp through a GWV filter (Method I) for ten minutes. The conversion of N-bromo-3,3-dimethylglutarimide in tubes A and B was determined to be 65.1% and 63.9 % respectively by NMR spectroscopy. The photolysates were washed and dried for GC analysis to afford $CHBrCl_2$ (0.027 mmol in tube A and 26.8 mmol in tube B), bromocyclohexane (0.00980 mmol in tube A and 0.00834 mmol in tube B), and

1,2-dibromocyclohexane (0.00637 mmol in tube A and 0.00543 mmol in tube B). The yields of these products were averaged and reported as experiment 70 in Table 2-11.

4.4.2.3. In the Presence of Cyclohexane and Benzene

Five dichloromethane solutions of N-bromo-3,3-dimethylglutarimide (0.10 M), cyclohexane (0.92 M), DCE (0.05 M) and various concentrations of benzene (0-0.80 M) were prepared as follows: N-bromo-3,3-dimethylglutarimide (1.37 g, 6.23 mmol), DCE (250 μl, 1.72 mmol), and cyclohexane (6.25 ml, 57.5 mmol) were dissolved in CH_2Cl_2 and filled up to 25.0 ml. Aliquots of the solution (2.00 ml each) were pipetted into each of five 5-ml volumetric flasks, and various amounts of benzene (0, 0, 140, 210, 290 μl) were added into each of these flasks with syringes. After diluting with CH_2Cl_2 to 5.0 ml, the solutions (2.00 ml) were transferred into five Pyrex tubes (1x10 cm). The concentration of benzene in these tubes were 0, 0, 0.40, 0.60, and 0.80 M respectively. The tubes were capped, and the solutions inside purged with nitrogen for five minutes. The degassed solutions were irradiated on a merry-go-round apparatus in a Rayonet Photochemical Reactor with RPR 3000 Å lamps (21 watts x 12) for 2.5 minutes at 15-18°C (Method II). The conversion of N-bromo-3,3-dimethylglutarimide in the two tubes containing no benzene was determined by NMR spectroscopy to be 12.5% and 12.7%. The photolysate (1.0 ml) was withdrawn from each of the five tubes,

washed and dried for GC analysis (column temperature 120-230°C at 10°/mimute, column pressure 20 psi, column length 25 m) to determine the yields of bromocyclohexane (retention time 1.96 minutes) and N-phenyl-3,3-dimethylglutarimide (retention time 8.52 minutes) using benzophenone as the internal standard (retention time 6.86 minutes). The results are listed as series E in Table 2-14.

4.4.2.4. Preparation of N-Phenyl-3,3-dimethylglutarimide (PhG)

To a 200 ml cylindrical photocell fitted with a side arm at the top and a gas inlet extended to the bottom, was added a solution of N-bromo-3,3-dimethylglutarimide (1.43 g, 6.47 mmol) and DCE (0.4 ml, 5 mmol) in benzene (160 ml). A Pyrex water-cooled lamp housing was inserted into the cell and the side arm connected to a condenser. A slow stream of nitrogen was allowed to bubble through the solution from the gas inlet and escape from a gas trap at the top of the condenser. The solution was irradiated with a 450-watt Hanovia medium pressure mercury lamp for thirty minutes. NMR analysis did not detect the singlet at 2.72 ppm due to the four methylene protons of 33NBG. Removal of the solvent left gum (2 g). GC analysis (200°C isothermal, 20 psi) showed the following products (retention time, peak area): 3,3-dimethylglutarimide (1.90 minutes, 53%) and PhG (3.41 minutes, 47%). The crude product was recrystallized from ethyl acetate-hexane (1:1) to give a solid (1.6 g) which contained 80%

PhG according to GC analysis. Chromatography of the solid (elution with 30% ethyl acetate-petroleum ether (30°-60°) gave twenty fractions of 15 ml each. Fractions 14-17 contained the title compound (250 mg) with >99% purity by GC analysis. Recrystallization of the crude product from methanol afforded PhG as colorless crystals (45 mg, 18%): mp 155-157°C; ^{1}H NMR ($CDCl_3$) 1.23 (s, 6H), 2.70 (s, 4H), 7.04-7.50 (m, 5H); IR (Nujol) 1730 (s), 1685 (s), 1600 (w), 1495 (m), 1457 (m), 1372 (s), 1335 (w), 1270 (s), 1250 (s), 1140(s), 770 (m), 700 (s), 640 (s); MS, *m/e* (relative intensity) 217 (M^+, 62), 189 (31), 174 (100), 119 (13), 94 (17), 83 (32), 55 (12). The tube 20 contained only 3,3-dimethylglutarimide shown by GC analysis.

4.4.2.5. In the Presence of Cyclohexane, 3,3-Dimethylbutene, and Benzene

A solution of N-bromo-3,3-dimethylglutarimide (200 mg, 0.909 mmol), cyclohexane (0.900 ml, 8.28 mmol), and 3,3-dimethylbutene (200 μl, 1.55 mmol) in dichloromethane (3.0 ml) was prepared. The solution (0.50 ml) was placed in each of the seven NMR tubes. Benzene (0, 0, 0.020, 0.040, 0.080, 0.20, 0.30 ml) and dichloromethane (0.50, 0.50, 0.48, 0.46, 0.42, 0.30, 0.20 ml) were added to these tubes respectively to form solutions of 0.11 M in N-bromo-3,3-dimethylglutarimide, 0.40 M in 3,3-dimethylbutene, and 1.0 M in cyclohexane. The concentration of benzene in these tubes was 0, 0, 0.22, 0.44, 0.88, 2.2, and 3.3 M

respectively. After the tubes were capped, the solutions were purged with nitrogen for four minutes and irradiated with RPR 3000 Å lamps (Method II) for four minutes. The volatile materials (the solvent, the olefin, benzene, bromocyclohexane, etc.) were vacuum distilled (2 mm Hg) into a 77°K trap (liquid nitrogen), and stored in seven 5-dram vials. To these vials was added $CHBr_3$ (10, 10, 8.0, 8.0, 6.0, 3.0, and 3.0 μl) as an internal standard. The solutions in these vials were analysed with GC (column temperature 50°C isothermal, column temperature 20 psi, column length 25 m) to determine the yields of bromocyclohexane (retention time 6.45 minutes). Under these conditions the retention time of $CHBr_3$ was 3.73 minutes. The nonvolatile materials were analysed with GC (column temperature 130-230°C at 10°/minute, column pressure 20 psi) after washing and drying. The yields of PhG (retention time 6.79 minutes) and N-(2-bromo-3,3-dimethyl)butyl-3,3-dimethylglutarimide **10** (retention time 7.26 minutes) were determined with benzophenone (retention time 5.32 minutes) as an internal standard. The molar response factor of **10** was assumed to be the same as that of benzophenone. The results are listed in Table 2-15.

The addition product **10** was prepared from N-bromo-3,3-dimethylglutarimide and 3,3-dimethylbutene by using the method described by U. Luning et al[38]. The crude product was purified by recrystallization from carbon tetrachloride and pentane (v/v 1:1) to afford **10** as white crytals: mp 90-92°C (lit.[38] mp 90°C);

^{1}H NMR ($CDCl_3$) 1.13 (s, 6H), 1.14 (s, 9H), 2.54 (s, 4H), 3,86 (m, 1H), 4.34 (m, 1H), 4.56 (m, 1H).

4.4.3. Photodecomposition of NBP

4.4.3.1. In the Presence of DCE

A solution of N-bromophthalimide (13.2 mg, 0.0579 mmol), DCE (3.0 μl, 0.038 mmol), and cyclohexane (20.0 μl, 0.184 mmol) in CH_2Cl_2 (2.00 ml) were prepared. The solution (1.0 ml) was placed in each of the two NMR tubes (A and B). The tubes were sealed, and the solutions inside purged with nitrogen then irradiated with a 200-watt lamp through a Pyrex filter (Method I) for 65 minutes. The proton signal at 7.76 ppm due to N-bromophthalimide (NBP) and 7.73 ppm due to phathalimide were used to estimate the conversion of NBP (the two signals were not well separated on the spectrum recorded with a Bruker SY 100, therefore the uncertainty associated with the reported NBP conversion was high). The photolysates were washed and dried, and mixed with $CHBr_3$ (1.0 μl, its retention time under the conditions was 4.57 minutes) for GC analysis (column temperature 50°C isothermal, column pressure 8 psi) to afford $CHBrCl_2$ (retention time 1.65 minutes, 0.00219 mmol in tube A and 0.00197 mmol in tube B) and bromocyclohexane (retention time 8.91 minutes, 0.0185 mmol in tube A and 0.0175 mmol in tube B). The GC analysis under different conditions (120°-230°C at 10°/minute, 8 psi) with $CHBr_3$ as an internal standard (retention time 1.20 minutes)

afforded phthalimide (retention time 4.52 minutes, 0.0190 mmol in tube A and 0.0204 mmol in tube B respectively). These results were averaged and are listed as experiment 73 in Table 2-12.

4.4.3.2. In the Presence of Br_2

A solution of NBP (43.6 mg, 0.192 mmol), Br_2 (2.0 μl, 0.040 mmol), and cyclohexane (20.0 μl, 0.184 mmol) in CH_2Cl_2 (2.00 ml) was prepared. The solution (1.0 ml) was placed in each of the two NMR tubes (A and B). After the tubes were capped, the solutions were purged with nitrogen for five minutes and irradiated with a 200-watt mercury lamp through a GWV filter (Method I). Precipitation of phthalimide occurred at time $t \simeq 6$ minutes. The irradiation was stopped at $t = 10$ minutes. Dichloromethane (0.5 ml) was added to the photolysates to form clear solutions. The NBP conversion in each of these two tubes was $\simeq$55%. Each solution was washed, dried, and combined with $CHBr_3$ (4.0 μl) for GC analysis to afford $CHBrCl_2$ (0.0261 mmol in tube A and 0.0241 mmol in tube B), bromocyclohexane (0.0138 mmol in tube A and 0.0130 mmol in tube B), and 1,2-dibromocyclohexane (0.00854 mmol in tube A and 0.00730 mmol in tube B). The results were averaged and are listed as experiment 76 in Table 2-13.

4.4.4. Photodecomposition of N-bromoimide 11

4.4.4.1. Preparation of Imide 13

A solution of hexanoyl chloride (22.4 ml, 0.138 mol) and pyridine (16 ml, 0.20 mol) in dichloromethane (400 ml) in a flask was cooled to -70°C with stirring. To the flask was added a solution of acetamide (10.2 g, 0.155 mmol) in acetone (125 ml). The solution temperature was maintained at -70°C for 48 hours, then warmed up to room temperature. A white precipitate of pyridine-hydrogen chloride was separated by filtration. After the solvent was removed from the filtrate under reduced pressure, the residue was dissolved in acetone (100 ml). It was combined with 100 ml of saturated aqueous $NaHCO_3$ solution. After the evolution of carbon dioxide ceased (*ca.* one hour), acetone was removed under reduced pressure on a warm water-bath. The aqueous solution was extracted with dichloromethane (80 ml x 5). The extract was washed with water (100 ml) and dried over anhydrous magnesium sulphate. Removal of the solvent under reduced pressure left a yellow solid (11.4 g) which contained 70% of **13** as shown by GC analysis. The crude product (7 g) was flash chromatographed using 30% ethyl acetate-hexane as the eluent. Ten fractions of 80 ml each were collected. Fractions 4-8, after removal of the solvent, afforded **13** (2.45 g) as white crystals: mp 64-65°C (lit.[151] mp 66°); ^{1}H NMR ($CDCl_3$) 0.90 (t, 3H, J=6.7 Hz), 1.35 (m, 4H), 1.66 (m, 2H), 2.37 (s, 3H), 2.52 (t, 2H, J=9.3 Hz), 9.07 (br s, 1H, NH); ^{13}C NMR ($CDCl_3$) 13.78, 22.30,

24.08, 24.98, 31.19, 37.27, 172.39, 174.05; IR (Nujol) 3260 (m), 3170 (m), 1736 (vs), 1456 (s), 1379 (m), 1256 (s), 1205 (m), 1165 (m) cm^{-1}; MS (EI), *m/e* 114 (22), 101 (68), 73 (25), 59 (40), 43 (100); (CI), 158 (M^++1, 100).

4.4.4.2. Preparation of C-Bromoimide 14

Hexanoyl chloride (2.86 g, 21.3 mmol) and bromine (1.0 ml, 20 mmol) were mixed in a 10 ml flask equipped with a condenser. The mixture was warmed to 80°C gradually with stirring. After evolution of the hydrogen bromide ceased (about 1 hour), the mixture was heated for an additional 2 hours to ensure completion. A change in colour of the mixture (brown then yellow then yellowish) was observed in three hours. To the yellowish liquid was added acetamide (1.24 g, 21 mmol). The mixture was heated at 90°C for five hours with stirring. The crude product was evaporated on a hot water-bath, the oily residue was washed with 100 ml of acetone-water (v/v 1:1) solution of $NaHCO_3$ and dried over anhydrous magnesium sulphate to afford a syrup (730 mg). Recrystallization from acetone gave crystalline **14** (300 mg): mp 103-105°C. HPLC analysis of compound **14** resulted in one peak. However, GC-MS (CI) analysis of the product gave rise to a minor peak (retention time 2.59 minutes, *m/e* 156) in addition to the major peak due to compound **14** (retention time 3.12 minutes, *m/e* 238, 236 (1:1)). The minor peak is presumably due to the dehydrobromination of **14**.

4.4.4.3. Preparation of C-Bromoimide 15

A heterogeneous mixture of **13** (314 mg, 2.0 mmol), bromine (0.6 ml, 11.g mmol), and K_2CO_3 (724 mg, 5.2 mmol) in CH_2Cl_2 (25 ml) was placed in a 25 ml Pyrex cell, stirred vigorously and irradiated through a GWV filter (Method I) under N_2 for 17 hours. GC analysis (column temperature 160°C isothermal, column pressure 10 psi) of the photolysate indicated five peaks at the retention times of 3.06 minutes (9.9%, **14**), 4.20 minutes (0.7%, **16**), 4.79 minutes (4.5%, **12**), 5.21 mintues (4.8%, **15**), 2.26 minnutes (2%), and 6.82 minutes (1.5%) in addition to the peak due to the parent imide **13** (retention time 1.96 minutes, 76%) and a very small peak (retention time 12.63 minutes). A yellow oil (498 mg) was obtained after the solvent was removed under reduced pressure. Chromatography of the crude product (elution with 25% ethyl acetate-petroleum ether) gave fifty fractions of 15 ml each. Fractions 12-19 contained C-bromoimide **14**, and fractions 20-24 contained mixtures of **14** and **13**. Elution with acetone (100 ml) afforded a yellowish gum (11 mg). It was purified by preparative TLC on silica gel (R_f=0.4) with 25% ethyl acetate-hexane and followed by recrystallization from CH_2Cl_2 to afford **15** (5 mg) as white crystals: mp 99-101°C.

4.4.4.4. Preparation of C-Bromoimide 16

A solution of α-bromoacetylbromide (0.46 ml, 5.2 mmol), hexanamide (0.566 g, 4.35 mmol), and pyridine (0.4 ml, 5 mmol) in CCl_4 (100 ml) was refluxed for two hours. After the solvent was removed under reduced pressure, the residue was dissolved in 100 ml of acetone-water (v/v 3:1) solution of $NaHCO_3$ (0.3 g). The solution was concentrated on a hot water bath under reduced pressure. The residue was extracted with dichloromethane (3 x 50 ml), and the combined extracts were dried over anhydrous magnesium sulphate. Removal of the solvent left a brownish solid (0.6 g). A peak at 4.25 minutes was observed when the solid was analysed by GC (160°C, isothermal, 10 psi). Chromatography of the crude product (elution with 20% ethyl acetate-hexane) followed by recrystallization from CH_2Cl_2 gave **16** as crystals: mp 117-119°C.

4.4.4.5. Preparation of N-Methylimide 18

N-methylacetamide (5.9 g, 81 mmol) was added to a 200 ml flask containing a solution of hexanoyl chloride (6.0 ml, 37 mmol) and pyridine (10 ml, 125 mmol) in dichloromethane (100 ml). A brownish solution was observed. It was stirred for 25 hours at room temperature. To the brown solution was added 0.5 N hydrochloric acid (200 ml). The organic layer was separated and the solvent was removed under reduced pressure, and the residue

was washed with acetone-water (v/v 1:1, 150 ml) solution of $NaHCO_3$ (5 g). After acetone was removed under reduced pressure, the mixture left was extracted with CH_2Cl_2 (3 x 40 ml). The combined extracts were washed with water (50 ml), dried over anhydrous magnesium sulphate, and filtered. Removal of the solvent left a yellow oil (6 g). Chromatography of the crude product (elution with 20% ethyl acetate-petroleum ether) gave ten fractions of 20 ml each. Fractions 5 and 6 contained 90% pure **18** (2.1 g), and fraction 9 (0.1 g) 97% pure **18** shown by GC analysis. Chromatography of the crude product collected from fractions 5 and 6 afforded **18** (1.5 g) as a yellowish oil: ^1H NMR ($CDCl_3$) 0.91 (t, 3H, J=7.0 Hz), 1.18-1.20 (m, 4H), 1.66 (m, 2H), 2.43 (s, 3H), 2.66 (t, 2H, J=7.5 Hz), 3.21 (s, 3H); ^{13}C NMR ($CDCl_3$)13.85, 22.43, 24.38, 26.68, 31.34, 31.47, 37.86, 173.34, 176.20; IR (CH_2Cl_2) 2960(s), 2938 (s), 2870 (s), 1695 (s), 1460 (w), 1415 (w), 1370 (s), 1305 (m), 1270 (m), 1140 (m), 980 (m); MS(EI), *m/e* 171 (M^+, 2), 156 (M^+-CH_3, 10), 128 (35), 115 (100), 99 (40), 86 (30), 73 (70), 58 (20), 43 (65); Anal. Calcd for $C_9H_{17}NO_2$: C, 63.16; H, 9.94; N, 7.93. Found: C, 63.30; H, 10.16; N, 7.93.

4.4.4.6. Preparations of C-Bromoimides 19 and 20

A solution of **18** (670 mg, 3.9 mmol), NBS (810 mg, 4.5 mmol), and bromine (100 μl, 2 mmol) in CH_2Cl_2 (20 ml) in a 25 ml Pyrex photocell was irradiated through a GWV filter (Method I) for one

hour. After the solvent was removed under reduced pressure, the residue was extracted with CCl_4 (3 x 100 ml). GC analysis of the CCl_4 solution (160°C isothermal, 10 psi) afforded (retention time, peak area) **19** (3.87 minutes, 15%), a decomposition product of **19** (1.90 minutes, 22%), **20** (6.10 minutes, 12%), the parent imide **18**, and several unidentified peaks. Chromatography of the mixture (elution with 10% ethyl acetate-petroleum ether) gave thirty fractions of 15 ml each. Fractions 20 and 21 contained **19** (60 mg) as a yellowish oil. The column was then eluted with 20% ethyl acetate-petroleum ether to give twenty fractions of 15 ml each. Fractions 9, 10, and 11 contained **20** contaminated by **18**. Removal of the solvent from fraction 10 left **20** (20 mg) as a yellowish oil. It was further purified with HPLC (Water Associates, Bondapak C_{18} column, 5% isopropanol-hexane as the eluent, 2 ml/minute). Under these conditions, **20** was eluted with the rention time of 4.48 minutes. Removal of the solvent afforded **20** (13 mg) with >99.99% purity shown by GC analysis. HPLC analysis of compound **19** resulted in one peak. However, GC-MS (CI) analysis of the product gave rise to a minor peak (retention time 1.87 minutes, *m/e* 170) in addition to the major peak due to compound **19** (retention time 3.88 minutes, *m/e* 252, 250 (1:1)). The minor peak is presumably due to the dehydrobromination of **19**.

4.4.4.7. Preparation of N-Bromoimide 11

The following reaction was carried out in the dark. A solution of imide **13** (157 mg, 1.00 mmol) in CH_2Cl_2 (10 ml) was placed in a 50 ml flask equipped with a drying tube and cooled down to -20°C with an ice-salt bath. One drop of cyclohexene was added to scavenge fortuitous bromine. Then 8 ml of Freon 11 solution of t-butylhypobromite[152] (5 mmol) was added in one portion. The solution was stirred at -20°C for 2.5 hours. Removal of the solvent under reduced pressure at 13-15°C left **11** as a colorless oil (240 mg): ^{1}H NMR ($CDCl_3$) 0.92 (t, 3H, J=6.7 Hz), 1.35 (m, 4H), 1.67 (m, 2H), 2.63 (s, 3H), 2.90 (t, 2H, J=7.5 Hz); IR (CCl_4) 3010 (m), 2990 (m), 2920 (w), 1720 (s), 1370 (w), 1230 (m), 1190 (w), 1160 (ms), 1025 (w), 640 (w). The conversion of the parent imide **13** to the N-bromoimide **11** was estimated to be, at least, >95%, since the IR absorption of N-H in 3300-3600 cm^{-1} region or the ^{1}H NMR signal of the acetyl group due to the parent imide **13** was not detected.

4.4.4.8. Photodecomposition of N-Bromoimide 11 in the Presence of an Olefin

A solution of **11** (236 mg, 1.0 mmol) and 3,3-dimethylbutene (0.10 ml, 2.5 mmol) in CH_2Cl_2 (25 ml) was placed in a 30 ml Pyrex photocell. The solution (0.5 ml) was analysed by NMR spectroscopy (EM 360), and a signal at 2.63 ppm due to the acetyl

group was recorded (the signal was well separated from the signal at 5.3 ppm due to dichloromethane). The photocell was kept in an ice-water bath and irradiated with a 200-watt mercury lamp (Method I) under nitrogen for one hour. The photolysate (0.5 ml) was analysed by NMR, and the intensity of the signal at 2.63 ppm was recorded. The conversion of **11**, C, was calculated to be ≃ 85% by the use of Eq. 4-7.

$$C = (I_{2.63}/I^{o}_{2.63})\times 100\% \qquad 4\text{-}7$$

where $I^{o}_{2.63}$ is the intensity of the signal at 2.63 ppm before the photolysis, and $I_{2.63}$ is that after *t* minutes of irradiation. The photolysate was washed with 5% aqueous $NaHSO_3$ solution, dried over anhydrous magnesium sulphate, and filtered. GC analysis of the filtrate (160°C, isothermal, 10 psi) afforded the peaks due to **13** (retention time 1.94 minutes, 8%), **12** (4.74 minutes, 80%), a decomposition product of **12** (2.25 minutes, ≃2%), and an unidentified monobrominated product **A** (7.45 minutes, 6%). Chromatography of the crude product (eluted with 20% ethyl acetate-hexane) gave fifty fractions of 10 ml each. Removal of the solvent from fraction 10 left **A** (6 mg) as a gum (98% purity as shown by GC analysis): MS (CI), *m/e* (relative intensity) 279.2 (M^+, 25), 277.1 (M^+, 27), 117.1 (40); ^1H NMR ($CDCl_3$) 0.90 (t, 3H, *J* ≃ 6 Hz), 1.33 (m, 6 H), 1.65 (m, 1H), 1.75 (m, 1H), 1.88 (m, 1H), 2.13 (m, 1H), 2.33 (m, 2H), 3.98 (ddd, 1H, *J* =5, 9, and 10 Hz), 4.92 (m, *J* = 5, 9, and 1 Hz); IR

(Nujol) 1730 (s), 1450 (br m), 1180 (br m), 1100 (w); ^{13}C NMR ($CDCl_3$) 172.80, 75.57, 52.86 (d), 35.69, 34.49, 31.28, 25.55, 24.69, 23.33, 22.28, 13.85 (q). Fractions 39-48 contained 4-bromoimide **12** with >99% purity, fractions 28-33 contained imide **13**, and fractions 34-38 mixtures of **13** and **12** as shown by GC analysis. Removal of the solvent from fractions 39-48 left a white solid (50 mg). Recrystallization of the solid from acetone afforded **12** as crystals (10 mg): mp 88-90°C. The experiment described above was repeated. After the photolysis the photolysate was combined with benzophenone (200 mg) as an internal standard, and the solution was analysed by GC to afford **12** (196 mg, 0.83 mmol, 83% based on the amount of **11** used), **13** (13.4 mg, 0.085 mmol, 8.5%), and the unidentified compound **A** (0.065 mmol, 6.5%) by assuming the molar respondance factor of **A** was twice[161] that of imide **13**.

4.4.4.9. Bromine-initiated Decomposition of 11

A solution of **11** (9.4 mg, 0.040 mmol) and bromine (1 μl, 0.02 mmol) in CCl_4 (1 ml) was placed in a NMR tube, sealed, purged with Argon for five minutes (see Section 4.4.1.2 for the detail). The tube was placed in an ice-water bath and irradiated with a ≥400-nm light source (Method I) for 10 minutes. The conversion of **11** was determined to be ≃85% by NMR analysis (see Section 4.4.4.8 for the detail). The photolysate was washed, dried over magnesium sulphate, and filtered (see Section 4.4.1.2

for the detail). To the filtrate was added 25 μl of CH_2Cl_2 solution of benzophenone (0.0220 M) as an internal standard. The mixture was analysed by GC (160°C isothermal, 10 psi) to afford **13** (retention time 1.97 minutes, 0.008 mmol, 20% based on the amount of **11** used), **14** (3.08 minutes, 0.0029 mmol, 7.3%), **16** (4.19 minutes, 0.00028 mmol, 0.7%), **12** (4.82 minutes, 0.021 mmol, 52%), **15** (5.32 minutes, 0.0036 mmol, 9.0%), an unidenfied compound **A** (7.45 min, 0.0014 mmol, 3.4%; its molar response factor relative to that of **13** was assumed to be two[161]) and a few very small peaks. The results are listed as experiment 154A in Table 2-16.

In a separate experiment a solution of **11** (9.4 mg, 0.040 mmol) and Br_2 (1μl) in carbon tetrachloride (1.0 ml) in a capped NMR tube was purged with nitrogen for five minutes. The tube was placed in a 100 ml Pyrex beaker full of ice-salt (about 3:1) and irradiated with a ≥400-nm light source (Method I). During the irradiation the wall of the beaker was wiped with a piece of tissue at about five minute intervals to remove the water condensed on it. The conversion of **11** was monitored by a Bruker SY 100 NMR spectrometer and was determined to be 81% after fifty five minutes of irradiation. The photolysate was washed, dried, and mixed with 100 μl of carbon tetrachloride solution of benzophenone (it was prepared by dissolving 100 mg of benzophenone in 25.0 ml of carbon tetrachloride) for GC analysis. The yields of products are reported as experiment 159 in Table 2-16.

4.4.4.10. Photobromination of Imide 13

4.4.4.10.1. With Br_2-NBS

A solution of **13** (6.3 mg, 0.040 mmol), bromine (1.0 μl, 0.02 mmol), and NBS (15 mg, 0.084 mmol) in CCl_4 (1.0 ml) was placed in a NMR tube, sealed, and purged with Argon (see Section 4.4.1.2 for the detail). The tube was placed in an ice-water bath and irradiated through a GWV filter and a filter solution (Method I) for 45 minutes. The photolysate was washed, dried, and filtered (see Section 4.4.1.2 for the detail) for GC analysis (160°C isothermal, 10 psi) to afford **13** (retention time 2.00 minutes, 92.6%), **14** (3.10 minutes, 4.93%), **16** (4.37 minutes, 0.32%), **12** (4.87 minutes, 0.64%), **15** (5.45 minutes, 1.57%), and two small peaks which were detected but not integrated. The results are listed as experiment 162 (Table 2-17).

4.4.4.10.2. With Br_2-K_2CO_3

13 (6.3 mg, 0.040 mmol), NBS (6.4 mg, 0.04 mmol), bromine (1.0 μl, 0.020 mmol), K_2CO_3 (0.12 mmol), and CCl_4 (2 ml) together with a magnetic bar were placed in a 1-cm fluorescence cuvette. After the cuvette was capped, the heterogeneous mixture was purged with nitrogen (see Section 4.4.1.2 for the detail) and irradiated similarly with stirring for 160 minutes. The photolysate was filtered and mixed with acetone (0.4 ml) for GC

analysis to afford **13** (retention time 1.97 minutes, 96.0%), **14** (3.13 minutes, 2.5%), **15** (5.41 minutes, 1.0%), and a small peak (2.59 min, 0.4%) due to the dehydrobromination of **14**. The signals due to **12** and **16** were detected but not integrated by GC. The results are listed as experiment 160 (Table 2-17).

4.4.4.11. Photobromination of 18

A solution of **18** (8.0 mg, 0.047 mmol), bromine (1.0 μl, 0.020 mmol), and NBS (20 mg, 0.11 mmol) in CCl_4 (1 ml) placed in a NMR tube was sealed, purged with Argon (see Section 4.4.1.2 for the detail), and irradiated with stirring, through a GWV filter and a filter solution (Method I) in an ice-water bath for 25 minutes. After work-up (see the previous paragraph), the photolysate was analysed by GC (column temperature 160°C isothermal, column pressure 10 psi) to afford **18** (retention time 2.29 minutes, 88%), **19** (3.86 minutes, 1.9%), **20** (6.06 minutes, 1.8%), and three unidentified compounds **X** (4.18 minutes, 1.8%), **Y** (4.71 minutes, 0.33%), and **Z** (5.46 minutes, 0.66%). GC-MS (CI) analysis showed the following data. **X:** *m/e* (relative intensity) 252 (90), 250 (100); **Y:** *m/e* (relative intensity) 252 (95), 250 (100); **Z:** *m/e* (relative intensity) 252 (90), 250 (100). A peak (retention time 1.86 minutes, 3.7%) due to the dehydrobromination of **19** was also detected. The results are listed as experiment 168 (Table 2-18).

18 (8.0 mg, 0.047 mmol), bromine (1.0 μl, 0.02 mmol), K_2CO_3 (15 mg, 0.11 mmol), CCl_4 (1 ml), and a magnetic bar were placed in a 1-cm fluorescence cuvette. The cuvette was sealed, purged with argon, and irradiated with vigorous stirring, through a GWV filter and a filter solution (Method I) at 0°C for 1.5 hours. The sample was heterogeneous throughout the irradiation. The photolysate was filtered, and the solvent was removed from the filtrate under reduced pressure. The residue was dissolved in 0.5 ml of acetone for GC analysis (160° isothermal, 10 psi): **18** (retention time 2.25 minutes, 95%), **19** (3.89 minutes, 0.95%), **20** (6.12 minutes, 1.3%), **X** (4.21 minutes, 0.64%), **Y** (4.75 minutes, 0.22%), **Z** (5.51 minutes, 0.51%), and the peak due to the dehydrobromination product of **19** (1.87 minutes, 2.10%). The results were listed as experiment 166 (Table 2-18).

4.4.4.12. Preparation of N-Bromo-N-Acetylacetamide

The title compound was prepared from N-acetylacetamide (50 mg) by using the method described in Section 4.4.4.7. The compound was obtained as yellowish oil: ^1H NMR ($CDCl_3$) 2.62 ppm (s, 6H); IR (Neat) 2950 (w), 1750 (m), 1720 (s), 1700 (m), 1500 (m), 1370 (m), 1235 (m), 1195 (m), 1022 (m), 585 (w). The conversion from the parent imide to the title compound was estimated to be ≃95% since the intensity of the proton signal at 2.29 ppm due to the parent imide to the intensity of that at 2.62 ppm due to the

Table 4-2

^{1}H NMR Parameters of Compounds 12, 14, 15, 16, 19, and 20 in $CDCl_3$ Solution

Cmpd.	Chemical Shift, ppm	Coupling Constant, Hz
12	1.07 (t, 3H, H_6), 1.89 (m, 2H, H_5), 2.07 (m, 1H, H_3'), 2.23 (m, 1H, H_3), 2.35 (s, 3H, H_2'), 2.78 (m, 2H, H_2), 4.03 (m, 1H, H_4), 7.88 (br s, NH)	$J_{5,6}$=7.5, $J_{4,5}$=5.0 $J_{5,3}$<1.2, $J_{2,3'}\simeq$8 $J_{4,3'}\simeq$6, $J_{3,3'}$=14.0 $J_{2,3}$=7.0, $J_{3,4}$=3.5 $J_{4,x}$=1.6
14	0.915 (t, 3H, H_6), 1.38 (m, 4H, H_4 & H_5), 2.0 (m, 1H, H_3'), 2.1 (m, 1H, H_3), 2.45 (s, 3H, H_2'), 4.43 (t, 1H, H_2), 8.57 (br s, NH)	$J_{5,6}$=7.5, $J_{2,3'}$=5.0 $J_{2,3}$=5.0, $J_{3',x}$=4.0 $J_{3',y}$=7.5 $J_{3,z}$=6.0
15	1.76 (d, 3H, H_6), 1.86 (m, 4H, H_3 & H_4), 2.38 (s, 3H, H_2'), 2.60 (t, 2H, H_2), 4.01 (m, 1H, H_5), 8.23 (br s, NH)	$J_{5,6}$=6.7, $J_{3,2}$=6.5 $J_{5,4}$=6.0
16	0.92 (t, 3H, H_6), 1.35 (m, 4H, H_5 & H_4), 1.67 (m, 2H, H_3), 2.59 (t, 2H, H_2), 4.18 (s, 2H, H_2'), 8.38 (br s, NH)	$J_{5,6}$=6.5, $J_{3,2}$=7.1

19	0.92 (t, 3H, H_6), 1.36 (m, 4H, H_4 & H_5), 2.07 (m, 1H, H_3 or H_3'), 2.16 (m, 1H, H_3' or H_3), 2.43 (s, 3H, H_2'), 3.28 (s, 3H, NCH_3), 5.10 (dd, 1H, H_2)	$J_{5,6}$=6.0, $J_{2,3}$=5.0 $J_{2,3'}$=5.5
20	1.73 (d, 3H, H_6), 1.77 (m, 4H, H_3 & H_4), 2.42 (s, 3H, H_2'), 2.75 (t, 2H, H_2) 3.22 (s, 3H, NCH_3), 4.15 (m, 1H, H_5)	$J_{5,6}$=6.5, $J_{2,3}$=6.0 $J_{5,4}$=6.0

Table 4-3

^{13}C NMR Paramerters of 12, 16, 19, and 20 in $CDCl_3$ Solution

Cmpd.	Chemical Shift, ppm
12	172.59, 171.24, 58.71, 34.42, 32.95, 32.41, 25.01, 12.01
16	173.38, 166.37, 37.25, 31.15, 29.36, 23.90, 22.30, 13.79
19	173.35, 172.49, 47.61, 34.32, 32.08, 29.55, 26.11, 22.13, 13.78
20	175.53, 173.23, 50.82, 40.41, 37.32, 31.57, 26.53, 26.35, 22.97

Table 4-4

IR Absorptions[a]

Cmpd.	ν, cm^{-1}
12	3423 (w), 2980 (w), 2945 (w), 1736 (s), 1684 (w), 1458 (m), 1379 (w), 1253 (m), 1202 (w), 1024 (w), 972 (w), 667 (w), 627 (w)
16	3230 (m), 3180 (m), 1735 (s), 1510 (m), 1170 (m)
19	2968 (m), 2880 (w), 1763 (w), 1720 (s), 1690 (m), 1448 (w), 1375 (w), 1306 (w), 1261 (m), 1138 (w), 1057 (w)
20	2945 (w), 1722 (s), 1373 (w), 1303 (w), 1261 (m), 1140 (w), 1082 (w)

a. The spectra of **12**, **19**, and **20** were recorded with a Bruker IFS-85 FT IR spectrophotometer from CH_2Cl_2 solution and the spectrum of **16** was obtained with a Perkin-Elmer 599B as a nujol mull.

Table 4-5

Mass Spectral Data

Cmpd.	*m/e* (rel. intensity, %)
12	(EI) 156 (22), 140 (25), 114 (87), 101 (100), 84 (21), 69 (43), 55 (28), 43 (62).
	(CI) 238 (24), 236 (25), 156 (100)
14	(EI) 181 (20), 179 (18), 114 (18), 100 (20), 55 (24), 43 (100)
	(CI) 238 (28), 236 (30), 158 (55), 156 (100)
15	(EI) 156 (27), 114 (100), 97 (40), 60 (57), 59 (56), 55 (30), 43 (90)
	(CI) 238 (41), 236 (41), 156 (100)
16	(EI) 237 (5), 235 (4), 208 (66), 206 (68), 194 (20), 193 (18), 181 (33), 179 (31), 156 (55), 140 (32), 138 (35), 100 (100), 99 (80), 72 (30), 55 (18)
19	(EI) 170 (82), 128 (100), 97 (47), 86 (20), 74 (87), 56 (23), 43 (21)
20	(EI) 170 (70), 128 (12), 114 (13), 97 (17), 69 (22), 55 (36), 43 (100).

Table 4-6

Microanalysis Data

12	Calcd	C: 40.68	H: 5.93	N: 5.93
$C_8H_{14}BrNO_2$	Found	C: 40.89	H: 6.20	N: 5.70
14	Calcd	C: 40.68	H: 5.93	N: 5.93
$C_8H_{14}BrNO_2$	Found	C: 40.86	H: 6.23	N: 5.69
15	Calcd	C: 40.68	H: 5.93	N: 5.93
$C_8H_{14}BrNO_2$	Found	C: 40.78	H: 6.21	N: 5.65
16	Calcd	C: 40.68	H: 5.93	N: 5.93
$C_8H_{14}BrNO_2$	Found	C: 40.87	H: 6.12	N: 5.81
19	Calcd	C: 43.20	H: 6.40	N: 5.60
$C_9H_{16}BrNO_2$	Found	C: 43.41	H: 6.69	N: 5.32
20	Calcd	C: 43.20	H: 6.40	N: 5.60
$C_9H_{16}BrNO_2$	Found	C: 43.38	H: 6.65	N: 5.33

title compound was 1:20. An weak absorption at 3240 cm^{-1} due to the parent imide was also detected.

Photobromination of **18** with Br_2 and the title compound as the bromination reagent was carried out in similar way as described in Section 4.4.4.11, and the results are reported as experiments 171 and 172 in Table 2-18.

4.4.5. Photodecomposition of N-Bromoimide 21

Imide **23** was synthesized from the corresponding dicarboxylic anhydride by using the methods described by Chow and Naguib[153] as white needles: mp 184-186°C (lit.[154] mp 186-188°C); ^1H NMR ($CDCl_3$) 1.65 (m, 2H), 3.34 (s, 2H), 3.38 (s, 2H), 6.22 (s, 2H), 7.53 (br s, 1H, NH); IR (Nujol) 3170 (s), 1710 (s), 1200 (s).

Imide **23** (410 mg, 2.51 mmol) was dissolved in CH_2Cl_2 (20 ml) in a 50 ml flask equipped with a drying tube. The solution was cooled in an ice-salt bath. To the solution was added 15 ml of CCl_4 solution of *t*-butylhypobromite (5.4 mmol) and the mixture was stirred for two hours. After the solvent was removed, N-Bromoimide **21** was obtained as a white solid (610 mg): ^1H NMR ($CDCl_3$) 1.65 (m, 2H), 3.47 (s, 4H), 6.17 (s, 2H); IR (Nujol) 1715 (s), 1686 (s), 1310 (ms), 1190 (ms), 840 (m), 749 (m), 700 (m), void of 3170 cm^{-1} (NH absent).

A solution of **21** (596 mg, 2.45 mmol) and DCE (130 μl, 1.6 mmol) in CH_2Cl_2 (20 ml) was placed in a 30 ml Pyrex photocell, sealed and purged with nitrogen. This solution was irradiated with RPR 3000 Å lamps (Method II) for two hours. Removal of the solvent left a yellow gum (700 mg). The crude product was analysed by GC (160°C isothermal, 20 psi) to show (retention time, peak area) **23** (3.43 minutes, 53%), **22** (3.85 minutes, 18%), **24** (5.72 minutes, 17%), a peak at 5.83 minutes, and four small peaks. The peak with retention time of 5.83 minutes (2%) showed the following MS pattern: *m/e* (relative intensity) 298, 296, 294 (4:8:4, M^++1), 217, 215 (100:98, M^+-Br), 107 (90), presumably an isomer of **24**. Chromatography of the crude product (elution with 40% ethyl acetate-hexane) gave forty fractions of 15 ml each. Fractions 11, 12, and 13 contained lactone **24** with 85%, 77%, and 54% purities respectively. It was further purified with preparative GC (stainless steel column, 3 ft x 0.25 in, 10% Carbowax 20M on Anakrom Q, 80-100 mesh; 160°C, isothermal) to give a colorless oil (5 mg). **24** crystallized on storage: mp 79-80°C. Fractions 33-37 contained imide **22** (30 mg, *ca* 95% purity). Recrystallization from aceton followed by washing with hexane afforded **22** as colorless crystals (10 mg): mp 165-166°C. Fraction 40 contained a mixture of imides **23** and **22** in a 1:1 ratio (7 mg) as shown by GC analysis.

In a separate experiment a solution of N-bromoimide **21** (163 mg, 0.67 mmol) and DCE (32 μl, 0.4 mmol) in CH_2Cl_2 (10 ml) were

photolyzed in the same way as described in the previous paragraph for 50 minutes. GC analysis of the photolysate (160°C isothermal, 20 psi) with 3,3-dimethylglutarimide added as an internal standard afforded **23** (0.34 mmol, 51% based on the amount of **21** used), **22** (0.14 mmol, 20%), lactone **24** (0.11 mmol, 16%), the isomer of **24** (0.02 mmol, 3%), and four very small unidentified peaks.

4.4.6. Photodecomposition of N-Bromoimide 25

N-Bromoimide **25** was prepared from imide **22** in the same way as described in Section 4.4.5, as a white solid: ^{1}H NMR ($CDCl_3$) 1.71 (br s, 3H), 1.76 (br s, 2H), 2.52 (br s, 1H), 2.98 (br s, 2H); IR ($CDCl_3$) 1695 (s), and no N-H absorption in 3200-3600 cm^{-1} region. The pertinent data of imide **22** are listed in Tables 4-7 and 4-9.

A solution of N-bromoimide **25** (22.4 mg, 0.092 mmol) and DCE (4 μl, 0.05 mmol) in CH_2Cl_2 (1.0 ml) in a NMR tube was purged with nitrogen (see Section 4.4.1.1 for the detail) and photolyzed in the same way as described in Section 4.4.5 for one hour. After the photolysate was kept in the dark for twenty four hours, it was mixed with 200 μl of CH_2Cl_2 solution of benzophenone (0.0140 M) as an internal standard for GC analysis (160°C isothermal, 20 psi). The yield of imide **22** in the photolysate was determined to be 0.073 mmol, 79% based on the amount

of **25** used. No imide **23** nor lactone **24** was detected. A small peak (retention time 8.70 minutes) was detected in addition to the peak due to imide **22**. The small peak had the following data obtained from GC-MS (CI) analysis, *m/e* 344 (M^++1, 2.9), 342 (M^++1, 22.6), 340 (M^++1, 46.1), 338 (M^++1, 30.0), 264 (M^+-Br, 9), 262 (M^+-Br, 60), 260 (M^+-Br, 100). The peak was assigned to the 1:1 adduct of N-bromoimide **25** to 1,1-dichloroethene (DCE). The area ratio of the peak to that of imide **22** was < 5/80. Several small unidentified peaks were also detected but not integrated by GC analysis.

4.4.7. Photodecomposition of N-Bromoimide 26

4.4.7.1. Preparations of 26 and 27

By reacting imide **28** with *t*-butylhypobromite (see Section 4.4.5 for the detail), N-bromoimide **26** was prepared as a white solid: ^{1}H NMR ($CDCl_3$) 2.17-2.72 (m, 4H), 3.30 (m, 2H), 5.95 (m, 2H); IR (Nujol) 1700 (s), 1300 (s), 1200 (ms), 1175 (ms), 695 (ms), void of 3230 cm^{-1} (NH absent). The pertinent data of imide **28** are as follows: ^{1}H NMR ($CDCl_3$) 2.10-2.70 (m, 4H), 3.12 (m, 2H), 5.94 (m, 2H), 8.29 (br s, NH); IR (Nujol) 3230 (s), 1695 (s).

Imide **28** (500 mg, 3.3 mmol), benzoylperoxide (5 mg), NBS (600 mg, 3.4 mmol), and CCl_4 (50 ml) in a 100 ml flask were heated under reflux for six hours in the dark. Succinimide

surfaced during the reaction. After the solvent was removed from the filtrate, the residue was recrystallized from acetone-hexane twice to give **27** (80 mg) as yellowish crystals: mp 105-108°C. HPLC trace showed only one peak when a CH_3CN solution of **27** was analysed. When the solution of **27** was analysed by GC-MS, two peaks (P_1 and P_2) were detected in addition to the peak due to the solvent. These two peaks showed the following MS data: P_1 *m/e* 149 (M^+-HBr, 15), 78 (100), 51 (15), 43 (8); P_2 *m/e* 149 (M^+-HBr, 30), 105 (100), 78 (95), 51 (40), 43 (10).

4.4.7.2. Photodecomposition of 26 in the Presence of DCE

To three Pyrex tubes (1x10 cm) was added a solution of **26** (600 mg, 2.6 mmol) and DCE (130 μl, 1.6 mmol) in 10 ml of CH_2Cl_2 (3, 3, and 4 ml respectively). Each tube was sealed, purged with nitrogen, and irradiated with RPR 3000 Å lamps (Method II) for 30 minutes. Cloudy material was formed during the irradiation. It did not dissappear after the tubes were shaken vigorously. The photolysates in the three tubes were combined, and kept in the dark overnight. CH_2Cl_2 (20 ml) was added to give a clear solution. It was analysed by GC (column temperature 160°C isothermal, column pressure 20 psi) to afford (retention time, peak area of signal) phthalimide (3.04 minutes, 1.3%), imide **28** (3.14 minutes, ≃45%), P_1 (3.16 minutes, ≃20%), P_2 (3.35 minutes, 25%), and a few small unidentified peaks. Small amounts of

amides **30** and **31** were detected (≃1%). Chromatography of the crude product (elution with 40% ethyl acetate-hexane) gave eighty fractions of 15 ml each. NMR analysis showed that fractions 17-21 contained **27** contaminated by a small amount of phthalimide (<4%), that fractions 23-28 contained **27** only, and that fractions 35-48 contained imide **28** (^{1}H NMR data of authentic **28** are listed in Table 4-7).

In a separate experiment, a solution of N-bromoimide **26** (18.5 mg, 0.0800 mmol) and DCE (40 μl, 0.48 mmol) in CH_2Cl_2 (1.0 ml) was placed in a Pyrex tube (1x10 cm). The solution was sealed, purged with nitrogen and irradiated with RPR 3000 Å lamps (Method II). The colorless solution turned cloudy in the first ten minutes and yellowish after one hour. The irradiation was stopped in three hours. The photolysate was filtered and mixed with 100 μl of tetrahydrofuran solution of benzophenone (0.00720 mmol) as an internal standard for GC analysis (column temperature 160°C isothermal, column pressure 20 psi) to afford **27** (0.0196 mmol, 24.5%), **28** (0.0112 mmol, 14.0%), **30** (0.0180 mmol, 22.5%) and **31** (0.0166 mmol, 20.8%).

4.4.7.3. Photodecomposition of 26 in the Presence of 1,3-Pentadiene

N-Bromoimide **26** (184 mg, 0.800 mmol) was dissolved in CH_2Cl_2 (5.0 ml). An aliquot (0.50 ml) of the solution was pipetted into each of the four Pyrex tubes (0.9x7 cm), and freshly distilled 1,3-pentadiene (10, 20, 40, and 130 μl) was added into each tube with a syringe. After diluting with CH_2Cl_2 to 1.0 ml, the solutions were sealed, purged with nitrogen and irradiated with RPR 3000 Å lamps (Method II) for three hours. To each photolysate was added 200 μl of CH_2Cl_2 solution of imide **23** (0.0076 mmol) as an internal standard. The yields of products **27**, **28**, **30**, and **31** were determined by GC analysis (column temperature 160°C isothermal, column pressure 20 psi), and the results are listed in Table 2-22.

In a separate experiment, a solution of **26** (550 mg, 2.4 mmol) and 1,3-pentadiene (110 μl, 1.1 mmol) in CH_2Cl_2 (25 ml) was placed in a 25 ml Pyrex photocell, sealed, purged with nitrogen, and irradiated with a 200-W mercury lamp (Method I) at 15-18 °C for three hours. A colorless solution was observed throughout the irradiation. A sample of the photolysate was transferred into an IR cell for IR analysis which showed strong absorptions at 2349 and 2245 cm^{-1}. Removal of the solvent under reduced pressure left a yellow oil (550 mg). Carbon dioxide evolved when the oil was transferred with a pipette to a vial. The oil, after being exposed to the air in the dark overnight,

was flash chromatographed on silica gel. Elution with 30% ethylacetate-hexane (1 l) afforded imide **28**. The column was eluted with 50% ethyl acetate-hexane to give 130 fractions of 10 ml each. Fractions 36-60 contained amide **30** (90 mg) with ≃90% purity as shown by GC analysis. Recrystallization from acetone gave **30** as white crystals (10 mg): mp 136-138°C. Fractions 100-127 contained amide **31** (70 mg) with >95% purity as determined by GC. Recrystallization from acetone afforded white crystals (8 mg): mp 127-129°C.

4.4.8. Photodecomposition of N-Bromoimide 32

N-Bromoimide **32** was prepared from imide **35** (mp 134-136°C, lit.[155] mp 137°C) which was prepared from the corresponding dicarboxylic anhydride by using the method described by Chow and Naguib[153]. In a typical experiment, imide **35** (590 mg, 3.86 mmol) was dissolved in dichloromethane (5 ml), and the solution was placed in a 100 ml flask equipped with a drying tube, and the flask was cooled in an ice-salt bath. To the solution was added 40 ml of CCl_4 solution of acetyl hypobromite[156] (8 mmol). The mixture was stirred for three hours to give a homogeneous solution. Removal of the solvent under reduced pressure left N-bromoimide **32** as a white solid (880 mg): ^{1}H NMR ($CDCl_3$) 1.49 (m, 4H), 1.84 (m, 4H), 3.09 (m, 2H); IR (CH_2Cl_2) 2945 (s), 2860 (s), 1720 (vs), 1165 (s), 815 (m), 620 (w), void of 3410 and 3210 cm^{-1} (NH absent). The pertinent data of imide **35** are as

follows: ^{1}H NMR ($CDCl_3$) 1.47 (m, 4H), 1.82 (m, 4H), 2.92 (m, 2H), 7.90 (br s, NH); IR (CH_2Cl_2) 3410 (s), 3210 (m), 2945 (s), 2860 (s), 1715 (vs), 1330 (s), 1270 (s).

A solution of **32** (880 mg, 3.85 mmol) and DCE (100 μl, 1.25 mmol) in CH_2Cl_2 (25 ml) placed in a 30 ml Pyrex photocell was sealed, purged with nitrogen, and irradiated with a 300-nm light source (Method II) for 15 minutes. The initial colorless solution turned brownish. To the photolysate was added DCE (15 μl, 1.88 mmol). The solution became colorless in five minutes. It was purged with nitrogen again and irradiated for 30 minutes. The solution remained colorless throughout irradiation. GC analysis (column temperature 160° isothermal, column pressure 20 psi) showed (retention time, peak area) **35** (3.13 minutes, 48%), **33** (3.63 minutes, 27%), **34** (3.93 minutes, 4.7%), 1-bromo-*cis*-cyclohexane-1,2-dicarboximide (4.87 minutes, 17%), and two small unidentified peaks. The photolysate was kept in the dark overnight. After the solvent was removed under reduced pressure, the residue was recrystallized from acetone to afford amide **33** (38 mg) as colorless crystals: mp 183.5-184.5°C. The mother liquor was flash-chromatographed. Elution with 40% ethyl acetate-hexane (3 x 500 ml) afforded no compound. Elution with pure ethyl acetate afforded three compounds. 1-bromo-*cis*-cyclohexane-1,2-dicarboximide was contained in fractions 10, 11, and 12 (15 ml eluent) with 80%, 96%, and 75% purities respectively as shown by GC analysis. Removal of the solvent

from fraction 11 gave a white solid: MS (CI), *m/e* (relative intensity) 234 (M^++1, 98), 232 (M^++1, 100); ^{1}H NMR ($CDCl_3$) 1.44 (m, 1H), 1.54 (m, 2H), 1.75 (m, 2H), 2.04 (m, 1H), 2.22 (m, 1H), 2.32 (m, 1H), 3.33 (m, 1H, H_1), 8.33 (br s, 1H, NH); ^{13}C NMR ($CDCl_3$) 21.35, 21.97, 24.55, 34.63, 52.38, 57.97, 174.76, 175.78. Imide **35** was contained in fractions 26-35, and amide **33** in fractions 100-104 as shown by GC analysis.

In a separate run, a solution of N-bromoimide **32** (15.5 mg, 0.0668 mmol) and DCE (5 μl, 0.06 mmol) in CH_2Cl_2 (1.0 ml) was placed in a NMR tube, sealed, purged with nitrogen, and irradiated with RPR 3000 Å lamps (Method II) for 15 minutes. The solvent was removed from the photolysate, and the residue was dissolved in $CDCl_3$ (0.6 ml) for NMR analysis. No signal at 3.09 ppm due to N-bromoimide **32** was detected. The $CDCl_3$ solution was mixed with benzophenone (as an internal standard) for GC analysis (column temperature 160°C isothermal, column pressure 20 psi) to afford amide **33** (0.050 mmol, 75% based on the amount of **32** used), amide **34** (0.0046 mmol, 6.9%), imide **35** (0.0099 mmol, 14.8%), and 1-bromo-*cis*-cyclohexane-1,2-dicarboximide (detected but not intergrated, <0.002 mmol, <3%).

4.4.9. Photodecomposition of N-Bromoimide 36

N-Bromoimide **36** was prepared from (±)-camphorimide **38**. The latter was synthesized from (±)-camphoric anhydride by using the

method described by Chow and Naguib[153] (mp 245-248°C, lit.[157] mp 249°C; ^{1}H NMR ($CDCl_3$) 1.00 (s, 3H), 1.06 (s, 3H), 1.20 (s, 3H), 1.7-2.5 (m, 4H), 2.64 (br d, 1H, J=6.6 Hz), 7.8 (br s, NH); IR ($CDCl_3$) 3210 (m), 1695 (s)).

A solution of **38** (230 mg, 1.1 mmol) in CH_2Cl_2 (5 ml) placed in a 50 ml flask equipped with a drying tube was cooled in an ice-salt bath. To the solution was added a CCl_4 solution of *t*-butyl hypobromite (25 ml, 4 mmol), and the mixture was stirred for 40 minutes. The solution was evaporated under reduced pressure to give N-bromoimide **36** as a yellowish solid (315 mg): ^{1}H NMR ($CDCl_3$) 0.98 (s, 3H), 1.02 (s, 3H), 1.31 (s, 3H), 1.99 (m, 4H), 2.98 (br d, 1H, J=6.2 Hz); IR ($CDCl_3$) 2980 (m), 1700 (s), void of 3210 cm^{-1} (NH absent).

A solution of **36** (315 mg, 1.1 mmol) and DCE (60 μl, 0.75 mmol) in CCl_4 (20 ml) was placed in a 30 ml Pyrex photocell, sealed, purged with nitrogen, and irradiated with RPR 3000 Å lamps (Method II) for twenty minutes. Removal of the solvent from the colorless photolysate left a yellowish solid (≃250 mg). The residue (4 mg) was dissolved in $CDCl_3$ (0.6 ml) for NMR analysis. No signal at 2.98 ppm due to N-bromoimide **36** was detected. The $CDCl_3$ solution was analysed by GC (column temperature 160°C isothermal, column pressure 20 psi) to show (retention time, peak area) amide **37** (2.01 minutes, 62%), imide **38** (2.27 minutes, 33%), and four small unidentified peaks. Chromatography of the crude product (elution with 60% ethyl acetate-hexane) gave

eighty fractions of 10 ml each. Fractions 10-14 contained imide **38**, and fractions 50-68 contained amide **37** (80 mg). Amide **37** used for microanalysis was recrystallized from acetone-hexane (1:5) as colorless needles: mp 97-98°C.

In a separate experiment, a solution of N-bromoimide **36** (365 mg, 1.27 mmol) and DCE (65 μl, 0.80 mmol) in CH_2Cl_2 (20 ml) was purged and irradiated in the same way as described above. To the photolysate was added benzophenone as the internal standard for GC analysis (200°C, isothermal, 20 psi). The products were amide **37** (0.76 mmol, 60% based on the amount of imide **36** used) and imide **38** (0.46 mmol, 36%).

4.4.10. Photodecomposition of N-Bromoimide 39

A solution of 3-methyl-3-ethylglutarimide **40** (250 mg, 1.61 mmol) in CCl_4 (40 ml) was placed in a 200 ml round-bottom flask. A CCl_4 solution of acetyl hypobromite[156] (15 ml, 2 mmol) was added, and the mixture was stirred for 30 minutes. After the solvent was removed under reduced pressure, N-bromoimide **39** was obtained as a white solid: ^{1}H NMR ($CDCl_3$) 0.92 (t, 3H, J=7.3 Hz), 1.07 (s, 3H), 1.44 (q, 2H, J=7.3 Hz), 2.72 (s, 4H); IR (Nujol) 1690 (s), 1270 (m), 1225 (s), 1145 (m), 1125 (ms), 635 (w), void of 3220 cm^{-1} (NH absent). The pertinent data of imide **40** are as follows: ^{1}H NMR ($CDCl_3$) 0.92 (t, 3H, J=7.4 Hz), 1.07 (s, 3H), 1.44 (q, 2H, J=7.4 Hz), 2.44 (s, 4 H), 7.9 (br s, NH);

IR (Nujol) 3220 (m), 1685 (s), 1280 (s).

A solution of **39** (12 mg, 0.051 mmol) and DCE (3 μl, 0.04 mmol) in CH_2Cl_2 (1.5 ml) was placed in a NMR tube, sealed, purged with nitrogen (see Section 4.4 1.1 for the detail), and irradiated with RPR 3000 Å lamps (Method II) for forty minutes. A colorless photolysate was obtained, and it was analyzed by GC (column temperature 230°C isothermal, column pressure 20 psi) to give a peak for imide **40** (retention time 1.93 minutes, 94%) as the major product and unidentified minor peaks at retention times 2.15 minutes (1%), 2.28 minutes (2%), 2.49 minutes (1%), and 2.93 minutes (2%). GC-MS (CI) analysis showed none of these peaks possessed *m/e* values of 220 and 222 (the M^++1 values of a C-brominated imide). The peak with retention time of 2.93 minutes showed the following MS pattern: *m/e* (relative intensity) 336, 334, 332, 330 (1:9:20:10, M^++1), presumably a 1:1 adduct of **39** to DCE.

Table 4-7

^{1}H NMR Parameters of Compounds

22, 24, 27, 30, 31, 33, and 37 in $CDCl_3$ Solution

Cmpd.	Chemical Shift ppm	Coupling Constant Hz
22	1.67 (m, 1H, H_4), 1.70 (br t, 2H, H_3 & H_5), 1.73 (m, 2H, H_7), 2.51 (m, 1H, H_1), 2.66 (m, 2H, H_2 & H_6), 7.78 (br s, 1H, NH)	$J_{2,1}=J_{6,1}=1.7$, $J_{1,7}=1.2$ $J_{4,7}=1.2$, $J_{2,4}=J_{6,4}=1.7$ $J_{1,3}=J_{1,5}\simeq 0.5$ $J_{3,4}=J_{5,4}=5.0$
24	2.45 (m, 2H, H_7 & $H_{7'}$), 2.95 (m, 1H, H_4), 2.98 (d m, 1H, H_2), 3.3 (m, 1H, H_1), 3.75 (m, 1H, H_3), 4.10 (m, 1H, H_5), 4.95 (m, 1H, H_6)	$J_{3,7'}\simeq 1.2$, $J_{2,1}=4.8$ $J_{6,1}\simeq 5.0$
27	2.15 (ddd, 1H, $H_{6'}$[a]), 2.52 (ddd, 1H, H_6[a]), 3.45 (ddd, 1H, H_1), 3.63 (dddd, 1H, H_2), 4.68 (m or dddd, 1H, H_3), 6.03 (ddd, 1H, H_5), 6.24 (dddd, 1H, H_4)	$J_{6',1}=10.3$, $J_{6',6}=14.5$ $J_{6',3}=4.0$[b], $J_{6,1}=6.0$ $J_{6,3}=4.5$, $J_{6,4}\simeq 0.6$ $J_{1,2}=8.5$, $J_{1,3}\simeq 0.5$ $J_{2,4}=2.6$, $J_{2,5}=4.0$ $J_{2,3}=1.0$, $J_{3,4}=5.0$ $J_{5,4}=9.8$, $J_{5,3}\simeq 0.7$

30	2.41 (m, 1H, H_{3e}), 2.48 (m, 1H, H_{3a}), 2.61 (m, 1H, H_{6a}), 2.73 (m, 1H, H_{4a}), 2.81 (m, 1H, H_{6e}), 4.38 (ddd, 1H, H_{5a}), 5.53 (m, 1H, H_1 or H_2), 5.71 (m, 1H, H_2 or H_1), 5.64 (br s, 2H, NH_2)	$J_{3e,3a}$=17, $J_{3a,4a}$=10 $J_{3e,4a}$=5.5, $J_{6a,6e}$=18 $J_{6a,5a}$=10, $J_{4a,5a}$=10 $J_{6e,5a}$=5.5, $J_{1,2}$=9.0 $J_{3a,x}$=2.5, $J_{3a,y}$=4.0 $J_{6a,u}$=2.5, $J_{6a,v}$=3.5 $J_{6e,z}$=5.4, $J_{6e,w}$=5.5
31	2.35 (m, 1H, H_{6e}), 2.55 (m, 1H, H_{3a}), 2.66 (m, 1H, H_{6a}), 2.88 (m, 2H, H_{3e}, H_{4a}), 4.84 (m, 1H, H_{5e}), 5.67 (m, 1H, H_1 or H_2), 5.75 (m, 1H, H_2 or H_1), 5.71 (br s, 2H, NH_2)	$J_{6a,6e}$=17, $J_{6e,5e}$=2 $J_{3a,4a}$=10, $J_{3e,4e}$=15 $J_{1,2}$=10, $J_{3a,x}$=2.0 $J_{3a,y}$=4.0, $J_{6a,z}$=5.0 $J_{6a,w}$=10, $J_{3e,u}$=2.5 $J_{3e,v}$=4.5, $J_{5e,q}$=5.0 $J_{5e,r}$=1.5
33	1.30 (m, 1H, H_5), 1.35 (m, 1H, H_{6a}), 1.62 (m, 1H, H_4), 1.80 (m, 3H, H_3, H_4 & H_5), 1.97 (m, 1H, H_{6e}), 2.42 (m, 1H, H_3), 2.42 (m, 1H, H_3), 2.50 (m, 1H, H_{1a}), 4.24 (ddd, 1H, H_{2a})	$J_{1a,6e}$=3.5, $J_{1a,6a}$=12.0 $J_{1a,2a}$=11.0, $J_{2a,3e}$=3.5 $J_{2a,3a}$=12.0, $J_{6e,6a}$=13.0 $J_{3e,4e}$=4.5*, $J_{3e,4a}$=3.0* $J_{6e,5a}$=5.0#, $J_{6e,5e}$=3.0# $J_{3a,3e}$=12.0

37	1.00 (s, 3H, C_3-Me), 1.19 (s, 3H, C_3-Me), 1.65 (m, 3H, C_2-Me), 2.38 (m, 1H, H_{5C}[c]), 2.62 (m, 1H, H_{5t}[c]), 2.66 (t, 1H, H_4), 5.27 (m, 1H, H_1), 5.43 (br s, 2H, NH_2)	$J_{1,5t}$=2.5†, $J_{1,5C}$=2.0† $J_{4,5t}$=7.5, $J_{4,5C}$=10.0 $J_{5C,5t}$=15.0, $J_{6,5C}\simeq$1.2‡ $J_{6,5t}$=2.0‡

a. H_6' and H_6 are hydrogens at C-6 position at the same side as, and at the opposite side to, the imidyl group.

b. Irradiation of the signal of H_3 simplifed the signal of H_6'; homoallylic coupling.

c. H_{5C} and H_{5t} are the two protons cis and trans to the $CONH_2$ group.

*, #, †, and ‡: These assignments are interchangeble.

Table 4-8

^{13}C NMR Parameters of Compounds

22, 24, 27, 30, 31, 33, and 37 in $CDCl_3$ Solution

Cmpd.	Chemical Shift, ppm
22	17.17, 17.26, 34.03, 37.10, 48.49, 175.14
24	33.90, 45.67, 46.81, 49.53, 50.02, 54.74 86.62, 174.98
27	31.96, 37.71, 40.69, 41.30, 123.45, 131.78 175.82, 178.36
30	29.70, 36.06, 47.94, 49.81, 124.83, 174.99
31	25.14, 35.61, 45.62, 49.19, 123.36, 124.89 173.67
33	24.50, 26.85, 31.24, 37.25, 51.95, 54.71 175.40
37	12.34, 20.87, 27.16, 32.45, 48.39, 56.72 121.02, 146.66, 175.8

Table 4-9

IR Absorptions of Compounds

22, 24, 27, 30, 31, 33, and 37[a]

Cmpd.	ν, cm^{-1}
22	3450 (m), 3180 (br s), 3080 (ms), 1685 (s), 1260 (s), 1005 (m)
24[b]	2998 (w), 2985 (w), 1788 (vs), 1402 (w), 1345 (m) 1170 (ms), 1014 (ms), 942 (m), 903 (m), 860 (w) 700 (w).
27	3257 (br s), 1775 (s), 1704 (br vs), 1640 (m), 1343 (s), 1187 (s), 1175 (s), 1004 (s), 771 (s).
30	3410 (m), 3220 (w), 1665 (s), 1620 (w)
31	3405 (m), 3200 (m), 1663 (s), 1650 (s)
33	3350 (s), 3160 (s), 1665 (vs), 1620 (s), 1186 (w) 1010 (w)
37[c]	3527 (ms), 3410 (ms), 2963 (s), 1682 (vs) 1589 (s).

a. in Nujol unless otherwise stated.

b. as a thin film.

c. as a CH_2Cl_2 solution.

Table 4-10

Mass Spectral Data of 22, 24, 27, 30, 31, 33, and 37

Cmpd.	Mode	*m/e* (rel. intensity)
22	EI	163 (M^+, 52), 91 (100), 65 (28)
24	EI	298 (M^+, 1), 296 (M^+, 2), 294 (M^+, 1) 217 (M^+-Br, 30), 215 (M^+-Br, 30) 107 (M^+-2Br, 40), 91 (40), 79 (80) 65 (25), 51 (20)
27	EI	150 (M^+-Br, 75), 105 (55), 79 (M^+-Br-CONHCO)
30	EI	205 (M^+, 0.5), 203 (M^+, 0.5), 124 (M^+-Br,95) 81 (100), 79 (80), 44 ($CONH_2^+$, 22)
31	EI	205 (M^+, 1.6), 203 (M^+, 1.8), 124 (M^+-Br,90) 81 (86), 79 (100), 44 ($CONH_2^+$, 20)
33	EI	207 (M^+, 2), 205 (M^+, 2), 126 (M^+-Br, 78) 81 (53), 67 (48), 55 (65), 44 (100)
	CI	208 (M^++1, 96), 206 (M^++1, 100), 126 (M^+-Br, 23)
37	EI	153 (M^+, 60), 138 (20), 110 (100), 95 (90) 79 (35), 67 (75), 55 (30), 41 (40)
	CI	154 (M^++1, 100)

Table 4-11

Microanalysis Data of Compounds 22, 24, 27, 30, 31, 33, and 37

22	Calcd	C: 66.26	H: 5.52	N: 8.59
$C_9H_9NO_2$	Found	C: 66.04	H: 5.40	N: 8.31
24	Calcd	C: 32.43	H: 2.70	
$C_8H_8Br_2O_2$	Found	C: 32.29	H: 2.55	
27	Calcd	C: 41.74	H: 3.48	N: 6.09
$C_8H_8BrNO_2$	Found	C: 41.84	H: 3.54	N: 6.00
31	Calcd	C: 41.18	H: 4.90	N: 6.86
$C_7H_{10}BrNO_2$	Found	C: 41.55	H: 4.90	N: 6.91
33	Calcd	C: 40.78	H: 5.83	N: 6.80
$C_7H_{12}BrNO_2$	Found	C: 40.80	H: 5.97	N: 6.67
37	Calcd	C: 70.59	H: 9.80	N: 9.15
$C_9H_{15}NO$	Found	C: 70.40	H: 9.92	N: 8.99

4.5. Reactions of NBS with Naphthols

General Conditions: The absorption spectra of dienone derivatives in dichloromethane were determined using a pair of normal UV cuvettes with a Varian Cary 210 spectrophotometer. The chemical shifts of the dienone derivatives prepared *in situ* were measured at 20°C on a Bruker SY 100 spectrometer. Rate constants for reactions of NBS with various naphthols were measured at 25±1°C, using a Varian Cary 210 spectrophotometer. All reactions were studied under pseudo-first-order conditions with at least a 15:1 ratio of naphthol to NBS.

4.5.1. UV Absorption Spectra

4.5.1.1. The Differential Spectra of Dienone 41

In the dark, dichloromethane solutions of 1-NpOH (5.00×10^{-3} and 1.52×10^{-3} M) and those of NBS (4.0×10^{-3}, 3.2×10^{-3}, and 6.4×10^{-4} M) were prepared by the volumetric method and kept in dark prior to use. Differential absorption spectra were recorded at 20°C using a pair of double-compartment cells. A typical run is shown in Figure 4-1, and the absorption spectra were recorded in Figure 2-15.

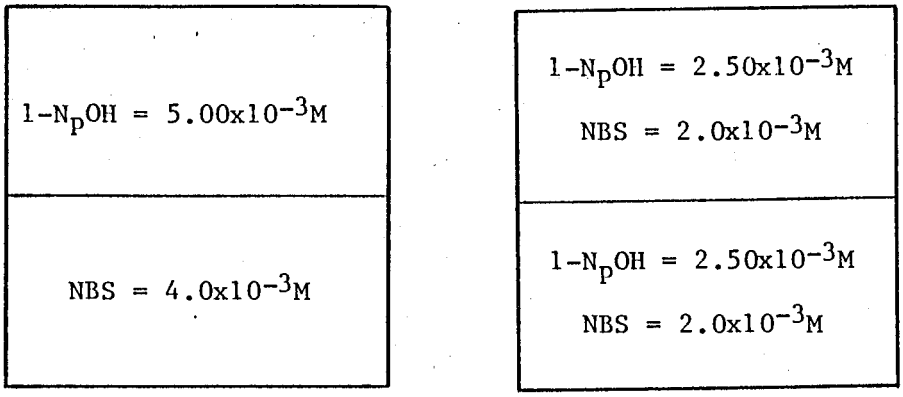

Figure 4-1. A pair of double compartment cells for the differential absorption spectra.

4.5.1.2. Isosbestic Points

2.0 ml of a dichloromethane solution of NBS (3.0×10^{-2} M) in a cuvette was placed in the sample compartment followed by injection with a syringe of 1.0 ml of CH_2Cl_2 solution of 1-NpOH (8.0×10^{-4} M) into the cuvette. The absorbances in 400-310 nm region were recorded at 100-second intervals with the first scan begining at t=10 seconds after the mixing. An isosbestic point at 324 nm was observed.

In a separate run, 0.050 ml of a CH_2Cl_2 solution of NBS (7.86×10^{-3} M) was diluted with CH_2Cl_2 (3.0 ml). The cuvette containing the solution was placed in the cuvette holder. Then 0.025 ml of CH_2Cl_2 solution of 1-NpOH (7.82×10^{-3} M) in CH_2Cl_2 was injected into the cuvette with a 25-μl syringe. The first scan from 330 to 240 nm started at t=5 seconds after the mixing. The scanning was repeated 18 times. A pair of isosbestic points at 324 and 269 nm were observed.

4.5.1.3. Determination of ϵ_{max} and λ_{max}

4.5.1.3.1. Dienones 41 and 42

Five dichloromethane solutions of 1-NpOH (3.75×10^{-3} M), cyclohexane (1×10^{-7} M), and various amounts of NBS (3.93×10^{-4}, 1.97×10^{-4}, 9.80×10^{-5}, 4.90×10^{-5}, and 2.50×10^{-5} M respectively) were prepared in the dark. Thirty minutes later, their absorption spectra in range 350-400 nm were recorded, and the absorbance at 365 nm was 0.761, 0.378, 0.174, 0.0905, and 0.0407 respectively. The λ_{max} was determined to be 357 nm, and the ratio of absorbance at 357 nm to that at 365 nm was 2.0:1.9.

To a dichloromethane solution of 2-naphthol (volumn of the solution 3.00 ml, the concentration of 2-NpOH 6.80×10^{-3} M) placed in a 1-cm UV cuvette was injected a dichloromethane solution of NBS (0.200 ml, 4.10×10^{-3} M), producing a working solution of 5.13×10^{-4} M in NBS and 6.38×10^{-3}M in 2-NpOH. The

increase in absorbance of the solution was monitored at 360 nm, and a maximum value of 0.67 was observed after 30 minutes. Then the absorbance of the solution at 332 nm (λ_{max}) was determined to be 1.45, and the absorbance at 350 nm 1.01. The absorbance at λ_{max} of dienones **43**, **44**, and **45** were recorded in the same way as described for **42** and the pertinent data are listed in Table 2-23.

4.5.2. Chemical Shifts of Dienones

To a NMR tube containing a $CDCl_3$ solution of NBS (0.2 ml, 5.78×10^{-2} M) was injected a $CDCl_3$ solution of 1-NpOH (0.25 ml, 1.4×10^{-1} M). The tube was placed inside the NMR cavity, the spinning adjusted, and the sample was locked as soon as possible. The spectrum was recorded ≃30 seconds after the mixing and at 30-second intervals. Some pertinent parameters used in this work were: NS=1, RG=64, AQ=5.4, O1=1900, SW=1500, RD=0, PW=4, and SR=1312.7. The hydroxyl signal at 5.3 ppm and the H_2 signal at 6.84 ppm of 1-naphthol kept decreasing, while the H_2 signal at 5.02 ppm, the H_3 signal at 6.38 ppm, and the H_4 signal at 6.70 ppm of **41** kept increasing.

In a separate run, the solution in the NMR tube was withdrawn and diluted ten times with dichloromethane after the signal intensity due to **41** did not increase any more. The absorption spectrum of the diluted solution in a 0.1-cm UV cell was

recorded. An absorption band (λ_{max}=357 nm, absorbance 0.513) was observed.

The chemical shifts of dienones **42**, **43**, and **44** were recorded in the same way as described for **41** and listed in Table 2-24.

4.5.3. UV Absorbance vs. Time

4.5.3.1. 1-Naphthol with NBS at 360 nm

In the dark, a dichloromethane solution of 1-naphthol (8.50×10^{-3} M) and one of NBS (8.42×10^{-3} M) were prepared and thermostated at 25°C prior to use. In a typical run, a UV cuvette containing the solution of 1-naphthol (3.00 ml) was placed in the thermostatically controlled sample compartment (25.0 ± 0.5°C) of a Varian 210 spectrophotometer. A cuvette containing 3 ml of dichloromethane was used as reference. Then the NBS solution (0.200 ml) was injected into the sample cuvette with a syringe to produce a working solution of 7.97×10^{-3} M in 1-naphthol and 5.26×10^{-4} M in NBS. The absorbance at 360 nm due to dienone **41** was recorded against time with a scanning rate of 10 sec/cm (time t, absorbance A_t): 10 sec, 0.0460; 20 sec, 0.075; 30 sec, 0.105; 40 sec, 0.135; 50 sec, 0.162; 60 sec, 0.200; 70 sec, 0.233; 1000 sec, 1.075 (A_∞). Fitting this data to $-\ln(A_\infty-A_t) = k_{obs}t$, where $k_{obs}=k_2[NBS]$, produced k_{obs} of 0.00333 sec^{-1} with a correlation coefficient of 0.998.

The rate constants for the reaction of NBS with other naphthols were determined in the same way as described for 1-naphthol and the results are listed in Table 2-25.

1-Naphthol (59.6 mg) in a 1-cm UV cuvette was dissolved with dichloromethane (3.0 ml). The cuvette was then placed in the sample compartment thermostated at 25.0±0.5°C. A UV cuvette containing dichloromethane (3.0 ml) was used as reference. To the sample cuvette was injected a dichloromethane solution of NBS (0.400 ml, 2.78×10^{-3} M) with a syringe, producing a working solution of 0.138 M in 1-naphthol and 3.27×10^{-4} M in NBS. The absorbance at 370 nm against time was recorded with a scanning rate of 5 sec/cm (time t, absorbance A_t): 3 sec, 0.29; 4 sec, 0.33; 5 sec, 0.36; 6 sec, 0.385; 200 sec, 0.62 (A_∞). Fitting this data to $-\ln(A_\infty - A_t) = k_{obs}t$, produced k_{obs} of 0.10 sec^{-1}.

4.5.3.2. 1-NpOH with NBS at 322 nm and 365 nm

In a UV cuvette held in the sample compartment of a Varian Cary 210, a working solution of 1.52×10^{-2} M in NBS, 3.18×10^{-4} M in 1-naphthol, and 2×10^{-4} M in cyclohexene was prepared, and thermostated at 25±1°C in the same way as described previously. The decrease in absorbance at 322 nm due to the consumption of 1-naphthol was monitored against time with a scanning rate of 10 sec/nm (time t, absorbance A_t): 10 sec, 0.775; 20 sec, 0.705; 30 sec, 0.650; 40 sec, 0.607; 50 sec, 0.577; 60 sec, 0.554; 70 sec,

0.534; 80 sec, 0.518; 90 sec, 0.507; 100 sec, 0.498. Fitting this data to $-\ln(A_t-A_\infty)=k_{obs}t$, where an optimized A_∞ of 0.465 was adopted[158], produced k_{obs} of 0.025 sec^{-1} with a correlation coefficient of 0.9999. Alternatively, from the slope of the plot of $\ln(A_t-A_{t40})$ against time[159] was obtained the same k_{obs} (0.025 sec^{-1}, c.c.=0.999, where A_{t40} is the absorbance at t+40 sec.). The experiment was repeated and a k_{obs} of 0.026 sec^{-1} was obtained. In a separate experiment, the same working solution was made, and the increase in the absorbance at 365 nm due to the formation of dienone **41** was monitored against time with a scanning rate of 10 sec/cm (time t, absorbance A_t): 10 sec, 0.110; 20 sec, 0.220; 30 sec, 0.305; 40 sec, 0.373; 50 sec, 0.425; 60 sec, 0.463; 70 sec, 0.491; 80 sec, 0.512; 90 sec, 0.530; 100 sec, 0.542. Fitting this data to $-\ln(A_{t20}-A_t)=k_{obs}t$, produced k_{obs} of 0.027 sec^{-1} with a correlation coefficient of 0.9999. The experiment was repeated, and a k_{obs} of 0.026 sec^{-1} was obtained.

4.5.3.3. FT-IR Spectra

A dichloromethane solution of NBS (0.2 ml, 5.17×10^{-2} M) was placed in a 0.2-ml IR cell, and capped with two rubber septums. Then 50 μl of CH_2Cl_2 solution of 1-NpOH (2.22×10^{-1} M) was injected quickly into the cell through one septum with a 100-μl syringe to form a working solution of 4.1×10^{-2} M in NBS and 4.4×10^{-2} M in 1-naphthol. The cell was placed in the sample

compartment of a Bruker IFS-85 FT IR spectrophotometer and the IR absorption of the solution was recorded 35 seconds after the mixing. After which, it was recorded at 1 minute intervals, each spectrum being recorded with eight scans within 10 seconds. In a separate experiment, IR absorption of succinimide in dichloromethane (3.0×10^{-3} M) was recorded: 3390 (br s), 1724 (s), 1161 (m), 895 (m) cm^{-1}.

4.5.4. Photodecomposition of Dienone 41

In a dark room, NBS (4.90 mg, 0.0275 mmol) was dissolved in dioxane (2.0 ml) in a flurescence cuvette. To the solution was added 7.5 mg (0.052 mmol) of 1-naphthol. A yellow solution was observed in two minutes. The cuvette was wrapped with a piece of aluminium foil. The solution was purged with nitrogen for ten minutes, and irradited with a 200-watt mercury lamp through a GWV filter (Method I) for fifteen minutes to give a yellowish-greenish solution. To the photolysate was added anthracene (2.59 mg, 0.0145 mmol) as an internal standard. The absolute yields of bromo-1-naphthols were determined, based on the NBS used, by GC (column temperature 190°C isothermal, column pressure 10 psi) to give 2-bromo-1-naphthol (retention time 2.26 minutes, 0.0206 mmol, 75% based on the amount of NBS used) and 4-Br-1-naphthol (4.09 minutes, 0.00165 mmol, 6.0%). The signal due to 2,4-dibromo-1-naphthol at 5.20 minutes was not detected. The remaining

1-naphthol (retention time 1.68 minutes) was 0.0289 mmol. Material balance based on 1-naphthol was calculated to be 98%.

The reaction was also carried out in dichloromethane, benzene, and acetonitrile. The results are listed in Table 2-26.

NBS (4.9 mg, 0.0275 mmol), 1-naphthol (8.5 mg, 0.059 mmol), and CCl_4 (3.0 ml) were placed in a 1-cm fluorescence cuvette. The heterogeneous mixture, after vigorous shaking, was purged with nitrogen for ten minutes, and irradiated through a GWV filter for 28 minutes. The mixture remained heterogeneous during the photolysis. The photolysate was filtered and the filtrate washed with 5% aqueous $NaHSO_3$ solution (2 ml) to destroy the remained NBS in it. The organic layer was separated and the aqueous layer was extracted with dichloromethane (2 ml). After the combined organic solutions were dried over anhydrous magnesium sulphate, it was mixed with athracene (0.0145 mmol) for GC analysis, and the yields of products were 2-bromo-1-naphthol (0.0102 mmol, 37% based on the amount of NBS used) and 4-bromo-1-naphthol (0.0019 mmol, 6.9%). 2,4-Dibromo-1-naphthol was not detected. The remaining 1-naphthol amounted to 0.0424 mmol). Material balance based on 1-naphthol was calculated to be 92.4%.

4.5.5. Bromination of 1-Naphthol and 1-MeO-Naphthalene with NBS

A solution of 1-naphtol (4.01 mg, 0.0277 mmol), 1-methoxynaphthalene (4.12 mg, 0.0259 mmol), and NBS (3.21 mg, 0.0180

mmol) in dichloromethane (3.0 ml) was sealed, purged with nitrogen, and irradiated with a 100-watt mercury lamp through a GWV filter for fifteen minutes. The colorless photolysate was analyzed by GC (190°C isothermal, 20 psi) with anthracene as the internal standard, and the yields of the products were 2-bromo-1-naphthol (0.0135 mmol, 75% based on the amount of NBS used), 4-bromo-1-naphthol (0.00115 mmol, 6.4%). The signals due to 2,4-dibromo-1-naphthol and 4-bromo-1-methoxy-naphthalene were detected but not integrated (<0.0005 mmol).

In a similar way, bromination of 1-methoxynaphthalene and 1-naphthol was carried out with Br_2-K_2CO_3 as bromination reagent. The results are listed in Table 2-27.

4.5.6. Preparation of 2-Bromo-4-chloro-1-naphthol

4-Chloro-1-naphthol (1.71 g) and NBS (0.71 g) were dissolved in dichloromethane (100 ml) at room temperature and kept under the room light for four hours. After the solvent was removed under reduced pressure, the blue residue was added into CCl_4 (80 ml) to obtain a heterogeneous mixture. The undissolved succinimide was filtered off, and a blue solution was obtained. After the solvent was removed under reduced pressure from the blue solution, the residue was sublimed to afford the title compound as white crystals: mp 92.5-93.5°C (lit.[160] mp 96°C); IR ($CDCl_3$ solution) 3520 (s), 1590 (s), 1580 (s), 1380(s), 1338 (ms), 1230 (vs), 1067 (ms); ^{1}H NMR ($CDCl_3$) 5.95 (s, OH), 7.56-7.67 (m, 2H),

7.61 (s, 1H), 8.13-8.31 (m, 2H). The singlet at 5.95 ppm disappeared after one drop of D_2O was added into the NMR sample and after shaking for about one minute.

4.5.7. Attempt to Detect Fluorescent Emission of 41

A solution of 1-naphthol (0.010 M) and NBS ($1.0x10^{-4}$ M) in dichloromethane (4.0 ml) was placed in a fluorescence cuvette and sealed with a rubber septum then purged with nitrogen through metallic neddles for ten minutes in a dark room. The formation of the dienone **41** was confirmed by UV spectroscopy, and an absorbance at 356 nm of 0.19 was observed. The solution was excited at 356 nm. No fluorescent emission was observed in region 385-600 nm.

4.5.8. Quantum Yield of Photodecomposition of 41

The quantum yield of photodecomposition of **41** was determined using an optical bench as shown in Figure 4-2. In a typical experiment, a fresh dichloromethane solution of NBS (0.0010 M) and 1-naphthol (0.011 M) was prepared and placed in a quartz cuvette. It was sealed and purged with nitrogen for ten minutes then kept in the dark at room temperature for ten minutes. Its absorbance at 365 nm was determined to be 1.95 ($\lg\epsilon$=3.28) before irradiation. Irradiation for 1.5 minutes decreased the absorbance at 365 nm to 1.74. The solution was taken out and its volume was measured to be $3.0x10^{-3}$ liter. The quantum yield of

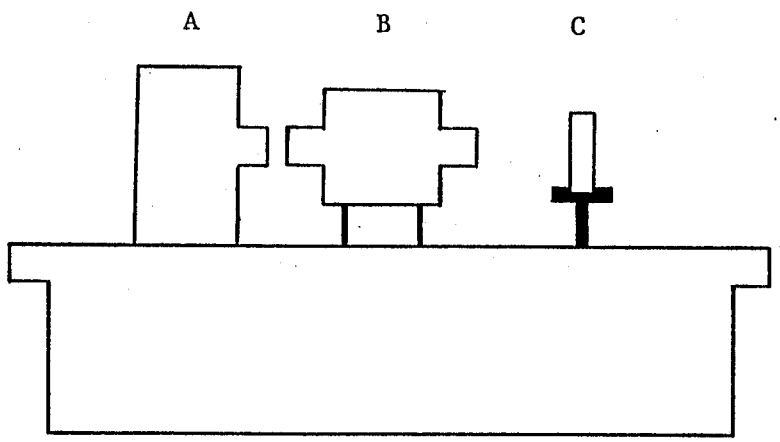

Figure 4-2. An optical bench used for the quantum yield determination

A: Light source (a 200-W Hg/Xe lamp)

B: Kratos high intensity monochrometer

C: Quartz cuvette (1-cm pathlength) containing sample.

The distance between A and B: 1 cm

The distance between B and C: 10 cm

photodecomposition of **41** was calculated to be 0.96 by the use of equation 4-8.

$$\Phi = (\Delta A \cdot V)/(\epsilon I_0 t) \qquad 4\text{-}8$$

where ΔA is the difference in absorbances, V is the volume of the sample solution in liter, ϵ is molar absorptivity of **41** , I_0 is the incident intensity of the light source being used in einstein/min, and t is the irradiation time in minutes. The experiment was repeated. A decrease in the absorbance at 365 nm from 1.89 to 1.66 was observed after 1.50 minutes of irradiation. Φ of 1.1 (rounded up from 1.05) was obtained. In both of the experiments the decrease in the absorbance at 365 nm due to the thermodecomposition of the sample was monitored before and after the irradiation. No correction was made for ΔA since the decrease due to the thermal process was too small.

The actinometer solution was prepared as follows. Benzophenone (456 mg, 2.50 mmol) and benzhydrol (921 mg, 5.00 mmol) were each dissolved in benzene (25.0 ml). Then a 10 ml aliquot was pipetted from each of the above two stock solutions and mixed in a volumetric flask to form an actinometer solution of 0.050M in benzophenone and 0.10 M in benzhydrol. The absorbance of the solution in a 0.1-cm UV cell was recorded first. Then 3 ml of the solution was transferred to a 1-cm fluorescence cuvette, sealed, and purged with nitrogen for 10 minutes, and

irradiated with the same light source for 10 minutes. Then the photolysate was transferred to a 0.1-cm UV cell and its absorbance recorded. The experiment was repeated, and the samples were irradiated for 25, 37, and 47 minutes respectively. The incident intensity of the light source was determined to be (2.3 ± 0.1)x10^{-7} einstein/minute by the use of equation 4-9, assuming there is no error associated with the data from each of the four experiments.

$$I_0 = (\Delta A \cdot V)/(\epsilon \Phi^0 t) \qquad 4\text{-}9$$

where ΔA is the difference in the absorbance of the sample before and after the irradiation, V is the volume of the photolysate in liter, ϵ is molar absorptivity of benzophenone at 365 nm and a value of 68 was adopted, Φ^0 is the quantum yield of benzophenone's reaction under the conditions and a value of 0.74 was assumed[78], and t is duration of the irradiation in minute.

4.6. Fluorescence Intensity Quenching by NBS

Uncorrected fluorescence spectra of naphthalene and anthracene in the presence of varied concentrations of NBS were measured in dichloromethane at room temperature after the sample solution in a sealed fluorescence cell was purged with nitrogen for 10 minutes. The fluorescence intensity ratio, I^0/I, was determined at the maximum-intensity wavelength. The Stern-Volmer

correlation of I^0/I vs. NBS, based on equation 4-10, was calculated from the least-square analysis.

$$I^0/I = k_q \tau_0 [NBS] \qquad 4\text{-}10$$

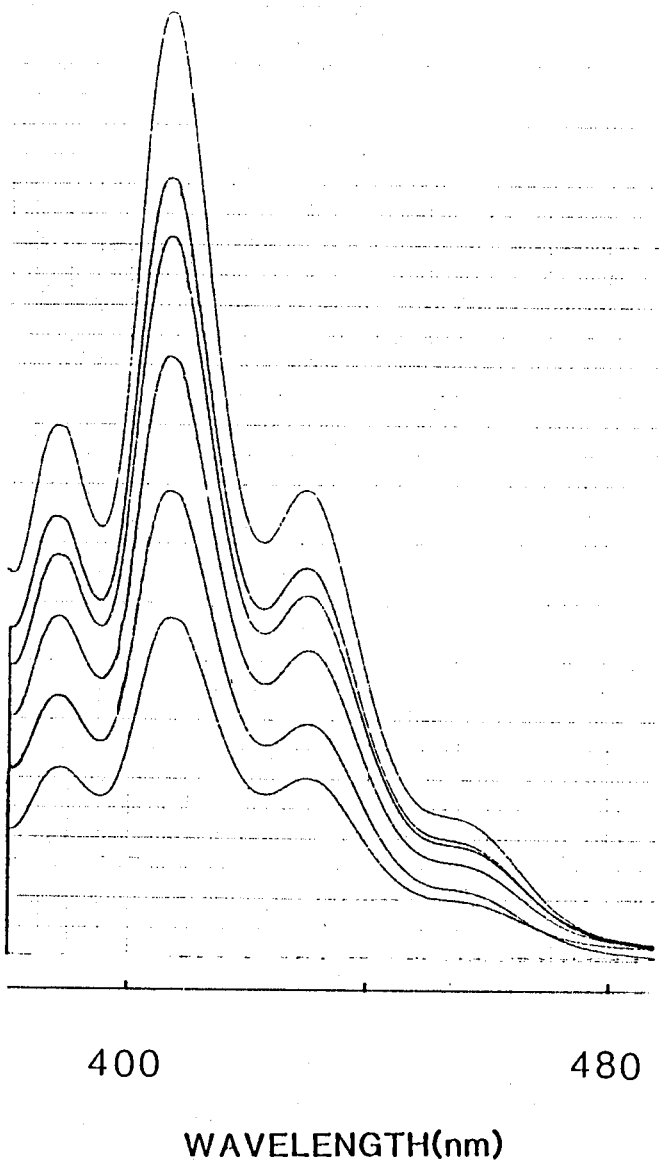

Figure 4-3. Fluorescence spectra of anthracene (9.4×10^{-5} M) in the absence and presence of NBS (Curve 1, [NBS]=0; 2, 6.41×10^{-3}; 3, 1.07×10^{-2}; 4, 1.78×10^{-2}; 5, 2.97×10^{-2}; 6, 4.94×10^{-2}) at room temperature. λ_{ex}= 370 nm (slit 3 nm).

Table 4-12

Quenching of Fluorescene Intensity of Anthracene (9.4×10^{-5} M) by NBS in CH_2Cl_2

10^3[NBS], M	I^a, cm	I^o/I	
0	16.0	1.00	
6.4	13.3	12.0	$k_q\tau_o = 36.5\ M^{-1}$
10.7	12.1	1.32	r=0.999
17.8	10.3	1.56	
29.7	8.10	1.98	
49.4	5.80	2.76	
0	20.4	1.00	
1.39	18.3	1.11	$k_q\tau_o = 38.6\ M^{-1}$
3.48	17.0	1.20	r=0.995
8.69	15.6	1.31	
13.6	13.7	1.49	
34.1	8.60	2.37	

a. Measured at 407 nm

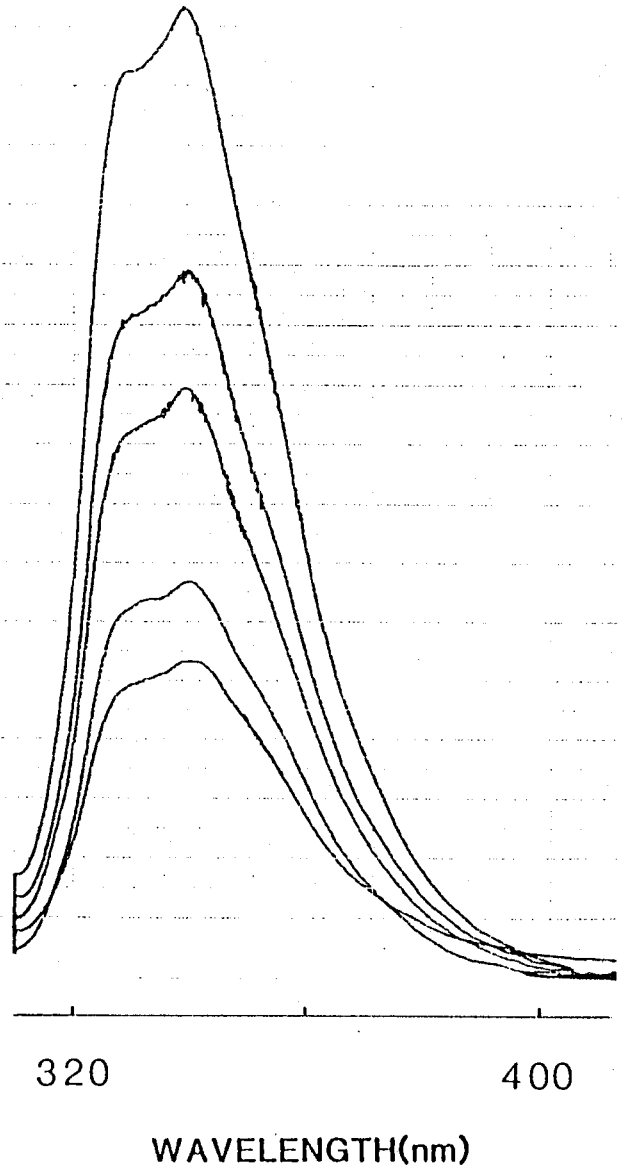

Figure 4-4. Fluorescence spectra of naphthalene (3.3×10^{-4} M) in the absence and presence of NBS (Curve 1, [NBS]=0; 2, 2.02×10^{-3}; 3, 3.37×10^{-3}; 4, 5.62×10^{-3}; 5, 9.36×10^{-3}) at room temperature. λ_{ex}=290 nm (slit 3 nm).

Table 4-13

Quenching of Fluorescence Intensity of Naphthalene (3.33×10^{-4} M) by NBS in CH_2Cl_2

10^3[NBS], M	I_f^a, cm	I^o/I	
0	16.3	1.00	
2.02	12.0	1.3	$k_q\tau_o = 300\ M^{-1}$
3.37	10.0	1.6	r=0.997
5.62	6.70	2.40	
9.36	5.00	3.25	
15.6	3.00	5.40	
0	17.0	1.00	
1.79	12.6	1.35	$k_q\tau_o = 303\ M^{-1}$
2.99	10.3	1.65	r=0.994
4.98	8.35	2.04	
8.31	5.70	2.98	
13.8	3.40	5.00	

a. Measured at 336 nm

APPENDIX

A1. Derivation of Equation 4-5

According to the definition of absorbance we have

$$\alpha = \lg(I_0/I) \qquad \text{A-1}$$

where α is the absorbance of the solution of benzophenone, I_0 is the intensity of the incident light striking the solution, and I is the intensity of the radiation emerging from the solution. Therefore,

$$10^{-\alpha} = I/I_0 \qquad \text{A-2}$$

and A-3 must be true

$$-10^{-\alpha} = -I/I_0 \qquad \text{A-3}$$

Adding 1 at the both side of A-3 simultaneously should not change the equality, and it is not difficult to obtain

$$1-10^{-\alpha} = [(I_0-I)/I_0] \qquad \text{A-4}$$

Similarly, we have

$$1-10^{-\beta} = [(I_0'-I')/I_0'] \qquad \text{A-5}$$

where β is the absorbance of the solution of NBS, and I'_0 and I' are the intensities of the incident light and transmitted light respectively. Since both the solutions were irradiated with the same light source on a merry-go-round , A-6 must hold.

$$I_0 = I'_0 \qquad \text{A-6}$$

Substituting I_0 for I'_0 in A-5 and dividing A-4 by A-5 gives

$$(1-10^{-\alpha})/(1-10^{-\beta}) = (I_0-I)/(I_0-I') \qquad \text{A-7}$$

The term on the right side of A-7 is the ratio of the quanta absorbed by benzophenone to that by NBS. Therefore the term on the left side can be used to correct the quantum yield obtained in Section 4.4.1.5 considering the absorbance of the solution of NBS is far less than 1 in the 290-310 nm region.

A2. Derivation of Equation 3-21

In order to derive the kinetic law from the mechanism which is expressed as Eq. 3-12, 3-13, 3-14, and 3-15, the stationary-state treatment is applied to the reactive intermediates, which must be present in low concentrations.

$$d[\dagger S]/dt = 0 = I-(k_{13}+k_{14})[\dagger S] \qquad \text{A-8}$$

$$d[(PI\cdot)]/dt = 0 = k_{14}[\dagger S]-k_{15}[(PI\cdot)][NBS] \qquad A\text{-}9$$

where I is the rate of light absorption in Einstein's liter^{-1}min^{-1} (see the text in Section 3.1.9 for the meaning of other symbols). The rate of (BPI) formation from (PI·) is

$$d[(BPI)]/dt = k_{15}[(PI\cdot)][NBS] \qquad A\text{-}10$$

Rearrangement of A-8 and A-9 gives A-11 and A-12 respectively.

$$I = (k_{13}+k_{14})[\dagger S] \qquad A\text{-}11$$

$$k_{14}[\dagger S] = k_{15}[(PI\cdot)][NBS] \qquad A\text{-}12$$

Substituting A-12 into A-10 produces

$$d[(BPI)]/dt = k_{14}[\dagger S] \qquad A\text{-}13$$

Dividing A-13 by A-11 gives the expression for the quantum yield of (BPI) formation from †S.

$$\Phi_e^0 = d[(BPI)]/I\,dt = k_{14}/(k_{13}+k_{14}) \qquad A\text{-}14$$

The quantum yields of BPI formation from S· in the absence and the presence of benzene [B], Φ_g^0 and Φ_g, can be derived in a similar way. Assuming a chain length of one, the quantum yields of BPI formation from S· in the absence and presence of benzene

can be written as A-15 and A-16.

$$k_{16}/(k_{16}+k_{18}[D]) \qquad \text{A-15}$$

$$k_{16}/(k_{16}+k_{18}[D]+k_{19}[B]) \qquad \text{A-16}$$

Multipling A-15 and A-16 by the chain length λ_b gives Equations 3-22 and 3-23. Equation 3-24 can be derived in similar way.

REFERENCES

1. C. Walling, *Free Radical Chemistry*, John Wiley and Sons, New York, N. Y., 1957, pp 381-386.

2. Leading references are given by Y. L. Chow and Y. M. A. Naguib, *Rev. Chemical Interm.*, 325 (1984).

3. (a) D. H. Hey, *Ann, Rpts. Chem. Soc.*, **41**, 184 (1944); (b) G. F. Bloomfield, *J. Chem. Soc.*, 114 (1944).

4. R. L. Tlumak, J. C. Day, J. P. Slanga, and P. S. Skell, *J. Am. Chem. Soc.*, **104**, 7257 (1982), in particular p 7259.

5. H. Schmid and P. Karrer, *Helv. Chim. Acta.*, **29**, 573 (1946).

6. (a) H. J. Dauben and L. L. McCoy, *J. Am. Chem. Soc.*, **81**, 4863 (1959); (b) H. J. Dauben and L. L. McCoy, *J. Org. Chem.*, **24**, 1577 (1959).

7. (a) J. Adam, P. A. Gosselain, and P. Goldfinger, *Nature*, **171**, 704 (1953); (b) P. A. Gosselain, J. Adam, and P. Goldfinger, *Bull. Soc. Chim. Belg.*, **65**, 533 (1956).

8. F. L. J. Sixma and R. H. Reim, *Proc. K. Ned. Akad. Wet., Ser. B: Phys. Sci.*, **B61**, 183 (1958).

9. B. P. McGrath and J. M. Tedder, *Proc. Chem. Soc. London*, 80 (1961)

10. R. E. Pearson and J. C. Martin, *J. Am. Chem. Soc.*, **85**, 354 (1963).

11. G. A. Russell, C. DeBoer, and K. M. Desmond, *J. Am. Chem. Soc.*, **85**, 365, 3139 (1963).

12. C. Walling, A. L. Reiger, and D. D. Tanner, *J. Am. Chem.*

Soc., **85**, 3129 (1963).

13. J. H. Incremona and J. C. Martin, *J. Am. Chem. Soc.*, **92**, 627 (1970).
14. W. A. Thaler, in *Methods in Free Radical Chemistry*, E. S. Huyser, Ed., Marcel Dekker, New York, 1969, Vol. 2, p 198, 204-209
15. R. C. Petterson and A. Wambsgans, *J. Am. Chem. Soc.*, **86**, 1648 (1964).
16. J. C. Day, M. J. Lindstrom, and P. S. Skell, *J. Am. Chem. Soc.*, **96**, 5616 (1974).
17. T. R. Beebe and F. M. Howard, *J. Am. Chem. Soc.*, **91**, 3379 (1969).
18. C. Walling, G. M. El-Taliawi, and C. Zhao, *J. Am. Chem. Soc.*, **105**, 5119 (1983).
19. C. Lagercrantz and S. Forshult, *Acta Chem. Scand.*, **23**, 708 (1969),
20. E. Hedaya, R. L. Hinman, V. Schomaker, S. Theodoropulos, and L. M. Kyle, *J. Am. Chem. Soc.*, **89**, 4875 (1967).
21. A. Lund, P. O. Samskog, L. Eberson, and S. Lunell, *J. Phy. Chem.*, **86**, 2458 (1982).
22. J. C. Scaiano, Private communication.
23. H. W. Johnson, and D. E. Bublitz, *J. Am. Chem. Soc.*, **80**, 3150 (1958).
24. J. C. Martin and P. D. Bartlett, *J. Am. Chem. Soc.*, **79**, 2533 (1957).
25. P.S. Skell, U. Luning, D. S. McBain, and J. Tanko, *J. Am.*

Chem. Soc., **108**, 121 (1986).

26. P. Kaushal, B. P. Roberts, and E. J. Ryan, *J. Chem. Soc., Chem. Commun.*, 1587 (1987).
27. J. M. Tanko, P. S. Skell, and S. Seshadri, *J. Am. Chem. Soc.*, **110**, 3221 (1988).
28. Y. L. Chow and Y. M. A. Naguib, *J. Am. Chem. Soc.*, **106**, 7557 (1984).
29. P. S. Skell and J. C. Day, *Acc. Chem. Res.*, **11**, 381 (1978).
30. U. Luning and P. S. Skell, *Tetrahedron*, **41**, 4289 (1985).
31. D. D. Tanner, D. W. Reed, S. L. Tan, C. P. Meintzer, C. Walling, and A. Sopchik, *J. Am. Chem. Soc.*, **107**, 6576 (1985).
32. R. W. Yip, Y. L. Chow, and C. Beddard, *J. Chem. Soc., Chem. Commun.*, 955 (1981).
33. D. D. Tanner, T. C-S Ruo, H. Takiguchi, A. Guillaume, D. W. Reed, B. P. Setiloane, S. L. Tan, and C. P. Meintzer, *J. Org. Chem.*, **48**, 2743 (1983).
34. P. S. Skell and S. Seshadri, *J. Org. Chem.*, **49**, 1650 (1984).
35. D. D. Tanner, C. P. Meintzer, and S. L. Tan, *J. Org. Chem.*, **50**, 1534 (1985).
36. J. C. Day, M. G. Katsaros, W. D. Kocher, A. E. Scott, and P. S. Skell, *J. Am. Chem. Soc.*, **100**, 1950 (1978).
37. F-L. Lu, Y. M. A. Naguib, M. Kitadani, and Y. L. Chow, *Can. J. Chem.*, **57**, 1967 (1979).
38. U. Luning, D. S. McBain, and P. S. Skell, *J. Org. Chem.*, **51**, 2077 (1986).

39. T. Kienig and R. A. Wielesek, *Tetra. Lett.*, **24**, 2007 (1975).

40. T. Clark, *J. Am. Chem. Soc.*, **101**, 7746 (1979).

41. O. Kikuchi, Y. Sato, and K. Suzuki, *Bull. Chem. Soc. Jpn.*, **53**, 2675 (1980).

42. M. J. S. Dewar, A. H. Pakiari, and A. B. Pierini, *J. Am. Chem. Soc.*, **104**, 3242 (1982).

43. P.S. Skell and J. C. Day, *J. Am. Chem. Soc.*, **100**, 1951 (1978).

44. R. L. Tlumak and P. S. Skell, *J. Am. Chem. Soc.*, **104**, 7267 (1982).

45. Y. Apeloig and R. Schreiber, *J. Am. Chem. Soc.*, **102**, 6144 (1980).

46. M. J. S. Dewar and S. Olivella, *J. Chem. Soc., Chem. Commu.*, 301 (1985).

47. S. A. Glover, A. Goosen, C. W. McCleland, and J. L. Schoonraad, *J. Chem. Soc., Perkin Trans. II*, 645 (1986).

48. P. S. Skell, R. L. Tlumak, and S. Seshadri, *J. Am. Chem. Soc.*, **105**, 5125 (1983).

49. D. D. Tanner and C. P. Meintzer, *J. Am. Chem. Soc.*, **107**, 6584 (1985).

50. V. Calo, L. Lopez, G. Pesce, F. Ciminale, and P. E. Todesco, *J. Chem. Soc., Perkin II*, 1189 (1974).

51. L. J. Bellamy, In *The Infra-red Spectra of Complex Molecules*, Methuen, London, 2nd Ed., 1958, in particular p 57.

52. Y. H. Zhang, M. H. Dong, X. K. Jiang, and Y. L. Chow,

private communication.

53. J. I. Musher, *Mol. Phys.*, **6**, 94 (1963).

54. C. M. Orlando, H. Mark, A. K. Bose, and M. S. Manhao, *J. Org. Chem.*, **33**, 2515(1968).

55. P. S. Skell and J. G. Traynham, *Acc. Chem. Res.*, **17**, 160 (1984).

56. U. Luning, S. Seshadri, and P. S. Skell, *J. Org. Chem.*, **51**, 2071 (1986).

57. P. S. Skell, *J. Am. Chem. Soc.*, **106**, 1838 (1984).

58. D. D. Tanner, R. J. Arhart, E. V. Blackburn, N. C. Das, and N. Wada, *J. Am. Chem. Soc.*, **96**, 829 (1974).

59. K. J. Shea, D. C. Lewis, and P. S. Skell, *J. Am. Chem. Soc.*, **95**, 7768 (1973) and earlier references therein.

60. R. M. Silverstein and G. C. Bassler, *Spectrometric Identification of Organic Compounds*, 4th Ed., John Wiley and Sons, New York, 1981; (a) P 130, (b) p 108, (c) p 226, (d) p 122, (e) p 125, (f) p 197.

61. Sadtler ^{13} NMR spectra No. 2558C.

62. Sadtler ^{1}H NMR spectra No. 19469M

63. W. Kemp, In *NMR in Chemistry*, MacMillan, London, 1986, in particular p 80.

64. For a review, see S. Sternhell, *Rev. Pure and Appl. Chem.*, **14**, 15 (1964).

65. E. I. Snyder and B. Franzus, *J. Am. Chem. Soc.*, **86**, 1166 (1964).

66. P. Laszlo and P. von Schleyer, *J. Am. Chem. Soc.*, **86**, 1171

(1964).

67. K. Tori, Y. Hata, R. Muneyuki, Y. Takano, T. Tsuji, and H. Tanida, *Can. J. Chem.*, **42**, 928 (1964).

68. M. Barfield, *J. Chem. Phys.*, **41**, 3825 (1964).

69. D. H. Williams and I. Fleming, *Spectroscopic Methods in Organic Chemistry*, McGraw-Hill, England, 1980, in particular p 161; M. E. Rose and R. A. W. Johnstone, *Mass spectrometry for Chemists and Biochemists*, Cambridge University Press, Cambridge, 1982, in particular p 272.

70. A. G. Schultz, F. P. Lavieri, M. Macielag, and M. Plummer, *J. Am. Chem. Soc.*, **109**, 3991 (1987); in particular p 4000, column 2.

71. E. Crundwell and W. Templeton, *J. Chem. Soc.*, 1400 (1964), in particular p 1401, Table 2.

72. K. Tori, K. Aono, Y. Hata, R. Wuneyuki, T. Tsuji, and H. Tanida, *Tetra. Lett.*, 9 (1966).

73. J. H. Noggle and R. E. Schirmer, *The Nuclear Overhauser Effect*, Academic Press, New York (1971).

74. For a recent review of NOE difference spectroscopy see: J. K. M. Sanders and J. D. Mersh, *Prog. Nucl. Magn. Reson. Spectroscopy*, 353 (1983).

75. B. I. Ionin and B. A. Ershov, *NMR Spectroscopy in Organic Chemistry*, Plenum Press, New York, 1970, in particular p 132.

76. P B. D. de la Mare and H. Suzuki, *J. Chem. Soc. C*, 648 (1968).

77. P. B. D. de la Mare, S. de la Mare, and H. Suzuki, *J. Chem. Soc. B,* 429 (1969).

78. G. S. Hammond and P. Leermakers, *J. Phys. Chem.*, **66**, 1148 (1962).

79. V. Calo, L. Lopez, G. Pesce, and P. E. Todesco, *J. Chem. Soc., Perkin II,* 1192 (1974).

80. S. Simakamasundari and R. Ganesan, *Intern. J. Chem. Kinetics,* **12**, 837 (1980).

81. A. J. Waring, *Adv. Alicyclic Chem.*, 1, 131 (1966).

82. W. G. Dauben, P. D. Hence, and W. K. Hayes, *J. Am. Chem. Soc.*, 77, 4609 (1955).

83. P. B. de la Mare and A. Singh, *J. Chem. Soc., Perkin II,* 59 (1973).

84. J. A. Kerr, In *Free Radicals*, J. K. Kochi Ed., John Wiley and Sons, New York 1973, Vol. I, p 15 (Table III).

85. G. C. Fettis, J. H. Knox, and A. F. Trotman-Dickenson, *J. Chem. Soc.*, 4177 (1960).

86. P. B. Howard and H. A. Skinner, *J. Chem. Soc. A,* 1536 (1966).

87. R. F. Barrow, T. C. Clark, J. Coxon, and K. K. Yee, *J. Mol. Spectrosc.*, **51**, 428 (1974).

88. K. P. Huberand and G. Herzberg, *Molecular Spectra and Molecular Structure Constants of Diatomic Molecules*, Van Nostrand, New York, 1979.

89. R. J. LeRoy, *J. Chem. Phys.*, **57**, 573 (1972).

90. For an excellent evaluation of gas-phase bromination

kinetics see S. W. Benson and J. H. Buss, *J. Chem. Phys.*, **28**, 301 (1958).

91. P. S. Skell, D. L. Tuleen, and P. D. Readio, *J. Am. Chem. Soc.*, **85**, 2850 (1963).

92. C. Walling, A. L. Rieger, and D. D. Tanner, *J. Am. Chem. Soc.*, **85**, 3129 (1963).

93. G. A. Russell and K. M. Desmond, *J. Am. Chem. Soc.*, **85**, 3139 (1963).

94. R. E. Pearson and J. C. Martin, *J. Am. Chem. Soc.*, **85**, 3142 (1963).

95. J. H. Incremona and J. C. Martin, *J. Am. Chem. Soc.*, **92**, 627 (1970).

96. G A. Russell, *J. Am. Chem. Soc.*, **80**, 4987 (1958).

97. N. Yamamoto, T. Kajikawa, H. Sato, and H. Tsubomoua, *J. Am. Chem. Soc.*, **91**, 265 (1969).

98. R. L. Strong, S. J. Rand, and J. A. Britt, *J. Am. Chem. Soc.*, **82**, 5053 (1960).

99. N. J. Bunce, K. U. Ingold, J. P. Landers, J. Lusztyk, and J. C. Scaiano, *J. Am. Chem. Soc.*, **107**, 5464 (1985).

100. E. F. Ullman and W. A. Henderson Jr., *J. Am. Chem. Soc.*, **88**, 4942 (1966).

101. J. C. Daton, K. Dawes. N. J. Turro, D. S. Weiss, J. A. Barltrop, and J. D. Coyle, *J. Am. Chem. Soc.*, **93**, 7213 (1971).

102. If the rate constants at 50°C for ring opening of the succinimidyl radical ($2x10^4$ s^{-1}) and for hydrogen

abstraction from dichloromethane by the succinimidyl radical (6 $M^{-1}s^{-1}$) reported by Walling[18] are taken as reasonable values, k_{16} and k_{18} at 20°C can be estimated to be $2x10^3$ s^{-1} and 1 $M^{-1}s^{-1}$ respectively. Since the lifetime of 3,3-dimethyl- glutarimidyl radical is about 45 μs at the room temperature[32], $2x10^3$ s^{-1} appears to be on the lower side. The rate constant for hydrogen abstraction from cyclohexane[32] by 3,3-dimethylglutarimidyl radical ($3.5x10^3$ M^{-1} s^{-1}) may be used for an estimation of the rate of reaction of the succinimidyl radical; $k_{18} = (3.5x10^3/200)x6 = 3$ M^{-1} s^{-1} where 200 is the relative selectivity $k(C_6H_{12})/k(CH_2Cl_2)$ per hydrogen (see Table 2-5) and 6 is the ratio of the number of hydrogens in cyclohexane to that in dichloromethane. The rate constant seems not too far from Walling's data.

103. H. E. Zimmerman and J. W. Wilson, *J. Am. Chem. Soc.*, **86**, 4036 (1964).

104. D. W. Placzek, B. S. Rabinovitch, and G. Z. Whitten, *J. Chem. Phys.*, **43**, 4071 (1965).

105. B. S. Rabinovitch and D. W. Stetser, *Advan. Photochem.*, **3**, 1 (1964).

106. E. F. Ullman, *Acc. Chem. Res.*, 1, 353 (1963).

107. For example, S-G Lee, *J. Chem. Soc., Chem. Commun.*, 1115 (1987).

108. Y. L. Chow and D. C. Zhao, *J. Org. Chem.*, **52**, 1931 (1987).

109. J. A. Barltrop and J. D. Coyle, in *Excited States in*

Organic Chemistry, Wiely, London, 1975, p 92.

110. G. B. Kistiakowski and J. C. Sternberg, *J. Chem. Phys.*, **21**, 2218 (1953).

111. N. K. Mathur and C. K. Narang, *The Determination of Organic Compounds with N-Bromosuccinimide and Allied Reagents*, Academic Press, London, 1975.

112. L. Horner and E. H. Winkelmann, *Angew., Chem.* **71**, 349 (1959).

113. N. P. Bau-Hoi, *Rec. Chem. Progr.*, **13**, 30 (1952).

114. C. Djerassi, *Chem. Rev.*, **43**, 271 (1948).

115. R. Filler, *Chem. Rev.*, **63**, 21 (1963).

116. R. C. Petterson and A. Wambsgans, *J. Am. Chem. Soc.*, **86**, 1648 (1964).

117. Y. L. Chow and R. A. Perry, *Can. J. Chem.*, **63**, 2203 (1985).

118. Y. L. Chow, T. W. Mojelsky, L. J. Magdzinski, and M. Tichy, *Can. J. Chem.*, **63**, 2197 (1985).

119. T. C. Joseph, J. N. S. Tam, M. Kitadani, and Y. L. Chow, *Can. J. Chem.*, **54**, 3517 (1976).

120. D. Griller and K. U. Ingold, *Acc. Chem. Res.*, **13**, 317 (1980).

121. D. F. Banks, E. S. Huyser, and J. Kleinberg, *J. Org. Chem.*, **24**, 3692 (1964).

122. D. D. Tanner and P. B. Bostelen, *J. Org. Chem.*, **32**, 1517 (1967).

123. R. Breslow, R. J. Corcoran, B. B. Snider, R. J. Doll, P. L. Khanna, and R. I. Kaleya, *J. Am. Chem. Soc.*, **99**, 905 (1977).

124. B. Blouri, C. Cerceau, and G. Lanchec, *Bull. Soc. Chim. Fr.*, 304 (1963).

125. B. Blouri, C. Cerceau, and J. E. Fauvet, *Bull. Soc. Chim. Fr.*, 477 (1962).

126. J. W. Wilt, in *Free Radicals*, KoChi Ed., John Wiley, New York, 1973, p 395.

127. Y. L. Chow and K. S. Pillay, unpublished work.

128. T. H. Lowry and K. S. Richardson, *Mechanism and Theory in Organic Chemistry*, Harper and Row, New York, 1976, p72.

129. E. C. Kooyman and G. C. Vegter, *Tetrahedron*, **4**, 382 (1958).

130. J. M. Brittain and P. B. D. de la Mare, in *The Chemistry of Halides, Pseudohalides and Azides, Part I, Supplement D*, S. Patai and Z. Rappoport Ed., John Wiley, New York, 1983, p 496.

131. P. B. D. de la Mare, O. M. H. El Dusouqui, J. G. Tillett, and M. Zeltner, *J. Chem. Soc.*, 5306 (1964).

132. E. Baciocchi and Illuminati, *J. Am. Chem. Soc.*, **89**, 4017 (1967).

133. M. Christen, W. Koch, W. Simon, and H. Zollinger, *Helv. Chim. Acta*, **45**, 2077 (1962).

134. W. Koch and H. Zollinger, *Helv. Chim. Acta*, **48**, 554 (1965).

135. J. M. Brittain, P. B. D. de la Mare and P. A. Newman, *J. Chem. Soc., Perkin II*, 32 (1981).

136. P. F. Kruse Jr., K. L. Grist, and T. A. McCoy, *Anal. Chem.*, **26**, 1319 (1954).

137. M. Z. Barakat, A. S. Fayzalla, and S. T. El-Aassan,

Analyst, **97**, 470 (1971).

138. D. S. Wilbur and H. A. O'Brien Jr., *J. Org. Chem.*, **47**, 359 (1982).

139. M. Anbar and I. Dostrovsky, *J. Chem. Soc.*, 1105 (1954).

140. R. A. Sneen and N. P. Matheney, *J. Am. Chem. Soc.*, **86**, 5503 (1964).

141. D. E. Pearson, R. D. Wysong, and C. V. Breder, *J. Org. Chem.*, **32**, 2358 (1967) and references 9 and 12 cited in this paper.

142. W. J. Moore, *Physical Chemistry*, Longmans, London, 4th Ed., 1963, p 266.

143. R. Haag, J. Wirz, and P. J. Wagner, *Helv. Chim.*, **60**, 2595 (1977).

144. X. Y. Li, H. Q. Pan and X. K. Jiang, *Tetra. Lett.*, 4937 (1984).

145. X. Y. Li, X. K. Jiang, Y. F. Gong and H. Q. Pan, *Acta Chim. Sinica*, **43**, 260 (1985); X. Y. Li, H. Q. Pan, X. K. Jiang, and Z. Y. Zhan, *Angew. Chem. Intern. Ed.*, **24**, 871 (1985).

146. H. Arzeno, D. H. R. Barton, R.-M. Berge-lurion, X. Lusinchi, and B. M. Pinto, *J. Chem. Soc., Perkin I*, 2069 (1984).

147. Y. L. Chow, D. C. Zhao, and C. I. Johansson, *Can. J. Chem.*, **66**, 2556 (1988).

148. G. Kortum, W. Vogel, and K. Andrussow, *Pure and Applied Chem.*, **1**, 190 (1960/61).

149. W. C. Still, M. Kahn, and A. Mitra, *J. Org. Chem.*, **43**, 2923

(1978).

150. S. L. Murov, *Handbook of Photochemistry*, Marcel Dekker, New York, 1973, p101.

151. M. V. Lock and B. F. Sagar, *J. Chem. Soc. B*, 690 (1966).

152. C. Walling and A. Padwa, *J. Org. Chem.*, **27**, 2976 (1962).

153. Y. L. Chow and Y. M. A. Naguib, *J. Chem. Soc., Perkin I*, 1165 (1984).

154. A. H. Andrist, M. J. Kovelan, *J. Chem. Soc., Perkin I*, 918 (1978).

155. S. S. G. Sircar, *J. Chem. Soc.*, 1252 (1927).

156. T. R. Beebe and J. W. Wolfe, *J. Org. Chem.*, **35**, 2056 (1970).

157. A. H. White and W. S. Bishop, *J. Am. Chem. Soc.*, **62**, 8 (1940).

158. M. J. J. Holt and A. C. Norris, *J. Chem. Educ.*, **54**, 426 (1977).

159. J. H. Espenson, *Chemical Kinetics and Reaction Mechanism*, McGraw-Hill, New York, 1981, p 25.

160. Willslatter and Schuler, *Chem. Ber.*, 61, 367 (1928).

161. Chuan-Jing Sun, *Principles and Technique of Gas Chromatography*, Chemical Industry Publishing House, Beijing, 1979, p 295.